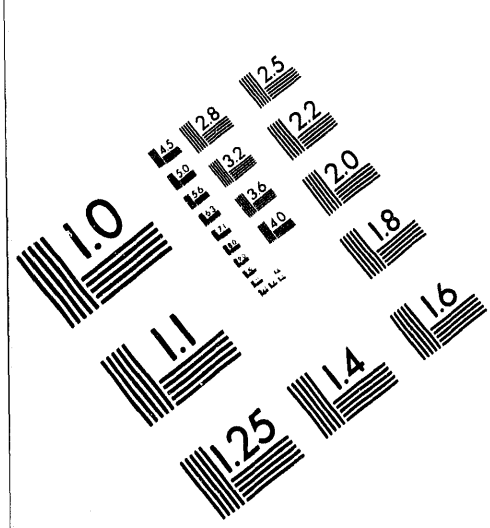

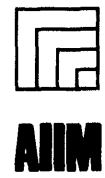

Association for Information and Image Management
1100 Wayne Avenue, Suite 1100
Silver Spring, Maryland 20910
301/587-8202

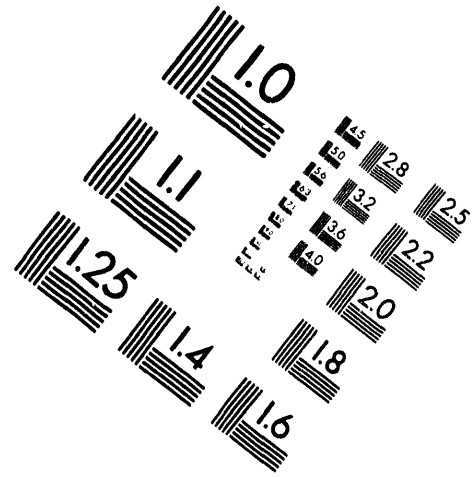

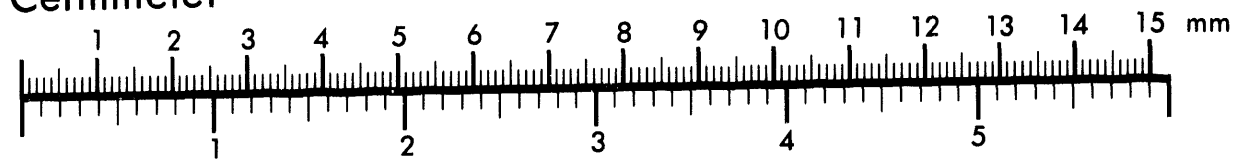

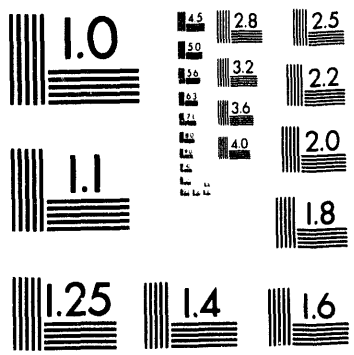

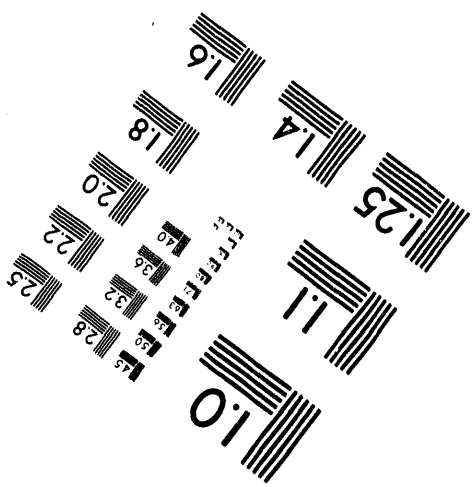

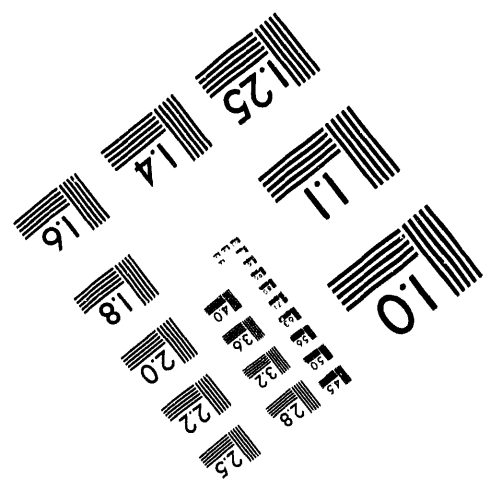

1 of 3

DOE/BC/14882-5
Distribution Category UC-122

RESPONSIVE COPOLYMERS FOR ENHANCED PETROLEUM RECOVERY

Annual Report

by
Charles McCormick
Roger Hester

August 1994

Work Performed Under Contract No. DE-AC22-92BC14882

Prepared for
U.S. Department of Energy
Assistant Secretary for Fossil Energy

Jerry Casteel, Project Manager
Bartlesville Project Office
P.O. Box 1398
Bartlesville, OK 74005

Prepared by
University of Southern Mississippi
Department of Polymer Science
Hattiesburg, MS 39406

TABLE OF CONTENTS

CHAPTER 9: POLYMER SOLUTION EXTENSIONAL BEHAVIOR IN POROUS MEDIA

NOMENCLATURE

A	Avogadro's number
A_o	Denn and Marucci model parameter
A_2	Second virial coefficient
a	Parameter relating permeability to porosity
B	Macromolecular stiffness parameter
B_o	Denn and Marucci model parameter
b	Parameter relating permeability to porosity
C	Polymer concentration
C_o	Denn and Marucci model parameter
C*	Critical overlap concentration
D_o	Denn and Marucci model parameter
D_o	Transitional diffusion coefficient
DP	Degree of polymerization
$\Delta\ell$	Length of bed
ΔP	Fluid pressure drop
d	Spherical particle diameter
d_n/d_c	Change in refractive index with respect to polymer concentration
ϵ	Polymer coil extensional strain
f	Fluid friction factor
f_m	Maximum fluid friction factor
f_p	Polymer solution friction factor
f_s	Solvent friction factor
Γ	Elongation rate
η_e	Solution extensional viscosity
η_s	Solvent shear viscosity
η_{red}	Solution reduced viscosity
$[\eta]$	Polymer intrinsic viscosity
$[\eta]_M$	Polymer intrinsic viscosity in brine
I	Ionic strength

I_E	Fluorescence emission intensity
I_M	Fluorescence emission intensity
I/I_o	Ratio of quenched to unquenched fluorescence intensities
k	Permeability
k'	Huggins constant
k_Q	Quenching rate constant
k_p	Rate constant for propagation
K_{sv}	Stern-Volmer constant
k_t	Rate constant for termination
κ	Debye-Huckel shielding length
Λ	Product of friction factor and Reynolds number
L	Reservoir pay thickness
ℓ_o	Polymer repeat unit length
M	Polymer molecular weight
m	Power law consistency index
M_{app}	Apparent molecular weight
M_o	Polymer repeat unit molecular weight
M_w	Weight average molecular weight
μ	Durst equation parameter
N	Number of polymer sub-elements
N_{De}	Deborah Number
N_{Re}	Reynolds number
Q	Volummetric flow rate
[Q]	Quencher concentration
ξ	Durst equation exponent
R	Gas law constant
R_f	Ratio of species travel to solvent travel
r	Radial distance from injection well
r_i	Reactivity ratio of the "i" species
ρ	Fluid density

σ	Durst equation parameter
T	Absolute temperature
t	Time for polymer coil extension
τ	Quenched fluorophore lifetime
τ	Polymer coil response time
τ_o	Unquenched fluorophore lifetime
υ	Fluid velocity
Φ	Fox-Flory constant
ϕ	Porosity
ψ	Normalized solution flow resistance
ψ_{max}	Maximum mobility flow resistance
X	Power law flow index

CHAPTER ONE
FIRST ANNUAL REPORT RESPONSIVE COPOLYMERS FOR ENHANCED PETROLEUM RECOVERY

I. Introduction

A coordinated research program involving synthesis, characterization, and rheology has been undertaken to develop *advanced polymer systems* which should be significantly more efficient than polymers presently used for mobility control and conformance. Unlike the relatively inefficient, traditional EOR polymers, these advanced polymer systems possess microstructural features responsive to temperature, electrolyte concentration, and shear conditions. Desired rheological behavior is accomplished by carefully controlling hydrophobic or ampholytic interactions between individual polymer chains. The polymers proposed circumvent major problems inherent in even the best conventional EOR polymers in which molecular weight is usually compromised in order to allow sufficient viscosity and uniform permeation without plugging the porous network. Additionally, conventional polymers are often poor mobility control agents in the presence of calcium, barium and sodium salts, precluding use in offshore recovery. By contrast, these advanced polymers would *maintain high viscosities* or behave as *gels* under low shear conditions and at *elevated electrolyte* concentrations expected in some reservoirs. At high fluid shear rates, intermolecular aggregates would dissociate yielding low viscosity solutions, subsequently reducing potential problems of face-plugging and shear degradation during injection. Also, certain copolymer compositions have been developed which emulsify hydrocarbons and viscosify the resulting fluid. Initial laboratory experiments have demonstrated the promise of such systems in higher salt, higher temperature reservoirs or as potential *surfactant/ viscosifiers* to mobilize entrapped oil.

Macromolecules can now be tailored for specific reservoir conditions. Most importantly, however, the development of new analytical techniques and screening tests now allows rapid feedback for systematic design of water-soluble polymers.

In our laboratories, DOE-sponsored research since 1978 has dealt with establishing unifying concepts regarding the relationships between structure of carefully synthesized molecules and fluid behavior under controlled salinity, pH, concentration, shear, and flow through porous media.

Virtually every behavioral property of polymer solutions important in EOR can be related to hydrodynamic volume and to macromolecular architecture.

Changes in molecular structure and hydrodynamic volume can directly affect:

- concentrations required for viscosity in mobility control
- degree of viscosity loss (or gain) in the presence of mono- and multivalent electrolytes
- solution phase stability as a function of temperature and ionic strength
- adsorption to porous media
- pore clogging
- chromatographic separation and excluded pore volume effects (sweep efficiency and slug dispersion)
- shear thinning effects
- molecular associations

The degree of shear, thermal and biological degradation are also affected by molecular structure and hydrodynamic size.

Partially hydrolyzed polyacrylamide HPAM and biopolymers such as xanthan have been extensively used due to their large solution dimensions in water; both have charged pendent groups. Additionally, the former usually is of high molecular weight and the latter contains chains stiffened by cyclic structures along the backbone.

The addition of electrolytes such as sodium and calcium salts to aqueous HPAM solutions results in viscosity loss and phase separation. The extent of loss depends upon temperature, concentration of polymer, concentration of added salt, and polymer microstructure. Similar effects are present with xanthan; however, they are of much less importance in rheological behavior and phase stability, probably due to molecular conformation, intermolecular interactions, and extended chain structure.

We are studying the effects of macromolecular structure on phase stability and salt sensitivity for polymers with carefully controlled structures and molecular weights. Table I below shows copolymer structure, molecular weight and zero shear intrinsic viscosity in 0.257 M NaCl of selected polymers from our research. This table illustrates the *dramatic enhancement of solution properties by proper molecular design.*

Copolymers with similar molecular weights and mole percent charged comonomers show hydrodynamic dimensions in sodium chloride decreasing greatly in the order NaAMB > NaAMPS > NaA. (See Table I for structure.) Additionally, *NaAMB and NaAMPS copolymers show no phase separation in NaCl or $CaCl_2$* solutions up to saturation even at elevated temperatures. The NaA copolymers (a class representative of hydrolyzed polyacrylamides) phase separate and/or precipitate in the presence of NaCl and $CaCl_2$. This behavior is a function of copolymer microstructure, concentration and molecular weight. The phase stability and high viscosity of the NaAMB copolymers were not expected and suggest the importance of hydrophobicity and conformational effects on ion binding of Ca^{++} and Na^{+} ions to the polymer.

Copolymers of DAAM were synthesized for comparative purposes since they contained similar but uncharged structures relative to those with NaAMPS and NaAMB units. Surprisingly, the viscosities in sodium chloride and calcium chloride solutions actually increased over those in distilled water. Even low molecular weight species showed high viscosity. In Table I, for example, DAAM-11 had a viscosity similar to that of NaA in NaCl solution despite having a molecular weight 4 to 5 times lower. This unexpected result has been the basis of studies in our laboratories on associative polymers detailed in suceeding chapters.

Recent discoveries in our laboratories and a few related reports in the literature suggest to us that *microheterogeneous ordering or aggregation might be used as a mechanism for developing advanced polymers for EOR.* These copolymers can be *tailored to be responsive to changes in salt concentration, pH, or added surfactants.* In addition to sweep efficiency improvement by viscosification, responsive rheological fluids could conceptually be used to improve reservoir conformance. Laboratory polymers responsive to changes in salt concentration and/or pH can form highly viscous fluids or gels. Unlike conventional cross-linked polymers, gelation can be reversed to restore original flow.

Table I
Salt Sensitivity (NaCl) of Model Copolymers of Acrylamide

Sample No.	Structure	Mol% Comonomer	Molecular Weight	η_0 (dL/g)
NaA-10	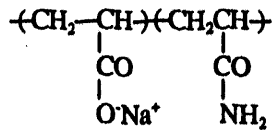	10	1,000,000	14.0
NaAMPS-1-5	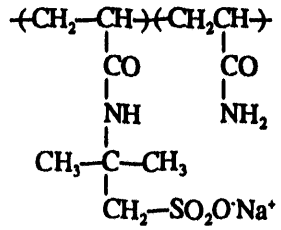	9.5	1,000,000	29.5
NaAMB-1-2	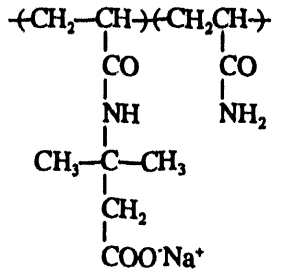	8.0	1,000,000	42.1
DAAM-11	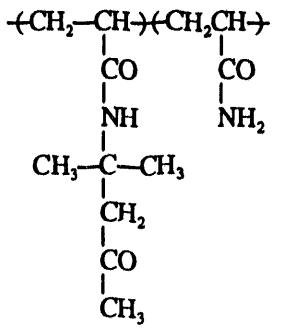	11	200,000	14.3

II. Overall Research Goals and Approach

The overall goal of this research is to prepare *advanced copolymers* for use as mobility control agents in EOR that rely on *microheterogeneous associations* (Scheme II-1) or *ampholytic associations* (Scheme II-2) to produce high viscosity in aqueous solutions yet are shear thinning. Such molecules would: (a) be efficient viscosifiers at low concentration and moderate molecular weight, (b) maintain or increase viscosity of the solution in the presence of mono- and/or multivalent electrolytes, (c) maintain or increase viscosity at higher temperatures or with pH changes, and (d) flow through relatively tight porous substrates under high shear stresses yet retard flow at low shear stress due to associative proper

Scheme II-1. Proposed interaction of associative, hydrophobically modified polymers. Association is favored by addition of NaCl or other electrolytes and by increasing temperature. Dissociation is favored by application of a shearing stress. Work in our laboratories and at Exxon clearly demonstrates this effect. Additionally, dissolution in aqueous media can be enhanced and adsorption onto porous substrate reduced by incorporating charged carboxylate or sulfonate groups onto the copolymers.

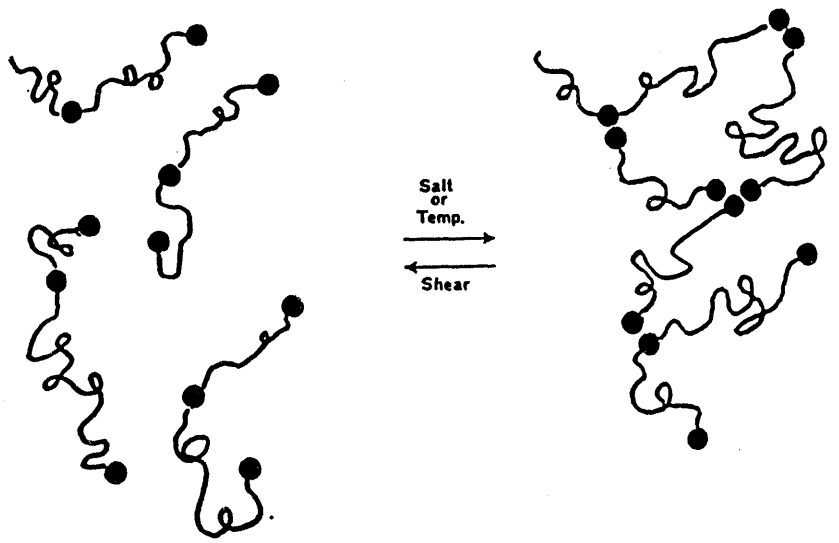

Scheme II-2. Polyampholyte expansion in salt solution. Copolymers with zwitterionic monomers or comonomer pairs exhibit low solution viscosity in water. As electrolyte is added expanded chain conformation results in enhanced viscosity. Gelation can occur with proper choice of monomers. This effect can be reversed.

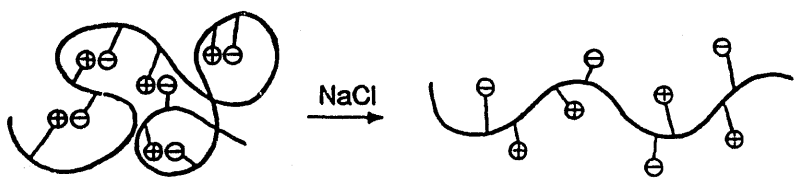

Compact Chain

Expanded Chain

A second major goal is to investigate the feasibility of utilizing a *hydrophobically modified polymer* as both the *surfactant* to emulsify oil and as a *viscosifying agent* (Scheme II-3) to increase sweep efficiency in EOR. The oil phase swells the polymer micelles which, in turn, would yield increased viscosity in the channels and pores. Such a polymer would eliminate the requirement of separate injections of a surfactant slug and a polymer slug and would avoid the attendant problems of polymer-surfactant mixing and slug dispersion normally encountered in micellar/polymer flooding.

Specific research objectives are

- Synthesis of advanced copolymers which rely on hydrophobic or ampholytic associations at low concentration for rheological control. Such associations are responsive to changes in pH and ionic strength.
- Synthesis and characterization of hydrophobically modified copolymers which can serve as both surfactant and viscosifier in EOR.
- Determination of hydrodynamic volume utilizing viscometry, low angle laser light scattering (LALLS), dynamic light scattering (DLS), and size exclusion chromatography (SEC) techniques.
- Development of predictive models based on interrelationships of molecular structure and solution behavior under operational conditions of temperature, shearing stress, concentration, and ionic strength.
- Technology transfer to the private sector for scale-up and field testing.
- Education and training of young scientists in innovative energy recovery research.

Scheme II-3. Polymeric surfactant-hydrophobic micelles swell upon contact with oil and interact cooperatively resulting in oil emulsification and an increase in viscosity.

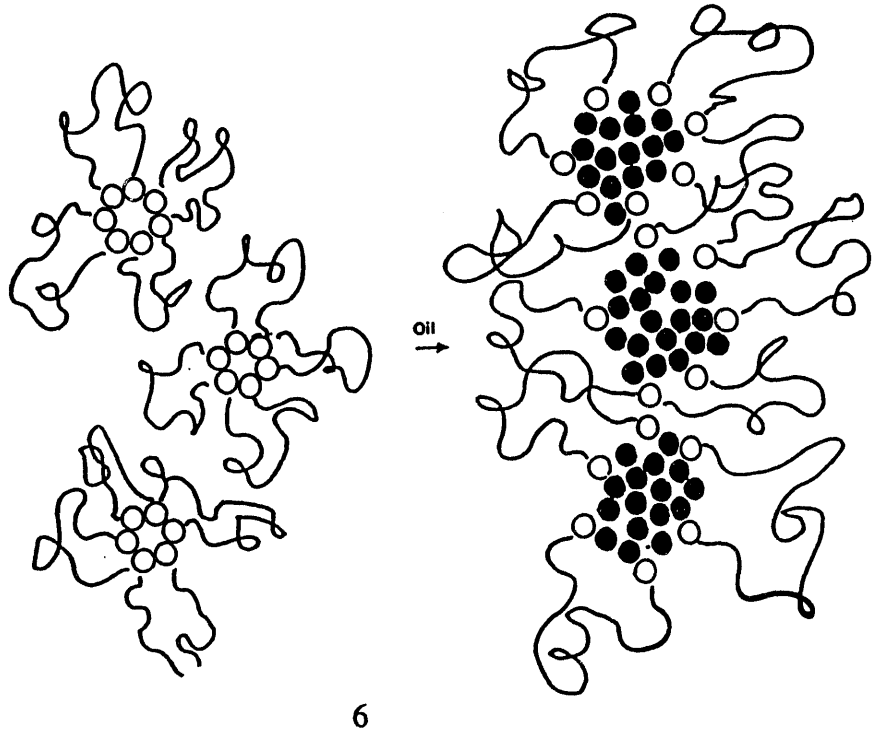

III. Advanced Copolymer Synthesis/Characterization/Solution Behavior

A. Conceptual Design

The three advanced copolymer systems conceptually described above are under preparation from the monomers shown in Scheme III-1. Acronyms have been assigned to each structure to aid in description of target copolymers. The *associative copolymers* rely on reversible hydrophobic interactions induced by RAM monomers appearing along a hydrophilic copolymer backbone composed of AM and ion containing monomers. For example, terpolymers of acrylamide (AM), 0.5 to 1.5% (RAM), and varying concentrations of NaA, NaAMPS, or NaAMB exhibit unexpected salt response and viscosity behavior which are being built into our advanced responsive systems. The remarkable viscosity responsiveness to changes in NaCl and polymer concentration are shown graphically in Scheme III-2. Clearly concentration-dependent, associative effects lead to marked increases in viscosity which persist at elevated salt concentrations. Conventional EOR polymers do not possess the important feature illustrated above.

Associative polymers without electrolyte comonomers present practical problems since they are slow to dissolve and would likely adsorb onto reservoir substrates. Choice of anionic (NaA, NaAMPS, NaAMB) comonomers aids dissolution and reduces adsorption particularly onto silicate surfaces. Additionally reversible rheological responsiveness to pH is anticipated. The above behavioral characteristics and predictions of cost effectiveness have dictated early study of RAM/NaA/AM, RAM/NaAMPS/AM, and RAM/NaAMB/AM terpolymers.

The *ampholytic* copolymers and terpolymers (Scheme II-2) rely on increased hydrodynamic volume upon addition of electrolytes. This viscosity increase is especially interesting for potential mobility control and conformance in high salt environments (for example off-shore EOR). Synthetic salt-responsive targets have been the sulfobetaine copolymer of AMPDAPS and AM and terpolymers AMPDAC/NaAMPS/AM or AMPTAC/NaAMPS/AM. Initial studies show significant viscosity increases with addition of NaCl to aqueous solutions of the above polymers. Substitution of NaAMB for NaAMPS results in hydrogel forming polymers. Reversibility of gel characteristics could be envisioned for "smart" profile modifiers.

The final group of advanced polymers are the polymeric surfactants (Scheme II-3). These co- and terpolymers associate in an intramolecular fashion to yield "polysoaps" which allow mobilization of residual oil. As well, rheology can be reversibly modified by changes in pH or salt concentration.

In a number of cases for synthesis of all three polymer systems it will be instructive to incorporate fluorescence labels into the copolymer backbone. The monomers NAS, APS, NaEAM, and PPAM (Scheme III-1) have been utilized as reporters of the reversible associations in aqueous media. These and other techniques are extremely important for optimizing macromolecular design.

Scheme III-1. Monomers for Synthetically Tailored EOR Polymers.

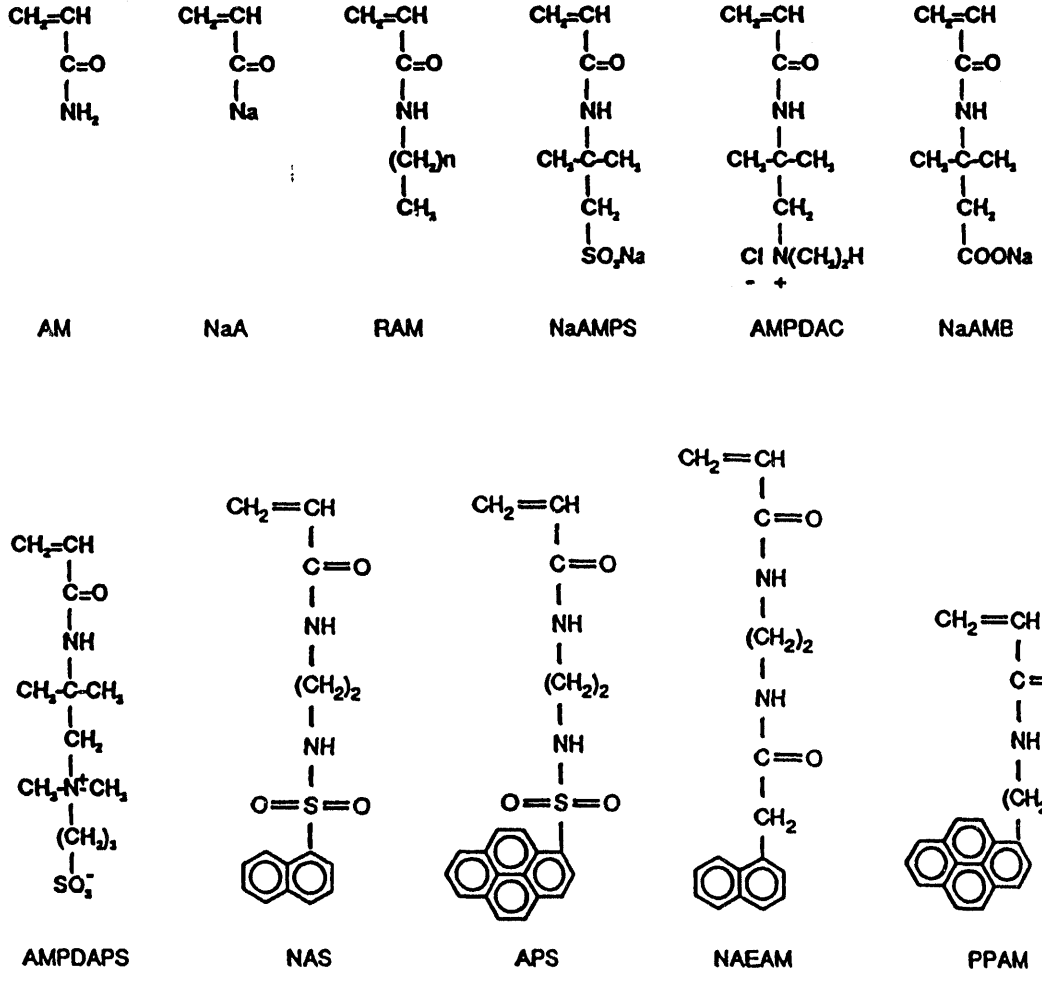

Scheme III-2. Viscosity behavior as a function of NaCl concentration and polymer concentration for the terpolymer of 5 mol% NaA; 0.5 mol% C-10 AM and 94.5 mol% AM.

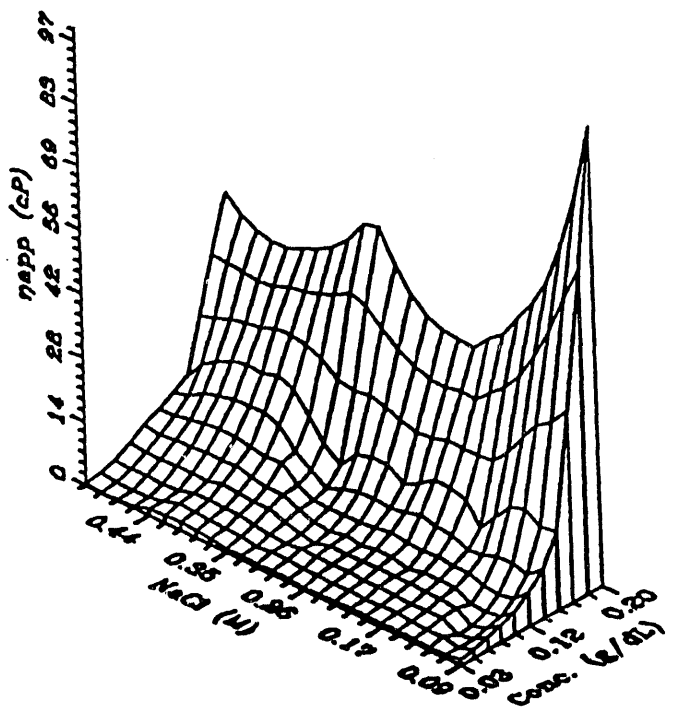

B. Copolymers of AM and NaAMB

Chapter 2 describes the synthesis, characterization and reactivity ratio studies of acrylamide (AM) with sodium-3-acrylamido methylbutanoate (NaAMB). Previous fundamental studies in our labs and core flow studies at Sun Oil and Refining indicated the potential of these systems as mobility control agents in EOR. We, therefore, have synthesized copolymers to further study extensional behavior under controlled conditions. Reactivity ratios were determined in 1M NaCl and compared to those in deionized water. Dilute solution properties were examined as a function of composition of added electrolytes and polymer microstructure. The remarkable viscosity maintenance at high salinity is the subject of sodium and celenium ion-binding studies utilizing ^{23}Na Nuclear Magnetic Resonance.

C. Terpolymers of AM, n-Decylacrylamide, and an anionic monomer

In Chapter 3 hydrophobically modified, water-soluble polyelectrolytes are discussed. The third anionic monomer chosen from among sodium-3-acrylamido-3-methylbutanoate (NaAMB), sodium acrylate (NaA), and 2-acrylamido-2-methylpropane-sulfonate (NaAMPS) imparts pH- and salt-responsive behavior. Solution and rheological behavior depends upon terpolymer composition, concentration, nature of the charged groups, and ionic strength. Within the carboxylate series, polymers with the carboxylate group closer to the polymer backbone exhibit greater viscosity increase with added electrolyte above the critical overlap concentration, C*. Spacing either the carboxylate or sulfonate group farther from the backbone disrupts associative intermolecular interactions, lowering viscosity. Significantly, both viscosity enhancement and ease of dissolution are possible in these systems.

D. Terpolymers of AM, N-(4-Butyl)phenylacrylamide (BPAM), and NaAMPS or NaAMB.

Hydrophobically modified terpolymers of acrylamide, and N-(4-butyl)phenylamide (BPAM) with either sodium-2-acrylamido-2-methyl propane sulfonate (NaAMPS) or sodium-3-acrylamido-3-methylbutanoate (NaAMB) are described in Chapter 4. These copolymers are like those described in Chapter 3; however, they possess the phenyl substituent which allows facile characterization via ultraviolet spectroscopic analysis. The carboxylated terpolymers exhibit high viscosities in the presence of NaCl and $CaCl_2$, but lose much of the viscosity at low pH or in the presence of urea. The sulfonate copolymers are less responsive to changes in pH or electrolyte concentration.

E. Associative Copolymers of AM with the APS Comonomer

In Chapters 5 and 6 the synthesis and solution properties of Copolymers of acrylamide with a fluorescent comonomer N-[(1-pyrenylsulfonamideo)ethyl]acrylamide are described. Copolymers were synthesized under both homogeneous and microheterogeneous conditions (micellar). The presence of the pyrene label allowed assessment of associative properties.

Copolymers prepared in the presence of sodium dodecyl sulfate surfactant exhibited associative behavior while those prepared under homogeneous conditions showed no association. The presence of a "blocky" microstructure is responsible for the associative thickening mechanism. This result unambiguously defines the role of the hydrophobic substituents in thickening and allows design of future systems.

F. Ampholytic Copolymers of NaAMPS with AMPTAC

Chapter 7 describes the synthesis and solution properties of high-density polyampholytes of sodium-2-(acrylamido)-2-methylpropanesulfonate (NaAMPS) with [2-(acrylamido)-2-methylproply]trimethylammonium chloride (AMPTAC). Reactivity ratios indicate an alternating microstructure. At a 1:1 composition, the copolymers exhibit increases in viscosity in the presence of electrolytes. Second virial coefficients from light-scattering measurements were used to detect polyampholyte/polyeltectrolyte transitions with compositional changes. Hydration in the presence of electrolytes is important in determining volume (viscosity behavior) and is discussed relative to composition and polymer concentration.

G. Ampholytic Terpolymers of AM, NaAMPS, and AMPTAC

The promising viscosity response of the NaAMPS/AMPTAC copolymers led us to synthesize terpolymers of AM, NaAMPS, and AMPTAC which possess significantly enhanced viscosity. Chapter 8 describes the synthetic procedures, structural characterization, and rheological behavior of these systems. Enhanced viscosities in saline solutions were observed for terpolymers containing as little as 0.5 mol% of each charged monomer. The outstanding solution properties of these novel terpolymers in brine will allow tailoring and optimization of these and similar systems for field application.

H. Polymer Solution Extensional Flow Behavior

In Chapter 9 the existing literature on dilute polymer solution extensional flow behavior is summarized. Two theoretical models were analyzed to reveal the effects of macromolecular properties in producing solutions that offer high resistance to flow through porous media. This high solution resistance is due to the uncoiling or extension of polymer molecules as they are forced through expanding and contracting flow channels. Both models did not explain all experimental data; however, the models provide a good understanding of what phenomena are important in controlling fluid flow resistance during flow through porous media.

RELATED DISSERTATIONS

"^{23}NMR Studies of Ion-Binding Homopolyelectrolytes and Conformational Changes in Hydrophobically-Modified Polyelectrolytes," J. Kent Newman, 1993

"Synthesis, Characterization and Solution Behavior of Hydrophobically Modified Polyececctrolytes, Yihua Chang, 1993.

"Structurally Tailored Water Soluble Polymers for the Study of Drag Reduction," Pavneet S. Mumick, 1993.

"Investigations of Polymeric Drag Reduction: A Proposed Model and Experimetnal Evidence," James P. Dickerson, 1993.

"Synthesis and Solution Behavior of Electrolyte-Responsive Polyampholytes," Luis C. Salazar, 1991.

"Photophysical Investigations of Hydrophobically-Modified Water-Soluble Polymers," M. D. Clark, 1990.

"Synthesis and Solution Properties of Pyrene-Labelled Water-Soluble Polymers," S. A. Ezzell, 1990.

"Synthesis and Characterization of Hydrophobically-Modified Polyacrylamides," J. C. Middleton, 1990.

"Effects of Polymer Parameters on Drag Reduction," Abbas M. Safieddine, 1990.

"Investigation of Applications and Limitations of the Lithium Chloride/N,N-Dimethylacetamide Solvent for Synthesis of Cellulose Derivatives," T. R. Dawsey - 1989.

"Effects of Chemical Structure on Drag Reduction Behavior of Water-Soluble Polymers," S. E. Morgan - 1988.

"Synthesis and Characterization of Associating Macromolecules: Hydrophobically Modified Copolymers," C. B. Johnson - 1987.

"Synthesis and Characterization of Auxin-Containing Polymers and Investigation of Controlled Release Behavior," K. Kim - 1987.

"Aqueous Solution Behavior and Microstructural Studies of N-Substituted Acrylamide Copolymers: Neighboring Group Effects," D. L. Elliott - 1986.

"Derivitization and Characterization of Cellulose in Lithium Chloride and N,N-Dimethylacetamide Solutions," P. A. Callais - 1986.

"Synthesis and Solution Property Studies of Structurally Tailored Acrylamide-Based Macromolecules," K. P. Blackmon - 1986.

"Characterization of High Molecular Weight, Water-Soluble Polymers Using Size Exclusion Chromatography and Fluorescence Spectroscopy," C. E. Lundy - 1986.

"C-13 NMR Characterization, and Dilute Solution Studies of Model Polysaccharide and Synthetic Acrylamide-Based Copolymers," B H. Hutchinson, Jr. - May 1985.

"Controlled Release Polymers Containing Labile Bonds to Pendant Metribuzin," K. W. Anderson - May 1983.

"Development of a New Calibration Technique for Size Exclusion Chromatography-Application to High Molecular Weight Water-Soluble Polymers," P. H. Mitchell, Jr. - May 1982.

"Synthesis, Characterization, and Rheological Studies of Model Graft Copolymers of Dextran," L. S. Park - May 1982.

"Synthesis, Characterization, and Dilute Solution Studies of Random Copolymers of Acrylamide," G. S. Chen - August 1982.

"Modification of Polymeric Substrates for Utilization as Biomedical Materials," J. A. Pelezo - August 1979.

"Synthesis and Characterization of Controlled Activity Polymers for Release of Pendent Pesticides," M. M. Fooladi - May 1979.

PATENTS

"Calcium-Tolerant N-Substituted Acrylamides as Thickeners for Aqueous Systems," C. L. McCormick and K. P. Blackmon, European Patent JHL/4900/EURO, October 17, 1985.

"Calcium Tolerant N-Substituted Acrylamides as Thickeners for Aqueous Systems," C. L. McCormick and K. P. Blackmon, U.S. Patent 4,584,358, Apr. 22, 1986.

"Calcium-Tolerant N-Substituted Acrylamides as Thickeners for Aqueous Systems," C. L. McCormick and K. P. Blackmon, German Patent 86303578.8-, June 30, 1986.

"Calcium-Tolerant N-Substituted Acrylamides as Thickeners for Aqueous Systems," C. L. McCormick and K. P. Blackmon, U. S. Patent 4,649,183, March 10, 1987.

RELATED PUBLICATIONS

1992

"Apparent Solubility Parameters from Photophysical Investigation of Copolymers with Pendent Naphthyl Chromophores," C. L. McCormick, C. E. Hoyle, M. D. Clark, and T. A. Schott, *Polymer International, 27(1)*, 63-65 (1992).

"Water-Soluble Copolymers. 37. Synthesis and Characterization of Responsive Hydrophobically-Modified Polyelectrolytes," C. L. McCormick, J. C. Middleton and D. F. Cummins, *Macromolecules, 25(4)*, 1201-1206 (1992).

"Water-Soluble Copolymers: 38. Synthesis and Characterization of Electrolyte Responsive Terpolymers of Acrylamide, N-(4-Butyl) Phenylacrylamide and Sodium Acrylate, Sodium-2-Acrylamido-2-Methylpropanesulfonate or Sodium-3-Acrylamido-3-Methylbulanoate," C. L. McCormick, J. C. Middleton and C. E. Grady, *Polymer, 33(19)*, 4184-4190 (1992).

"Water-Soluble Copolymers. 39. Synthesis and Solution Properties of Associative Acrylamido Copolymers with Pyrenesulfonamide Fluorescence Labels," C. L. McCormick and S. A. Ezzell, *Macromolecules, 25(7)*, 1881-1886 (1992).

"Water-Soluble Copolymers. 40. Photophysical Studies of the Solution Behavior of Associative Pyrenesulfomide-Labeled Polyacrylamides," C. L. McCormick, C. E. Hoyle, D. Creed and S. A. Ezzell, *Macromolecules, 25(7)*, 1887-1895 (1992).

"Water Soluble Copolymers. XLI. Copolymers of Acrylamide and Sodium 3-Acrylamido-3-Methylbutanoate," C. L. McCormick and L. C. Salazar, *J. Macro. Sci.—Pure Appl. Chem., A29(3)*, 193-205 (1992).

"Water Soluble Copolymers 43. Ampholytic Copolymers of Sodium 2-(Acrylamido)-2-Methylpropanesulfonate with 2-(Acrylamido)-2-Methylpropanetrimethylammonium Chloride," C. L. McCormick and L. C. Salazar, *Macromolecules, 25(7)*, 1896-1900 (1992).

"Water Soluble Copolymers: 44. Ampholytic Terpolymers of Acrylamide with Sodium 2-Acrylamido-2-Methylpropanesulfonate and 2-Acrylamido-2-Methylpropanetrimethylammonium Chloride," C. L. McCormick and L. C. Salazar, *Polymer, 33(20)*, 4384-4387 (1992)

"Water Soluble Copolymers 46. Hydrophilic Sulfobetaine Copolymers of Acrylamide and 3-(2-Acrylamido-2-Methylpropanedimethylammodio)-1-Propanesulfonate," C. L. McCormick and L. C. Salazar, *Polymer, 33(21)*, 4617-4624 (1992).

1991

"Structural Design of Water-Soluble Copolymers," C. L. McCormick, in *Water Soluble Polymers: Synthesis, Solution Properties and Applications*, ACS Symposium Series 467, Chapter 1, 2-24 (1991).

"Copolymers of Acrylamide and a Novel Sulfobetaine Amphoteric Monomer," L. C. Salazar and C. L. McCormick, in *Water Soluble Polymers: Synthesis, Solution Properties and Applications*, ACS Symposium Series 467, Chapter 7, 119-129 (1991).

"Synthesis and Solution Characterization of Pyrene-Labeled Polyacrylamides," S. A. Ezzell and C. L. McCormick, in *Water Soluble Polymers: Synthesis, Solution Properties and Applications*, ACS Symposium Series 467, Chapter 8, 130-150 (1991).

"Photophysical and Rheological Studies of the Aqueous-Solution Properties of Naphthalene-Pendent Acrylic Copolymers," M. D. Clark, C. L. McCormick and C. E. Hoyle, in *Water Soluble Polymers: Synthesis, Solution Properties and Applications*, ACS Symposium Series 467, Chapter 19, 291-302 (1991).

"Roles of Molecular Structure and Solvation on Drag Reduction in Aqueous Solutions," C. L. McCormick, S. E. Morgan and R. D. Hester, in *Water Soluble Polymers: Synthesis, Solution Properties and Applications*, ACS Symposium Series 467, Chapter 21, 320-337 (1991).

"Rheological Properties of Hydrophobically Modified Acrylamide-Based Polyelectrolytes," J. C. Middleton, D. F. Cummins and C. L. McCormick, in *Water Soluble Polymers: Synthesis, Solution Properties and Applications*, ACS Symposium Series 467, Chapter 22, 338-348 (1991).

"Water-Soluble Copolymers-Major Structural Types and Applications," C. L. McCormick, *Proceedings of the Eighteenth Annual Water-Borne, Higher-Solids, and Powder Coatings Symposium*, New Orleans, LA, February 1991.

1990

"Fundamental Studies of Hydrophobically Modified, Associative Copolymers in Aqueous Solution: Implications in Rheology Modification and Drag Reduction," C. L. McCormick and Roger D. Hester, *Proceedings of the 1990 Water-Borne and Higher-Solids Coatings Symposium*, 17, 85-101, New Orleans, LA (1990).

"Water-Soluble Copolymers. 35. Photophysical and Rheological Studies of the Copolymer of Methacrylic Acid with 2-(1-Naphthylacetyl)ethyl Acrylate," C. L. McCormick, C. E. Hoyle and M. D. Clark, *Macromolecules, 23(12)*, 3124-3129 (1990).

"Water-Soluble Copolymers. 36. Photophysical Investigations of Water-Soluble Copolymers of 2-(1-Naphthylacetamido)ethylacrylamide," C. L. McCormick, C. E. Hoyle and M. D. Clark, *Macromolecules, 24(9)*, 2397-2403 (1991).

"Water-Soluble Copolymers. 30. Effects of Molecular Structure on Drag Reduction Efficiency," C. L. McCormick, R. D. Hester, S. E. Morgan and A. M. Safieddine, *Macromolecules, 23(8)*, 2124-2131 (1990).

"Water-Soluble Copolymers. 31. Effects of Molecular Parameters, Solvation, and Polymer Associations on Drag Reduction Performance," C. L. McCormick, R. D. Hester, S. E. Morgan and A. M. Safieddine, *Macromolecules, 23(8)*, 2132-2139 (1990).

"Water-Soluble Copolymers XXXII: Macromolecular Drag Reduction. A Review of Predictive Theories and the Effects of Polymer Structure," S. E. Morgan and C. L. McCormick, *Prog. Polym. Sci., 15(3)*, 507-549 (1990).

"Water-Soluble Polymers: 33. Ampholytic Terpolymers of Sodium 2-Acrylamido-2-Methylpropanesulfonate with 2-Acrylamido-2-Methylpropanedimethylammonium Chloride and Acrylamide: Synthesis and Aqueous-Solution Behavior," C. L. McCormick and C. B. Johnson, *Polymer, 31*, 1100-1107 (1990).

"Water-Soluble Polymers. XXXIV. Ampholytic Terpolymers of Sodium 3-Acrylamido-3-Methylbutanoate with 2-Acrylamido-2-Methylpropane-Dimethylammonium Chloride and Acrylamide: Synthesis and Absorbency Behavior," C. L. McCormick and C. B. Johnson, *J. Macromol. Sci.—Chem., A27(5)*, 539-547 (1990).

1989

"Synthetically Structured Water-Soluble Copolymers: Associations by Hydrophobic or Ionic Mechanisms," C. L. McCormick and C. B. Johnson, chapter in *Polymers in Aqueous Media*, J. E. Glass, Ed., ACS Books, Advances in Chemistry Series No. 223, 437-454 (1989).

"Water-Soluble Copolymers. XXXII. Macromolecular Drag Reduction, A Review of Predictive Theories and the Effects of Polymer Structure," S. E. Morgan and C. L. McCormick, *Progress in Polymer Science, 15(3)*, 507-549 (1989).

"Water Soluble Polymers," C. L. McCormick, J. Bock, and D. N. Schulz, *Encyclopedia of Polymer Science and Engineering, 17*, John Wiley and Sons, New York, 730-784 (1989).

Polymers for Mobility Control in Enhanced Oil Recovery—Third Annual Report, C. L. McCormick and R. D. Hester, DOE/BC/10844-15, U. S. Department of Energy, Bartlesville, OK (1989). 108 pp.

"Copolymers of Acrylamide with (2-Acrylamido-2-Methylpropyl)Trimethyl Ammonium Chloride," C. L. McCormick, J. R. Danford, J. K. Newman, and L. C. Salazar, *Polymer Preprints, 30(2)*, 193 (1989).

"Volume Fraction Normalization Technique for the Study of Drag Reduction Efficiency," C. L. McCormick, P. S. Mumick and S. E. Morgan, *Polymer Preprints, 30(2)*, 256 (1989).

"Structural Design of Water-Soluble Copolymers for Specific Solution Properties and Behavior," C. L. McCormick, *Polymer Preprints, 30(2)*, 327 (1989).

"Synthesis of Pyrene-Labeled High Molecular Weight Acrylamide Copolymers," C. L. McCormick and S. A. Ezzell, *Polymer Preprints, 30(2)*, 340 (1989).

"Copolymers of Acrylamide and a Novel Sulphobetaine Amphoteric Monomer," C. L. McCormick and L. C. Salazar, *Polymer Preprints, 30(2)*, 344 (1989).

"Synthesis and Characterization of Hydrophobically Modified Acrylamide-Based Polyelectrolytes," C. L. McCormick, J. C. Middleton and D. Cummins, *Polymer Preprints, 30(2)*, 348 (1989).

"Photophysical and Rheological Studies of the Aqueous Solution Properties of a Naphthalene Containing Polyacid," C. L. McCormick, M. D. Clark and T. A. Schott, *Polymer Preprints, 30(2)*, 375 (1989).

"Size Exclusion Chromatography of High Molecular Weight Water-Soluble Polymers," R. D. Hester and A. M. Safieddine, *Polymer Preprints, 30(2)*, 369 (1989).

"Determination of Molecular Weight Distributions of Large Water Soluble Macromolecules," R. D. Hester and M. J. Mettille, *Polymer Preprints, 30(2)*, 380 (1989).

1988

"Water-Soluble Copolymers. 28. Ampholytic Copolymers of Sodium 2-Acrylamido-2 methylpropanesulfonate with (2-Acrylamido-2-methylpropyl) dimethylammonium Chloride: Synthesis and Characterization," C. L. McCormick and C. B. Johnson, *Macromolecules, 21*, 686-693 (1988).

"Water-Soluble Copolymers. 29. Ampholytic Copolymers of Sodium 2-Acrylamido-2-methylpropanesulfonate with (2-Acrylamido-2-methylpropyl) dimethylammonium Chloride: Solution Properties," C. L. McCormick and C. B. Johnson, *Macromolecules, 21*, 694-699 (1988).

"Structurally Tailored Macromolecules for Mobility Control in Enhanced Oil Recovery," C. L. McCormick and C. B. Johnson, chapter in *Water-Soluble Polymers for Petroleum Recovery*, G. A. Stahl and D. N. Schulz, eds., Plenum Publishing Company, 161-180, 1988.

"Size Characterization of EOR Polymers in Solution," R. D. Hester and A. D. Puckett, chapter in *Water-Soluble Polymers for Petroleum Recovery*, G. A. Stahl and D. N. Schulz, eds., Plenum Publishing Company, 201-213, 1988.

"Second Generation Copolymers for EOR," C. L. McCormick and C. B. Johnson, *Petroleum Preprints, 33(1)*, 53-58 (1988).

"A Study of Hydrophobic Association in Water-Soluble Polymers Using a Covalently Bound Fluorescence Probe," C. L. McCormick and M. D. Clark, *Polymer Preprints, 29(1)*, 309 (1988).

"Determination of Molecular Weight Distributions of Large Water-Soluble Macromolecules Using Dynamic Light Scattering," R. D. Hester and M. J. Mettille, *Proceedings of the ACS Division of Oil Field Chemistry, 33*, 20-24 (1988).

1987

"Water-Soluble Copolymers. 27. Synthesis and Aqueous Solution Behavior of Associative Acrylamide/N-Alkylacrylamide Copolymers," C. L. McCormick, T. Nonaka, and C. B. Johnson, *Polymer, 29(4)*, 731-739 (1987).

"Water-Soluble Copolymers, XVI. Studies of the Behavior of Acrylamide/N-(1,1-Dimethyl-3-Oxobutyl)Acrylamide Copolymers in Aqueous Salt Solutions," C. L. McCormick, B. H. Hutchinson, and S. E. Morgan, *Makromol. Chem., 188*, 357-370 (1987).

Associative Polymers for Mobility Control in Enhanced Oil Recovery - First Annual Report, C. L. McCormick and R. D. Hester, DOE/BC/10844-5, U. S. Department of Energy, Bartlesville, OK (1987). 258 pp.

Polymers for Mobility Control in Enhanced Oil Recovery - Second Annual Report, C. L. McCormick and R. D. Hester, DOE/BC/10844-10, U. S. Department of Energy, Bartlesville, OK (1987). 211 pp.

"Photophysical Properties of Pyrene in Solutions of Water-Soluble Acrylamide Copolymers," C. L. McCormick, C. E. Hoyle, and M. D. Clark, *Proceedings PMSE, 57*, 643 (1987).

"Hydrophobically Modified Polymers for Release of Bioactive Agents," C. L. McCormick and J. C. Middleton, *Proceedings PMSE, 57*, 700 (1987).

"Model Water-Soluble Acrylamide Copolymers for the Study of Polymeric Drag Reduction," C. L. McCormick, R. D. Hester, S. E. Morgan, and A. M. Safieddine, *Proceedings PMSE, 57*, 840 (1987).

"Synthesis and Characterization of Polyampholytes," C. L. McCormick and C. B. Johnson, *Proceedings PMSE, 57*, 154 (1987).

1986

"Water-Soluble Copolymers XV. Studies of Random Copolymers of Acrylamide with N-Substituted Acrylamides by Carbon 13-NMR," B. H. Hutchinson and C. L. McCormick, *Polymer, 27(4)*, 623-626 (1986).

"Water-Soluble Copolymers XIV. Potentiometric and Turbidimetric Studies of Water-Soluble Copolymers of Acrylamide: Comparison of Carboxylated and Sulfonated Copolymers," C. L. McCormick and D. L. Elliott, *Macromolecules, 19*, 542-547 (1986).

"Water-Soluble Copolymers XIII. Copolymers of Acrylamide with Sodium-3-Acrylamido-3-Methylbutanoate: Solution Properties," C. L. McCormick, K. P. Blackmon and D. L. Elliott, *J. Poly. Sci., Chem.: Poly. Chem., A24*, 2619-2634 (1986).

"Water-Soluble Copolymers XII. Copolymers of Acrylamide with Sodium-3-Acrylamido-3-Methylbutanoate: Synthesis and Characterization," C. L. McCormick, K. P. Blackmon, *J. Poly. Sci., Chem.: Poly. Chem., A24*, 2635-2645 (1986).

"Aqueous Solution Behavior of Copolymers of Acrylamide with Sodium-3-Acrylamido-3-Methylbutanoate (NaAMB): Neighboring Group Effects," C. L. McCormick and D. L. Elliott, *Polymer Preprints, 27(2)*, 280-281 (1986).

"Structurally Tailored Macromolecules for Mobility Control in Enhanced Oil Recovery," C. L. McCormick and C. B. Johnson, *Proceedings PMSE, 55*, 366-370 (1986).

"Water-Soluble Copolymers, XXV. Ion-Binding Studies of N-Substituted Acrylamide Copolymers Using Potentiometric and Spectroscopic Methods," C. L. McCormick and D. L. Elliott, *J. Poly. Sci. Chem.: Poly. Chem., A25*, 1329-1337 (1986).

"Water-Soluble Copolymers, XXIV. Copolymers of Acrylamide with N-(1,1-Dimethyl-3-Oxobutyl)-N-(n-Propyl)Acrylamide: Solution Properties," C. L. McCormick, K. P. Blackmon, and D. L. Elliott, *D. Angew. Makro. Chem., 144*, 87-99 (1986).

"Water-Soluble Copolymers, XXIII. Copolymers of Acrylamide with N-(1,1-Dimethyl-3-Oxobutyl)-N-(n-Propyl)Acrylamide: Synthesis and Characterization," C. L. McCormick and K. P. Blackmon, *D. Angew. Makro. Chem., 144*, 73-86 (1986).

"Water-Soluble Copolymers: XXII. Copolymers of Acrylamide with 2-Acrylamido-2-Methylpropanedimethylammonium Chloride: Aqueous Solution Properties of a Polycation," C. L. McCormick, K. P. Blackmon, and D. L. Elliott, *Polymer, 27*, 1976-1980 (1986).

"Water-Soluble Copolymers: XXI. Copolymers of Acrylamide with 2-Acrylamido-2-Methylpropanedimethylammonium Chloride: Synthesis and Characterization," C. L. McCormick and K. P. Blackmon, *Polymer, 27*, 1971-1975 (1986).

"Water-Soluble Copolymers XX. Copolymers of Acrylamide with Sodium-3-(N-Propyl) Acrylamido-3-Methylbutanoate: Solution Properties," C. L. McCormick and K. P. Blackmon and D. L. Elliott, *J. Macromol. Sci., Chem., A23(12)*, 1469-1486 (1986).

"Water-Soluble Copolymers XIX. Copolymers of Acrylamide with Sodium-3-(N-Propyl) Acrylamido-3-Methylbutanoate: Synthesis and Characterization," C. L. McCormick and K. P. Blackmon, *J. Macromol. Sci., Chem., A23(12)*, 1451-1467 (1986).

"Water-Soluble Copolymers XVIII. Copolymers of Acrylamide with Sodium-2-Methacrylamido-3-Methylbutanoate: Microstructural Studies and Solution Properties," C. L. McCormick, D. L. Elliott and K. P. Blackmon, *Macromolecules, 19*, 1516-22 (1986).

"Water-Soluble Copolymers XVII. Copolymers of Acrylamide with Sodium-2-Methacrylamide-3-Methylbutanoate: Synthesis and Characterization," *Macromolecules, 19*, 1512-5 (1986).

"Characterization of Large Water-Soluble Macromolecules by Size Exclusion Chromatography," R. D. Hester and C. E. Lundy, *Proceedings PMSE, 54*, 190 (1986).

"Size Characterization of EOR Polymer," R. D. Hester and A. D. Puckett, *Proceedings PMSE, 55*, 499-502 (1986).

"Characterization of Large Water-Soluble Macromolecules by Size Exclusion Chromatography," R. D. Hester and C. E. Lundy, *J. Polymer Science, Chem.*, *24*, 1829 (1986).

"A Comparison of Methods for Determining Macromolecular Polydispersity from Dynamic Laser Light Scattering Data," R. D. Hester, R. A. Vaidya and M. J. Mettille, Chapter 4, *ACS Symposium Series Book 332* (1986).

1985

"A Comparison of Methods for Determining Macromolecular Polydispersity from Quasi-Elastic Laser Light Scattering Data," R. D. Hester, R. A. Vaidya and M. J. Mettille, *Proceedings PMSE, 53* (1985).

Improved Polymers for Enhanced Oil Recovery - Final Report, C. L. McCormick and R. D. Hester, U. S. Department of Energy, DOE/BC/10321-20, Bartlesville, OK (1985). 219 pp.

"Synthetic Random and Graft Copolymers for Enhanced Oil Recovery," C. L. McCormick and C. B. Johnson, in *Biotechnology of Marine Polysaccharides*, McGraw-Hill, R. Colwell, E. R. Pariser, A. J. Sinskey, Eds., pp. 414-428 (1985).

"Water-Soluble Copolymers XI. Selectivity in the Graft Copolymerization of Acrylamide/N-(1,1-Dimethyl-3-Oxybutyl) Acrylamide Comonomers Onto Dextran by Ce(IV) Induced Initiation," C. L. McCormick and L. S. Park, *J. Appl. Polym. Sci.*, *30*, 45-59 (1985).

"Water-Soluble Random and Graft Copolymers for Utilization in Enhanced Oil Recovery," C. L. McCormick, *J. Macromol. Sci., Chem., A22(5-7)*, 955-982 (1985).

1984

"Water-Soluble Copolymers X. Copolymers of Acrylamide with N-(1,1-Dimethyl-oxybutyl) Acrylamide - Solution Properties," C. L. McCormick and G. S. Chen, *J. Poly. Sci., Chem.*, *22*, 3649-3660 (1984).

"Water-Soluble Copolymers IX. Copolymers of Acrylamide with N-(1,1-Dimethyl-oxybutyl) Acrylamide - Synthesis and Characterization," C. L. McCormick and G. S. Chen, *J. Poly. Sci., Chem.*, *22*, 3633-3649 (1984).

"Water-Soluble Copolymers of Acrylamide - Effects of Macromolecular Structure on Solution Properties," C. L. McCormick, *Preprints PMSE, 51*, 471-474 (1984).

"Synthesis Characterization, and Solution Behavior of Water-Soluble Polymers for Enhanced Oil Recovery," C. L. McCormick, G. S. Chen, and H. H. Neidlinger, *Preprints*, Am. Chem. Soc., Div. Pet. Chem., d., *29(4)*, 1159-67, 1984.

"Effects of Molecular Structure of Solution Behavior of Polymers for Utilization in Enhanced Oil Recovery," C. L. McCormick, K. P. Blackmon, D. L. Elliott, *Preprints*, Am. Chem. Soc., Div. Pet. Chem., d., *29(4)*, 1159-67, 1984.

"Water-Soluble Copolymers VIII. Synthesis and Dilute Solution Rheological Studies of Dextran-g-poly(acrylamide-co-sodium acrylates)," C. L. McCormick, L. S. Park, and R. D. Hester, *Polym. Eng. and Sci., 24(2)*, 163 (1984).

"Water-Soluble Copolymers VII. Cerium (IV) Induced Graft Copolymerization of Acrylamide and Sodium-2-Acrylamido-2-Methylpropane Sulfonate onto Dextran," C. L. McCormick and L. S. Park, *J. Poly. Sci., Chem., 22*, 49 (1984).

"Water-Soluble Copolymers VI. Dilute Solution Viscosity Studies of Random Copolymers of Acrylamide with Sulfonated Comonomers," H. H. Neidlinger, G. S. Chen, and C. L. McCormick, *J. Appl. Poly. Sci., 29*, 713-730 (1984).

Improved Polymers for Enhanced Oil Recovery - Sixth Annual Report, C. L. McCormick and R. D. Hester, DOE/BC/10321-16, U.S. Department of Energy, Bartlesville, OK (1984). 144 pp.

1983

"Polymers for Enhanced Oil Recovery," C. L. McCormick, *Mississippi Energy Research Journal*, 5-9, February (1983).

Improved Polymers for Enhanced Oil Recovery - Fifth Annual Report, R. D. Hester and C. L. McCormick, DOE/BC/10321-12, U. S. Department of Energy, Bartlesville, OK (1983). 219 pp.

1982

"Water-Soluble Copolymers. V. Compositional Determination of Random Copolymers of Acrylamide with Sulfonated Comonomers by Infrared Spectroscopy and C^{13} Nuclear Magnetic Resonance," C. L. McCormick, G. S. Chen, and B. H. Hutchinson, Jr., *J. Appl. Poly. Sci., 27*, 3103 (1982).

"Water-Soluble Copolymers. IV. Random Copolymers of Acrylamide with Sulfonated Comonomers," C. L. McCormick and G. S. Chen, *J. Polymer Science, Polymer Chemistry, 20*, 817 (1982).

"Effects of Synthetic Parameters on Microstructure and Solution Properties of Random- and Graft-Copolymers of Acrylamide with Sulfonate-Containing Monomers," C. L. McCormick, G. S. Chen and L. S. Park, *Proceedings IUPAC Macro 82*, Amherst, MA, 142 (1982).

"Structure and Dilute Aqueous Solution Property Relationships of Model Graft Copolymers, Dextran-g-Poly(acrylamide-co-sodium acrylates)," C. L. McCormick and L. S. Park, *Polymer Preprints, 23(2)*, 122 (1982).

Improved Polymers for Enhanced Oil Recovery - Fourth Annual Report, C. L. McCormick, DOE/BC/10321-5, U. S. Department of Energy, Bartlesville, OK (1982). 274 pp.

"Dextran-g-Acrylamide Copolymers for Enhanced Oil Recovery," C. L. McCormick, *Proceedings of the Second Conference on Water-Soluble Polymers*, State University of New York, New Paltz, 1-22 (1982).

1981

"Random- and Graft-Copolymers for Utilization in Enhanced Oil Recovery," R. D. Hester, C. L. McCormick, and H. H. Neidlinger, *Proceedings of the SPE/DOE Joint Symposium on Enhanced Oil Recovery*, Tulsa, OK (1981).

"Model Acrylamide Random and Graft Copolymers for Utilization in Enhanced Oil Recovery," C. L. McCormick, R. D. Hester and G. C. Wildman, *ACS Symposium Series - Enhanced Recovery Methods*, R. Berg, Ed., ACS, Washington, DC (1981).

"Synthetic Random- and Graft-Copolymers of Acrylamide for Enhanced Oil Recovery," C. L. McCormick, H. H. Neidlinger, R. D. Hester, and G. C. Wildman, *Polymer Preprints, 22(2)*, 74 (1981).

"Solution Properties of Random- and Graft-Copolymers of Acrylamide Utilized in Enhanced Oil Recovery," H. H. Neidlinger, G. S. Chen, F. Arai, and C. L. McCormick, *Polymer Preprints, 22(2)*, 90 (1981).

"Synthetic Random- and Graft-Copolymers for Utilization in Enhanced Oil Recovery," C. L. McCormick, R. D. Hester, H. H. Neidlinger, and G. C. Wildman, *Surface Phenomena in Enhanced Oil Recovery*, D. O. Shah, Ed., Plenum Press: New York, 741-772 (1981).

"Model Copolymers for Enhanced Oil Recovery," C. L. McCormick, H. H. Neidlinger and R. D. Hester, *Preprints*, Petroleum Division, ACS, Atlanta, GA, *26(1)*, 156 (1981).

"Model Acrylamide Random- and Graft-Copolymers (I) - Synthesis and Characterization," C. L. McCormick, L. S. Park, G. S. Chen, and H. H. Neidlinger, *Polymer Preprints, 22(1)*, 137 (1981).

"Model Acrylamide Random- and Graft-Copolymers (II) - Viscosity Studies in Aqueous Solutions," H. H. Neidlinger, C. L. McCormick and G. S. Chen, *Polymer Preprints, 22(1),* 139 (1981).

"Water-Soluble Copolymers. III. Dextran-g-Acrylamides, Control of Grafting Sites and Molecular Weight by Ce(IV) Induced Initiation in Homogeneous Solutions," C. L. McCormick and L. S. Park, *J. Polymer Science, Polymer Chemistry, 19,* 2229-2241 (1981).

"Water-Soluble Copolymers. II. Synthesis and Characterization of Model Dextran-g-Acrylamides by Ce(IV)/HNO_3 Induced Initiation," C. L. McCormick and K. C. Lin, *J. Macromolecular Science, Chemistry, A16(8),* 1441-1462 (1981).

"Water-Soluble Copolymers. I. Synthesis of Model Dextran-g-Acrylamides by Fe(II)/H_2O_2 Initiation and Characterization by Aqueous Size Exclusion Chromatography," C. L. McCormick and L. S. Park, *J. Applied Polymer Science, 26,* 1705-1717 (1981).

Improved Polymers for Enhanced Oil Recovery - Third Annual Report, C. L. McCormick, R. D. Hester, H. H. Neidlinger, and G. C. Wildman, DOE/BETC/5603-15, U. S. Department of Energy, Bartlesville, OK (1981). 294 pp.

1980

"Dextran-g-Acrylamide Copolymers for Potential Utilization as Displacement Fluids in Enhanced Oil Recovery," C. L. McCormick, L. S. Park and K. C. Lin, *Polymer Preprints, 21(1),* 171 (1980).

"Viscosity Studies of Acrylamide Random Copolymers," H. H. Neidlinger, G. S. Chen and C. L. McCormick, *Polymer Preprints, 21(1),* 175 (1980).

"Applications of the Southern Method of GPC Calibration to Aqueous Polymer Systems," P. H. Mitchell, C. L. McCormick and R. D. Hester, *Polymer Preprints, 21(1),* 109 (1980).

Improved Polymers for Enhanced Oil Recovery: Synthesis and Rheology - Second Annual Report, C. L. McCormick, G. C. Wildman, R. D. Hester, and H. H. Neidlinger, DOE/BETC/5603-10, U. S. Department of Energy, Bartlesville, OK (1980). 242 pp.

"Synthesis, Characterization and Rheological Behavior of Model Acrylamide Random- and Graft-Copolymers for Utilization in Enhanced Oil Recovery," H. H. Neidlinger, C. L. McCormick, R. D. Hester, and G. C. Wildman, *EOR - Chem. Flooding, 2,* F-29/1-21/14, DOE/BETC/IC-80/3, Bartlesville, OK (1980).

1979

"Synthesis, Characterization and Rheological Behavior of Model Random- and Graft-Copolymers for Utilization in Enhanced Oil Recovery," C. L. McCormick, R. D. Hester, H. H. Neidlinger, and G. C. Wildman, *Proceedings of the Fifth DOE Symposium on Enhanced Oil Recovery, Volume I*, Tulsa, OK, D4/1-D4/26 (1979).

"Synthesis and Viscosity Behavior of Acrylamide Random- and Graft-Copolymers," H. H. Neidlinger and C. L. McCormick, *Polymer Preprints, 20(1)*, 901 (1979).

"Synthesis and Dilute Solution Behavior of Acrylamide Random- and Graft-Cpolymers Utilized as Mobility Control Agents in Enhanced Oil Recovery," H. H. Neidlinger and C. L. McCormick, *Preprints IUPAC 26th International Symposium on Macrocolecules, 3*, 1584, Mainz, Germany (1979).

Improved Polymers for Enhanced Oil Recovery: Synthesis and Rheology - First Annual Report, C. L. McCormick, G. C. Wildman, R. D. Hester, and H. H. Neidlinger, BETC-5603-5, U. S. Department of Energy, Bartlesville, OK (1979). 123 pp.

CHAPTER TWO: COPOLYMERS OF ACRYLAMIDE AND SODIUM 3-ACRYLAMIDO-3-METHYLBUTANOATE

Abstract

Copolymers of acrylamide (AM, M_1) with sodium 3-acrylamido-3-methylbutanoate (NaAMB, M_2) synthesized in 1M NaCl (the ABAM2 series) are compared to those synthesized in deionized water (the ABAM1 series). At fixed feed ratios, higher incorporation rates were found for NaAMB with increasing ionic strength of the polymerization solvent. Reactivity ratios calculated by the methods of Kelen-Tüdös changed from r_1=1.23 and r_2=0.50 in deionized water to r_1=1.00 and r_2=0.64 in 1M NaCl. This change is in accord with a decrease in electrostatic repulsion between the macroradical and unreacted NaAMB. Dilute solution properties, examined as a function of composition and added electrolytes, indicate differences in microstructure for the ABAM1 and ABAM2 copolymers.

Introduction

Water soluble polymers that maintain high solution viscosities in the presence of added electrolytes have been the subject of our continuing research[1-3]. We have previously studied the copolymers of sodium 3-acrylamido-3-methylbutanoate (NaAMB, M_2) with acrylamide (AM, M_1) synthesized in deionized water[4,5]. NaAMB (Figure 1) is the carboxylated version of the pH stable monomer sodium 2-acrylamido-2-methylpropanesulfonate (NaAMPS). These monomers feature two geminal methyl groups which protect the amide functionality from hydrolysis. The acrylamido functionality allows polymerization to high molecular weights due to a high value of k_p^2/k_t.

Homopolymers of NaAMB and copolymers with AM are chain extended water-soluble polymers known for their phase stability in the presence of Na^+ and Ca^{++} and in high temperature environments[4,5]. Their attractive viscosity characteristics and electrolyte tolerance have been attributed to neighboring group and intra-unit interactions.

In this study, we examine the effects of changing the ionic strength of the polymerization solvent (water) on polymer microstructure and on solution properties. By synthesizing the homopolymer of NaAMB, and the copolymers with AM, in the presence of electrolytes we anticipate changes in microstructure and thus solution behavior[6].

Experimental

Materials and Monomer Synthesis

3-Acrylamido-3-methylbutanoic acid (AMBA) monomer was synthesized via a Ritter reaction of equimolar amounts of 3,3-dimethylacrylic acid with acrylonitrile as reported by Hoke and Robins[7] and modified by Blackmon[4]. Acrylamide (AM) from Aldrich was recrystallized twice from acetone prior to use. Potassium persulfate from Aldrich was recrystallized twice from water prior to use. Reagent grade sodium chloride from Fisher Scientific was used without further purification.

Synthesis of Copolymers of Sodium 3-Acrylamido-3-methylbutanoate and Acrylamide in the presence of NaCl

The ABAM2 series of copolymers was synthesized by free radical polymerization of sodium 3-acrylamido-3-methylbutanoate (NaAMB) with acrylamide (AM) in 1M NaCl solution. These copolymers were compared with the copolymers of the analogous ABAM1 series previously synthesized in deionized water by Blackmon[4]. In both cases potassium persulfate was used as the initiator; the reactions were conducted at 30°C and pH with a 0.46M monomer concentration. For each series the amount of acrylamide in the feed varied from 25 to 90 mol %.

A typical synthesis involved the dissolution of specified quantities of the monomers in separate solutions. The sodium salt NaAMB was obtained by the addition of NaOH to AMBA. The monomers were then mixed to form a single solution. Following adjustment of the pH to 9, the reaction mixture was transferred to a 500ml, 3-necked round bottom flask equipped with a mechanical stirrer, nitrogen inlet, and gas bubbler. The mixture was sparged with nitrogen for twenty minutes then initiated with 0.1 mol % potassium persulfate. Samples were taken at low and moderate conversions to study copolymer drift. The polymers were precipitated in acetone, redissolved in deionized water, then dialyzed using Spectra/Por 4 dialysis bags with molecular weight cutoffs of 12,000 to 14,000 daltons. After isolation by lyophilization, the copolymers were stored in desiccators. IR: ABAM2-100 homopolymer, N-H (broad), 3400-3300 cm^{-1}; C-H, 2955 cm^{-1}; amide C=O, 1655 cm^{-1}; sodium salt C=O, 1580 cm^{-1}. Typical copolymer: ABAM2-40, N-H (broad), 3450-3300 CM^{-1} ; AM amide C=O, 1665 cm^{-1} ; NaAMB amide C=O,1665 cm^{-1} ; (s), 1520 cm^{-1} (m); sodium salt C=O, 1580 cm^{-1}. ^{13}C NMR: ABAM2-40, Acrylamido C=O, 182.3 ppm; NaAMB C=O, 178.1 ppm; chain CH_2, 38.0 ppm; chain CH,44.6 ppm; gem CH_3, 29.0 ppm; NaAMB C, 55.4 ppm; NaAMB CH_2, 50.8 ppm.

Copolymer Characterization

Elemental analyses for carbon, hydrogen, and nitrogen were conducted by M-H-W Laboratories of Phoenix, AZ on both the low and high conversion copolymer samples. ^{13}C NMR spectra were obtained using 10 wt % aqueous (D_2O) polymer

solutions. The procedure for quantitatively determining copolymer compositions from ^{13}C NMR has been discussed in detail elsewhere[8]. FT-IR spectra for all materials synthesized were obtained using a Perkin-Elmer 1600 Series FT-IR spectrophotometer. Light scattering studies were performed on a Chromatix KMX-6 low-angle laser light scattering spectrophotometer and refractive index increments were obtained using a Chromatix KMX-16 laser differential refractometer. All measurements were conducted at 25°C in 0.512 M NaCl at a pH of 7.0 ± 0.1.

Viscosity Measurements

Stock solutions of sodium chloride (0.042, 0.086, 0.257, and 0.514 NaCl) were prepared by dissolving the appropriate amount of salt in deionized water in volummetric flasks. Polymer solutions were then made by dissolution and dilution to appropriate concentrations. After aging for two to three weeks, the solutions were analyzed with a Contraves LS-30 rheometer.

Results and Discussion

Copolymers of NaAMB and AM synthesized in deionized water (the ABAM1 series) are expected to be different from those synthesized in a 1M NaCl aqueous solution (the ABAM2 series). At pH 9, well above the pKa of the carboxylic acid group, 3-acrylamido-3-methylbutanoic acid (AMBA) exists in its changed form, sodium 3-acrylamido-3-methylbutanoate (NaAMB) (Figure 1). During polymerization the presence of NaCl should shield electrostatic interactions between charged groups, minimizing charge-charge repulsion between the NaAMB units on the growing macromolecular chain and the unreacted NaAMB.

Effects of NaCl on Composition

Varying comonomer feed compositions were used to synthesize the ABAM2 copolymer series with aqueous 1M NaCl as the polymerization solvent (Table I). The low conversion aliquots were taken when the reaction mixture first showed signs of increased viscosity. The polymerizations were then allowed to proceed to high conversion for optimum polymer yield. The compositions in Table I show a small amount of compositional drift as a result of the increased conversion. For example the copolymerization conducted at a 60:40 ratio of AM:NaAMB showed a 1.2% increase in M2 composition at 24% conversion over that observed at 4.1% conversion. The copolymers synthesized in deionized water did not exhibit copolymer drift with increased conversion.

Elemental analysis was used to determine the copolymer compositions. The weight percentages of carbon and nitrogen obtained from elemental analysis can be represented by equations (1) and (2).

$$\% C/12.01 = 3A + 8B \quad (1)$$

$$\% N/14.01 = A + B \quad (2)$$

The coefficients A and B are the number of moles of AM and NaAMB, respectively, in a normalized amount of copolymer, e.g. one gram. The mole percent of each monomer in the copolymer may then be determined using equations (3) and (4).

$$mol\% AM = A/(A + B) \times 100\% \quad (3)$$

$$mol\% NaAMB = B/(A + B) \times 100\% \quad (4)$$

A second set of copolymers was synthesized in which the ionic strength of the polymerization solvent was varied while the copolymer composition was maintained at 25:75 AM:NaAMB (Table II). As illustrated in Figure 2, increasing the ionic strength of the polymerization solvent allows more NaAMB to be incorporated into the copolymers up to a limiting composition. These results are similar to those of Breslow and Kutner[9] who prepared polymers of sodium ethylenesulfonate. They found an increase in the rate of polymerization and molecular weight upon the addition of sodium acetate. This was attributed to the reduction of an electrostatic effect which repels the ionic monomer from the negative charges on the growing chain. The compositions of the copolymers in Table II indicate that a similar reduction in electrostatic repulsion has occurred in the presence of NaCl. However, the relative hydrophobic character of NaAMB may also enhance its reactivity with the terminal NaAMB mer on the propagating chain.

Effects of NaCl on Reactivity Ratios

The compositions of the low conversion copolymers of the ABAM1 and ABAM2 series are compared in Table III. For every feed composition, the copolymers synthesized in the presence of NaCl had greater amounts of NaAMB incorporated. This information is presented graphically in Figure 3. The data for the ABAM2 copolymers lie closer to the dashed line which represents completely random copolymerization. The reactivity ratios (Table IV) derived by the methods of Fineman-Ross[10] and Kelen-Tüdös[11] are closer to "ideal" ($r_1 = r_2 = 1$) with added NaCl; r_1 , r_2 values are 1.2, 0.5 in water and 1.0, 0.6 in NaCl solution respectively. It is interesting that the product $r_1 r_2$ does not change significantly for the copolymers made in the absence or presence of salt (Table IV).

Changes in Copolymer Microstructure

Statistical microstructural information can be obtained using the equations of Igrashi[12] and Pyun[13]. These methods allow calculation of the fractions of M_1-M_1, M_2-M_2, and M_1-M_2 units in the copolymers from experimentally determined reactivity ratios and copolymer composition.

The results obtained for the copolymers (Table V) support the premise that changing the ionic strength of the polymerization solvent should lead to different copolymer microstructures. However, when the number of NaAMB centered triads are plotted as a function of copolymer composition (Figure 4) the ABAM1 and the ABAM2 series data fall on the same curve. The dashed line represents the triad distribution for an r_1 r_2 value of 0.64. Igarashi's equations depend on the inverse of r_1 r_2 and as long as this product remains the same the outcome of the equations will be the same.

Harwood, Park, and Santee have discussed the inadequacies of reactivity ratios by examining the microstructure of acrylamide copolymers using a catalyzed intrasequence cyclization technique[14]. They found that synthesizing copolymers of acrylamide with styrene in a variety of solvents led to copolymers with the same microstructure despite extreme differences in reactivity ratios.

Viscometric Studies

Effects of Copolymer Composition

The viscosity data obtained in this work indicate a change in the microstructure of the copolymers upon changing the ionic strength of the polymerization solvents. The intrinsic viscosities, obtained from Huggins plots, for the ABAM1 and ABAM2 series copolymers are shown in Figure 5. For both series the highest intrinsic viscosities were obtained from the copolymers contain less than 40 mol % NaAMB. Counterion condensation likely occurs at compositions with more NaAMB. Additionally decreasing molecular weight occurs with increasing NaAMB incorporation yielding lower viscosities.

The differences in location of the viscosity maxima may be due to neighboring group effects. At certain compositions the monomer units along the backbone can interact via hydrogen bonding for form chain-stiffening structures[2]. The frequency of these interactions will depend on the polymer microstructure. From Figure 6 it appears that the highest viscosities in deionized water are produced when the composition of NaAMB lies between 10 and 25 mol % for the ABAM1 series and 20 to 40 mol % for the ABAM2 series. The lack of smoothness of the viscosity copolymer composition curve from the ABAM1 series has been reported previously and may be due to conformational restrictions due to nearest neighbor interactions[5].

Effects of Molecular Weight

Molecular weight affects the dilute solution behavior of copolymers. Table VI compares the molecular weights and 2nd virial coefficient values of the copolymers made in deionized salt water. Samples ABAM1-10-2 and ABAM2-25-2 have molecular weights of 15.6 x 10^6 and 16.0 x 10^6 g/mol respectively. These two copolymers also have similar zero-shear intrinsic viscosities. Second virial coefficients indicate that even though ABAM1-10-2 has less charge than ABAM2-25-2, it is better solvated.

Samples ABAM1-25-2 and ABAM2-40-2 also have similar molecular weights but their viscosities are markedly different. The dissimilar second virial coefficients indicate the importance of polymer solvation on hydrodynamic volumes in solution. The small A_2 values for both ABAM1-25-2 and ABAM2-25-2 suggest the existence of microstructural interactions like those discussed above.

Effects of Added Electrolytes

The relationship of zero shear intrinsic viscosity to ionic strength for a number of ABAM1 and ABAM2 copolymers as a function of ionic strength are illustrated in Figure 6. Typical polyelectrolyte behavior is oberved. The polymer chains collapse as the ionic strength of the sovlent increases. The change of intrinsic viscosity with ionic strength has been used as a qualitative measure of chain flexibility. Smidsrod and Huag[15] obtained what they called a "stiffness parameter", B, utilizing equation (5) in which S is the slope of the plot of $[\eta]$ as a function of the inverse square root of the ionic strength and $[\eta]_M$ is the intrinsic viscosity at a given salt concentration. The exponent r is assumed invariant to polymer type and has an approximate value of 1.3

$$S = B \cdot ([\eta]_M)^r \qquad (5)$$

Values of B are generally low for polymers which retain their viscosity (remain extended) with increasing electrolyte concentration. Higher B values are reported for flexible polymers. It should be noted that B is inversely related to measures of stiffness such as persistence length on the steric factor[15]. In general B values (Table VII) for the copolymers in this work are higher for the ABAM2 series than the ABAM1 series for similar overall compositions up to 65 mole%. Differences in the aqueous solution viscosities for very similar molecular weights can only be attributed to microstructural differences.

Interestingly, ABAM1-10-2 with 8.4 mole percent NaAMB in the copolymer exhibits the best electrolyte tolerance over a wide range of NaCl concentrations consistent with our previous observations[2,4,5]. Neighboring group interactions between isolated NaAMB units and acrylamide are suggested to be responsible for chain stiffening. More random placement of NaAMB units as experimentally observed in synthesis from NaCl solutions lead to higher B values and less stiffening. Finally, above 65 mole% few isolated NaAMB units are available for placement between neighboring acrylamide units and smaller differences in stiffness are observed in the

two series of copolymers.

Conclusions

The addition of NaCl to the aqueous reaction medium results in more random copolymerization of acrylamide with sodium-3-acrylamido-3-methylbutanoate. Reactivity ratios determined experimentally at pH 9 changed from $r_1 = 1.23$ and $r_2 = 0.50$ for AM, NaAMB (M_1, M_2) in deionized water to $r_1 = 1.00$ and $r_2 = 0.64$ in NaCl. The change is in accord with screening of electrostatic repulsion between the growing chain and the charged monomer[16,17]. As a result 7.1% more NaAMB is incorporated at a 25:75 AM:NaAMB feed ratio.

It was anticipated that reactivity ratio changes might lead to significantly different distributions of monomer sequences and persistence length changes. Calculations using Igarashi's method show nearly identical NaAMB-centered triad distributions for copolymerizations in deionized or 1M NaCl solutions. Unfortunately the calculated distributions only reflect that the mathematical product $r_1 \cdot r_2$ is approximately 0.6 in both cases. This has no apparent physical significance.

Dilute solution behavior of the respective ABAM1 and ABAM2 series as a function of electrolyte concentration reveals significant microstructural differences. Qualitative comparisons of chain stiffness using the Smidsrod-Huag treatment[15] indicate microstructural effects - likely hydrogen bonding interactions of NaAMB with adjacent AM units - are more effective in maintaining chain dimensions. Such interactions are more effectively attained in synthesis at pH 9 from deionized water rather than 1M NaCl.

Technologically the NaAMB/AM copolymers continue to be of great interest owing to their unusually high viscosity maintenance and phase stability in high electrolyte and temperature environments.

References

1. G. S. Chen, Ph.D. Dissertation, University of Southern Mississippi (1982).

2. K. P. Blackmon, Ph.D. Dissertation, University of Southern Mississippi (1986).

3. L. C. Salazar, Ph. D. Dissertation, University of Southern Mississippi (1991).

4. C. L. McCormick and K. P. Backmon, *J. Poly. Sci., Polym. Chem. Ed., 24*, 2635 (1986).

5. C. L. McCormick, K. P. Blackmon, and D. L. Elliot, *J. Poly. Sci., Polym. Chem. Ed., 24*, 2619 (1986).

6. C. L. McCormick and L. C. Salazar, *Polym. Mat. Sci. Eng., 57* 859 (1987).

7. D. Hoke and R. Robins, *J. Polym. Sci., 10*, 3311 (1971).

8. C. L.. McCormick and B. H. Hutchinson, *Polymer, 27(4)*, 623 (1988).

9. D. S. Breslow and A. Kutner, *J. Polym. Sci., 27,* 295 (1958).

10. M. Fineman S. Ross, *J. Polym. Sci., 5(2)*, 259 (1950).

11. T. Kelen and F. Tüdös, *J. Macromol. Sci. Chem., A9*, 1 (1975).

12. S. Igarashi, *J. Polym. Sci. Polym.-Lett. Ed., 1*, 359 (1963).

13. C. W. Pyun, *J. Polym. Sci., A2(8)*, 1111 (1970).

14. H. J. Harwood, K. Y. Park, and E. R. Santee, *Polym. Preprints, 27(2)*, 81 (1986).

15. O. Smidsrod and A. Huag, *Biopolymers, 10*, 1213 (1971).

16. V. A. Kabonov, D. A. Topchiev, and T. M. Karaputadze, *J. Polymer Sci., ACS Symp. 42,* 173 (1973).

17. D. A. Kangas and R. R. Pelletier, *J. Polymer Sci.: Part A-1, 8*, 3543 (1970).

Table I

Reaction Parameters for the Copolymerization of Acrylamide (AM) with Sodium 3-Acrylamido-3-methylbutanoate (NaAMB) Synthesized in 1M Na Cl.

Sample Number	Feed Ratio AM:NaAMB	Reaction Time (hrs)	Conversion %	Weight (% C)	Weight (% N)	NaAMB in Copolymer (mol %)[a]
ABAM2-10-1	90:10	2.25	8.6	46.47	15.42	9.6 ± 0.2
ABAM2-10-2	90:10	4.42	20.1	45.66	15.08	10.6 ± 0.2
ABAM2-25-1	75:25	1.33	3.8	46.64	12.98	23.8 ± 0.5
ABAM2-25-2	75:25	10.25	14.1	--	--	24.8 ± 1.2[b]
ABAM2-40-1	60:40	1.5	4.1	47.21	11.44	36.3 ± 0.9
ABAM2-40-2	60:40	8.0	24.0	46.46	11.12	37.5 ± 0.9
ABAM2-60-1	40:60	1.5	11.4	47.62	9.83	53.0 ± 1.4
ABAM2-60-2	40:60	4.0	17.8	45.63	9.15	56.4 ± 1.5
ABAM2-75-1	25:75	1.5	8.6	46.87	8.57	67.6 ± 1.9
ABAM2-75-2	25:75	3.0	30.6	45.49	8.15	70.2 ± 1.9
ABAM2-100	0:100	5.42	5.5	44.76	6.27	100[c]
ABAM2-0	100:0	6.5	50.3	--	--	0[c]

[a] Determined from Elemental Analysis

[b] Determined from ^{13}C NMR

[c] Theoretical value

Table II

Reaction Parameters for the Copolymerization of Acrylamide (AM) with Sodium 3-Acrylamido-3-methylbutanoate (NaAMB) Synthesized in Solvents of Varying Ionic Strengths at a Fixed Feed Ratio

Sample Number	Feed Ratio AM:NaAMB	Ionic Strength (mol/L)	Reaction Time (hrs)	Conversion %	Weight (% C)	Weight (% N)	NaAMB in Copolymer (mol %)[a]
ABAM2-75(D.I)	25:75	0.00	2.66	4.0	44.36	8.53	61.3 ± 1.6
ABAM2-75(0.15)	25:75	0.15	2.66	7.1	44.39	8.60	60.4 ± 1.7
ABAM2-75(0.20)	25:75	0.20	4.00	3.5	46.34	8.76	63.4 ± 1.7
ABAM2-75(0.30	25:75	0.30	3.75	23.6	46.88	8.58	67.5 ± 1.8
ABAM2-75(0.45)	25:75	0.45	2.33	7.0	45.86	8.23	70.0 ± 1.9
ABAM2-75(1.00)	25:75	1.00	1.50	8.6	45.49	8.15	67.6 ± 1.2

[a] Determined by Elemental Analysis

Table III

Compositions of Copolymers of Acrylamide (AM) with Sodium 3-Acrylamido-3-methylbutanoate (NaAMB) Synthesized in Deionized Water (the ABAM1 series) and in 1M NaCl (the ABAM2 series).

Sample Number	Feed Composition (mol %)		Polymer Composition[a] (mol %)	
	AM	NaAMB	AM	NaAMB
ABAM1-10-1	90	10	92.0	8.0
ABAM1-25-1	75	25	79.7	20.3
ABAM1-40-1	60	40	68.6	31.2
ABAM1-60-1	40	60	51.6	48.4
ABAM1-75-1	25	75	37.9	63.1
ABAM2-10-1	90	10	90.4	9.6
ABAM2-25-1	75	25	76.2	23.8
ABAM2-40-1	60	40	63.7	36.3
ABAM2-60-1	40	60	47.0	53.0
ABAM2-75-1	25	75	32.4	67.6

[a] Determined from Elemental Analysis

Table IV
Reactivity Ratios for the ABAM1 and ABAM2 Copolymer Series
Determined using the Methods of Kelen-Tüdös and Fineman-Ross

	ABAM1			ABAM2		
Method	r_1	r_2	r_1r_2	r_1	r_2	r_1r_2
Kelen-Tüdös	1.23 ± 0.02	0.50 ± 0.04	0.62	1.00 ± 0.03	0.64 ± 0.05	0.64
Fineman-Ross	1.20 ± 0.02	0.47 ± 0.05	0.56	0.98 ± 0.03	0.59 ± 0.05	0.58

Table V

Structural Data for the Copolymers of Acrylamide (AM, M1) with Sodium 3-Acrylamido-3-methylbutanoate (NaAMB, M2) Synthesized in Deionized Water and 1M NaCl.

Sample Number	NaAMB in Copolymer (mol %)	Blockiness (mol %)		Alternation (mol %)	Mean Sequence Length	
		M_1-M_1	M_2-M_2	M_1-M_2	M_1	M_2
ABAM1-10-1	8.0	84.3	0.4	15.3	11.8	1.1
ABAM1-25-1	20.3	62.2	2.8	35.0	4.6	1.2
ABAM1-40-1	31.2	44.8	7.2	48.0	2.8	1.3
ABAM1-60-1	48.4	21.3	19.9	57.0	1.8	1.7
ABAM1-75-1	63.1	10.6	36.8	52.6	1.4	2.4
ABAM2-10-1	9.6	81.4	0.6	18.1	9.8	1.1
ABAM2-25-1	23.8	56.4	4.0	39.6	3.9	1.2
ABAM2-40-1	36.3	37.8	10.4	51.9	2.5	1.4
ABAM2-60-1	53.0	18.7	24.8	56.5	1.7	1.9
ABAM2-75-1	67.6	8.0	43.2	48.8	1.3	2.8

Table VI

Molecular Weight and Second Viral Coefficient Data for the ABAM1 and ABAM2 Copolymer Series.

Sample Number	Composition AM	NaAMB	Mw ($x10^{-6}$g/mol)	A_2 ($x10^4$ml mol/g^2)
ABAM1-10-2	91.6	8.4	15.6	4.28
ABAM1-25-2	79.9	20.1	12.9	1.52
ABAM1-60-2	50.2	49.8	14.0	3.49
ABAM2-10-2	90.4	9.6	6.8	4.39
ABAM2-25-2	76.2	23.8	16.0	3.60
ABAM2-40-2	63.7	36.3	11.9	4.02

Table VII

Comparison of the ABAM1 and ABAM2 Copolymer Series
Based on the Smidsrod and Haug Stiffness Parameter

Sample Number	NaAMB in Copolymer (mol %)	B ($[\eta]_{0.514M}$)
ABAM1-10-2	8.4	0.03
ABAM1-25-2	20.1	0.07
ABAM1-40-2	31.4	0.12
ABAM1-60-2	49.8	0.12
ABAM1-75-2	63.6	0.11
ABAM2-10-2	10.6	0.06
ABAM2-25-2	24.8	0.15
ABAM2-40-2	37.5	0.20
ABAM2-60-2	56.4	0.16
ABAM2-75-2	70.2	0.11

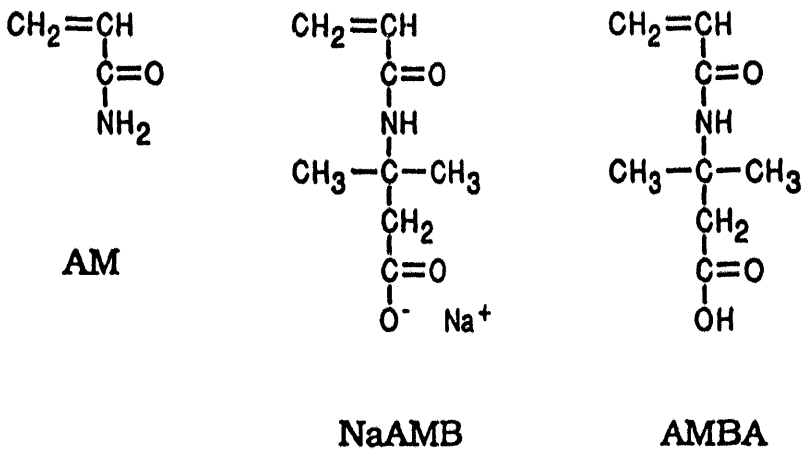

Figure 1 - Structures of comonomers: Acrylamide (AM); Sodium 3-Acrylamido-3-methylbutanoate (NaAMB); and 3-Acrylamido-3-methylbutanoic Acid (AMBA).

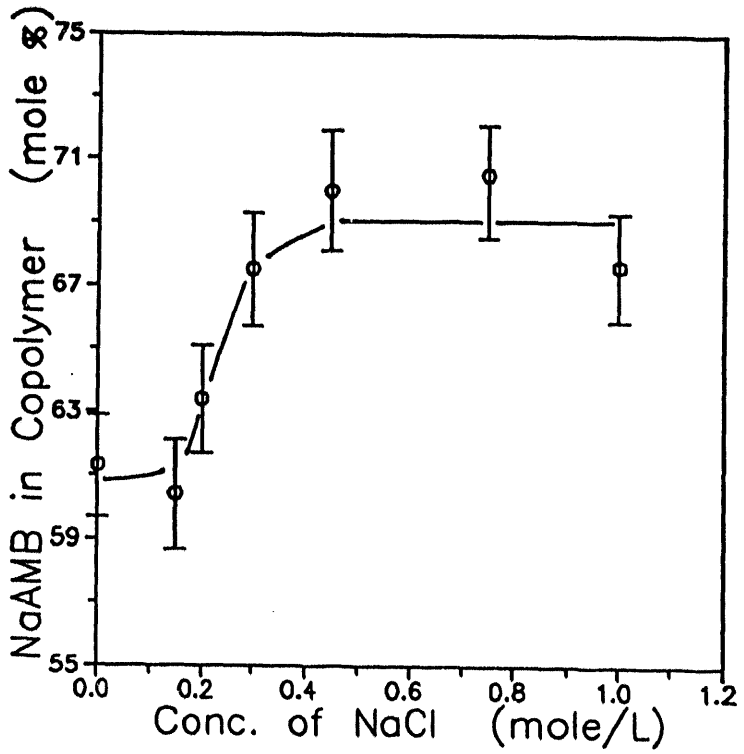

Figure 2 - Mole percent NaAMB incorporated into a copolymer as a function of salt concentration when the feed ratio is kept constant at 25/75 mol % AM/NaAMB.

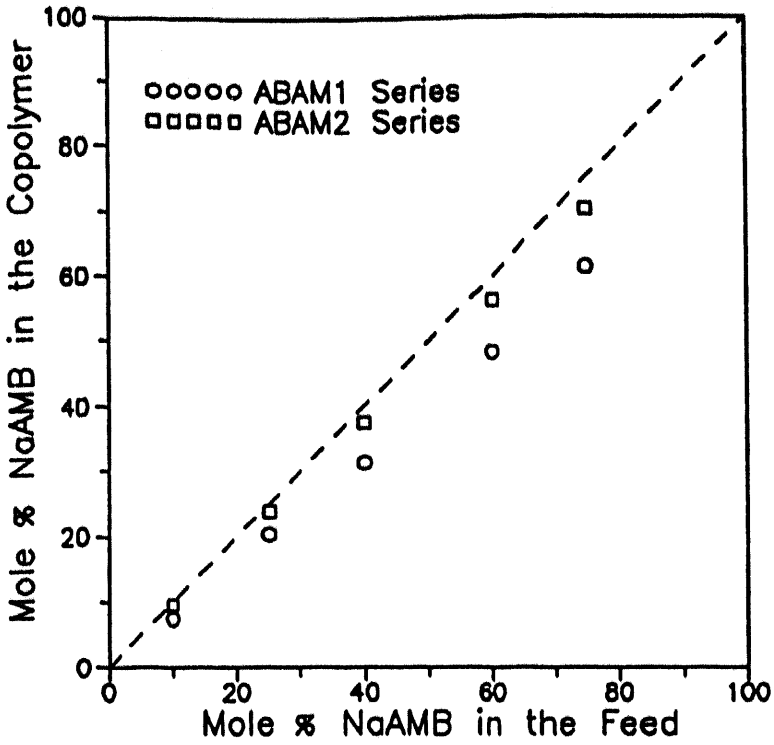

Figure 3 - Mole percent NaAMB incorporated into the copolymers as a function of comonomer feed ratio for the copolymers synthesized in deionized water (ABAM1 series) and in 1M NaCl (ABAM2 series). The dashed line represents $r_1 = r_2 = 1.0$.

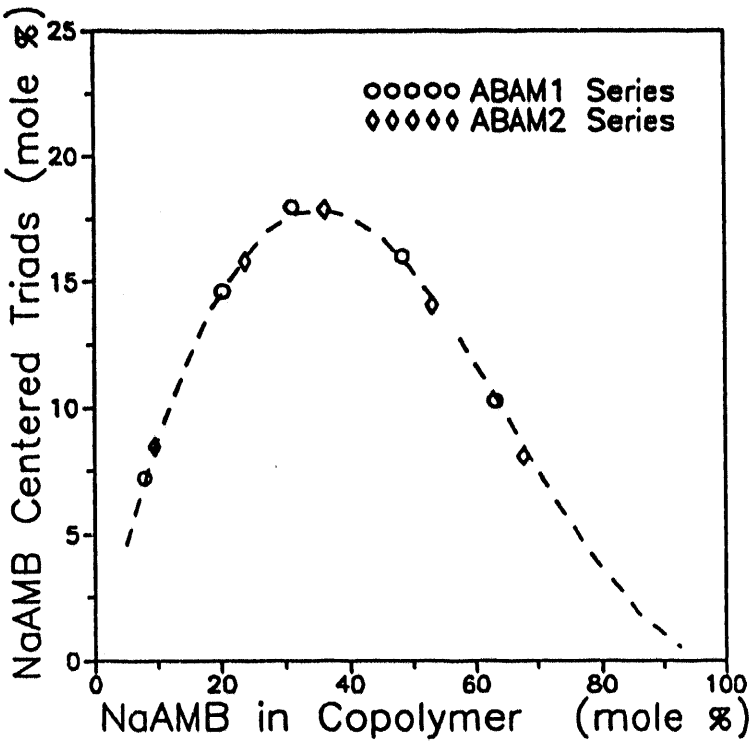

Figure 4 - Number of NaAMB monomer unit centered triads as a function of polymer composition for ABAM1 and ABAM2 copolymers. The dashed line represents the triad distribution for any polymer with $r_1 r_2 = 0.64$ regardless of the values of r_1 and r_2.

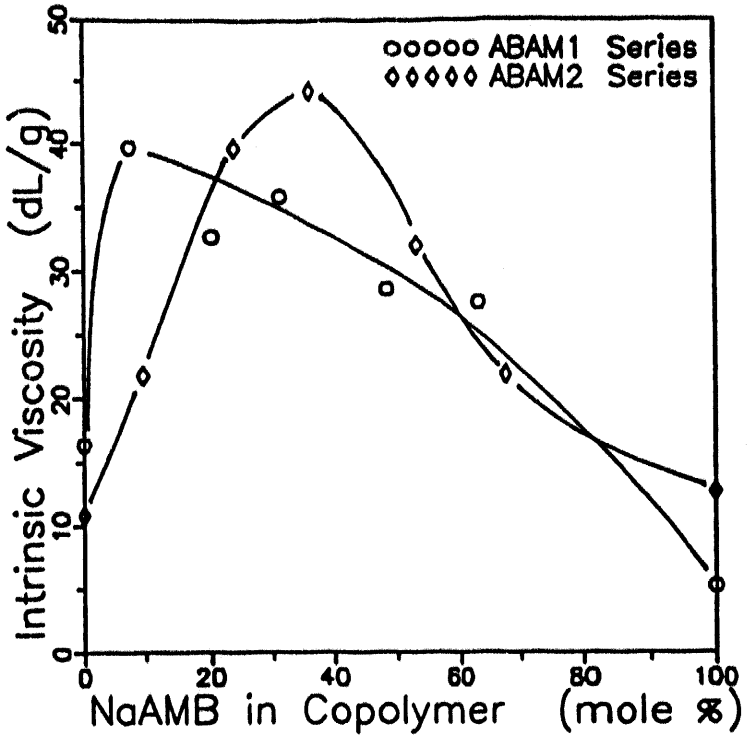

Figure 5 - Compositional effect on intrinsic viscosity for the ABAM1 and ABAM2 copolymer series in 0.514M NaCl determined with a shear rate of 1.75 sec^{-1} at 30°C.

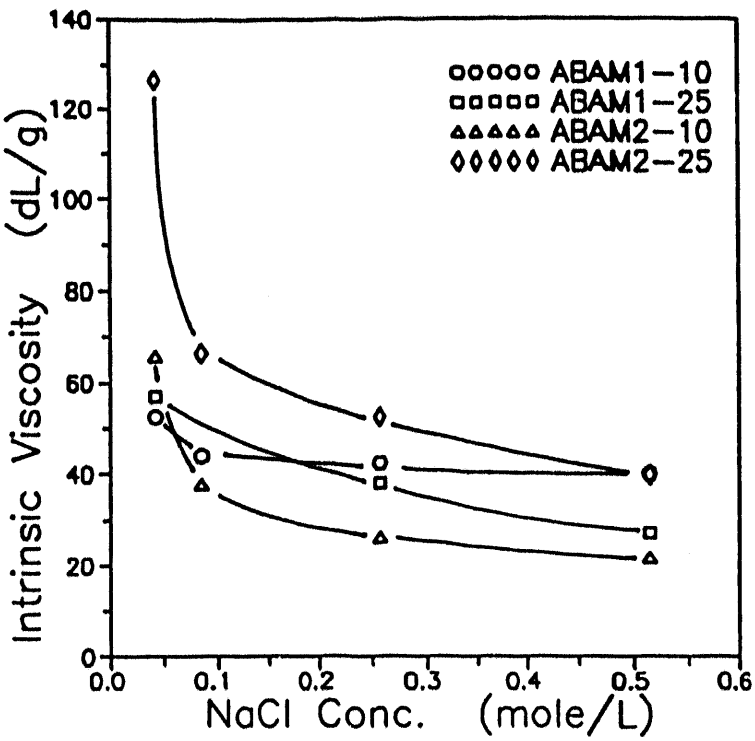

Figure 6 - Effect of sodium chloride concentration on the intrinsic viscosities of ABAM1 and ABAM2 copolymers determined at 30°C with a shear rate of 1.25 sec^{-1}.

CHAPTER THREE: TERPOLYMERS OF NaAMB, AM, AND n-DECRYLACRYLAMIDE

Abstract

Hydrophobically-modified, water-soluble, polyelectrolytes have been prepared by a micellar technique from acrylamide, n-decylacrylamide and a third monomer, sodium-3-acrylamido-3-methylbutanoate, sodium acrylate, or sodium-2-acrylamido-2-methypropanesulfonate. These terpolymers exhibit rheological behavior dependent upon the terpolymer composition, nature of the charged monomer, ionic strength, and pH. Although the hydrophobic monomer is incorporated in low concentration, the associative effects are profound with some compositions maintaining high viscosity in NaCl concentrations of up to 0.514M. Hydrophobic associations in terpolymers with the carboxylate anion are stronger than structurally analogous terpolymers containing the sulfonate anion, especially at high NaCl concentrations. Within the carboxylate series, copolymers with the carboxylate group closer to the polymer backbone exhibit greater viscosity increases with added electrolyte above a critical overlap concentration. Presence of carboxylate or sulfonate groups farther from the macromolecular backbone disrupts to a greater extent such hydrophobic associations.

Introduction

Studies in our laboratories have focused on developing macromolecules that can maintain or increase the viscosity of aqueous solutions in the presence of mono- or multivalent electrolytes[1-10]. Such polymers may have important commercial applications in enhanced oil recovery, drag reduction, flocculation, super absorbency and in personal care and coatings formulations. Hydrophilic polymers containing a small number of water-insoluble groups can undergo microphase separation and associations in aqueous solution.[11-17]

Recent work by our research group involved the synthesis and characterization of copolymers of acrylamide with n-alkylacrylamides with alkyl lengths of 8, 10, and 12 carbons. These polymers exhibit microheterogeneous associative behavior with the incorporation of less than one mole % of n-alkylacrylamide.[18,19] While such copolymers yield high viscosity solutions in the presence of added electrolytes above a critical concentration, they are difficult to hydrate from the dry state. In order to enhance dissolution and provide potential responsiveness to salt or pH changes, terpolymers containing acrylamide (AM), 0.5 mole percent of N-*n*-decrylacrylamide (C10AM) as the hydrophobic monomer, and sodium-3-acrylamido-3-methylbutanoate (NaAMB), sodium

acrylate (NaA), or sodium-2-acrylamido-2-methylpropanesulfonate (NaAMPS) were synthesized.[20,21] The two carboxylate monomers and one sulfonate monomer were selected to evaluate the differences in pK_B of pendent anions and to observe the influence of the distance of the charged group from the polymer backbone. Rheological properties were determined by low shear viscometry in deionized water and sodium chloride solutions.

Experimental Section

Materials

Acrylamide (AM), obtained commercially from Aldrich Chemical Co., was recrystallized twice from acetone, dried under vacuum, and stored in a desiccator prior to use (mp 81-84 °C). Acrylic acid, also obtained from Aldrich, was purified by vacuum distillation in the presence of cupric sulfate to remove inhibitor prior to use. 2-Acrylamido-2-methylpropanesulfonic acid (AMPS) was obtained from Fluka Chemical Co. and recrystallized twice from a mixture of methanol and 2-propanol. N-*n*-decylacrylamide [18] (C10AM) and 3-acrylamido-3-methylbutanoic acid (AMBA)[22] were synthesized and purified by previously reported methods. The monomers (Figure 1) were polymerized in their sodium salt forms.

Potassium persulfate from J. T. Baker Co. was recrystallized twice from deionized water prior to use. Sodium dodecyl sulfate, received from Aldrich Chemical Co., was used without further purification. Reagent grade sodium chloride from Fisher Scientific Co. was used without further purification. All aqueous solutions were prepared using deionized water.

Polymer Synthesis

The incorporation of water-soluble and water-insoluble monomers into the polymer backbone was accomplished by a micellar polymerization method.[16] In this technique, use of a surfactant is necessary in order to solubilize the hydrophobic monomer. Sodium dodecyl sulfate (SDS) was chosen as the surfactant in this instance. Each reaction was conducted in a 500-mL, three-necked, round-bottomed flask equipped with a mechanical stirrer, nitrogen inlet, and condenser. The appropriate amount of ionizable monomer was placed in DI water and the pH adjusted to 9 with NaOH to form the water-soluble salt. This amount was recorded and the solution diluted to a final volume of 230 mls (13.0 mol). The acrylamide monomer was dissolved in this solution, placed in a round-bottomed flask and was deaerated with purified nitrogen for thirty minutes. Surfactant (7.93 g; 2.8×10^{-2} mol) and 0.109 g (5.2×10^{-4} mol) of C10AM monomer were then added and the solution heated to 50°C with stirring under a nitrogen atmosphere. Potassium persulfate (0.005 g; 1.8×10^{-5} mol) dissolved in 5 ml of deionized water was added for a total water volume of 235 ml and a total monomer concentration of 0.44 M. The polymerizations were conducted for 4-6

hours followed by dilution with an equal amount of water and precipitation into acetone. The polymers were washed extensively in acetone and then dried under vacuum for 24 hours. Molecular weights for four acrylamide homopolymers prepared under the above conditions were determined to be from 1.0 to 1.5 x 10^6 by light scattering. Associative interactions precluded meaningful molecular weight measurements for the hydrophobically modified terpolymers; however, molecular weights would be expected to be in the same range.

Polymer Composition

Elemental analyses for carbon, hydrogen and nitrogen content of the terpolymers were conducted by M-H-W Laboratories of Phoenix, AZ. In addition, sulfur analyses of representative samples (of polymers not containing NaAMPS) were performed to confirm the absence of residual surfactant (Table 1). The low amount of C10AM incorporated into the polymer could be neglected in elemental analysis calculations without introducing significant error.

Viscometry

Stock solutions of sodium chloride (0.085, 0.170, 0.257, 0.342 and 0.514 M) were prepared by dissolving the appropriate amount of salt in deionized water contained in volummetric flasks. Polymer samples were dissolved by gentle shaking on an orbital shaker for 14 days to allow complete hydration before further dilutions of these stock solutions were made.

Viscosity experiments were conducted on the Contraves LS 30 low shear rheometer at a shear rate of $6s^{-1}$ at 30°C. The upper limit of the Contraves is 250 cP at a shear rate of $6s^{-1}$. Several polymers exceeded this value in the concentration range investigated. These polymer solutions were gels and a value of 250 cP was assigned to them for graphical purposes.

Results and Discussion

Electrostatic interactions and hydrophobic effects for terpolymers of the type prepared in this study may lead to microheterogeneous phase separation of important consequence in aqueous solution. The electrostatic interactions of carboxylate or sulfonate groups along the backbone generally increase the hydrodynamic volume while hydrophobic moieties aggregate in aqueous solution by intramolecular (closed) or intermolecular (open) associations dependent upon polymer microstructure, concentration, and molecular weight. Proper selection of synthetic conditions can lead to technologically important systems responsive to changes in pH or electrolyte concentration

Feed Composition

Three series of terpolymers were prepared by a modified micellar polymerization technique reported in the patent literature by Turner, Siano, and Bock[16]. The reaction conditions (Table 1) were chosen in order to have feed compositions of 0.5 mol % of the hydrophobic monomer C10AM, specified (5,10,25, and 40 mol%) concentration of the anionic monomers, NaAMB, NaAMPS, or NaA and the remainder AM. Our initial objectives were to achieve an associative viscosifier with properties of the uncharged C10AM/AM copolymer previously prepared[19] but with pH or electrolyte responsiveness. Additionally, it was our desire to assess the roles of the carboxylate and sulfonate groups on hydrophobic domain disruption.

Terpolymer Composition

Data from elemental analysis show agreement between feed ratios and copolymer composition up to 20 mole percent of the anionic monomer (Table 1). Above 20 mole percent, the incorporation likely decreases as electrostatic repulsions between structopendent charged groups of the growing polymer chain and charged monomer units become significant. While the incorporation of C10AM cannot be determined by conventional methods such as elemental analysis or NMR, Valint, *et al*[23] have shown greater than 85% incorporation of a chromophore labeled hydrophobic monomer by ultraviolet spectroscopy. Terpolymers with ionizable monomer feed compositions of 5 and 25 mole percent are representative samples of a low-charge-density and high-charge-density terpolymers, respectively. Terpolymers (Table 1) are named according to the type and concentration of ionic monomer present. For example, the terpolymer with a feed composition of 0.5 mole percent C10AM, 94.5 mole percent AM, and 5 mole percent NaAMB is referred to as NaAMB-5.

Solution Studies

Apparent viscosity (η_{app} in centipoise) is plotted as a function of polymer concentration (grams per 100mL or g/dL) and of solution ionic strength (NaCl) in three-dimensional plots to clearly illustrate solution behavior. Reduced viscosity (η_{red} in deciliters per gram) is plotted as a function of polymer concentration for each polymer sample at specific NaCl concentrations to further illustrate rheological changes (Figures 2-13).

NaAMPS Terpolymers

Both NaAMPS-5 and NaAMPS-25 show typical polyelectrolyte behavior at low solution ionic strengths (Figures 2 and 3). The apparent viscosities of both systems are high at low ionic strength characteristic of typical hydrated polyelectrolytes. Viscosity then decreases with increasing ionic strength as the charged groups are shielded by the addition of NaCl. However, above a critical polymer concentration (C*), η_{app} and η_{red} of NaAMPS-5 increase with increasing solution ionic strength above 0.26 M NaCl,

atypical of traditional polyelectrolytes (Figures 2(a) and 2(b)). The low charge-density polymer (Figure 2b) shows a linear increase in η_{red} only for the low ionic strength solution. At higher ionic strength, η_{red} increases rapidly indicative of interpolymer associations. The high-charge-density NaAMPS-25 polymer shows linear behavior at all ionic strengths investigated; apparently the increased charge-density effectively prevents hydrophobic aggregation (Figures 3a and 3b) by disrupting water structure ordering necessary for associative thickening behavior.

NaAMB Terpolymers

The NaAMB terpolymers exhibit unusual behavior as demonstrated by an increase in apparent viscosity with increasing solution ionic strength (Figures 4a and 5a). The NaAMB-5 terpolymer does not show associative behavior at NaCl concentrations less than 0.17M. The electrostatic repulsions of the NaAMB groups are sufficient to prevent interpolymer aggregation through hydrophobic associations. At 0.26 M NaCl; however, a rapid increase in apparent viscosity is observed above 0.10g/dL indicative of associative behavior. In 0.51 M NaCl, no further aggregation occurs above 0.10 g/dL. However, because the coil is further collapsed by the large excess of NaCl, apparent viscosity is lower than that of the polymer in 0.34 M NaCl. This also is clearly illustrated in the reduced viscosity plots for the NaAMB-5 polymer, where linear behavior is observed only for the 0.17 M NaCl solution. Above 0.17 M NaCl, η_{red} again increases nonlinearly indicating associative behavior (Figure 4b).

The NaAMB-25 terpolymer (Figures 5a and 5b) behaves in a different manner from NaAMB-5. The higher polymer charge-density results in a more expanded coil at low solution ionic strength. Initially, coil collapse due to ionic shielding occurs with increasing NaCl concentration followed by an increase in viscosity. The NaAMB-25 curve does not exhibit the maximum seen in the low-charge-density polymer system suggesting insufficient electrolyte to effectively reduce charge-charge repulsions. Reduced viscosity solution behavior is linear for the high-charge-density NaAMB-25 polymer up to a concentration of 0.15 g/dL. Above this concentration the polymers associate and η_{red} increases exponentially.

NaA Terpolymers

An initial decrease and the leveling of apparent viscosity with increasing ionic strength at high concentration is observed for NaA-5 (Figure 6a). The polymer has nonlinear reduced viscosity solution behavior at all ionic strengths (Figure 6b). The higher charge-density polymer (NaA-25) has low viscosity in low ionic strength solution and apparent viscosity rapidly increases with increasing salt solution to form gels with viscosities greater than 250 cP measured at 6/sec shear rate (Figure 7a). Similar behavior is seen in the η_{red} plot; viscosity increases even more rapidly at higher ionic strength (Figure 7b).

Comparison of the NaAMPS, NaAMB and NaA Terpolymers

NaAMPS terpolymers demonstrate associative behavior only at low-charge-densities and moderate-to-high ionic strength. However, the NaAMB and NaA terpolymers, apparent viscosity increases linearly with sample concentration up to a critical value of solution ionic strength. Above this NaCl molarity, the viscosity exponentially increases with polymer concentration indicative of intermolecular hydrophobic association. The salt concentration necessary for this transition is higher for the NaAMB polymer than for the NaA. It is also apparent that the terpolymers containing NaA have much higher viscosities than the other systems investigated.

Conceptual Models

At low ionic strength and high charge density, the electrostatic repulsive forces dominate the polymer solution behavior and all the polymers act as polyelectrolytes with similar viscosities. Armstrong and Strauss[24] have depicted a typical polyelectrolyte as an extended chain with the ionic atmosphere projecting out radially to a distance on the order of the Debye-Hückel shielding length (κ^{-1}) where for a 1:1 simple electrolyte $\kappa^{-1} = (0{,}304)/I^{1/2}$ (e.g. for a 0.1 M NaCl solution κ = 0.1 nm). The entire chain may be envisioned as enclosed by a tube with an average diameter of $2\kappa^{-1}$. Even in excess electrolyte, where the chain may form a random coil, the local geometry may be represented by the above model if the radius of curvature is greater than $2\kappa^{-1}$.

The presence of pendent C10AM hydrophobic groups along the polymer backbone apparently changes the aqueous solution behavior from that of a typical polyelectrolyte at higher ionic strengths; the nonpolar *n*-decyl groups are excluded from the polar environment[25] resulting in network formation. The onset value of interaction at low C* values has yet to be explained; however, Israelachvili *et al.*[26,27] and Pashley *et al.*[28] have demonstrated long range attractive interaction of crossed cylinders of hydrophobically modified mica surfaces. They reported attractive forces 10-100 times stronger than expected van der Waals forces over distances up to 10 nm. These forces decay exponentially with a force proportional to exp(-D/1.0) where D is equal to distance in nm.

In our terpolymer systems, as the charge density decreases and solution ionic strength increases, the electrostatic potential along the polymer chain decreases allowing long-range hydrophobic attractions well below that of C* for unmodified polyacrylamides[19,29]. Israelachvili has predicted aggregation for charged, hydrophobically-modified colloid particles where the Debye-Hückel parameter approaches the decay length of 1.0 nm for hydrophobic associations corresponding to a solution ionic strength for NaCl of 0.1M.[27] This is consistent with our finding that significant associative behavior occurs only at ionic strengths greater than or equal to 0.17 M NaCl.

Strauss *et al.* observed similar behavior with poly-4-vinylpyridine derivatives[30,31] hydrophobically modified with ethyl and dodecyl side chains. Low hydrophobic group incorporation resulted in polymers that displayed intermolecular association above C*; with increasing hydrophobic group incorporation, the polymers associated intramolecularly resulting in polysoaps. Above a critical polymer concentration, sufficient hydrophobic groups were present to associate either in an inter-or intramolecular fashion. The associations of bound hydrophobic groups were discussed in terms of a critical micelle concentration similar to that for small molecule surfactants. At low dodoecyl group incorporation, an insufficient number of hydrophobic groups are present on any individual polymer chain to form a stable ensemble. When a critical polymer concentration is reached, the polymer chains associate to form an intermolecular network in the aqueous system.

The association of polymer chains results in a rapid increase in apparent molecular weight (M_{app}). Below this critical molecular weight η_{app} and η_{red} increase in a linear fashion and reduced viscosity as a function of concentration may be plotted according to the Huggins equation[32]. Above a critical M_{app}, (M_c) viscosity increases exponentially instead of linearly[33] as seen by the increases in both apparent and reduced viscosity (Figures 2-7).

The terpolymers containing NaAMPS are the least affected by changing ionic strength, reflecting the insensitivity of the sulfonate anion. The carboxylate anions of NaAMB and NaA polymers on the other hand, show aggregation as ionic shielding causes collapse of the Debye-Hückel radius. The much higher viscosities of the NaA terpolymers may also be explained by the thickness of the Debye ionic layer. The NaAMB and NaAMPS mers are farther from the polymer backbone and may interfere with hydrophobic association more than the NaA mer. Additionally, the *gem*-dimethyl groups of the NaAMB and NaAMPS may have sufficient hydrophobic character to disrupt associations of the *n*-decyl groups into stable micelle like domains (Figure 8).

Conclusions

Associative polymers of acrylamide and n-decylacrylamide with sodium-3-acrylamido-3-methylbutanoate, sodium acrylate, or sodium-2-acrylamido-2-methylpropanesulfonate have been prepared by a micellar technique. The NaAMPS terpolymers display typical polyelectrolyte behavior at low solution ionic strength and high charge density. The sulfonate groups are not sufficiently shielded by the Na^+ counterions to prevent electrostatic repulsions and hydrophobic aggregation at charge densities of 25 mole percent. The NaAMB and NaA terpolymers exhibit associative properties at lower ionic strengths and higher charge densities due to hydrophobic associations among the decyl groups along the polymer chain as the Debye-Hückel reciprocal shielding length (κ^{-1}) is reduced to the order of the decay length for long-range hydrophobic interactions.

Distance of the ionic group from the backbone seems to influence hydrophobic association also. The NaAMB and NaAMPS monomers allow charged groups to extend out farther from the polymer backbone apparently preventing associations among the hydrophobic decyl groups at low solution ionic strengths and high polymer charge density. This is not observed for the NaA monomer with charge much closer to the backbone. As the polymer coils interact, a critical apparent molecular weight is reached and viscosity exponentially increases with increasing polymer concentration.

Although the goals of achieving facile dissolution of associative viscosifiers and understanding more fully the effects of ionic monomer composition on solution behavior have been realized, a number of significant problems remain unresolved. First, the precise composition of these n-alkyl type terpolymers is not determinable by current methods of analysis. Secondly, although preliminary data has been presented and discussed at major symposia, [17-18] the precise nature of micellar polymerization has not been elucidated, in particular sequence length of hydrophobic monomers produced by the method and its importance on macroscopic viscosity. Finally, molecular weight data for associative polymers, particularly those with blocky microstructures, is suspect since intermolecular associations during dissolution may not be completely disrupted. Therefore, comparisons can only be made (and then cautiously) on systems prepared under similar synthetic conditions. Each of these concerns will be addressed in subsequent papers in this series.[35]

References

1. McCormick, C. L.; Elliot, C. L.; Blackmon, K. P. *Macromolecules*, **1986**, 19, 1516.
2. McCormick, C. L.; Blackmon, K. P. *J. Macromol. Sci. (A), Chem.*, **1986**, 25, 1451.
3. McCormick, C. L.; Elliot, D. L. *J. Macromol. Sci. (A), Chem.*, **1986**, 23, 1469.
4. McCormick, C. L., Blackmon, K. P., *Polymer*, **1986**, 27, 1971.
5. McCormick, C. L.; Elliot, D. L.; Blackmon, K. P., *Polymer*, **1986**, 27, 1976.
6. McCormick, C. L.; Blackmon, K. P., *Angew. Makromol. Chem.*, **1986**, 144, 73.
7. McCormick, C. L.; Elliot, D. L.; Blackmon, K. P., *Angew. Makromol. Chem.*, **1986, 144**, 87.
8. McCormick, C. L.; Elliot, D. L.; *Polym. Sci., Polym. Chem. Ed.*, **1986**, A25, 1329.
9. McCormick, C. L.; Johnson, C. B. *Macromolecules*, **1988**, 21, 686.
10. McCormick, C. L.; Johnson, C. B. *Macromolecules*, **1988**, 21, 694.

11. Bikales, N. M. Ed. *Water-Soluble Polymers,* Plenum, New York, 1973.

12. Volk, H.; Friedrich, R. E. in *Handbook of Water-Soluble Gums and Resins,* Davidson, R. L. Ed., McGraw-Hill, New York, 1980; Chapter 16.

13. Finch, C. A. Ed. *Chemistry and Technology of Water-Soluble Polymers,* Plennum, New York, 1981.

14. Landoll, L. M. U. S. Patent 4 228 277, 1980.

15. Evani, S.; Carson, F. P. U.S. Patent 3 963 684, 1976.

16. Turner, S. R.; Siano, D. B.; Bock, J. U. S. Patent 4 520 182, 1985.

17. Shalaby, S. W., McCormick, Charles L., and Butler, G. B. *Water-Soluble Polymers,* ACS Symposium Series 467, American Chemical Society, Washington D.C. 1991.

18. Peer, W. J. "Polymerization of Hydrophobically Modified Polyacrylamide Chapter 20, 391-397. Valint, P.L.; Bock, J.; Schulz, D. M. "Synthesis and Characterization of Hydrophobically Associating Polymers" Chapter 21, 399-410 In Glass, J. E. Ed. *Polymers in Aquous Media*, Advances in Chemistry Series 223, Amer. Chem. Soc., Washington, D.C., 1989.

19. McCormick, C. L.; Johnson, C. B. *Polym. Mater. Sci. Eng.*, **1986**, 55, 366.

20. McCormick, C. L.; Johnson, C. B.;Tanaka, T. *Polymer*, **1988**, 29, 731.

21. McCormick, C. L.; Middleton, J. C. *Polym. Mater. Sci. Eng.*, **1987**, 57, 700.

22. McCormick, C. L.; Middleton, J. C.; Cummins, D. F. *Polym. Preprints*, 1989, 30(2), 348.

23. McCormick, C. L.; Blackmon, K. P. J. *Polym. Sci.; Part A; Polym. Chem.*, **1986**, 24, 2635.

24. Valint, P.L.; Bock, J.; Schultz, D. N. *Polym. Mat. Sci. Eng.*, **1987**, 57, 482.

25. Armstrong, R. W. Strauss, U. P. in *Encyclopedia of Polymer Science 1st Ed.*, Volume 10, p 731 John Wiley and Sons, New York, 1971.

26. Tanford, C. W. *The Hydrophobic Effect*, John Wiley and Sons, New York, 1973.

27. Israelachvili, J.; Pashley, R. *Nature*, **1982**, 300, 341.

28. Israelachvili, J.; Pashley, R. *J. Coll. Int. Sci.*, **1984**, 98(2), 500.

29. Pashley, R.; McGuiggan, P.M.; Ninham, B. W.; Evans, D. F., *Science,* **1985**, 229, 1088.

30. Klein, J.; Heitzmann, R. *Makromol. Chem.*, **1974**, 174, 1895.

31. Strauss, U. P.; Gershfeld, N. L. *J. Phys. Chem,* **1954**, 58, 747.

32. Strauss, U. P.; Gershfeld, N. L.; Crook, E. H. *J. Phys. Chem.*, **1956,** 60, 577.

33. Tanford, C. W. *Physical Chemistry of Macromolecules*, John Wiley and Sons, New York, 1961.

34. Klein, *J. Macromolecules,* **1978**, 11(5), 852.

35. McCormick, C. L.; Middleton, J. C. and Grady, C. E. "Water Soluble Co-Polymers 38: Synthesis and Characterization of Electrolyte Responsive Terpolymers of Acrylamdie, N-(4-Butyl)Penylacrylamide, and Sodium Acrylate, Sodium-2-Acrylamideo-2-Methylpropansulfonate or Sodium-3-Acrylamido-3-Methylbutanoate," submitted for publication 1991.

36. McCormick, C. L.; Ezzell, S. A. "Water-Soluble Copolymers. 39. Synthesis and Solution Properties of Associative Acrylamido Copolymers with Pyrensulfonamide Fluorescence Labels," Submitted for publication 1991.

37. McCormick, C. L.; Hoyle, C. E.; Creed, D.; Ezzell, S. A. "Water-Soluble Polymers 40. Photophysical Studies of the Solution Behavior of Associative Pyrenesulfonamide-Labelled Polyacrylamides," submitted for publication 1991.

Table 1

Copolymer Composition of C10AM Terpolymers
from Elemental Analysis Neglecting C10AM

	Feed Ratio	Elem. Analy.		Polymer Composition	
Sample	M_1:M_{2b}	%C	%N	Mol% AM	Mol% NaAMPS
NaAMPS-40[a]	59.5:40	39.39	10.12	68.8	31.2
NaAMPS-25	74.5:25	42.01	11.18	65.6	34.4
NaAMPS-10	89.5:10	45.17	14.37	83.7	16.3
NaAMPS- 5	94.5: 5	41.25	14.64	92.5	7.3
					NaAMB
NaAMB-40	59.5:40	48.90	12.34	67.0	33.0
NaAMB-25	74.5:25	45.67	12.80	76.9	23.1
NaAMB-10	89.5:10	48.80	16.17	89.6	10.4
NaAMB- 5	94.5: 5	45.85	16.09	93.9	6.1
					NaA
NaA-40	59.5:40	41.50	11.94	73.9	26.1
NaA-25	74.5:25	42.43	13.19	79.7	20.3
NaA-10	89.5:10	45.00	15.33	87.2	12.8
NaA- 5	94.5: 5	45.11	16.11	94.4	5.6

(a) feed composition of ionizable monomer
(b) M1 = AM; M2 = NaAMPS, NaAMB, or NaA

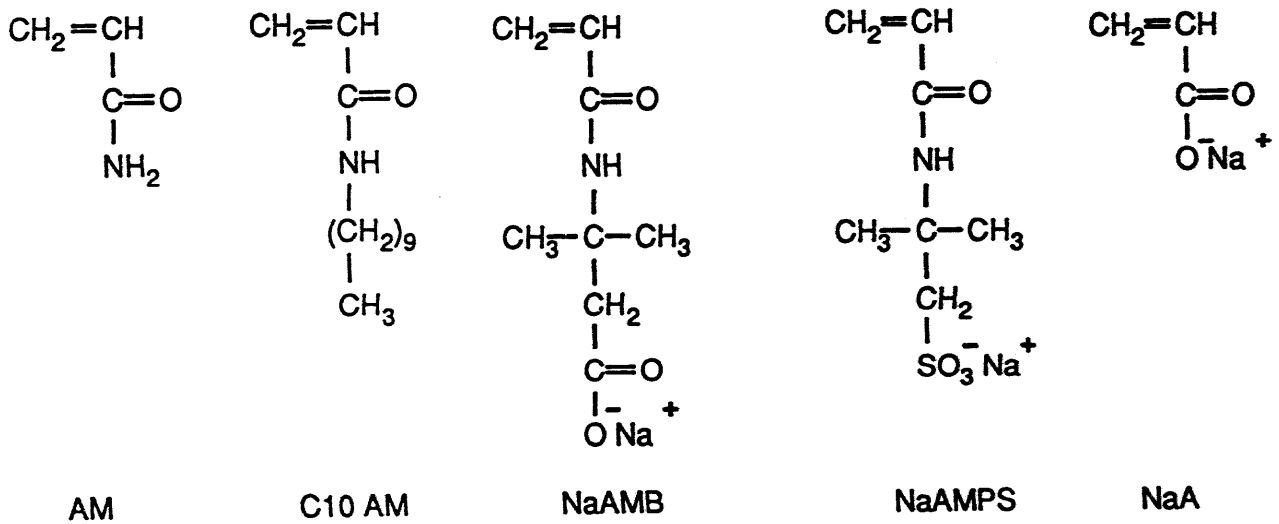

Figure 3-1 Structures of monomers used to prepare terpolymers

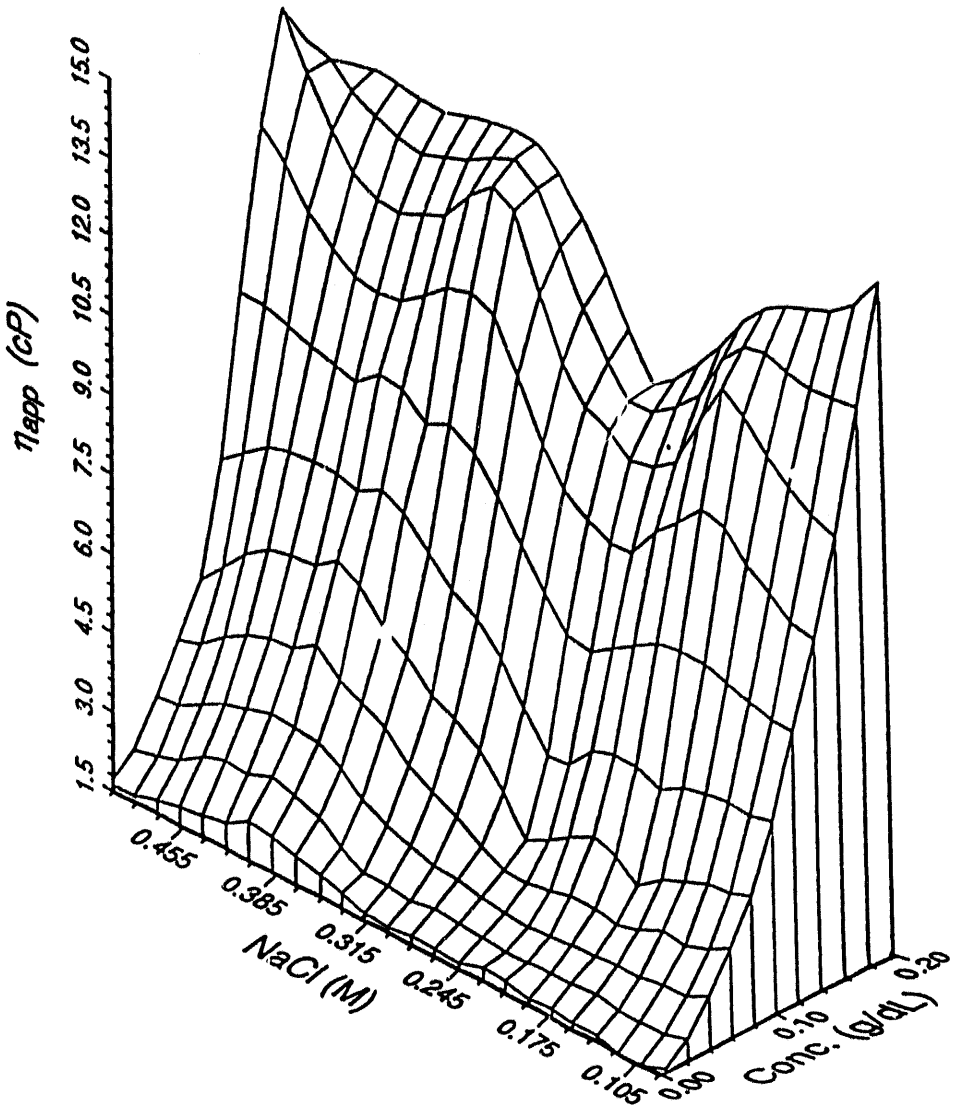

Figure 3-2a. η_{app} as a function of polymer concentration and solution ionic strength for the NaAMPS-5 terpolymer.

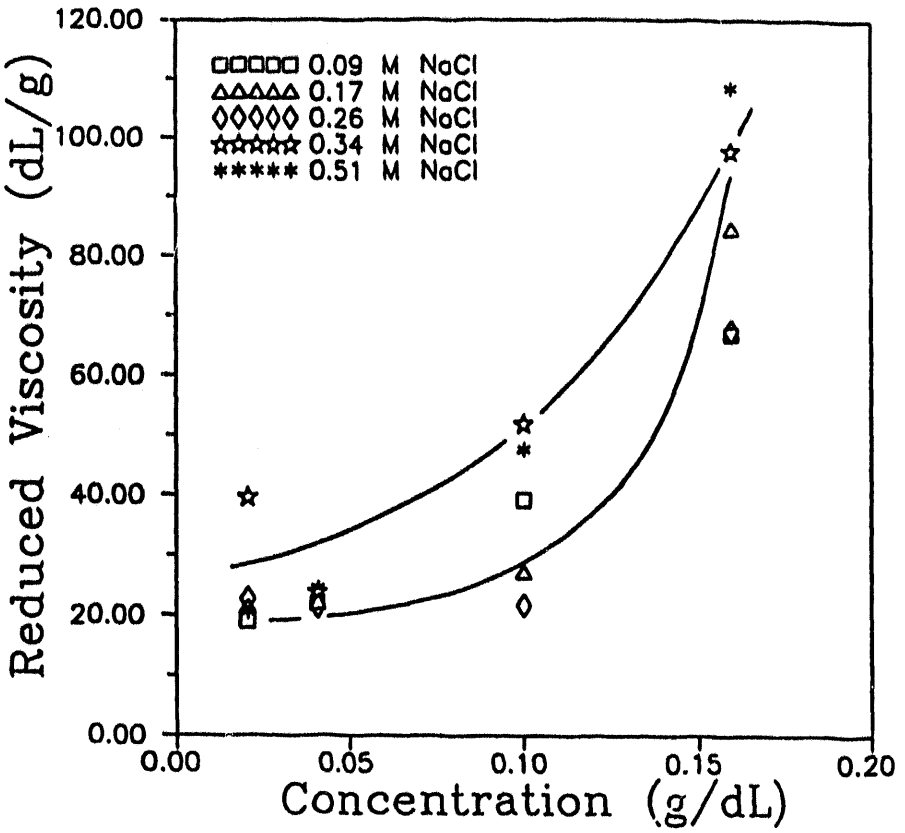

Figure 3-2b. η_{red} versus polymer concentration for the NaAMPS-5 terpolymer at 5 different solution ionic strengths.

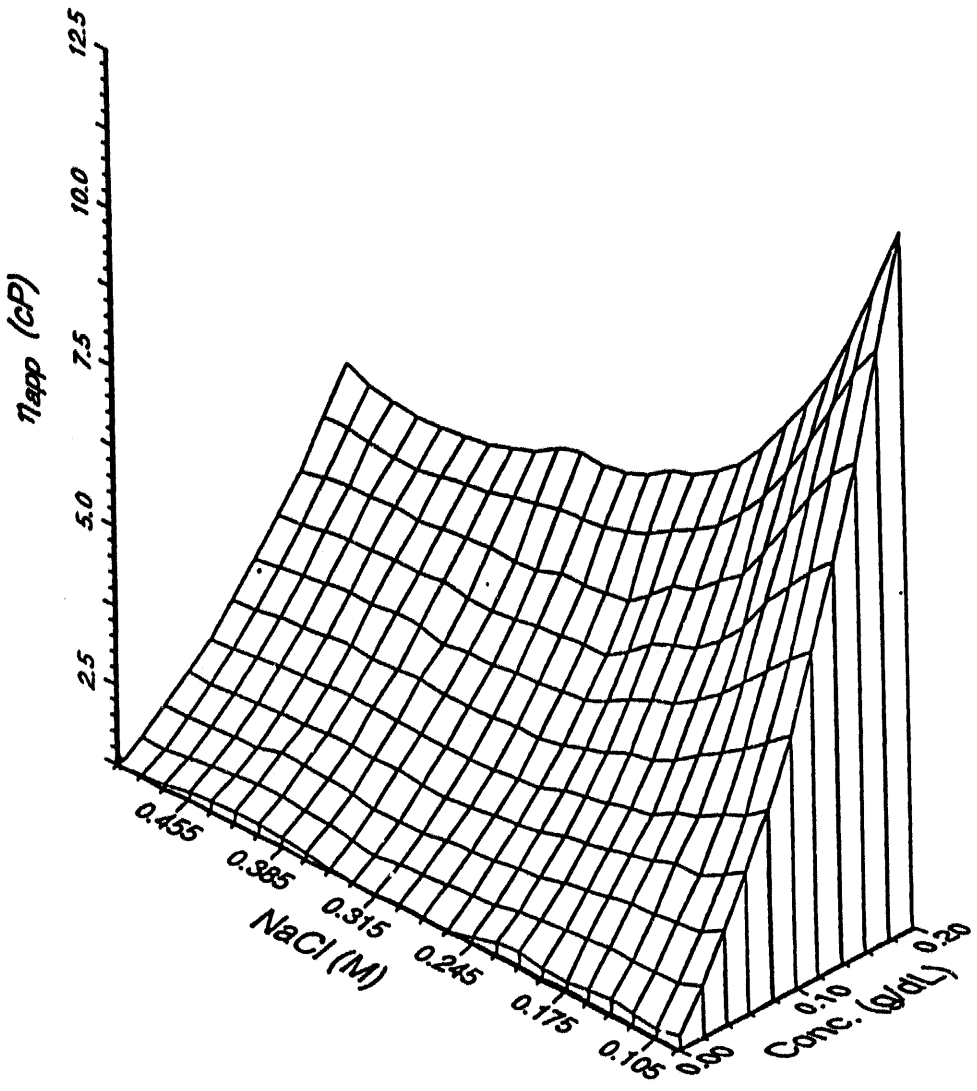

Figure 3-3a. η_{app} as a function of polymer concentration and solution ionic strength for the NaAMPS-25 terpolymer.

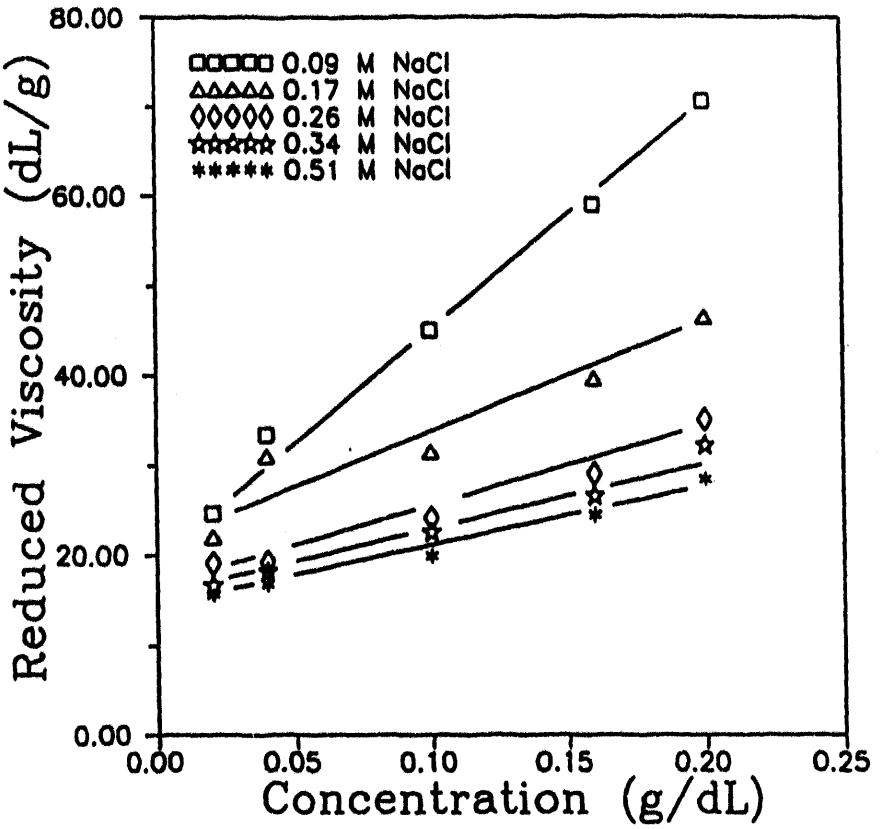

Figure 3-3b. η_{red} versus polymer concentration for the NaAMPS-25 terpolymer at 5 different solution ionic strengths.

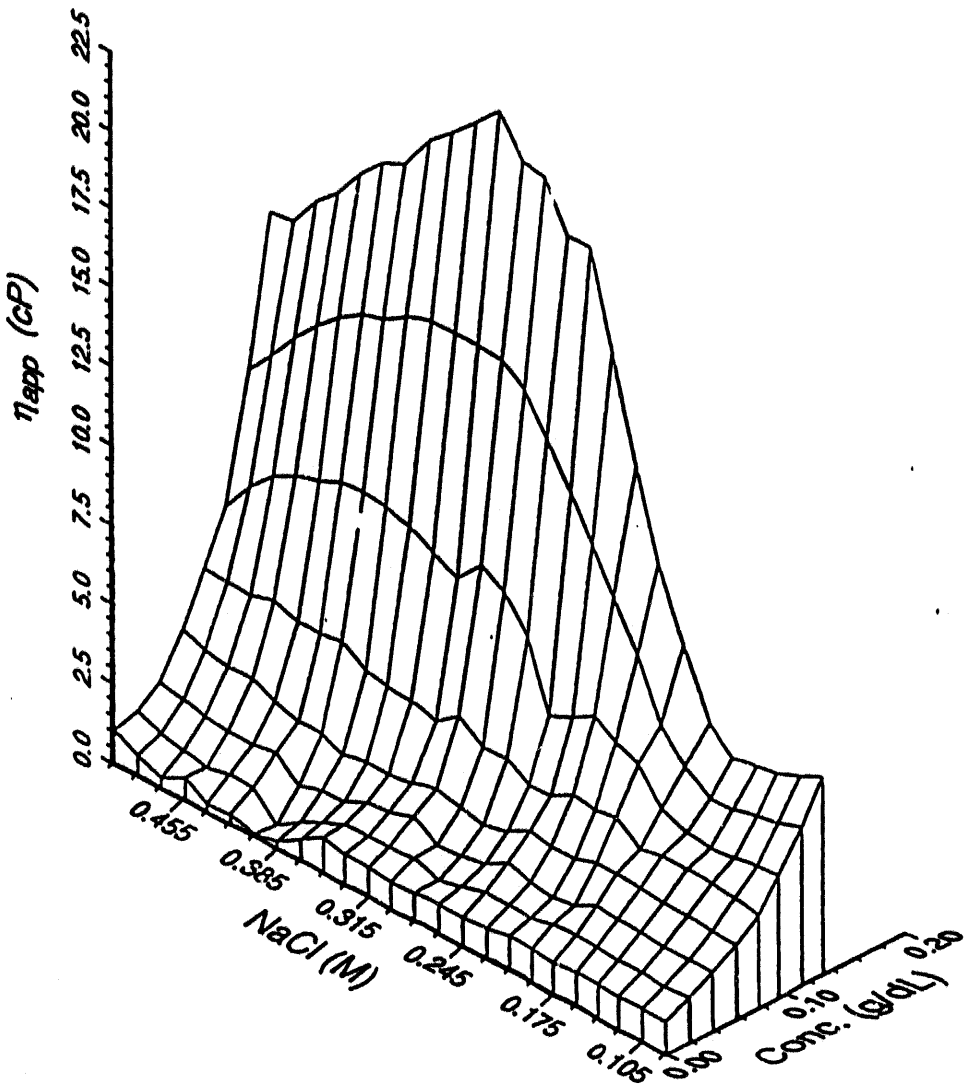

C10AM/NaAMB-5

Figure 3-4a η_{app} as a function of polymer concentration and solution ionic strength for the NaAMB-5 terpolymer.

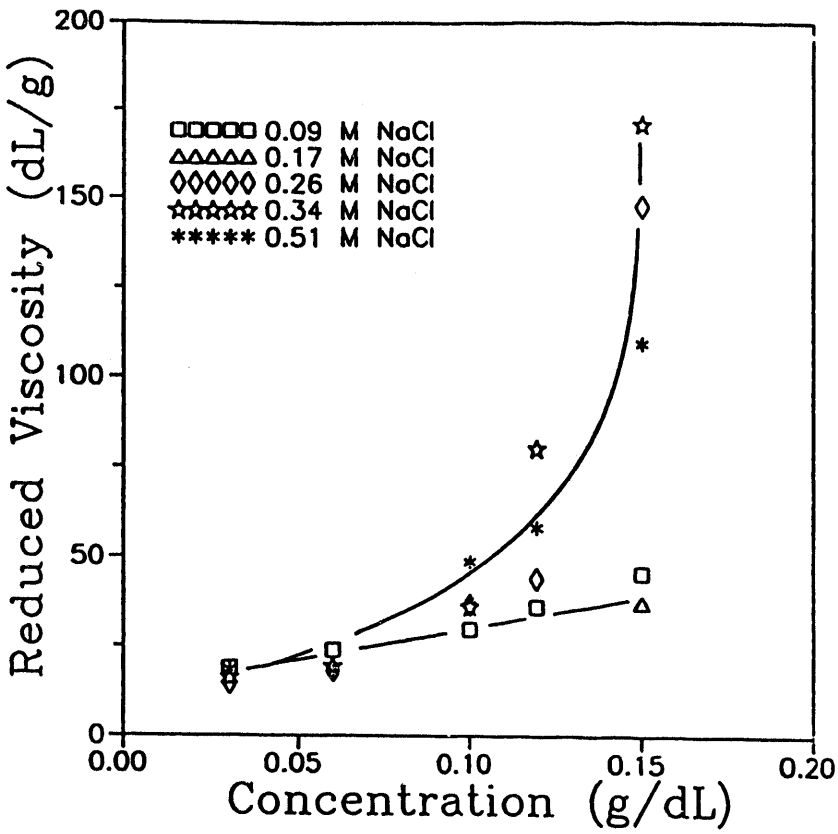

Figure 3-4b. η_{red} versus polymer concentration for the NaAMB-5 terpolymer at 5 different solution ionic strengths.

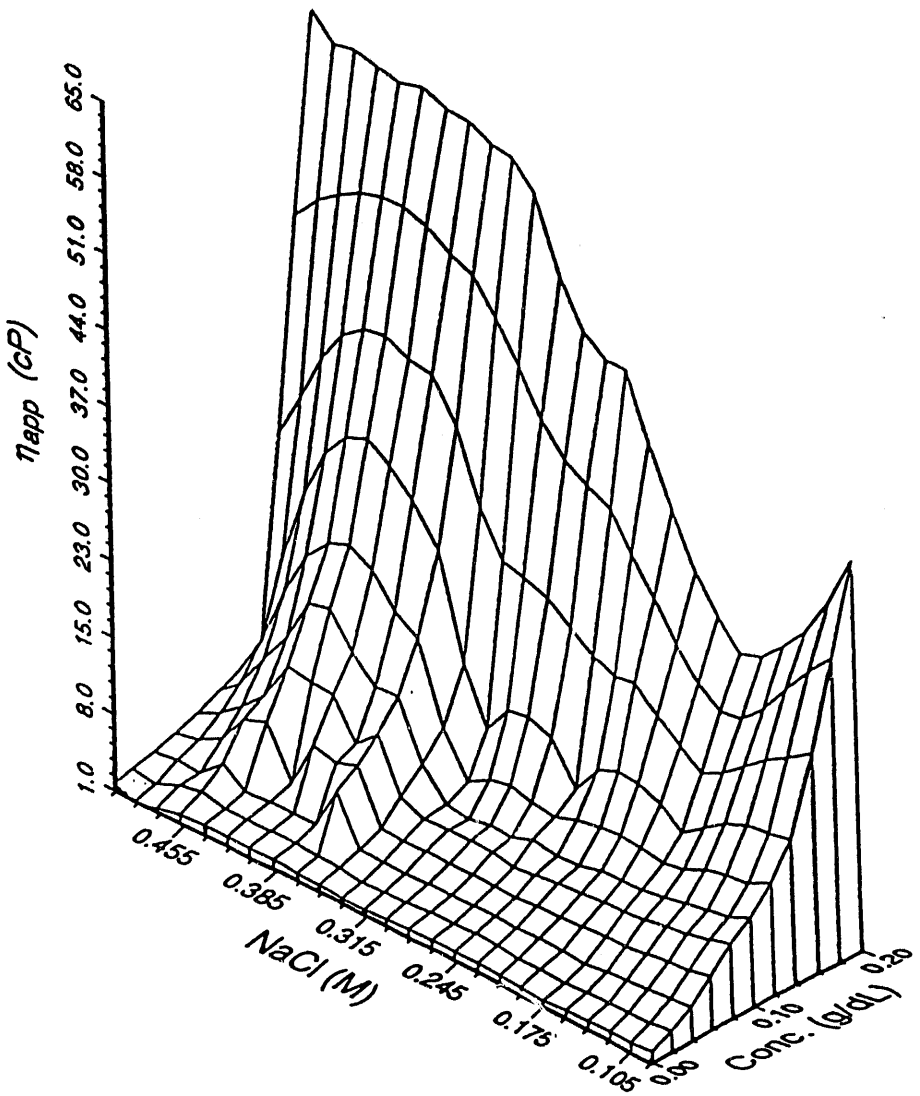

Figure 3-5a η_{app} as a function of polymer concentration and solution ionic strength for the NaAMP-25 terpolymer.

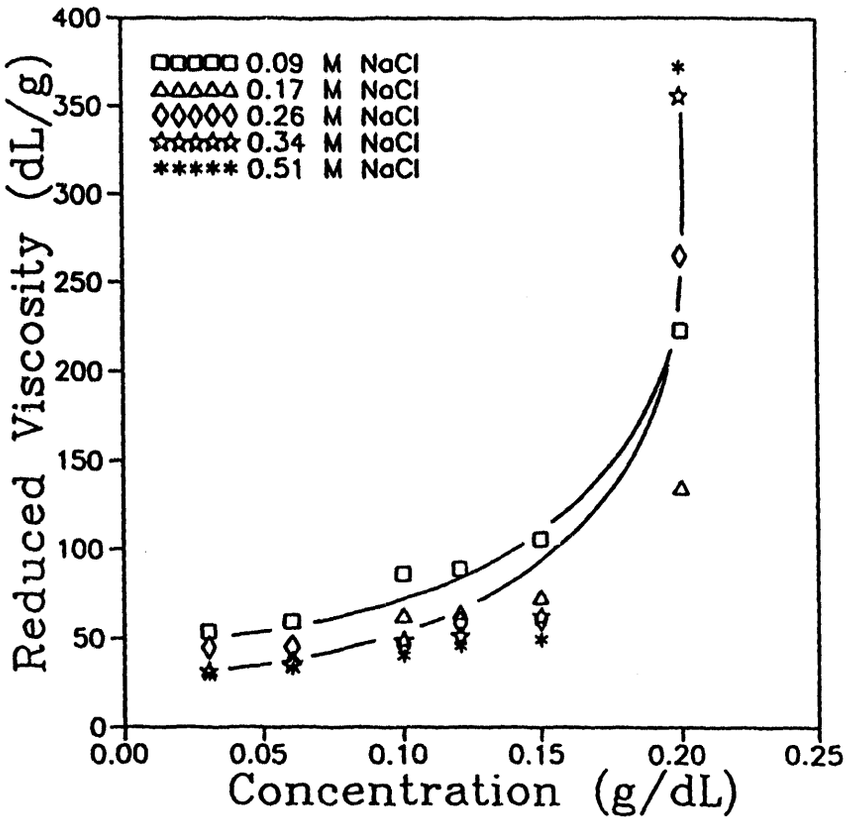

Figure 3-5b η_{red} versus polymer concentration for the NaAMP-25 terpolymer at 5 different solution ionic strengths.

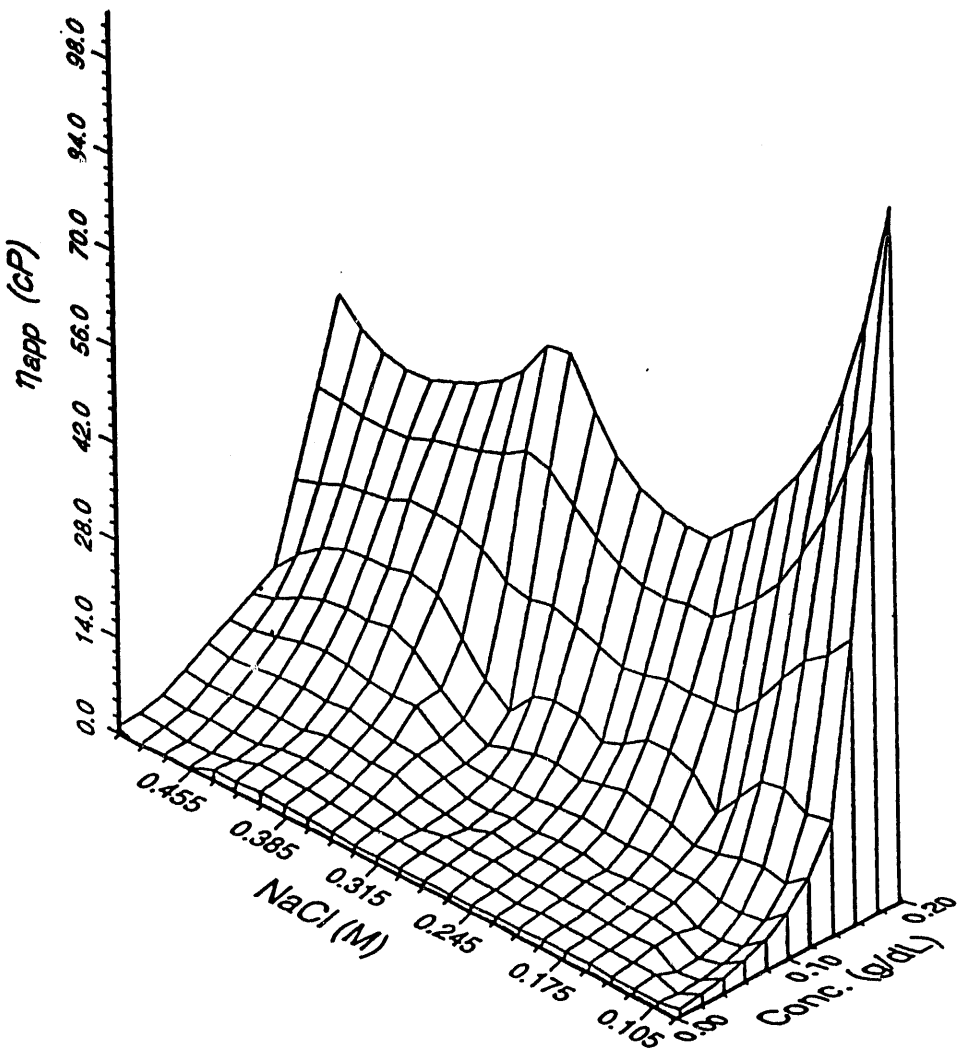

Figure 3-6a. $\tau_{|_{app}}$ as a function of polymer concentration and solution ionic strength for the NaA-5 terpolymer.

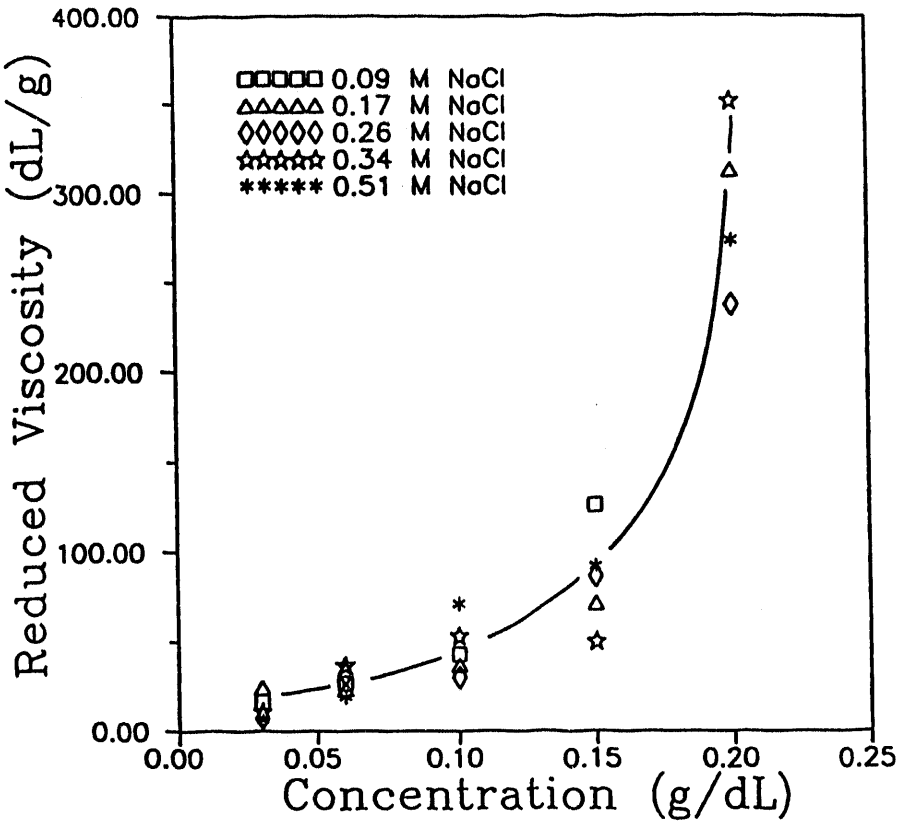

Figure 3-6b. η_{red} versus polymer concentration for the NaA-5 terpolymer at 5 different solution ionic strengths.

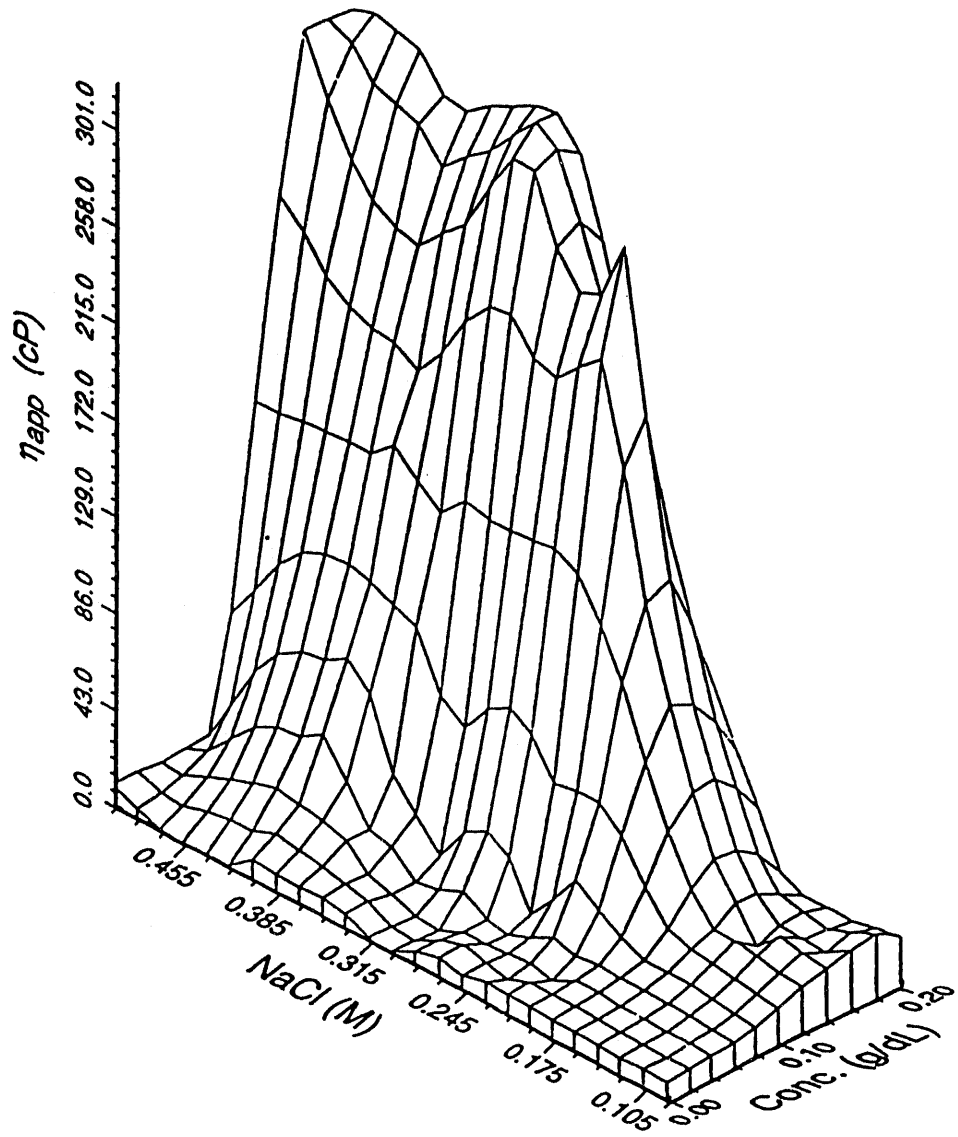

Figure 3-7a. η_{app} as a function of polymer concentration and solution ionic strength for the NaA-25 terpolymer.

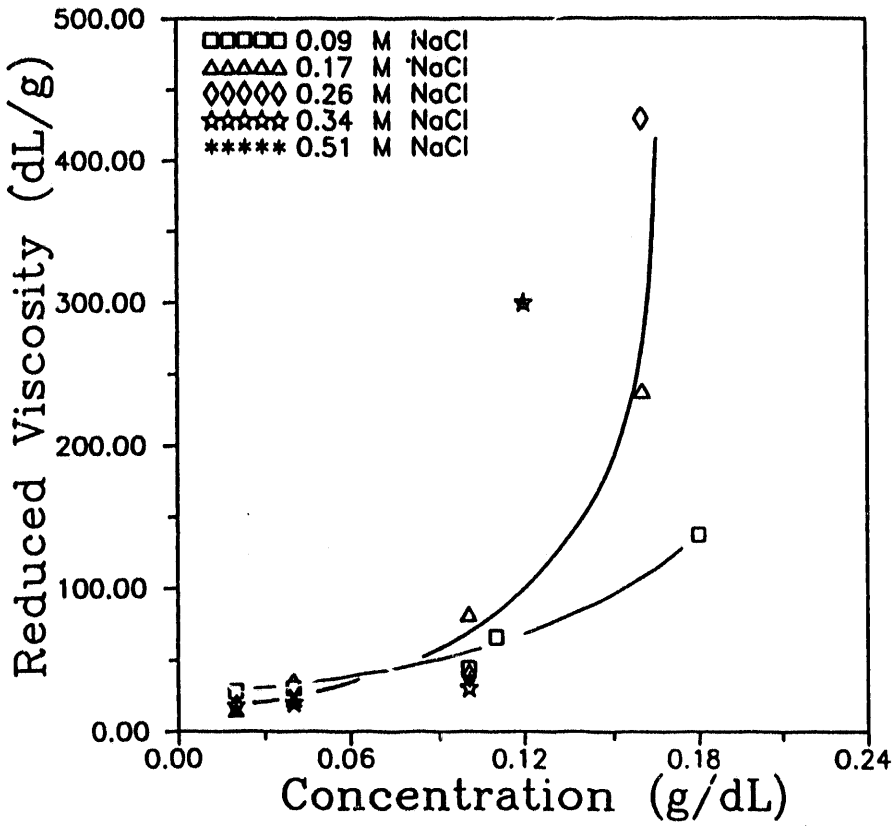

Figure 3-7b. η_{red} versus polymer concentration for the NaA-25 terpolymer at 5 different solution ionic strengths.

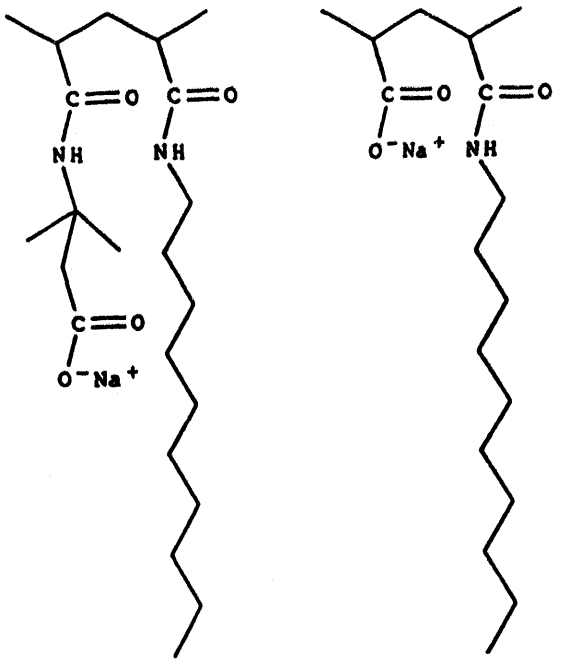

Figure 3-8 Schematic comparison of NaAMB terpolymer versus NaA terpolymer illustrates how hydrophobic associations might be disrupted by the more extended NaAMB ionic group resulting in less aggregation and lower viscosity.

CHAPTER FOUR: SYNTHESIS AND CHARACTERIZATION OF ELECTROLYTE RESPONSIVE TERPOLYMERS OF ACRYLAMIDE, N-(4-BUTYL)PHENYLACRYLAMIDE, AND SODIUM ACRYLATE, SODIUM-2-ACRYLAMIDO-2-METHYLPROPANESULFONATE OR SODIUM-3-ACRYLAMIDO-3-METHYLBUTANOATE

Abstract

Responsive associative terpolymers of acrylamide, 0.5 mole percent N-(4-butyl)phenylacrylamide and 5 and 25 mole percent of one of the following: sodium acrylate, sodium-2-acrylamido-2-methylpropanesulfonate, or sodium-3-acrylamido-3-methylbutanoate were synthesized by a micellar polymerization method. Terpolymer composition was determined by a combination of UV spectroscopy and elemental analysis. Solution properties were determined by low shear rheometry as functions of polymer concentration, solution ionic strength, pH and urea concentration. The carboxylate terpolymers demonstrate high viscosities in the presence of up to 0.5 M NaCl and 0.17 M $CaCl_2$, but lose much of their viscosity at low pH and high urea content. The sulfonate-containing terpolymers are less responsive at low pH and high electrolyte concentration then the carboxylate-containing terpolymers.

Introduction

Hydrophobically associating, water-soluble polymers are important in a number of areas including enhanced oil recovery, drag reduction, and for formulation in coatings and personal care items.[1-6] Intermolecular associations of the hydrophobic groups in aqueous solution result in network formation and a rapid increase in solution viscosity. Typically, less than two percent incorporation of the hydrophobic monomer into the polymer backbone is necessary to obtain associative behavior. This concentration is below the detection limit of standard techniques such as NMR or elemental analysis. Valint et al.[7-9] have overcome this difficulty by synthesizing N-aryl substituted acrylamides, including N-4(butyl)phenylacrylamide used in this report; these are easily detected by ultraviolet spectroscopy.

Research in our labs has concentrated on modified polyacrylamides to gain a fundamental understanding of hydrophobic associations and to develop structure-property relationships.[10-14] In this work we report the synthesis and solution properties of electrolyte-responsive terpolymers of acrylamide (AM) with N-(4-butyl)phenylacrylamide (BPAM) and one of the following ionic monomers: sodium acrylate (NaA), sodium-2-acrylamido-2-methylpropanesulfonate (NaAMPS), or sodium-3-acrylamido-3-methylbutanoate (NaAMB) (Figure 1). Comparisons may be made between the sulfonate group (NaAMPS) and the carboxylate moiety (NaAMB and NaA). In addition comparisons may be made between the two carboxylates where the NaAMB has a spacer group that decouples the charged group from the polymer backbone. Previously we reported structure-property relationships for similar terpolymers with the non chromophore containing N-decyl acrylamide monomer.[13-15] Hydrophobic group incorporation into a polyelectrolyte allowed the interaction of hydrophobic attractions and electrostatic charge-charge repulsions to be investigated.

Here the interaction of repulsive electrostatic and attractive, hydrophobic forces, both intra- and intermolecular are examined as functions of parameters such as pH, temperature, and polymer concentration. Importantly, precise compositions of the hydrophobic monomer can be determined in each study.

Experimental

Materials and Monomer Synthesis

All chemicals were obtained from Aldrich Chemical Company. Reagent grade solvents were used without further purification. Acrylamide (AM) was recrystallized twice from acetone, dried under vacuum, and stored in a desiccator (mp 81-84 °C). Acrylic acid (AA) was purified by vacuum distillation in the presence of cupric sulfate to remove inhibitor prior to use. 2-Acrylamido-2-methylpropanesulfonic acid (AMPS) was obtained from Fluka Chemical Co. and recrystallized twice from a mixture of methanol and 2-propanol.

3-Acrylamido-3-methylbutanoic acid (AMBA) was synthesized via a Ritter reaction using acrylonitrile and 3,3-dimethylacrylic acid in the presence of water and excess sulfuric acid. The procedure of Hoke and Robbins[16] was employed for the synthesis of AMBA.

N-(4-Butyl)phenylacrylamide (BPAM) was synthesized from the reaction of 4-butylaniline with acryloyl chloride with triethylamine as the acid receptor using the method described by Valint, Bock and Schulz.[7]. 4-Butylaniline was recovered as a clear liquid after vacuum distillation at 100 °C/6-9 mm Hg. The crude product (90% yield) was recrystallized from a mixture of acetone and cyclohexane at -5 °C and a white product was recovered (mp 101-102 °C). Anal.; FTIR (KBr): N-H 3290, C=C-H 3120, aliphatic CH_2, CH_3 2930 and 2860, C=O 1650, disubstituted aromatic 810 and 730 cm^{-1}. ^{13}C NMR ($CDCl_3$): δ 13.6 (CH_3), 22.0 (CH_3-$\underline{CH_2}$), 33.3 (CH_3-CH_2-$\underline{CH_2}$-), 34.8 (benzyl-CH_2), 120.1, 126.9, 135.2, 139.0 (aromatic CH) 128.5 (=CH), 131.2 (CH_2=), 163.0 (C=O).

The model compound of N-(4-butyl)phenylacrylamide, N-(4-butyl)phenylamidopropionic acid (BPAP), was synthesized in a one-step reaction of 4-butylaniline with succinic anhydride as follows. Distilled 4-butylaniline (0.01 mol) was dissolved in 75 mL of dichloromethane in a 250-mL flask equipped with a mechanical stirrer, thermometer, and addition funnel sealed with a drying tube. Succinic anhydride (0.01 mol) was dissolved in 100 mL of dichloromethane and added to the reaction mixture over 1 h at room temperature. A white precipitate formed and was filtered. The product was recrystallized from a mixture of acetone and hexane at -5 °C resulting in white crystals (mp 154-156 °C).

Polymer Synthesis

A micellar polymerization technique[4] was used to prepare terpolymers with monomer feeds of 0.5 mole percent of the BPAM and 5 and 25 mole percent AA, AMBA, or AMPS. The remaining polymer was composed of acrylamide (AM). The ionic surfactant, sodium dodecyl sulfate (SDS), is necessary to dissolve BPAM in the aqueous solution.

Each reaction was conducted in 500-mL, three necked, round-bottomed flasks equipped with mechanical stirrer, nitrogen inlet, and condenser. The appropriate amount of ionizable monomer was placed in 240 mL deionized water and the pH adjusted to 9 with NaOH pellets to form the water-soluble sodium salt (NaA, NaAMB, or NaAMPS). SDS surfactant (7.93 g; 2.8 x 10^{-2} mol) and 0.1117 g (5.5 x 10^{-4} mol) of BPAM hydrophobic monomer were then added respectively and stirred under N_2 until a clear solution was observed. The acrylamide monomer was then dissolved in this solution and heated to 50 °C with stirring. The water-soluble initiator, potassium persulfate (0.010 g; 3.7 x 10^{-5} mol) dissolved in 10 mL of deionized water, was added for a total water volume of 250 mL and a total monomer concentration of 0.44 M. The polymerizations were conducted for 4-6 hours followed by dilution of the polymer mixtures with equal amounts of water and precipitation into acetone. The polymers were washed extensively in acetone and then dried under vacuum for 24 hours.

Polymer Characterization

Polymer Purification.

After precipitation the polymers were dried and redissolved in deionized water. The samples were then dialyzed against deionized water through SpectraPor No. 4 dialysis tubing with a molecular weight cut off of 12-14000 daltons for a minimum of seven days. The purified samples were then lyophilized to a constant weight. Attempts to determine molecular weights by light scattering were unsuccessful due to the associative nature of the terpolymers. Homopolyacrylamide prepared under identical conditions yielded molecular weights of 1.0 to 1.5 x 10^6. Since all polymer series were prepared under identical conditions comparisons of solution behavior should be qualitatively valid.

Elemental Analysis.

Elemental analyses for carbon, hydrogen, and nitrogen of the terpolymers were conducted by M-H-W Laboratories of Phoenix, AZ. In addition, sulfur analysis of representative samples of polymers not containing a sulfur based monomer was performed to confirm the absence of residual surfactant.

UV Analysis.

Ultraviolet spectroscopy was used in determining polymer composition of those polymers containing monomers with chromophoric groups. All spectra were obtained in a Perkin-Elmer Lambda 6 Spectrometer. Beer's Law Plots were obtained at 250 nm for the water-soluble sodium salt of the model compound and compared with polymer absorbance. Polyacrylamide was used as a reference to remove any background absorbance.

Solution Rheology.

Stock solutions were prepared by dissolving the appropriate amount of salt in deionized water contained in volumetric flasks. The appropriate amount of dried polymer was weighed into a glass container and solvent added. Typical polymer concentrations were 0.2 g/dL. The polymers were dissolved by gentle shaking on an orbital shaker for 14 days to allow complete hydration before further dilutions of these stock solutions were made. Viscosity experiments were conducted on a thermostatically controlled Contraves LS 30 low shear rheometer.

Compositional Calculations.

Polymer compositions were determined using a combination of UV spectroscopy and elemental analysis. The concentration of BPAM was determined directly from a Beer's law plot in mol/L. For terpolymers, three variables and two equations were used where variable C represents the moles of BPAM in 100 g of polymer determined from UV, A the moles of ionic monomer in 100 g of polymer, and B the moles of AM in 100 g of polymer as determined from matrix algebra. The coefficients are the number of carbons and nitrogens in each monomer. After determining A and B (with C known from UV) for each polymer sample, mole percent compositional data were calculated to determine the relative abundance of each of the monomers. Equations (1) through (5) were used for BPAM/NaAMPS where A is NaAMPS and B is AM.

$$\% \text{ C}/12.01 = 7A + 3B + 13C \quad (1)$$
$$\% \text{ N}/14.01 = 1A + 1B + 1C \quad (2)$$
$$\text{Mole } \% \text{ NaAMPS} = 100A/(A + B + C) \quad (3)$$
$$\text{Mole } \% \text{ AM} = 100B/(A + B + C) \quad (4)$$
$$\text{Mole } \% \text{ BPAM} = 100C/(A + B + C) \quad (5)$$

Similar equations [(6) through (10)] were used to determine terpolymer compositions for the BPAM/NaAMB series where A, B, and C are NaAMB, AM, and BPAM respectively.

$$\% \text{ C}/12.01 = 8A + 3B + 13C \quad (6)$$
$$\% \text{ N}/14.01 = 1A + 1B + 1C \quad (7)$$
$$\text{Mole } \% \text{ NaAMB} = 100A/(A + B + C) \quad (8)$$
$$\text{Mole } \% \text{ AM} = 100B/(A + B + C) \quad (9)$$
$$\text{Mole } \% \text{ BPAM} = 100C/(A + B + C) \quad (10)$$

Equations (11) through (15) were used to determine terpolymer compositions for the BPAM/NaA series. A, B, and C represent monomers NaA, AM, and BPAM respectively.

$$\% \text{ C}/12.01 = 3A + 3B + 13C \quad (11)$$
$$\% \text{ N}/14.01 = 0A + 1B + 1C \quad (12)$$
$$\text{Mole } \% \text{ NaA} = 100A/(A + B + C) \quad (13)$$
$$\text{Mole } \% \text{ AM} = 100B/(A + B + C) \quad (14)$$
$$\text{Mole } \% \text{ BPAM} = 100C/(A + B + C) \quad (15)$$

Results and Discussion

Previous work in our laboratory has led to successful preparation of hydrophobically modified polyelectrolyte terpolymers with pH-and salt- responsive viscometric behavior.[15] However, we were concerned with the inability to absolutely quantify the decylacrylamide content. However the introduction of the phenyl moiety into the hydrophobic monomer reported by Valint, Bock, and Schulz[7] allowed us to substitute BPAM for decylacrylamide. The resulting terpolymers had similar properties to those prepared previously,[15] but importantly, compositions could be successfully determined by a combination of elemental analysis and ultraviolet spectroscopy. Terpolymers containing 5 and 25 mole percent ionic monomer in the feed were prepared to represent low-charge

density and high-charge density polymers, respectively. The hydrophobic group was incorporated into the polymer at approximately 0.5 mol% via the micellar polymerization and the remaining backbone was composed of acrylamide. Monomer structures are shown in Figure 1.

Ionic strength of the terpolymer solutions was varied from 0.01 to 0.5 to evaluate the effects on polymer rheology. The effects of the divalent cation Ca^{2+} were also investigated in 0.17 M $CaCl_2$ (ionic strength of 0.5). The effects of urea, a water structure breaker which interferes with hydrophobic associations, and pH were also evaluated.

Compositional analysis

Compositional data (Table I) indicate agreement between the feed ratios and copolymer composition for the acrylamide and ionic comonomer, but hydrophobic monomer incorporation decreases as much as 50% with increasing ionic group incorporation. Analogous nonionic copolymers were reported to result in BPAM monomer incorporation greater than 85% of the feed ratio[7,14]; therefore, the introduction of charged groups into the backbone must interfere with hydrophobic group incorporation. The growing polymer chain bearing anionic charge groups is less likely to interact with the anionically charged surface of the micelle where the hydrophobic monomer is solubilized. This also implies that the hydrophobic monomers are less likely to have a charged group as a nearest neighbor. Parallel studies in our research group support a somewhat blocky incorporation of hydrophobic monomers at low surfactant/monomer ratios.

Solution properties of BPAM terpolymers

Effect of ionic strength

Three dimensional plots can be used to topologically show relationships among apparent viscosity, terpolymer concentrations, and ionic strength. For simplicity we have also plotted reduced viscosity for each polymer as a function of ionic strength in the traditional manner. Polymer concentration varies from 0.04 to 0.20 g/dL and NaCl concentrations 0.01, 0.05, 0.10, and 0.50 M NaCl. When gels with viscosities greater than the upper range of the Contraves (operating at 25 °C and a shear rate of 6 s-1) were formed, an upper limit of 250 cP is placed on the graphs.

The BPAM/NaAMPS-5 polymer has a high viscosity at low ionic strength typical of polyelectrolytes. However unlike traditional polyelectrolytes which completely lose hydrodynamic volume with added electrolyte, this terpolymer above the overlap concentration (C*) maintain viscosity due to intermolecular hydrophobic associations (Figure 2). Gel formation occurs at concentrations above 0.16 g/dL at all ionic strengths investigated.

The BPAM/NaAMPS-25 polymer has higher apparent viscosity than the low-charge density analogs at concentrations below C*. Above C*, however the low-charge density polymers have higher viscosities (Figure 3).

The BPAM/NaAMB-5 polymer has behavior similar to that of the BPAM/NaAMPS-5 terpolymer. Viscosity is maintained with increasing ionic strength above C* (Figure 4). The BPAM/NaAMB-25 terpolymer behaves like a typical polyelectrolyte (Figure 5), while the

BPAM/NaA-5 terpolymer behaves in a fashion similar to the other low-charge density polymers (Figure 6). The BPAM/NaA-25 (Figure 7) also has a higher η_{sp} viscosity at low polymer concentration and a lower viscosity above C* than its low-charge density analogs.

The low-charge density terpolymers have lower viscosities below the overlap concentration (C*) and higher viscosities above C* than the high-charge density systems. Below C* the ionic forces determine the solution behavior, but above C* the hydrophobic interactions dominate the solution rheology. Below C*, the increase in charge density from 5 to 25 mole percent results in polymers with larger hydrodynamic volumes. Above C*, where viscosity enhancement is due to interpolymer associations, the low-charge density, charge-charge repulsions act to expand the polymer coil and to enhance water solubility; however, these are not sufficient to disrupt hydrophobic interactions. Higher charge densities both reduce the amount of hydrophobic group incorporated during polymerization and disrupt hydrophobic interactions.

The BPAM/NaAMPS-25 terpolymer (Figure 3) contains one-third less hydrophobic monomer than the BPAM/NaAMB-25 polymer (Figure 5), yet has a much higher viscosity at higher salt concentrations. This indicates that the polyelectrolyte and hydrophobic interactions are acting in concert and that microstructural placement of the hydrophobic groups is as important as the hydrophobic monomer concentration. The soft NaAMPS anions are less affected by solvent ionic strength and therefore the polymer retains a higher viscosity in salt solutions. The NaAMB charged group repulsions are effectively shielded by the counterions (site binding) resulting in a loss of hydrodynamic volume. The BPAM/NaA terpolymers (Figures 6 and 7) maintain high viscosity at all ionic strengths. The proximity of the charged group to the backbone may result in less hydrophobic disruption, although some reduction in viscosity above C* is also seen by increasing charge density in these systems.

Viscosity plots also illustrate that the high-charge-density NaAMPS and NaAMB polymers possess higher viscosities at low concentration; however, the low-charge-density polymers associate efficiently at concentrations between 0.08 and 0.12 g/dl resulting in a rapid rise in the η_{sp} vs concentration plot. The NaA containing polymers are qualitatively different in that the high-charge-density systems maintain higher viscosity up to a limiting ionic strength.

Effects of calcium salt

The effect of calcium salt addition is demonstrated for the BPAM/NaAMPS-5 (Figure 8) and BPAM/NaAMB-5 (Figure 9) solutions. As might be expected, the Ca^{2+} ion causes greater reduction in hydrodynamic volume than the Na^{1+} ion. Although phase separation often occurs in some polyelectrolyte systems, these low charge density copolymers retain solubility and high reduced viscosities up to concentrations of 0.2 g/dl. At higher terpolymer concentrations gellation occurs.

Effects of urea

Reduced viscosity was evaluated as a function of added urea, reported to be a disrupter of hydrophobic interactions. Reduced viscosity was measured at 0.5 (Figure 10) and 0.01 M NaCl (Figure 11) in 0, 1, 3, 5, and 7 M urea at a solution concentration of 0.1 g/dL. The low-charge-density polymers BPAM/NaAMPS-5, BPAM/NaAMB-5, and BPAM/NaA-5 were selected because they appear to have the most numerous hydrophobic associations. A tenfold decrease in reduced

viscosity was observed while increasing urea concentration from 0 to 7 M urea at low ionic strength for the BPAM/NaAMB system; the least drop in viscosity was observed for the BPAM/NaA polymers. In 0.5 M NaCl, the viscosity decrease is much less pronounced for BPAM/NaAMB (55 to 30 dL/g) with increasing urea concentration (0 to 3 M). At both ionic strengths in 7 M urea, the viscosities of the terpolymers decrease to approximately the value of their analogous, unmodified copolymers. The urea clearly disrupts the hydrophobic interactions, resulting in deaggregation of the polymer network. The large apparent molecular weight resulting from the interaction of several polymer chains decreases to that of the unmodified coil in solution.

Conclusions

Terpolymers of BPAM, AM, and anionic monomers NaA, NaAMPS, and NaAMB were prepared by a micellar polymerization method and characterized utilizing elemental analysis and ultraviolet spectroscopy. UV comparisons of the model compound BPAP with the terpolymers allowed direct analysis of hydrophobe content.

The low-charge density polymers exhibit lower viscosities below C* and higher viscosities above C* than their high-charge-density analogs. All of the low-charge-density polymers formed gels at concentrations of 0.20 g/dL. Below C*, the electrostatic repulsions dominate solution behavior and the polymers with the most ionic monomer content have larger hydrodynamic volumes. Above C* interpolymer aggregation and network formation is responsible for the large apparent viscosities. The low-charge-density polymers have the higher viscosities above C* due to less electrostatic interference from charge-charge repulsions resulting in more hydrophobic association.

The order of the high-charge-density systems with the most efficient aggregation and therefore highest viscosities at a given concentration and ionic strength is BPAM/NaA > BPAM/NaAMPS > BPAM/NaAMB. The presence of ionic groups adjacent to hydrophobic groups may result in a disruption of the hydrophobic effect through water restructuring. If runs of acrylamide separate the ionic groups from the hydrophobic blocks, synergistic effects might be observed where the electrostatic repulsions can result in chain expansion and the hydrophobic groups may also maintain interpolymer associations. In this instance the NaAMPS terpolymers are less shielded by counterions and maintain larger hydrodynamic volumes than NaAMB terpolymers which collapse with increasing ionic strength.

The reduced viscosities of the systems are sensitive to pH. The viscosities show a maximum at pH 7-8. At low pH values, the charged groups are neutralized and the coil collapses, except for the NaAMPS containing polymers. At high pH the presence of excess counterions reduces electrostatic repulsions and results in a slight decrease in viscosity.

Reduced viscosity decreases measurably with increasing urea content. Urea interferes with hydrophobic interactions and reduces the intermolecular associations. In 7 M urea the associative polymers approach viscosities similar to those of unmodified analogs.

The difficulty of determining precise molecular weights due to polymer associations in dilute solution continues to be a major obstacle. Additionally the mechanism of the micellar polymerization

and evidence for block hydrophobic runs at low hydrophobic monomer feed ratios are being investigated.

References

1. McCormick, C.L.; Schulz, D.N.; Bock, J. *Encyclopedia of Polymer Science and Engineering*, 1989, 730-784.

2. Landoll, L. M. U.S. Patent 4 228 277, 1980.

3. Landoll, L. M. U.S. Patent 4 243 802, 1981.

4. Turner, S. R.; Siano, D. B.; Bock, J. U.S. Patent 4 520 187, 1985.

5. Evani, S. U.S. Patent 4 432 881, 1984.

6. Hoy, K. L.; Hoy, R. C. U.S. Patent 4 426 485, 1984.

7. Valint, Jr., P. L.; Bock, J. and Schulz, D. *Polym. Mat. Sci. Eng. Preprints*, **1987**, 57, 482.

8. Siano, D. B.; Bock, J.; Myer, P.; and Valint, Jr., P. L. *Polymers in Aqueous Media, Performance Trough Association*, 1989, 425-435.

9. Valint, Jr., P. L.; Bock, J.; Ogletree, J.; Zushma, S.; Pace, S. J. *Polym. Preprints*, 1990, 31(2), 67.

10. McCormick, C. L.; Johnson, C. B. *Polym. Mater. Sci. Eng.*, **1986**, 55, 366.

11. McCormick, C. L.; Johnson, C. B.; Tanaka, T *Polymer*, **1988**, 29, 731.

12. Johnson, C. B. *Ph.D. Dissertation*, University of Southern Mississippi, May 1987.

13. McCormick, C. L.; Middleton, J. C.; and Cummis, D. *Polymer Preprints*, *30(2)*, 348 (1989).

14. Middleton, J. C. *Ph. D. Dissertation*, University of Southern Mississippi, December 1990.

15. McCormick, Charles L.; Middleton, J. C.; and Cummins, D. F. submitted for publication (1990).

16. Hoke, D.; Robins, R. *J. Polym. Sci.*, **1972**, 10, 3311.

17. Ezzell, S. *Ph.D. Dissertation*, University of Southern Mississippi, December 1990.

Table I

BPAM Terpolymer Compositional Data from UV and Elemental Analysis

Sample No.	M1:M2:M3[a]	%C	%N	UV[b] x10^3	AM mol%	NaAMB mol%	BPAM mol%
BPAM/NaAMB-5	95: 5:0.5	47.51	16.54	5.32	93.4	6.2	0.45
BPAM/NaAMB-25	75:25:0.5	49.39	12.86	3.41	70.8	28.9	0.37
						NaAMPS	
BPAM/NaAMPS-5	95: 5:0.5	46.46	46.16	5.26	91.8	7.7	0.46
BPAM/NaAMPS-25	75:25:0.5	40.45	11.59	2.09	73.5	26.2	0.25
						NaA	
BPAM/NaA-5	95: 5:0.5	44.18	15.42	5.47	90.7	10.5	0.45
BPAM/NaA-25	95:25:0.5	41.80	11.76	2.99	72.7	27.1	0.26

(a) M1-acrylamide; M2-ionic group NaAMB, NaAMPS, NaA; M3-BPAM feed compositions
(b) UV absorbance scanned at 250 nm
(c) from UV determination

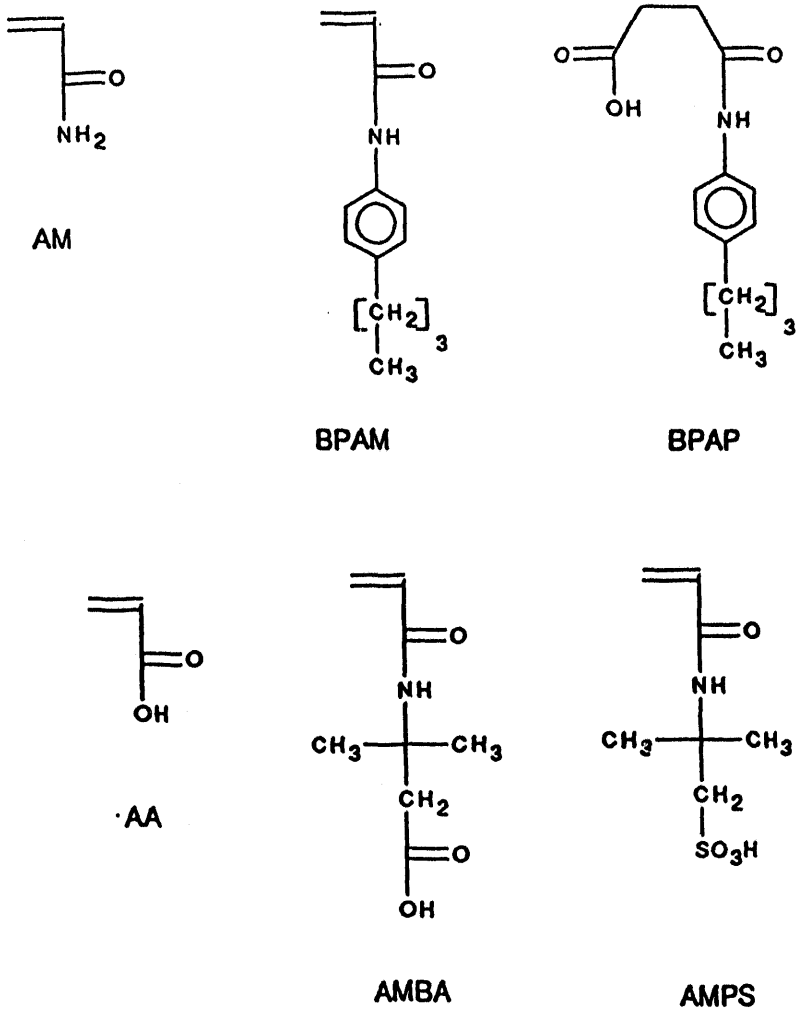

Figure 4-1. Monomers used in polymer synthesis and BPAM model compound.

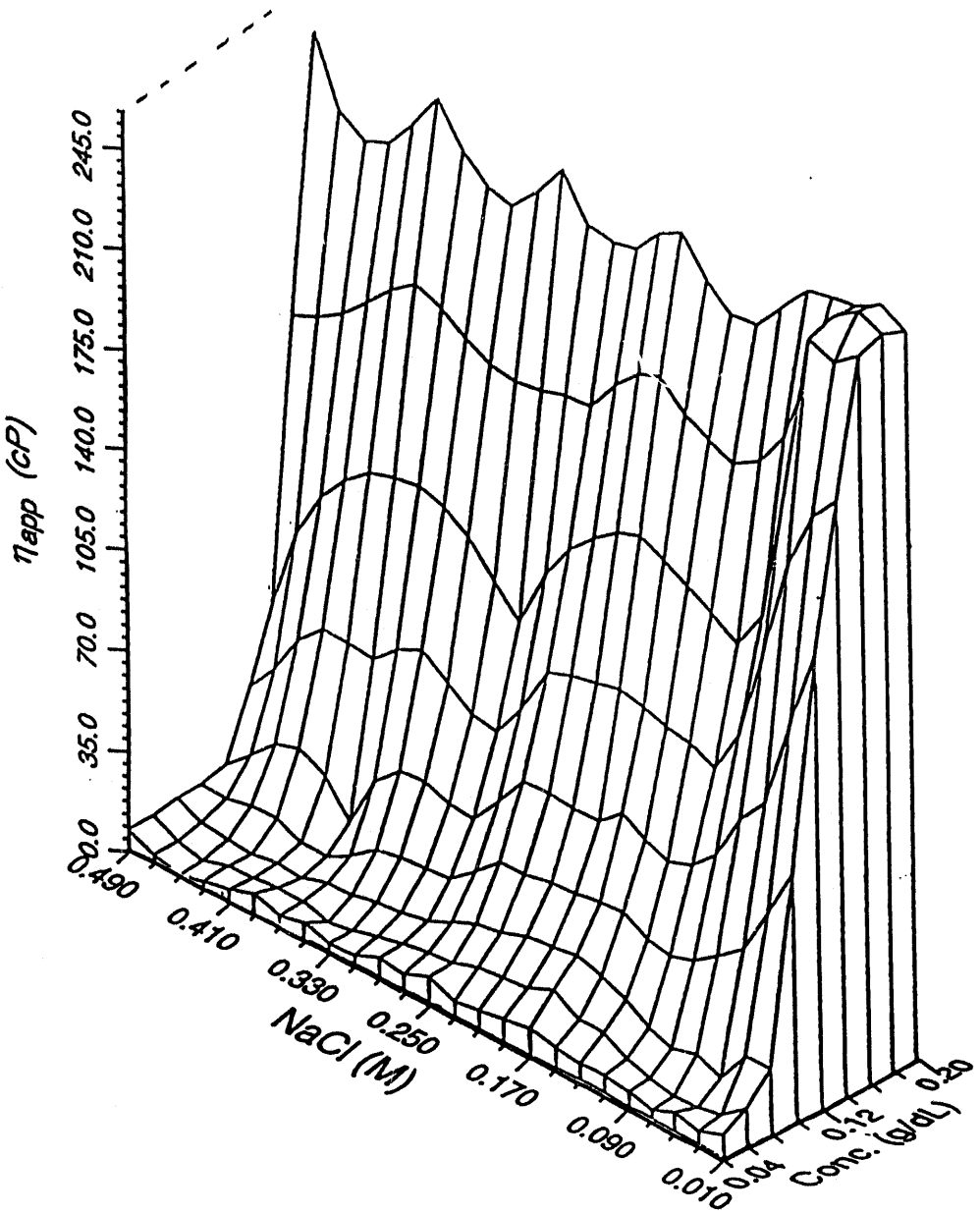

Figure 4-2. η_{app} as a function of polymer concentration and solution ionic strength for the BPAM/NaAMPS-5 terpolymer.

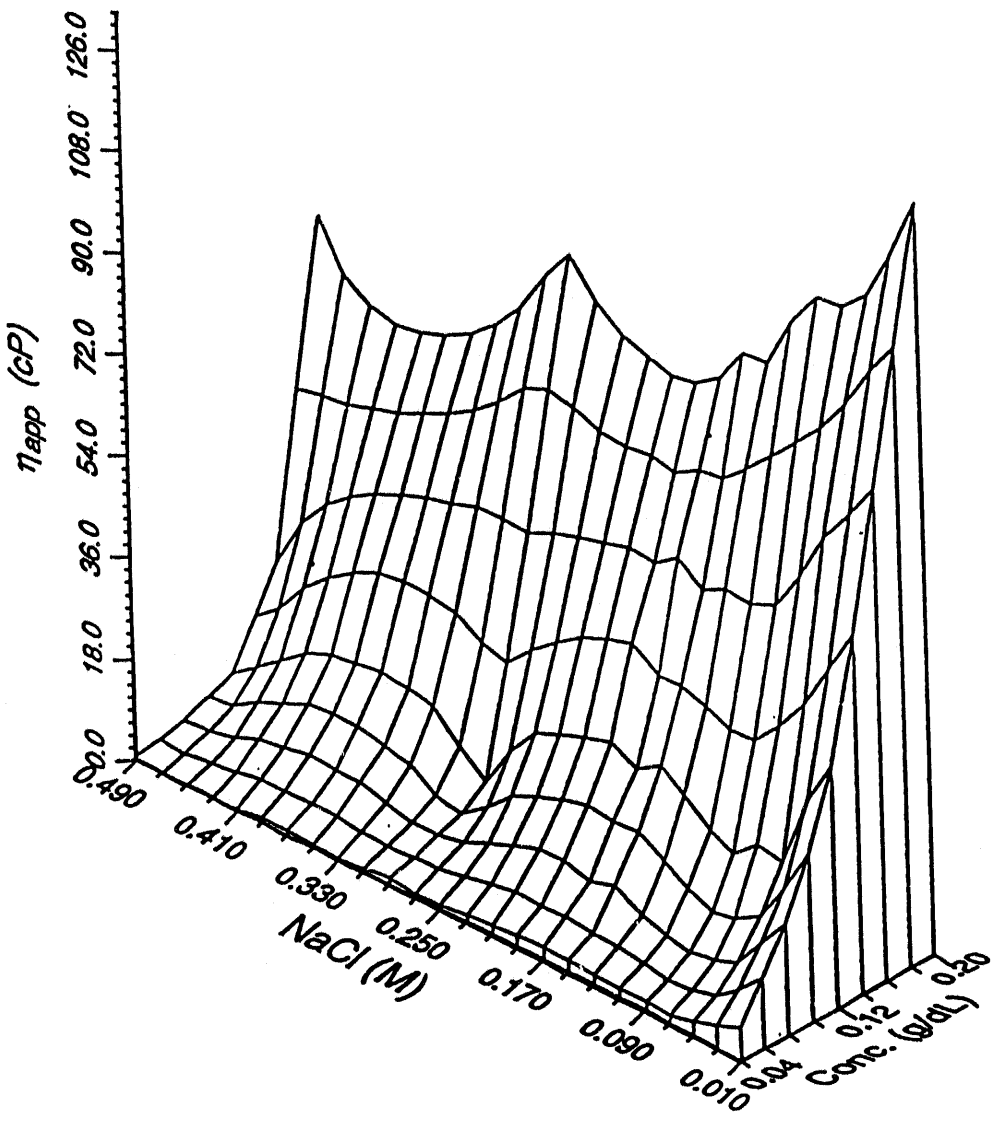

Figure 4-3. η_{app} as a function of polymer concentration and solution ionic strength for the BPAM/NaAMPS-25 terpolymer.

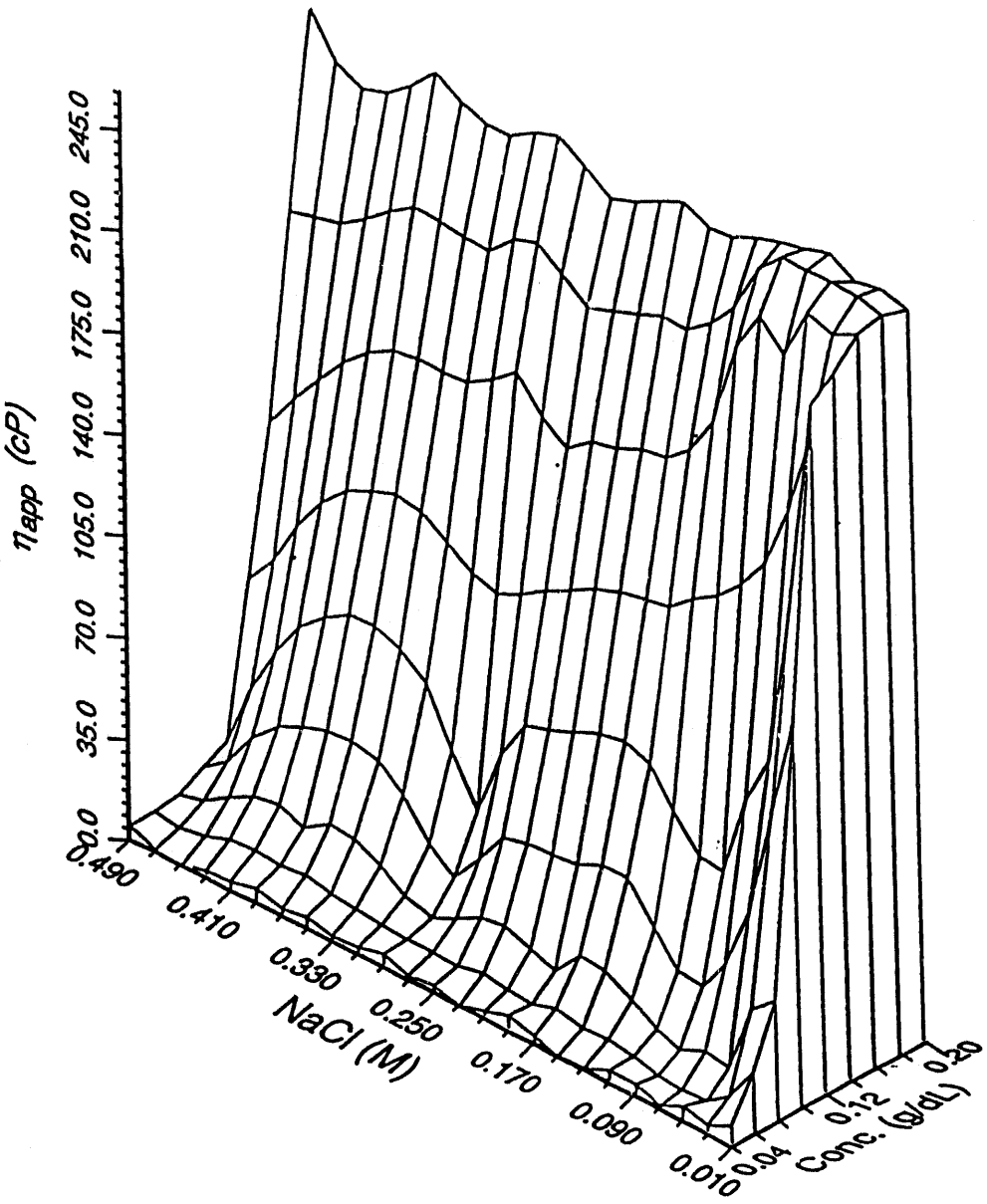

Figure 4-4. η_{app} as a function of polymer concentration and solution ionic strength for the BPAM/NaAMB-5 terpolymer.

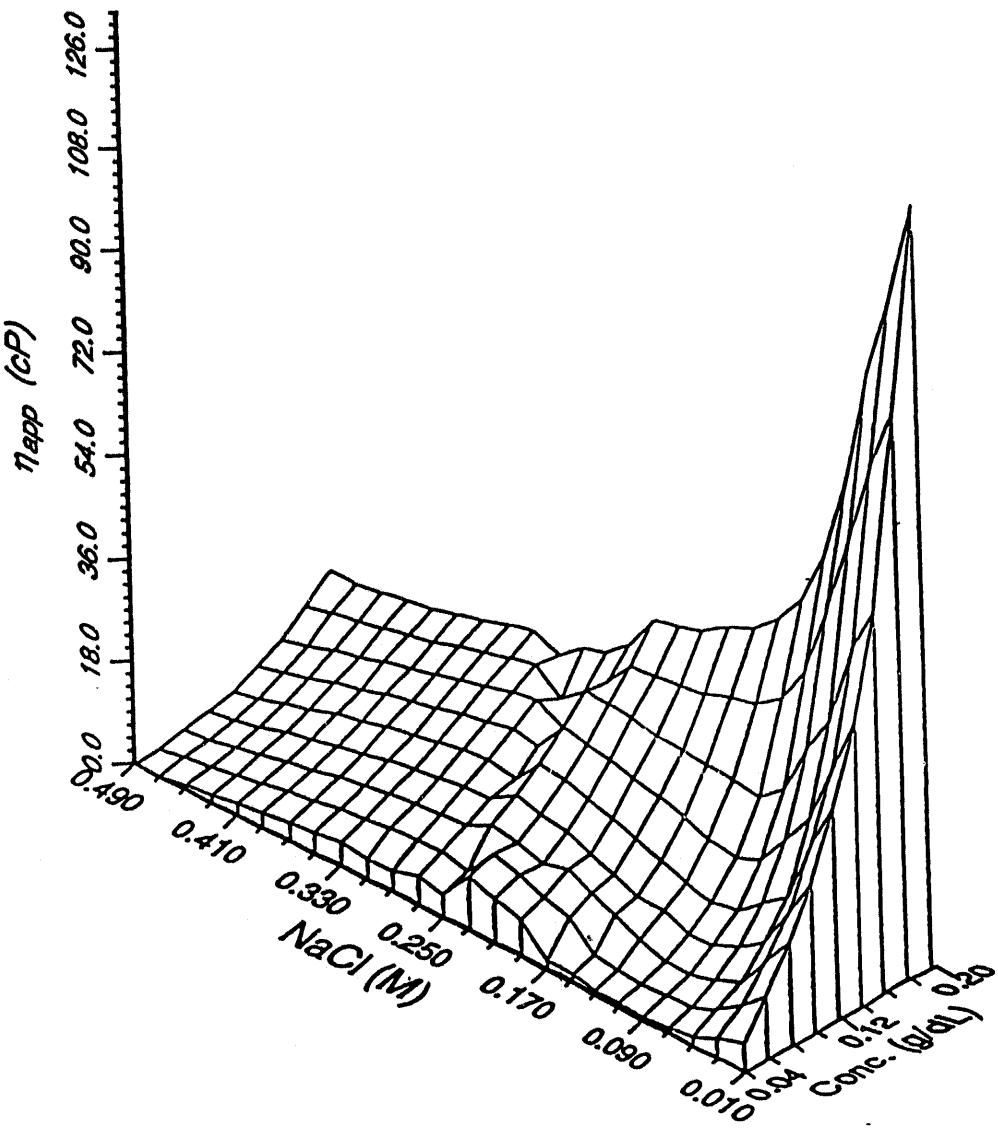

Figure 4-5. η_{app} as a function of polymer concentration and solution ionic strength for the BPAM/NaAMB-25 terpolymer.

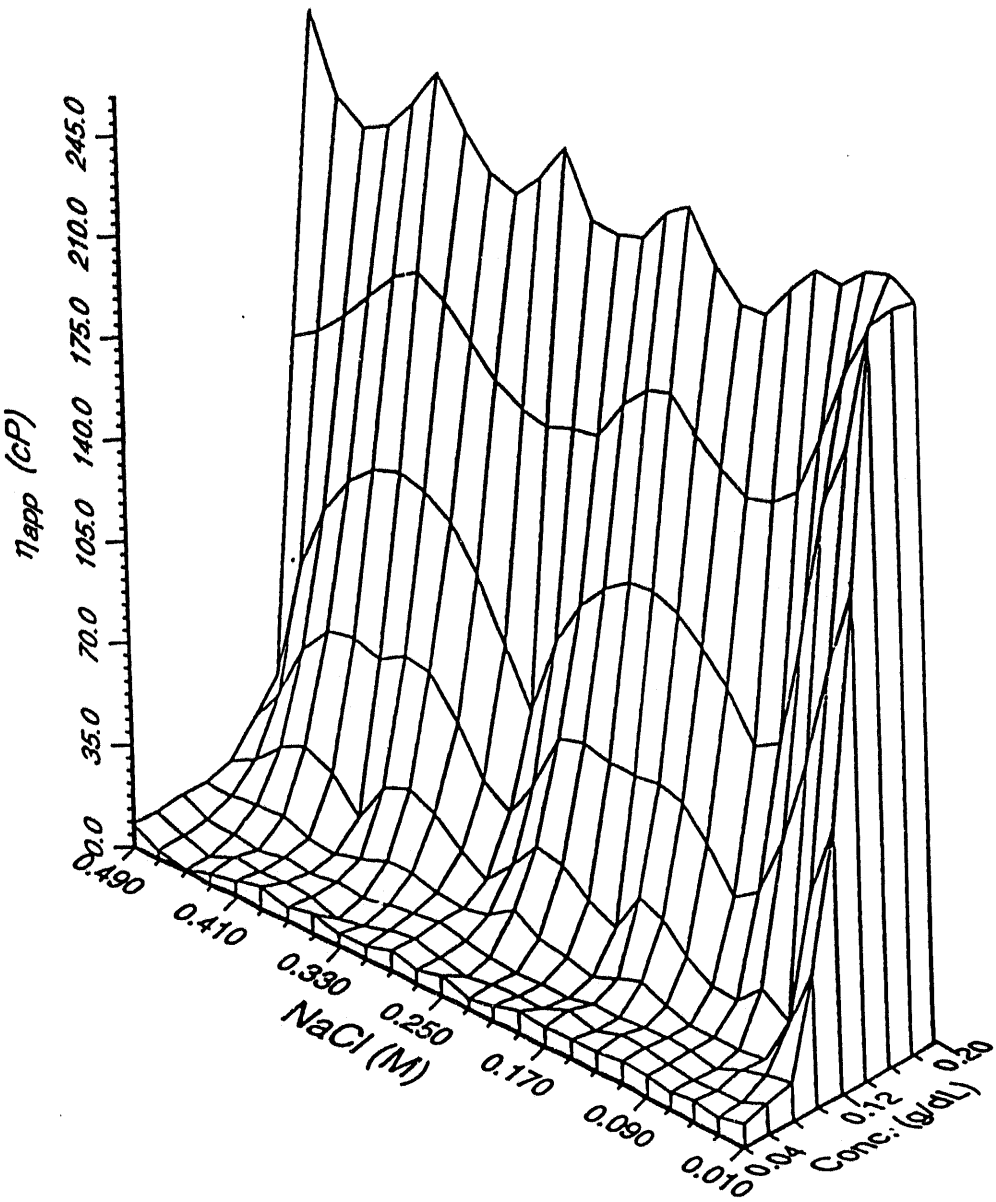

Figure 4-6. η_{app} as a function of polymer concentration and solution ionic strength for the BPAM/NaA-5 terpolymer.

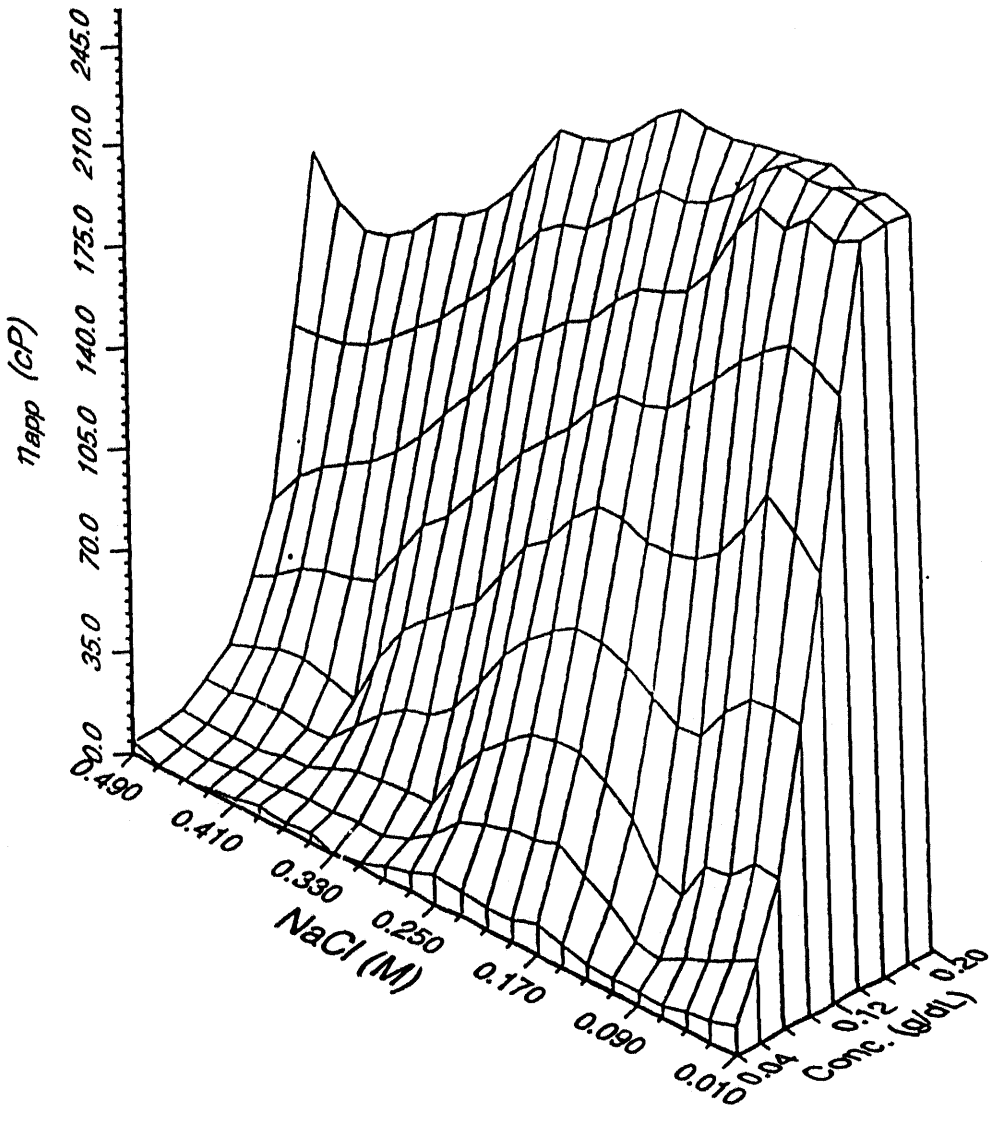

Figure 4-7. η_{app} as a function of polymer concentration and solution ionic strength for the BPAM/NaA-25 terpolymer.

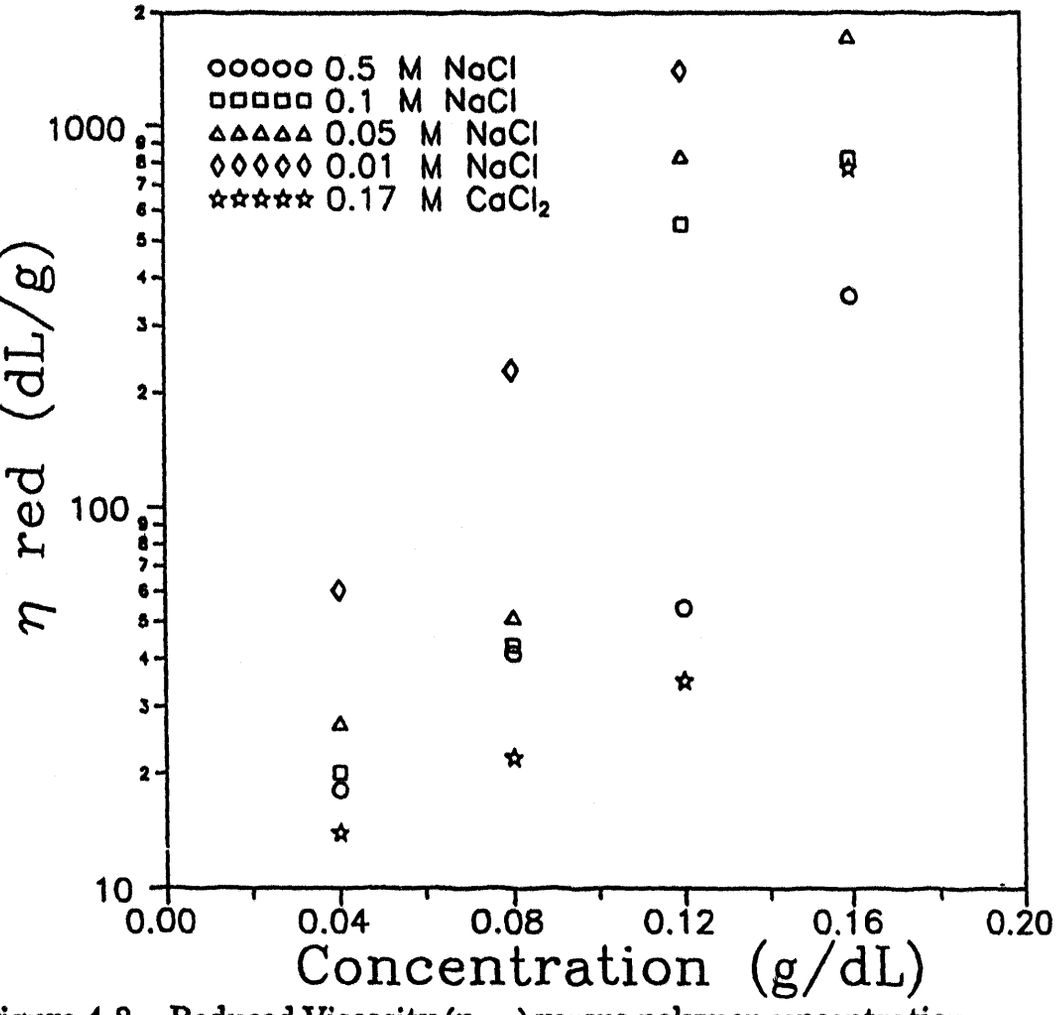

Figure 4-8. Reduced Viscosity (η_{red}) versus polymer concentration for the BPAM/NaAMPS-5 terpolymer in NaCl and $CaCl_2$.

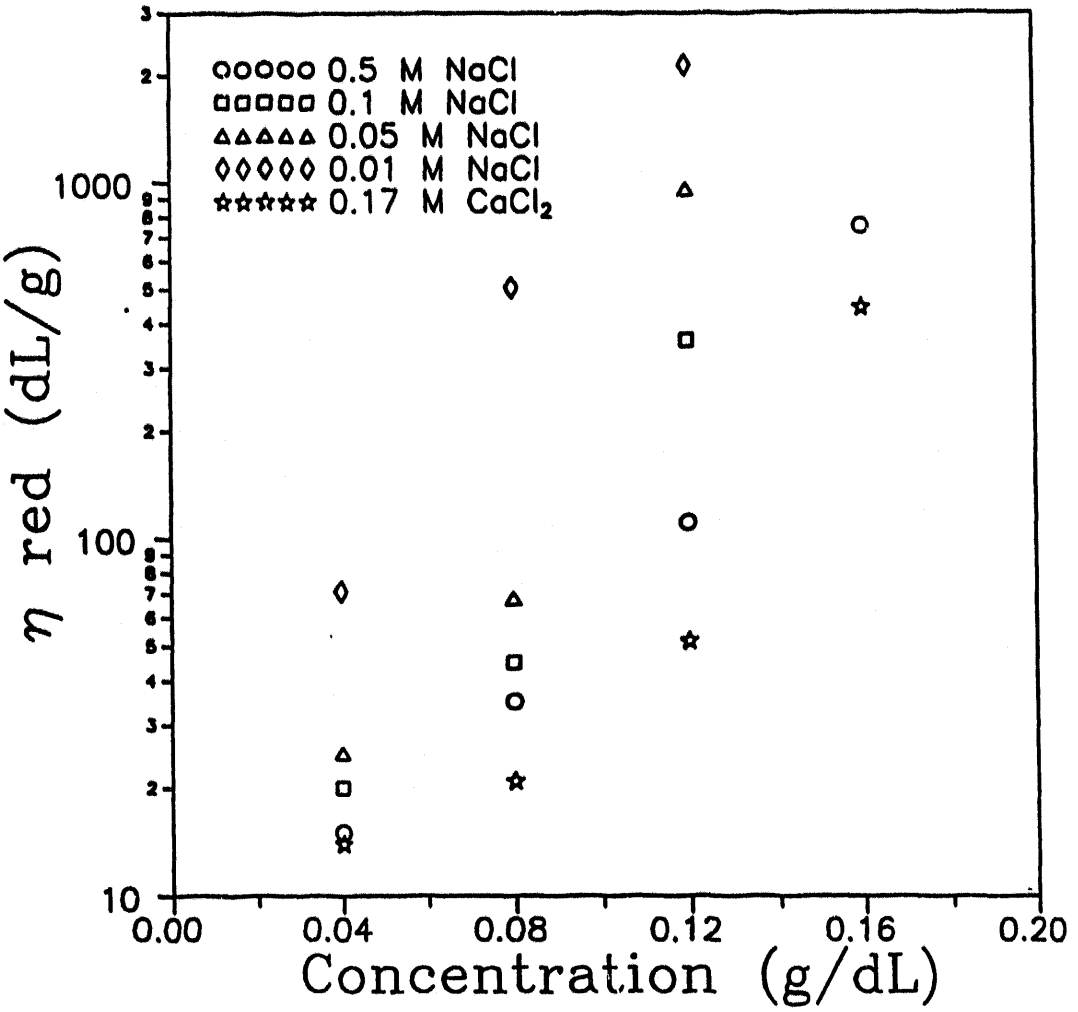

Figure 4-9. Reduced Viscosity (η_{red}) versus polymer concentration for the BPAM/NaAMBA-5 terpolymer in NaCl and $CaCl_2$.

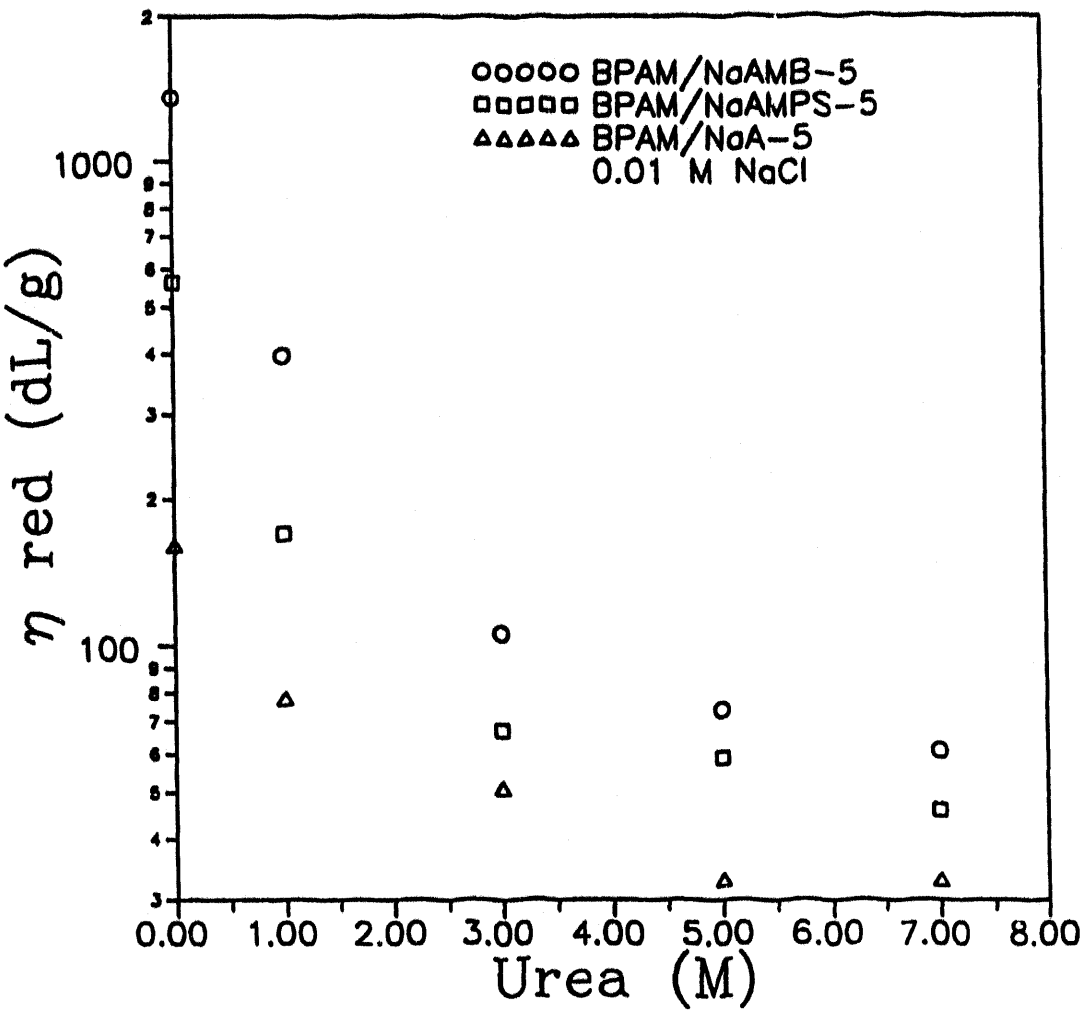

Figure 4-10. Reduced Viscosity (η_{red}) versus urea concentration for the low charge density terpolymers in 0.01M NaCl. Polymer concentration 0.1g/dL.

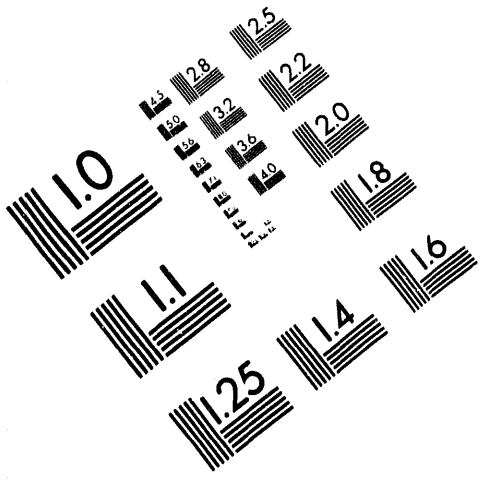

Association for Information and Image Management

1100 Wayne Avenue, Suite 1100
Silver Spring, Maryland 20910

301/587-8202

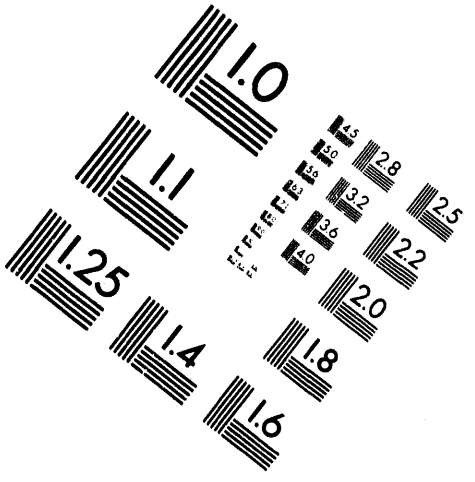

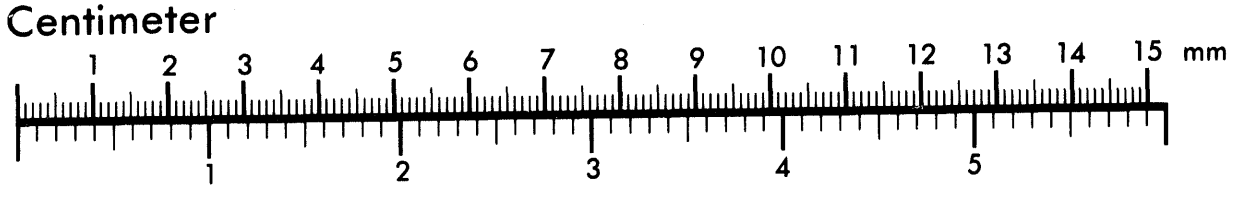

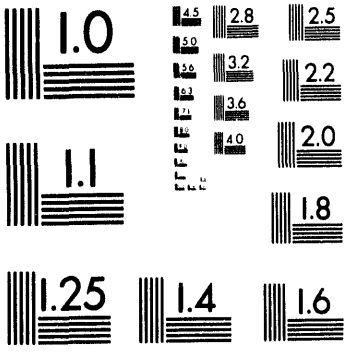

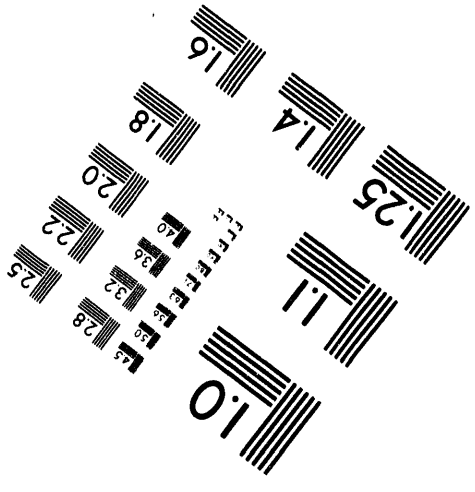

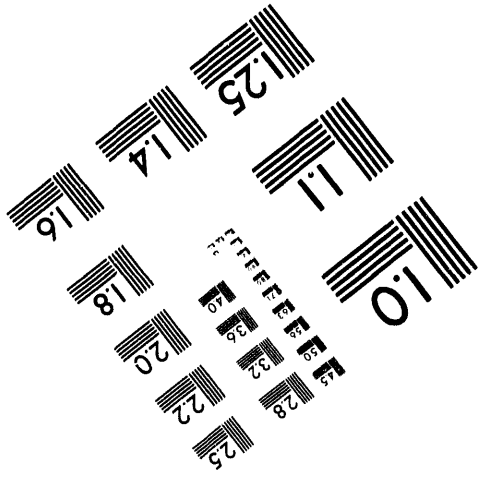

2 of 3

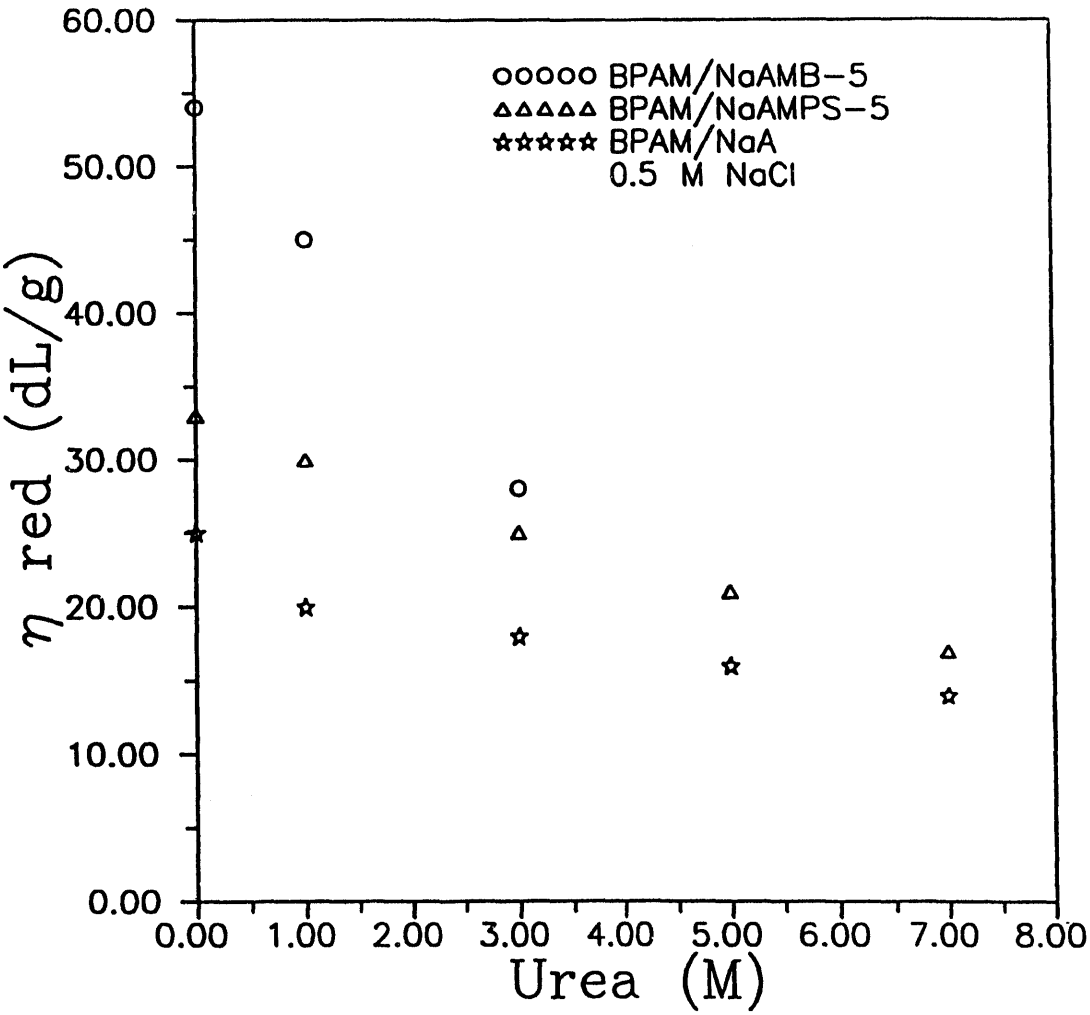

Figure 4-11. Reduced Viscosity (η_{red}) versus urea concentration for the low charge density terpolymers in 0.5M NaCl. Polymer concentration 0.1g/dL.

CHAPTER FIVE: SYNTHESIS AND SOLUTION PROPERTIES OF ASSOCIATIVE ACRYLAMIDO COPOLYMERS WITH PYRENESULFONAMIDE FLUORESCENCE LABELS

Abstract

Pyrenesulfonamide-labelled model associative polymers have been prepared via the copolymerization of acrylamide with 0.5 mole % [1-β-aminoethyl)sulfonamido-1-pyrene]acrylamide. Synthesis of this monomer and details of copolymerization with acrylamide via surfactant and solution copolymerization techniques are described. The microheterogeneous surfactant technique yields a copolymer which exhibits intermolecular associative behavior in aqueous media as demonstrated by rheological and steady state fluorescence studies. Conversely, classical light scattering studies indicate the compact nature of copolymer prepared by the homogeneous solution technique. Intramolecular hydrophobic associatives, indicated by a low second virial coefficient and a small hydrodynamic volume, dominate rheological behavior.

Introduction

Microheterogeneous phase separation in hydrophobically-modified water-soluble copolymers can be achieved by appropriate structural tailoring yielding systems with unique rheological characteristics. Among such materials are rheology modifiers known as "associative thickeners" which demonstrate significant increases in viscosity above the critical overlap concentration, C*[1]. For example, the copolymer of acrylamide containing 0.75 mole percent of n-decylacrylamide prepared under suitable conditions [2] exhibits a sixteen-fold increase in apparent viscosity (Figure 1) as the copolymer concentration increases from 0.05 to 0.20 g/dl. Homopolyacrylamide, by comparison, prepared under the same reaction conditions shows only a gradual increase in viscosity with concentration.

Although associative thickeners based on hydrophobic modification of a number of polymer types including polyacrylamides, cellulosics, polyethers, etc have been reported, the mechanism(s) responsible for their rheological behavior(s) have yet to be fully elucidated. The low concentration of "hydrophobes" and the nature of the interactions preclude study by traditional spectroscopic techniques such as IR or NMR due to insufficient resolution. Photophysical techniques with appropriately labelled copolymers, however, have been used by our group and others [3,4] to study such systems.

In this paper we report synthesis and solution properties of copolymers of acrylamide with [(1-B-aminoethyl)sulfonamido-1-pyrene]acrylamide. The pyrene sulfonamide comonomer serves in two capacities in this study; it provides a fluorescence label for

photophysical measurements and it serves as the hydrophobic monomer. Under selected reaction conditions discussed herein associative properties are observed. The subsequent paper in this series details photophysical evidence for the associations.

Experimental

Materials

Acrylamide (AM) was recrystallized from acetone three times and vacuum-dried at room temperature prior to use. Pyrene was purified by flash chromatography [5] (silica gel packing, CH_2Cl_2 eluent). N,N-Dimethylformamide (DMF) was allowed to stand overnight over 4 Å molecular sieves and was then distilled at reduced pressure. H_2O was deionized and had a conductance less than $1x10^{-7}$ mho/cm. Other starting materials were purchased commercially and used as received. Solvents were reagent-grade, unless otherwise noted.

Monomer and Model Compound Synthesis

[1-(β-Aminoethyl)sulfonamido-1-pyrene]acrylamide [5] and Its Precursors
(Schemes 1 and 2)

Sodium(1-pyrenesulfonate) (7). A literature method [6] was modified for the preparation of sodium(1-pyrenesulfonate) (Scheme 1). Pyrene [1] (47.60 g, 0.235 mol) was dissolved in 300 ml CH_2Cl_2. Chlorosulfonic acid (16 ml, 0.24 mol) dissolved in 50 ml CH_2Cl_2 was added dropwise to the pyrene solution with brisk stirring, at 0°C, under a steady N_2 stream. The reaction progress was followed by thin layer chromatography (TLC) (CH_3OH eluent); 1-pyrenesulfonic acid appears at $R_f = 0$ (R_f= distance traveled by substrance divided by distance traveled by solvent front) while pyrene has a higher R_f value. The resulting dark green solution was poured (with extreme caution) into 500 ml of ice and stirred, allowing the CH_2Cl_2 to evaporate over a two-day period. This solution was filtered twice through celite to remove particulates; each time the celite pads were washed with 150 ml H_2O. NaOH (10.0 g, 0.25 mol) was added as an aqueous solution. Aqueous NaCl (500 mL) was also added. The yellow sodium salt **6** was precipitated via slow solvent evaporation. Filtered and vacuum-dried at 65°C. Elemental analysis of this product indicated that this product was a dihydrate and contained residual NaOH. This product was used successfully in the subsequent reaction without further purification. Yield: 51.0 g (71 %). Anal. Calcd. for $C_{16}H_{13}O_5SNa$: C, 56.46; H, 3.85; S, 9.42; Na, 6.76. Found: C, 55.64; H, 3.15; S, 9.33; Na, 8.71. IR: 3100-3700 (OH stretch due to H_2O); 3045 (aromatic CH stretch); 1194 and 1060 (asymmetric and symmetric S=O stretch). ^{13}C NMR (DMSO-d_6): 123.72, 124.82, 125.34, 126.26, 126.74, 126.80, 126.88, 127.29, 127.69, 130.11, 130.71, 131.29, 141.81 (all aromatic resonances).

1-Pyrenesulfonylchloride (8).

A hydrochloric acid solution in diethyl ether, 30 ml (3×10^{-2} mol) was added to a slurry of (9.1 g, 3×10^{-1} mol) in DMF (200 ml) to generate the sulfonic acid. Thionyl chloride

(22 ml, 0.18 mol) was then added dropwise. TLC with 3:1 CH_2Cl_2: acetone eluent showed the disappearance of the starting material ($R_f = 0$) and the appearance of **8** ($R_f = 0.6$). Stirring was continued for 3 hrs., then the solution was poured into 400 mL ice. The orange-yellow precipitate was filtered and washed with 500 ml H_2O. This material was air-dried overnight on the filter, then vacuum-dried for 18 hr. at 100°C. Yield: 7.7 g (85 %). m.p. 172°C. Anal. Calcd. for $C_{16}H_9SO_2Cl$: C, 63.89; H, 3.00; S, 10.57; Cl, 11.78. Found: C, 63.85; H, 3.09; S, 10.61; Cl, 11.59. IR: 3107, 3145 (aromatic CH stretch); 1590 (S-Cl stretch); 1361, 1173 (asymmetric and symmetric S=O). ^{13}C NMR (DMSO-d_6): 123.79, 123.90, 124.34, 124.93, 125.52, 126.40, 126.73, 126.99, 127.36, 127.91, 130.19, 130.78, 131.52, 141.55 (all aromatic resonances).

N-(1-Pyrenesulfonyl)ethylenediamine.hydrochloride (9).

A modification of a literature procedure for the reaction of acid chlorides with symmetrical diamines [7], via a high-dilution technique (Scheme 1), was used for the synthesis of **9**. Ethylenediamine (10.0 ml, 0.15 mol) was added to 1 L CH_2Cl_2 and stirred rapidly at 0°C under a N_2 blanket. **8** (3.0 g, 1.0 x 10^{-2} mol) was dissolved in 1 L CH_2Cl_2 and added dropwise to the stirred diamine solution. After addition was completed (about 2 hr.), the CH_2Cl_2 layer was extracted with 2 x 3 L H_2O and 1 x 2 L 5% NaCl. The CH_2Cl_2 layer was slowly filtered through a pad of $MgSO_4$, then treated with 15 ml of 1.0 N HCl dissolved in diethyl ether. The resulting fine pale-yellow precipitate was vacuum-dried at room temperature. TLC of this material (3:1 CH_2Cl_2: acetone eluent) exhibited only one component at $R_f = 0$. HPLC purity was determined to be > 99.9 %. Anal. Calcd. for $C_{18}H_{17}SO_2N_2Cl$: C, 59.92; H, 4.72; N, 7.77; S, 8.89; Cl, 9.83. Found: C, 59.92; H, 4.59; N, 7.57; S, 8.64; Cl, 9.81. IR: 2800-3600 (NH_3Cl stretch); 3318 (H-N-SO_2- stretch); 3028 (aromatic CH stretch); 2912 (aliphatic CH stretch); 1325, 1159 (asymmetric and symmetric S=O); 1085 (S-N stretch). ^{13}C NMR (DMSO-d_6): 38.61, 39.87 (ethylene resonances); 123.06, 123.28, 124.15, 126.77, 126.96, 129.63, 129.96, 130.40, 131.60, 134.05 (aromatic resonances).

The free amine of **9** was prepared via addition of a concentrated aqueous solution of a molar equivalent of NaOH to **9** dissolved in the minimum amount of DMF. After brief stirring, the solution was poured into H_2O which precipitated **9** in the free amine form, designated here as **10**. This yellow solid was washed with H_2O, then vacuum-dried at room temperature. A downfield shift of the ethylene resonances was observed in the ^{13}C NMR spectrum, confirming the formation of the free amine[8]. ^{13}C NMR (DMSO-d_6): 42.62, 46.03 (ethylene resonances); 123.20, 123.46, 124.17, 126.77, 126.96, 129.70, 129.87, 130.53, 131.60, 134.05 (aromatic resonances).

[1-(β-Aminoethyl)sulfonamido-1-pyrene]acrylamide (5).

Synthesis of **5** is depicted in Scheme 2. The amine hydrochloride salt **9** (1.0 g, 2.8 x 10^{-3} mol) and [1,8-bis-(dimethylamino) napthalene] (1.19 g, 5.6 x 10^{-3} mol) were stirred with 7 ml DMF under a nitrogen stream for 15 minutes at 0°C. Acryloyl chloride (2.2 ml, 2.8x10^{-2} mol) in 7 ml DMF was then added dropwise to the amine solution. TLC (acetone eluent) was

used to follow the depletion of starting amine ($R_f = 0$) and the generation of product (R_f = 0.70). After the addition was complete, the reaction mixture was poured into 150 mL ice. The product precipitated overnight as a yellow solid which was subsequently filtered and vacuum-dried at room temperature. Yield: 0.90 g (88 %). Product recrystallization was performed by dissolution of 0.9 g **5** in 300 ml boiling CH_2Cl_2, decolorization with Norit RB 1 0.6 charcoal pellets, and filtration through a celite pad. Pale green crystals were recovered in 69 % yield. Purity of this material was determined to be > 99.9 % via HPLC. Anal. Calcd. for $C_{21}H_{18}SO_3N_2$: C, 66.67 %; H, 4.76; S, 8.47; N, 7.41. Found: C, 66.83; H, 5.00; S, 8.48; N, 7.49. IR: 3050-3600 (N-H stretch); 3370, 3289 (H-N-SO_2 stretch); 3084 (aromatic CH stretch); 2938, 2864 (aliphatic CH stretch); 1659, 1540 (amide I and II bands); 1312, 1159 (S=O asymmetric and symmetric stretch). ^{13}C NMR (DMSO-d_6): 38.77; 41.95 (ethylene carbons); 127.14, 129.58 (vinylic carbons); 123.09, 123.32, 124.07, 124.27, 125.02, 126.63, 126.79, 126.86, 129.44, 129.73, 130.36, 131.44, 132.23, 133.88 (aromatic carbons); 164.84 (acrylamido ketone carbon).

Pyrenesulfonamide Model Compounds

[1-(β-Aminoethyl)sulfonamido-1-pyrene]2,4-dimethylglutaric acid (3)

Synthesis of **3** required first the preparation of 2,4-dimethylglutaric anhydride, followed by amination with **10** (Scheme 3).

2,4-Dimethylglutaric anhydride (11).

2,4-Dimethylglutaric acid (2.0 g) was added to 5 ml acetic anhydride. Vacuum distillation of this solution at 90°C gave acetic anhydride as the first fraction. The anhydride product **11** then distilled over as a clear liquid which cooled to form a hygroscopic, hard white solid. Although an IR of this product showed the presence of some diacid (O-H stretch 2500-3500 cm^{-1}; C=O stretch due to diacid at 1698 cm^{-1}), this material was successfully used in subsequent reactions without purification. Yield: 1.1 g (62 %). IR: 3500-2500 (OH stretch due to acid), 1794, 1752 (asymmetrical and symmetrical anhydride ketone stretching modes); 1698, 1459 (acid ketone stretching modes).

Synthesis of 3. (Scheme 3)

The amine sulfonamide **10** (0.75 g, 2.31 x 10^{-3} mol) was dissolved in 6 ml DMF. This solution was added dropwise to **11** (0.41 g, 2.54 x 10^{-3} mol) dissolved in 2 ml DMF under N_2 at 0°C. The reactant mixture was stirred for 5 hr. then poured into 50 ml saturated NaCl solution, which was acidified (HCl). A yellow oil immediately formed. The H_2O was decanted and the product dissolved in 30 ml CH_2Cl_2. Extraction of this solution with 50 ml H_2O precipitated the product as a pale green solid. TLC (CH_3OH eluent) gave a R_f = 0.82 for the product; traces of impurities near $R_f = 0$ were also present. Purification of **3** was performed via dissolution of 0.61 g in DMF, followed by flash chromatography on 250 ml silica gel, with CH_3OH as the eluent. This procedure was tedious since the product was very slow to elute. Vacuum solvent removal from the pure fractions gave about 0.2 g (33 %) yield of a pale yellow-green product. HPLC purity of this material was determined to be >

99.9 %. Anal. Calcd: C, 64.35; H, 5.63; N, 6.01; S, 6.87. Found: C, 64.20; H, 5.69; N, 5.94; S, 6.73. IR: 3500-2500 (acid OH stretch); 3378, 3284 (H-N-SO_2 stretching); 1737 (asymmetric C=O stretch of the acid residue); 1684 (amide I); 1549 (amide II); 1302, 1167 (asymmetric and symmetric S=O stretch). ^{13}C NMR (DMSO-d_6): 20.37, 21.13, 21.56 (aliphatic resonances of the glutaric residue); 42.84, 45.30 (aliphatic resonances of the ethylenediamine residue); 126.94, 127.92, 130.63, 133.23, 135.99, 137.62 (aromatic resonances); 179.01, 180.80 (ketone resonances of the glutaric residue).

[1-(β-Aminoethyl)sulfonamido-1-pyrene]gluconamide heptahydrate (4)

Synthesis of **4** is depicted in Scheme 5. The free amine of **10** (0.44 g; 1.36 x 10^{-3} mol) was added to δ-gluconolactone (0.30 g; 1.68 x 10^{-3} mol) in 2 ml of CH_3OH. A clear green solution was obtained upon heating; a reflux was maintained for 18 hours. Compound **4** precipitated from solution as a yellow-green solid. After filtration and washing with CH_3OH, **4** was vacuum-dried overnight at room temperature. HPLC purity of this compound was determined to be 99.9%. Elemental analysis determined **4** to be a heptahydrate. Yield: 0.31 g (45 %). m.p: 171-173°C. Anal. Calcd. (heptahydrate): C, 46.67; H, 4.90; N, 4.53; S, 5.19. Found: C, 46.16; H, 4.55; N, 4.24; S, 5.31. IR: 3600-3000 (OH stretch); 3379 (H-N-SO_2 stretch); 1657 (amide I); 1533 (amide II); 1419 (C-N stretch); 1307, 1161 (asymmetric and symmetric S=O). ^{13}C NMR (DMSO-d_6): 38.24, 41.20 (ethylene resonances); 63.27 (1′ C-OH); 69.89, 71.44, 72.25, 72.45 (2′ C-OH); 123.17, 123.35, 124.22, 126.65, 126.81, 127.09, 129.51, 129.68, 129.62, 130.51, 133.93 (aromatic resonances); 172.77 (amide ketone).

Synthesis of Pyrenesulfonamide-Labelled Polymers

Poly[[1-(β-Aminoethyl)sulfonamido-1-pyrene]acrylamide-co-acrylamide] (1). Surfactant Polymerization Technique.

The general method of Turner et al., was employed (Scheme 4)[9]. Monomer feed ratio in this copolymerization was 99.50 mol % AM: 0.50 mol % **5**. The polymerization was performed by adding 7.38 g (0.1048 mol) AM, 7.92 g (2.74 x 10^{-2} mol) sodium dodecyl sulfate, 0.20 g (5.29 x 10^{-4} mol) **5**, and 235 g H_2O to a 500 ml flask equipped with mechanical stirrer, nitrogen inlet, condenser, bubbler, and heating bath. This mixture was heated to 50°C under a nitrogen purge. Stirring rate was maintained at approximately 60 rpm. All of the monomer **5** had dissolved after 15 minutes; polymerization was then initiated via syringe addition of 9.25 x 10^{-6} mol $K_2S_2O_8$, as a deaerated solution in 2 ml of H_2O. Polymerization was allowed to continue at 50°C for 12 hours, after which time the polymer was recovered via precipitation into acetone. Purification was accomplished by redissolving the polymer in H_2O and dialyzing against H_2O using 12,000-14,000 molecular weight cutoff dialysis tubing. This polymer was recovered by freeze-drying. Conversion was 22%.

Poly[[1-(β-Aminoethyl)sulfonamido-1-pyrene]acrylamide-co-acrylamide] (2). Solution Polymerization Technique.

Monomer feed ratios, quantities, and equipment in this preparation (Scheme 5) were the same as in the previous procedure. Comonomers were dissolved in a mixture of 130 ml DMF and 100 ml H_2O. Three freeze-pump-thaw cycles were performed to remove residual oxygen. Initiation procedure was as described for the surfactant polymerization. In this case, polymer precipitated from solution as the polymerization continued (12 hr.). Pouring the suspension into acetone allowed recovery of the polymer product. Purification procedures were as described for the surfactant polymerization. Conversion was 21 %. UV analysis determined **2** to contain 0.35 mol % **5** (70 % incorporation).

Characterizational Methods—Pyrenesulfonamide Derivatives

^{13}C NMR spectra were recorded with a Bruker AC-300 instrument. Most samples were dissolved in DMSO-d_6; chemical shift assignments are relative to the central DMSO peak (^{13}C - 39.50 ppm). UV-VIS spectra were recorded with a Perkin-Elmer Lambda 6 Spectrophotometer. A Mattson Model 2020 FTIR was used to obtain infrared spectra.

Sample purity was determined in most cases by both TLC and high performance liquid chromatography (HPLC). TLC was performed on Merck Kieselgel 60 silica gel plates. Developed plates were generally viewed under 254 nm light for napthalene derivatives and 325 nm for pyrene derivatives. HPLC was performed on a Hewlett-Packard Model 1050 system equipped with a photodiode-array detector. A Waters μ-Bondapak C18 column was employed with methanol as the mobile phase. Sample effluent was typically monitored at 220 nm for napthalene derivatives or 350 nm. Alternately, multiple wavelengths were monitored—depending on the nature of suspected impurities.

Solution Preparation.

Polymer stock solutions were prepared in H_2O or 2 % (w/w) NaCl at ca. 200 mg/dl. Several weeks of constant mechanical shaking were required for complete solubilization. Solutions were filtered through an 8 μm filter; a peristaltic pump was employed to pump the solution at a low flow rate. Polymer and fluorphore concentrations of stock solutions are shown in Table I.

Copolymer Composition

Copolymer composition was determined by UV analysis of the aqueous copolymer solutions. The pyrenesulfonamide chromophore was determined to have $\epsilon = 24120\ M^{-1}\ cm^{-1}$.

Rheological Studies

Viscosity measurements were performed on solutions ranging from 20-200 mg/dl in concentration. Measurements were recorded with a Contraves Low-Shear 30 Rheometer at 25°C and a shear rate of 6.0 s^{-1}.

Classical Light Scattering

Classical light scattering measurements were performed on a Chromatix KMX-6 instrument. A 1.2 μm filter was used in the filter loop. Measurements were made at 25°C. dn/dc measurements were taken on a Chromatix KMX-16 differential refractometer also at 25°C.

Results and Discussion

The synthetic objective of this work was to prepare a pyrene-containing monomer which could be copolymerized with acrylamide to yield a copolymer with associative thickening behavior. Our concept was to utilize a hydrolytically stable monomer with both the necessary hydrophobic characteristics and photophysical response. Although fluorescence probes and labels have been used to study organization, we know of no other reports utilizing the fluorescence label as the sole hydrophobic moiety for domain formation.

The monomer [1-(β-aminoethyl)sulfonamide-1-pyrene]acrylamide **5** proved to have the necessary properties to achieve our synthetic objective. This monomer was initially synthesized by Winnik's group[10] and subsequently synthetic procedures modified and scaled up to provide a highly purified monomer suitable for photophysical studies.

Several features of **5** should be noted. The acrylamido functionality of the monomer allows rapid copolymerization with the acrylamide monomers. Monomers of this type have large ratios of $(k_p^2/k_t)^{1/2}$ where k_p and k_t represent the rate constants for propagation and termination in free radical polymerization. The amide and sulfonamide linkages are hydrolitically stable in aqueous media and thus protect the integrity of the label during photophysical analysis. The monomer **5** has no benzylic hydrogens for chain transfer as do most pyrene labels reported in the literature. The spacer length (in this case ethylene) can be altered in the synthetic procedure to decouple the pyrene from the polymer backbone. Finally the pyrene sulfonamide chromophore has a high molar absorptivity value and a high quantum yield of fluorescence[11].

The synthesis of **5** deserves some comment. The first synthetic step (Scheme 1), chlorosulfonation of pyrene, proceeded smoothly. Product **7**, sodium-1-pyrenesulfonate, contained a small amount of NaOH but was used without further purification. The compound was isolated as a dihydrate; similar compounds have been reported to exist as hydrates—for example 1-pyrenesulfonic acid[11]. Transformation to pyrene sulfonylchloride **8** was also facile.

Reaction of **8** with ethylenediamine to give N-(1-pyrenesulfonyl)ethylenediamine hydrochloride **9** was problematic. Initial attempts, despite dilute reaction conditions, led to

production of significant amounts of the ethylenediamine bis(sulfonamide) which was difficult to separate from **9**. Apparently, the reaction is diffusion-controlled. Reaction of **8** with ethylenediamine is quite rapid and if the desired monosulfonamide product **10** encounters another molecule of **8**, the sequential reaction will occur.

Recent literature has addressed control of such reactions. Monoacylation of symmetrical diamines can be achieved by a "high-dilution" technique[7,12]. Therefore very dilute solution of **8** was added dropwise to a solution of excess ethylenediamine with rapid mixing to reduce the disubstitution reaction. A pure product was obtained by extraction in methylenechloride and conversion to the aminehydrochloride **9** by addition of HCL in diethylether.

Reaction of **9** with acryloyl chloride (Scheme 2) was facilitated by using two equivalents of the acid scavenger 1,8-bis(dimethylamino)naphthalene. This base is sterically hindered[14] and will not deprotonate the sulfonamide proton **5**. The sulfonamide proton of **5** is acidic; triethylamine and other bases deprotonate **5** to give the sulfonamide salt, which is nonfluorescent. The pyrenesulfonamide monomer **5** was recrystallized from methylene chloride. HPLC analysis utilizing dual ultraviolet detection at 330 nm and 220 nm indicated sample purity greater than 99.9%.

In addition to the desired sample purity, monomer **5** is soluble in aprotic solvents such as dimethylformamide and dimethylacetamide. It is insoluble in water but, importantly, is readily solubilized by sodium dodecylsulfate micelles.

Model compounds **3** [1-(β-amidoethyl)sulfonamido-1-pyrene]2,4-dimethylglutaric acid and **4** [1-(β-aminoethyl)sulfonamido-1-pyrene] gluconamide heptahydrate were synthesized as water-soluble species bearing the pyrenesulfonamide moiety for model studies (Scheme 3). Neither **3** nor **4** has been previously reported. Structural and purity evaluation of both were satisfactory. Interestingly, despite extended drying, **3** remained a heptahydrate. Other hydrophobic gluconamides have also been reported to have highly hydrated structures[15].

Synthesis of Model Polymers

Two synthetic methods were chosen to prepare copolymers with approximately 0.5 mole percent of **5** but different microstructures. In the first procedure, often called the "micellar technique", 99.5 mole % of acrylamide and 0.5 mole % of **5** were copolymerized in aqueous solution in the presence of sodium dodecyl sulfate at concentrations well above its critical micelle concentration (Scheme 4). Potassium persulfate was used as the initiator.

Concurrent studies in our laboratories with phenyl and naphthyl chromophore-containing monomers have shown that in this microheterogeneous procedure the surfactant/hydrophobic monomer ratio is important in dictating final rheological properties[16].

These findings are consistent with a proposed mechanism of successive chain propagation of hydrophobic monomers present in the separate SDS micelles and solution polymerization of acrylamide resulting in short runs of the comonomer randomly distributed along the polymer backbone. The importance of this distribution will be addressed later in this report.

In a second synthetic procedure (Scheme 5) the two monomers in the same molar ratios were copolymerized under homogeneous reaction conditions in a DMF/H_2O mixture again with potassium persulfate initiation. This polymerization might be expected to occur in a more random fashion than the micellar polymerization with monomers of **5** randomly distributed along the backbone.

Copolymer Characterization

The micellar copolymer **1** was purified by successive precipitation into acetone, redissolution into water, dialysis performed to remove surfactant and freeze dried. Verification of removal of SDS was obtained using $BaCl_2$ reagent. Copolymer **2** precipitated as a suspension during polymerization and was purified by sequential addition to acetone, filtration, redissolution into water, and lipholization.

Copolymer compositions were determined by ultraviolet spectroscopic analysis in water of the pyrenesulfonamide chromophore at 35/nm (ϵ = 24, 120 M^{-1} cm^{-1}). Copolymer **1** was found to contain 0.25 mole % **5** (50% incorporation) while copolymer **2** contained 0.35 mole % (70% incorporation). Fluorescence studies which include characterization of microstructure of copolymers **1** and **2** are reported in Chapter Six.

Rheological Studies

Rheological studies were performed on diluted stock solutions (Table I). The copolymer **1** prepared by the micellar technique, like many other associative copolymers synthesized previously in our labs, required several weeks with continuous shaking for complete dissolution. A contraves Low-Shear 30 Rheometer operating at $6s^{-1}$ was utilized for viscometric studies.

Equations 1 (the Huggins equation) and 2 (the "Modified Einstein-Simha" equation) are often utilized to study polymer solution viscosity behavior as a function of polymer concentration, C..

$$\eta_{red} = [\eta] + k'[\eta]^2C \qquad (1)$$

$$\eta_{rel} = 1 + [\eta]C \qquad (2)$$

The utility of the Huggins equation (1) is well recognized for solvated polymers; alternately, Equation (2) has been proposed for the analysis of polymers which behave as suspensions in solution[15]. Plots of relative viscosity versus concentration for **2**, the solution-polymerized system, are illustrated in Figure 2 in deionized H_2O and 2% NaCl. The linearity of the data and an intercept value of one suggest that this polymer behaves as a suspension in solution. The higher order terms of the Huggins equation, which account for interpolymer interactions, appear to be unimportant here. Huggins plots of these data in water and NaCl are given in Figure 3. The reduced viscosity is insensitive to polymer concentration (within experimental error), giving a value of zero for the Huggins constant, k'.

These data and fluorescence data to be presented later suggest the presence of intramolecular hydrophobic associations of the pyrenesulfonamide label. Such associations could result in compaction of the polymer coil, giving the observed suspension-like behavior. Classical light scattering was performed on copolymer **2** in DI H_2O indicating $M_w = 1.6 \times 10^5$ with the second virial coefficient, A_2, equal to 0.

Structure **1** is a representative sample of copolymers of **5** with AM prepared by the micellar polymerization technique. Relative viscosity profiles are illustrated in Figure 4 for deionized water and NaCl solutions. At low concentrations (< 0.10 g/dl) intermolecular association is apparent. Increased ionic strength (2 % NaCl) contracts the polymer coil yielding a lower viscosity. The low C* value likely represents the onset of intermolecular hydrophobic associations of the hydrophobic pyrenesulfonamide moieties. By comparison, a homopolymer of acrylamide exhibits linear viscosity behavior through this concentration range. Attempts at Huggins plots for **1** are given in Figure 5. The nonlinearity of these profiles indicates the first two terms of the Huggins equation are insufficient to model these data. Such a nonlinear response is strong evidence for intermolecular associative behavior. It should also be noted that the associative tendencies at copolymer **1** in solution preclude analysis by light scattering.

Conclusions

Our objectives in the synthesis and study of model associative polymers first necessitated the synthesis of a fluorophore-containing hydrophobic monomer and model compounds. These materials were purified to a degree appropriate for polymerization and subsequent photophysical studies. The hydrolytically stable, pyrenesulfonamide-labelled monomers were readily copolymerizable with acrylamide via homogeneous (solution) and heterogeneous (micellar) polymerization techniques. Labelled copolymers prepared by the two procedures have significantly different rheological behaviors. The surfactant polymerized copolymer **1** in aqueous media exhibited a low critical overlap concentration—typical of associative thickener behavior. Conversely, the solution copolymerization yields copolymer **2** which is more spherical in nature. The Huggins profile of this polymer in aqueous solutions

has zero slope demonstrating a compact conformation. Light-scattering analysis of this polymer in H_2O gives a second virial coefficient value of zero. Photophysical analysis of these systems has been conducted and is reported in the next paper in this series.

References

1. C. L. McCormick, J. Bock, and D. N. Schulz, *Encyclopedia of Polymer Science and Engineering, 17,* John Wiley and Sons, New York, **1989** 730-784.

2. McCormick, C. L.; Nonake, T,; Johnson, C. B. **Polymer**, 1988, 29, 731.

3. Winnik, F. M.; Winnik, M. A.; Tazuke, S.; Ober, C. K. *Macromolecules*, **1987**, 20, 38.

4. Char, K.; Frank, C. W.; Gast, A. P.; Tang, W. T. *Macromolecules*, **1987**, 20, 1833.

5. Still, W. C.; Kahn, M.; Mita, A. *J. Org. Chem.*, **1978**, 43, 2923.

6. Tietze, E.; Bayer, *O. Ann,* 1939, 540, 189; *Chem. Abstr.*, **1939**, 9318.

7. Jacobson, A. R.; Mahris, A. M.; Sayre, L. M. *J. Org. Chem.*, **1987**, 52, 2592.

8. Silverstein, R. M.; Bassler, G. C.; Morrill, T. C. *Spectrometric Identification of Organic Compounds*; Wiley: New York, 1981, 267.

9. Turner, S. R.; Siano, D. B.; Bock, J. (to Exxon Research and Engineering), US Patent 4 520 182, **1985.**

10. Winnik, M. A.; Private Communications, University of Toronto, **1987.**

11. Tesler, J.; Cruikshank, K. A.; Morrison, L. E.; Netzel, T. L. *J. Am. Chem. Soc.*, **1989**, 111, 6966.

12. Menger, F. M.; Whitsell, L. G. *J. Org. Chem.*, **1987**, 52, 3793.

13. Bourne, J. R.; Ravindranath, K.; Thoma, S. *J. Org. Chem.*, **1988**, 53, 5167.

14. Alder, R. W.; Bowman, P. A.; Steele, W. R. S.; Winterman, D. R. *Chem. Comm.*, **1968**, 723.

15. Fuhrhop, J. H.; Svenson, S.; Boettcher, C.; Tossler, E.; Vieth, H. M. *J. Am. Chem. Soc.*, **1990**, 112, 4307.

16. Middleton, J. C.; Ph.D. Dissertation, University of Southern Mississippi, **1990.**

17. Salomone, J. C.; Tsai, C. C.; Olson, A. P.; Watterson, A. C. In I*ons in Polymers, Advances in Chemistry* Series No. 187, American Chemical Society; Washington, DC, 1978, 337.

Table I
Stock Solutions of Labelled Polymers

Polymer #	Polymer Conc. (mg/dl)	Fluorophore Conc. (mol/l)
29	218	7.13×10^{-5}
33	193	9.28×10^{-5}

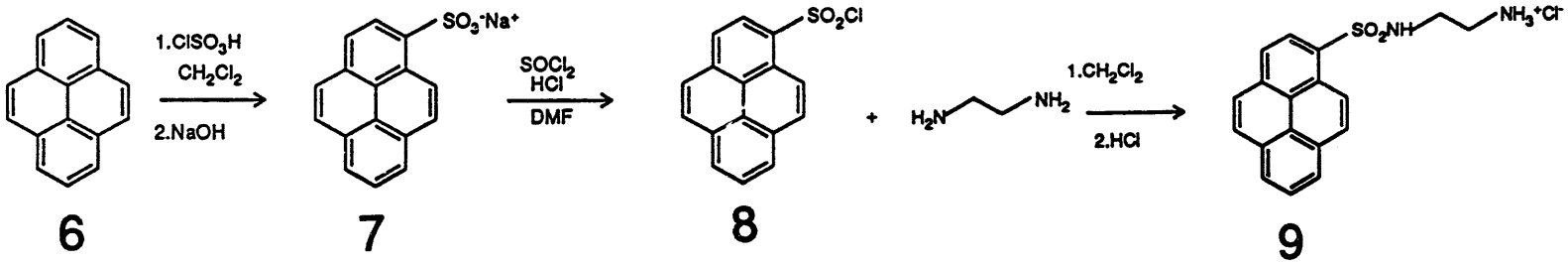

Scheme 5-1. Synthesis of N-(1-Pyrenesulfonyl)ethylenediamine Hydrochloride 9.

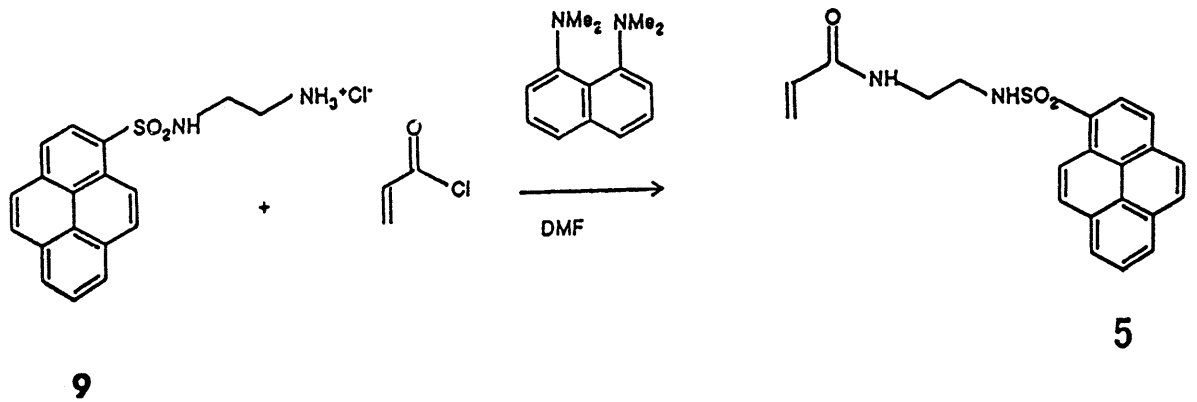

Scheme 5-2. Synthesis of [1-(β-Aminoethyl)sulfonamido-1-Pyrene]Acrylamide 5.

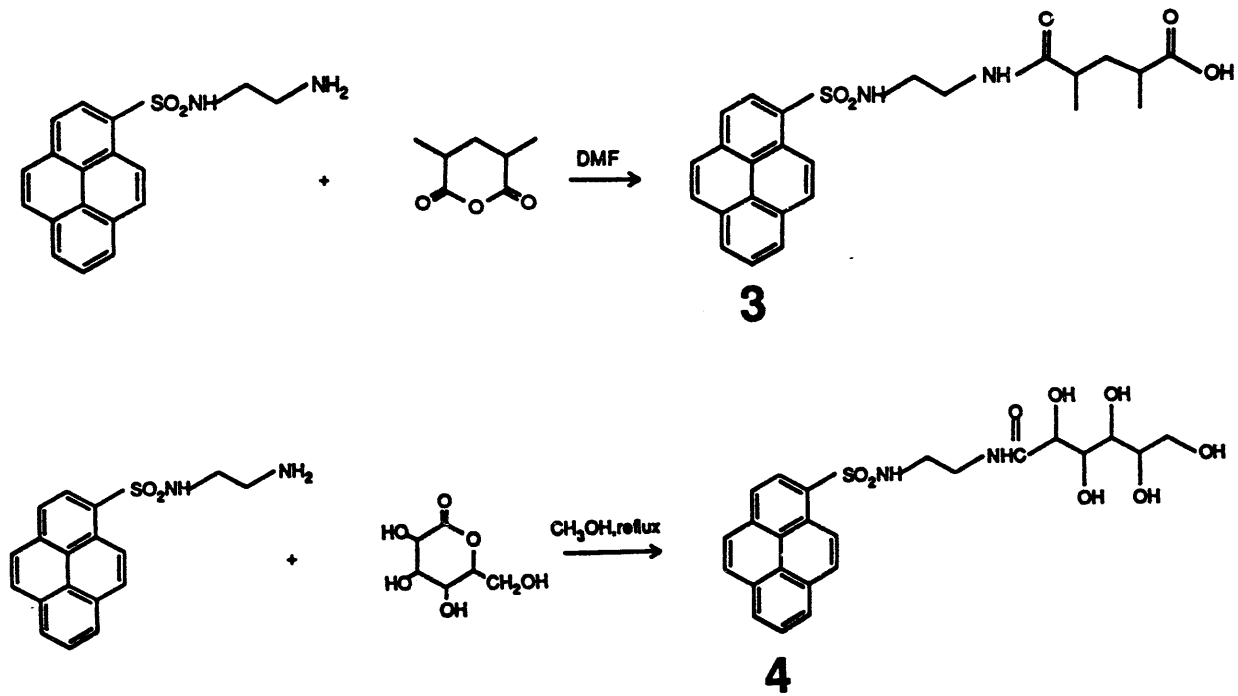

Scheme 5-3. Synthesis of Pyrene-Containing Model Compounds 3 and 4.

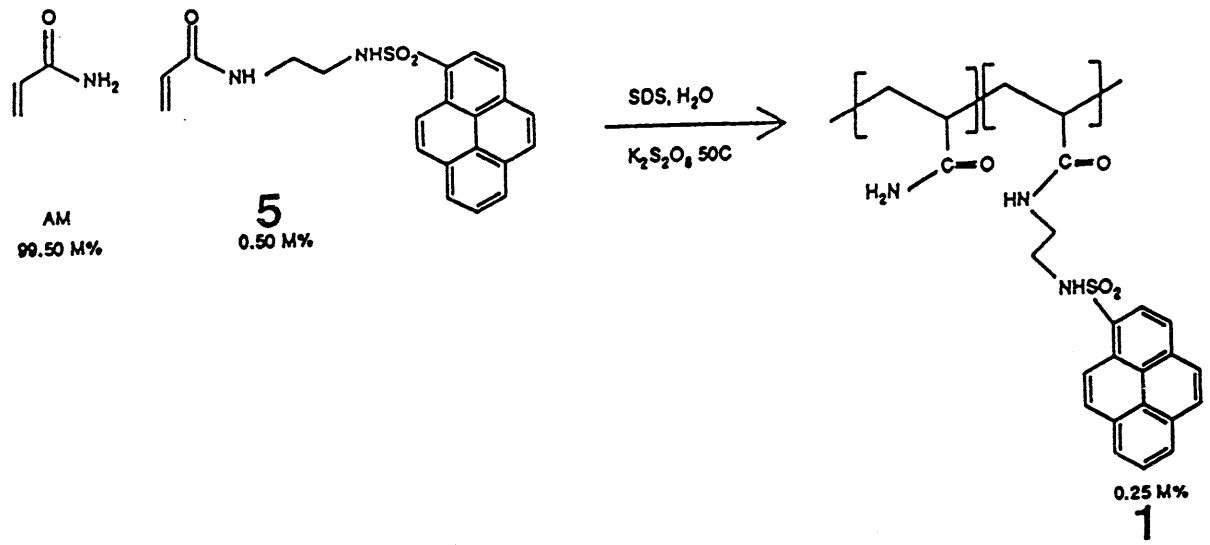

Scheme 5-4. Synthesis of Copolymer 1 via Surfactant Polymerization Technique.

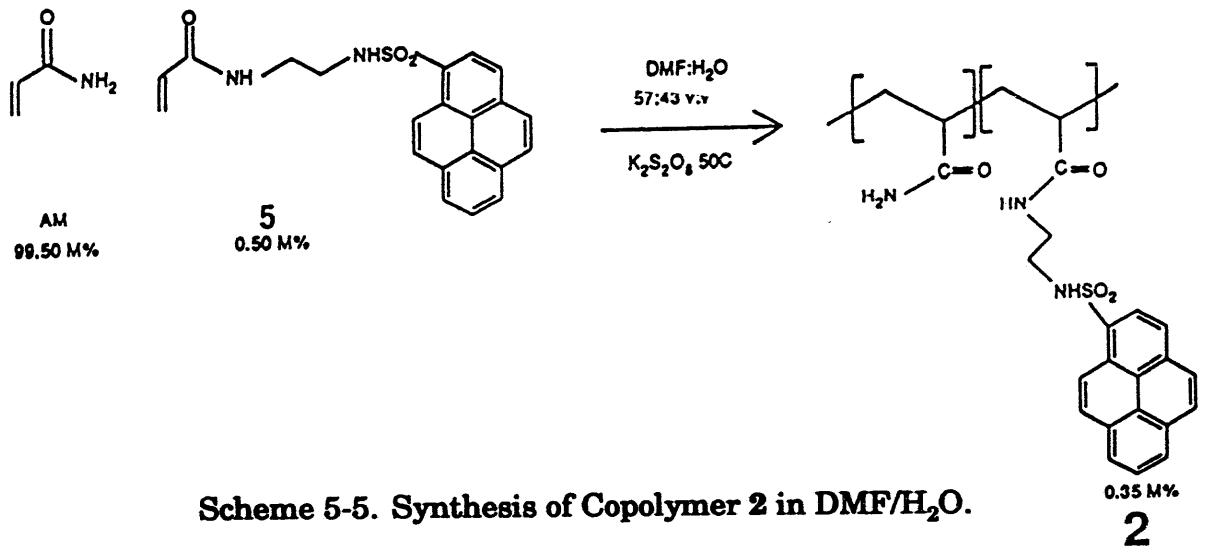

Scheme 5-5. Synthesis of Copolymer 2 in DMF/H_2O.

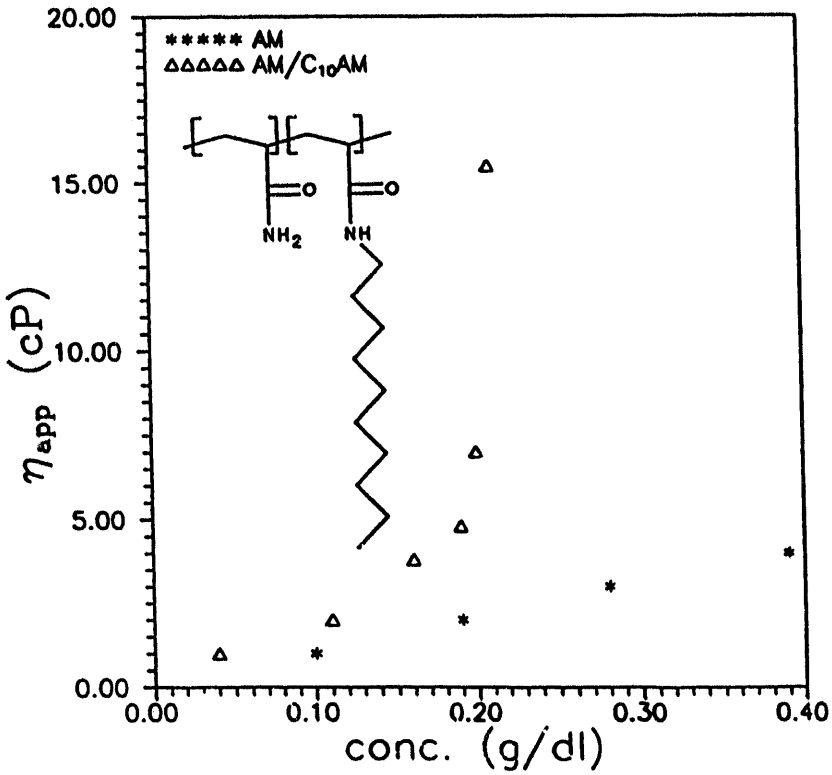

Figure 5-1. Illustration of Associative Behavior of Polyacrylamide Modified with 0.75 Mole % N-Decylacrylamide via Surfactant Polymerization.

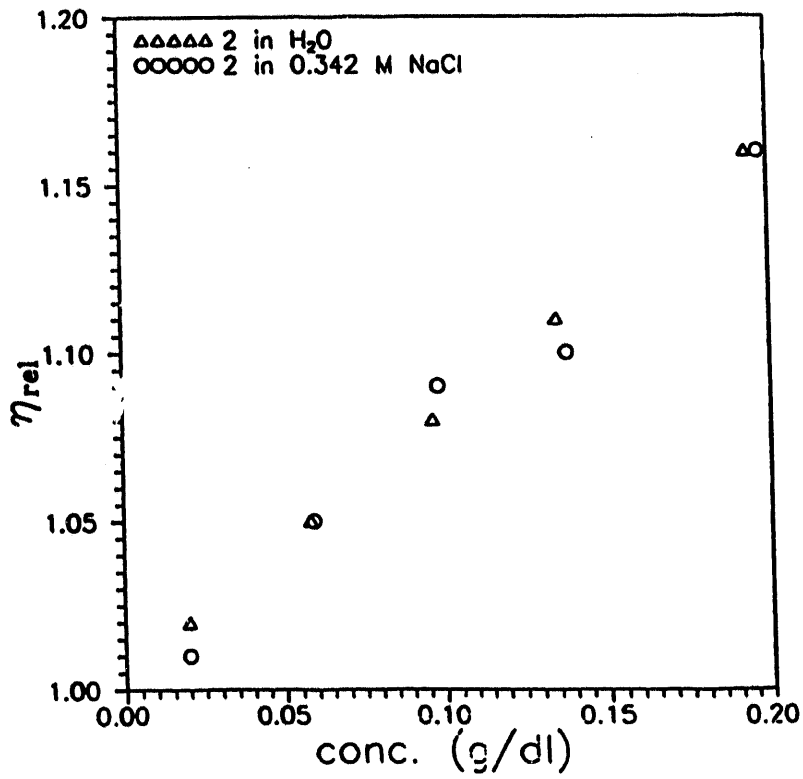

Figure 5-2. Relative Viscosity for Copolymer 2 in H_2O (Δ) and in NaCl (O) Solution.

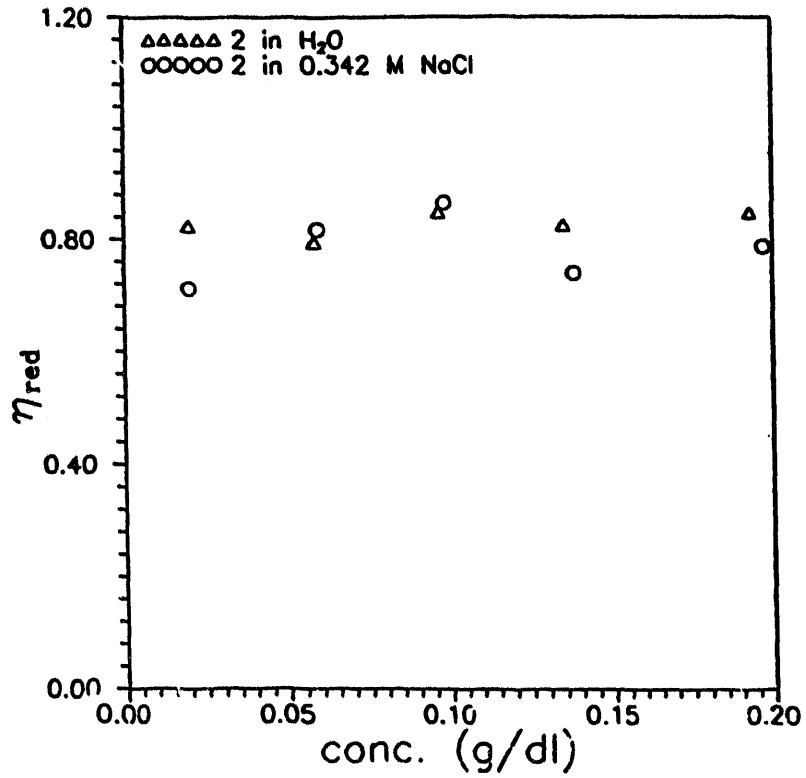

Figure 5-3. Reduced Viscosity vs. Concentration for Copolymer 2 in H_2O (Δ) and in NaCl (O).

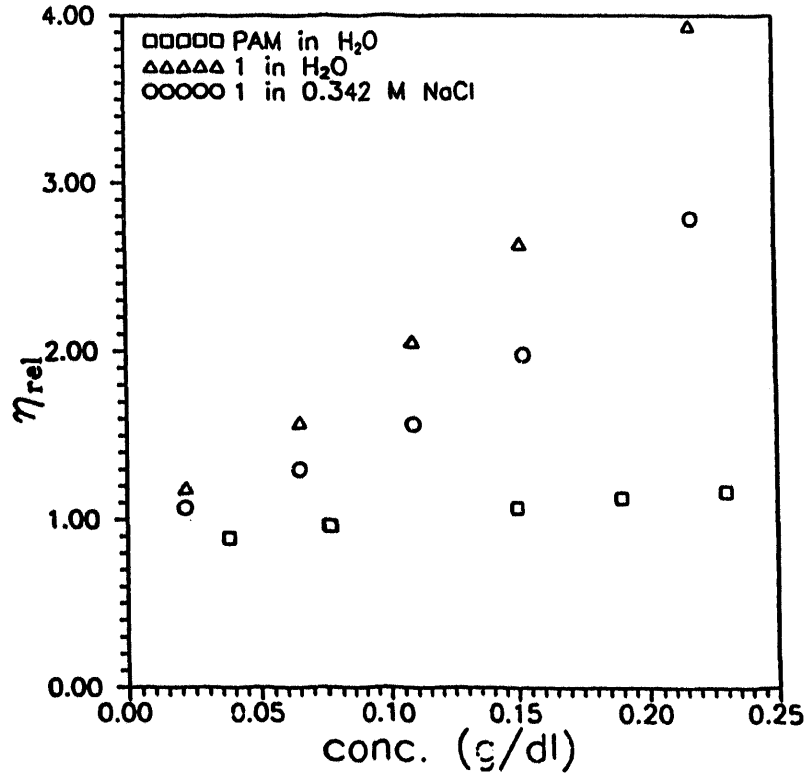

Figure 5-4. Relative Viscosity for Copolymer 1 in H_2O (Δ) and in NaCl (○) and for Acrylamide Homopolymer in H_2O (□).

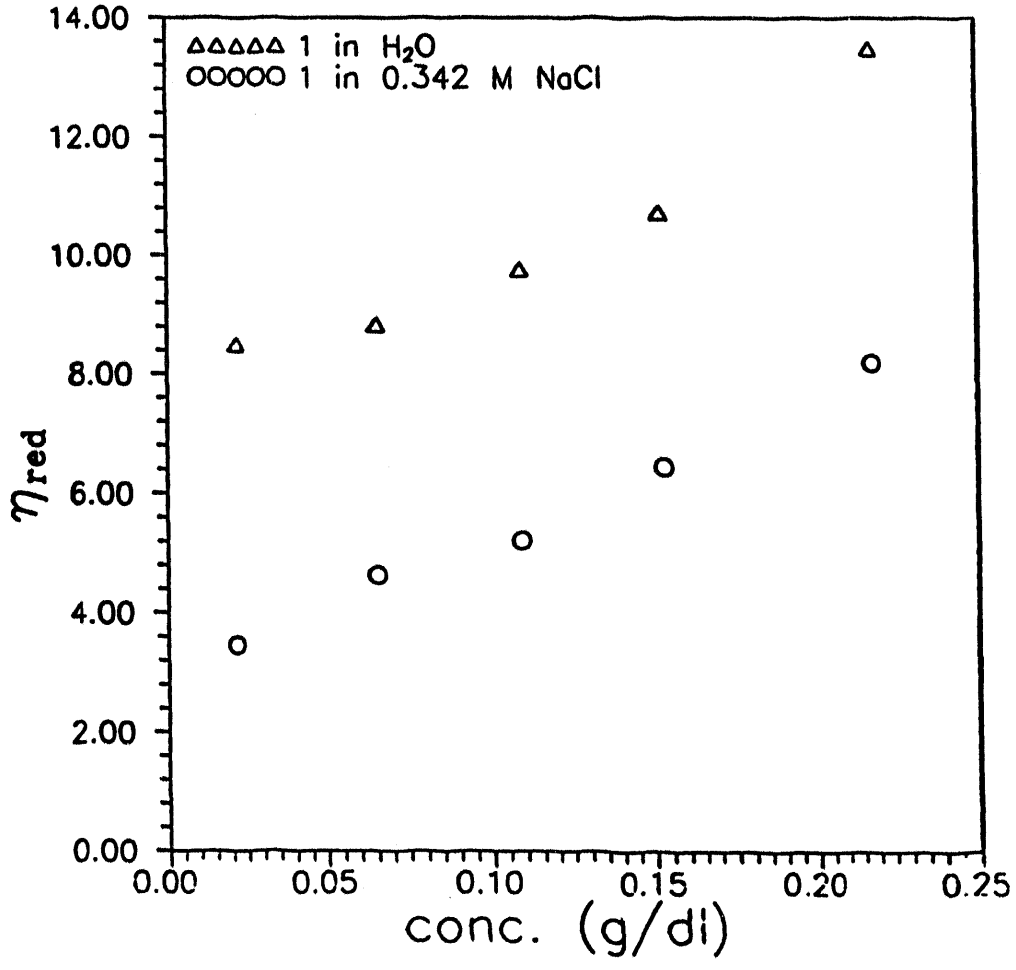

Figure 5-5. Reduced Viscosity vs.Polymer Concentration for Copolymer 1 in H_2O (Δ) and in NaCl (O).

CHAPTER SIX: PHOTOPHYSICAL STUDIES OF THE SOLUTION BEHAVIOR OF ASSOCIATIVE PYRENESULFONAMIDE-LABELLED POLYACRYLAMIDES

Abstract

Photophysical studies were conducted on copolymers of acrylamide containing less than 0.5 mole% of [1-β-aminoethyl sulfonamido-1-pyrene]acrylamide in order to relate aqueous solution behavior to molecular structure. The copolymer prepared via a surfactant technique was shown to possess some inherent blockiness or short runs of the pyrenesulfonamide label in dilute solution. Intermolecular associations were observed above a critical concentration of polymer. I_E/I_M values from steady state fluorescence paralleled the rheological response as a function of concentration. The copolymer prepared by solution polymerization showed random incorporation of the pyrenesulfonamide comonomer and no intermolecular association tendency over the concentration range studied. The pyrenesulfonamide labels were shown to form ground state aggregates within relatively accessible hydrophilic environments in both polymers. Associative thickening behavior observed in the surfactant-polymerized copolymer is consistent with microphase organization of hydrophobic pyrenesulfonamide aggregates above a critical concentration. Fluorescence quenching has been used to probe the micorenvironment around the label.

Introduction

Polymer solution behavior of polyelectrolytes has previously been elucidated via photophysical studies of pyrene-labelled water-soluble polymers including polyelectrolytes[1-5], poly(ethylene oxide)[6], (hydroxypropyl) cellulose[10-11] and poly(N-isopropylacrylamide)[12,36,37]. Particularly relevant work includes that of Winnik *et al.*[7-10] who studied pyrene-labelled hyroxypropyl(celluloses) which serve as model associative thickeners. Photophysical analysis demonstrated the aggregation of neutral hydrophobic polymers in aqueous media[7-10] and the interaction with surfactants[10-11] at the molecular level. Frank *et al.*[6] investigating the pyrene end-labelled poly(ethylene glycol) in aqueous media, showed the associative behavior at the molecular level via the photophysical response of the pyrene label. Molecular aspects of poly(ethylene glycol):poly(methyl methacrylate) polymer complexation have also been reported[13-15].

In this study, we have employed photophysical techniques and model compounds to analyze the molecular solution behavior of previously reported pyrensulfonamide-labelled polyacrylamides which display associative behavior in aqueous media[35] (Scheme 1). Copolymer **1** was synthesized by a surfactant or "micellar" technique, copolymer **2** in homogeneous solution using a cosolvent. Our goal is to correlate molecular solution behavior with macroscopic solution viscosity response in order to develop overall structure-property relationships for associative water-soluble polymers.

Experimental

Materials

Deionized water (DI H_20) used in these studies had a conductance less than $1x10^{-7}$ mho/cm. Cetylpyridinium chloride was recrystallized from methanol/diethyl ether. Nitromethane was distilled at atmospheric pressure. Other starting materials were purchased commercially and used as received.

Labelled Polymers/Model Compounds (Scheme 1)

The syntheses of pyrenesulfonamide-labelled copolymers **1** and **2** and model compounds, **3** and **4** are described in Chapter 5[35]. Labelled copolymer **1** and prepared via a surfactant copolymerization technique, and contains 0.25 mol% of a pyrenesulfonamide label. Copolymer **2** was synthesized via a solution copolymerization technique and contains 0.35 mol% of the pyrenesulfonamide label.

Synthesis of the Fluorescence Quencher N-methylpyridinium chloride

The method of Nakaro *et al.*[16] was modified. The basic procedure involves synthesis of N-methylpyridinium iodide with subsequent ion-exchange to give N-methylpyridinium chloride.

N-Methylpyridiunium iodide

Anhydrous pyridine, (26 ml, 25 g, 0.32 mol), was added to diethyl ether (250 ml). Methyl iodide (39 ml, 0.63 mol) in diethyl ether (50 ml) was added dropwise with stirring to the pyridine solution. After the addition was completed, the addition funnel was replaced with a condenser. Refluxing overnight resulted in a white solid precipitate. N-methylpyridinium iodide is very hygroscopic, therefore purification was accomplished by washing with multiple portions of diethyl ether under N_2. The ether washings were removed via a filter stick[17] which allowed a continuous inert atmosphere to be maintained. Vacuum drying at room temperature overnight gave a white solid, yield 53 g (76%).

N-Methylpyridinium chloride

N-methylpyridiunium iodide, (39 g, 16 mol), and silver chloride (35 g, 0.26 mol) were added to water (50 ml). This suspension was allowed to stir overnight in the dark under a nitrogen blanket. Filtration removed the lime-green silver iodide; the filter cake was washed with additional water (25 ml). To ensure completeness of exchange, the aqueous solution was then passed through a column containing Bio-Rad AG 1-X8 ion-exchange resin (10 cc, quaternary ammonium type, chloride form). The aqueous effluent tested negative for iodide (persulfate test) and positive for chloride (silver nitrate test). Freeze-drying of the aqueous solution produced a syrup which was

further dehydrated via azeotropic distillation with toluene. The resulting off-white solid mass was extremely hygroscopic; a nitrogen atmosphere was consistently maintained during all manipulations. Residual toluene was removed via a filter stick. Recrystallization from the minimum amount of boiling anhydrous 1-propanol gave N-methylpyridinium chloride as white crystals, which were washed with diethyl ether and vacuum-dried at room temperature. All weighings and transfers of this material as a solid were performed under dry nitrogen; storage was over phosphorus pentoxide. Elemental analysis of this compound indicated that 8.15% H_2O was retained. Recovery: 18 g (88 %). m.p. 138-140°C (sealed tube). Anal. Calcd. for C, 50.87; H, 6.99; Cl, 25.03; N, 9.88. Found: C, 50.58; H, 6.77; Cl, 24.66; N, 9.84. ^{13}C NMR (D_2O), TMS insert): 48.25 (-$\underline{C}H_3$); 128.04, 145.07, 145.30 (aromatic resonances). ^1H NMR (D_2O), TMS insert): 3.68 (-$\underline{C}H_3$); 7.33, 7.80, 8.07 (aromatic C-$\underline{H}$).

Polymer Characterization-General

Solution Preparation

Polymer stock solutions were prepared in water of 2% (w/w) aqueous sodium chloride at ca. 200 mg/dl. Several weeks of constant mechanical shaking were required for complete solubilization. Stock solutions were filtered through an 8 μm filter; a peristaltic pump was employed to pump the solution at a low flow rate. Dilution of stock solutions was performed gravimetrically. Samples were allowed to equilibrate for minimum of one week with constant mechanical shaking before characterization.

Characterization

Characterization techniques (other than photophysical) are described in Chapter 5[35].

Pyrenesulfonamide-Labelled Polymers and Model Compounds: Photophysical Characterization

Steady-State Fluorescence Studies

Steady-state emission studies were performed on a Spex Fluorolog-2 fluorescence spectrometer equipped with a DM3000F data system. All samples were run in the front-face mode to avoid inner filter effects. Slit widths were varied from 0.5-2.5 nm, depending on sample concentration. Samples were deaerated by bubbling with nitrogen for 25-30 min. Particularly "foamy" samples were sparged by first bubbling with helium, followed by argon. Excitation spectra were obtained via excitation from 250 to 400 nm while monitoring the emission intensity at either 418 nm (monomer emission) or 510 nm (excimer emission). Wavelength-dependent variations in lamp intensity were corrected by an instrumental correction function; rhodamine B was the internal reference. Detector and emission grating variations were also corrected via an internal function.

Steady-State Fluorescence Quenching

Approximately 200 mg of sample solution were degassed in a septum-capped fluorescence cuvette; a quencher solution was likewise degassed. The emission spectrum was then recorded as described previously. Intensities of the (0,2) (monomer, 400 nm) band were recorded in the absence of quencher (I_o). A microliter syringe was used to deliver aliquots, generally 1-3 μL, of the quencher solution to the sample. The sample cuvette was shaken and the diminished values of fluorescence intensity were recorded. A positive inert gas pressure was maintained in both the cuvette and quencher vial in order to exclude oxygen.

Transient Fluorescence Studies

A Photochemical Research Associates IPRA) single-photon counting instrument equipped with an H_2-filled 510-B flashlamp was used to obtain fluorescence decay curves. Fluorescence decay times were fit from decay profiles using either a Digital Micro PDP-11 or an IBM-PC. In either case, PRA software was used which employs a nonlinear iterative deconvolution technique to analyze decay curves.

Sample degassing was as described previously. Pyrensulfonamide-labelled materials were excited at 340 nm; decays were measured at 400 nm (monomer emission), 519 (excimer emission). We have found it important to use a minimal time-per-channel setting to avoid placement of counts in the lower time decades. An appropriate setting for these materials is 0.1786 ns/channel for a range of 512 channels; 10^4 counts were generally taken in the maximum channel.

Transient Fluorescence Quenching Studies

Sample handling was as described for the steady-state quenching experiments, except 400 mg of sample solution were employed. Excitation was at 340 nm; fluorescence decay profiles were obtained of the 400 nm (monomer) band as a function of quencher concentration.

Results and Discussion

Model Compound Photophysics

To assist in analyzing the photophysical properties of synthetic copolymers **1** and **2** containing the pyrenesulfonamide monomer, we prepared water soluble model compounds **3** and **4** with the pyrensulfonamide chromophore. The solubility of compound **4** in water is limited to $3x10^{-5}$ M despite the hydrophilic gluconamide group. Likewise the solubility of **3** is $6x10^{-5}$M at pH 7. At higher pH values the salt is more soluble ($1x10^{-2}$M).

The UV absorption spectra of **3** and **4** in DI H_2O are displayed in Figure 1 for comparative purposes. These spectra are essentially identical as would be expected since both possess the same chromophore. Steady-state fluorescence spectra of **3** and

4 (Figure 2) were recorded upon excitation at 340 nm, over the range of 350-600 nm. The three peak maxima characteristic of the monomer emission are 360 nm [0,0], 400 nm [0,2] and 418 nm [0,3]. In the concentration regime employed (10^{-5} M), the solutions are sufficiently dilute to preclude the formation of excimer. The fluorescence spectrum of a concentrated (ca 10^{-2} M) aqueous solution of the sodium salt of 3 is shown in Figure 3. The structureless red-shifted emission centered at about 520 nm can be assigned to excimer which forms at higher concentration levels. It should be noted that the salt of 3 may have surfactant characteristics which contribute to excimer formation.

The sulfonamide proton of the pyrenesulfonamide group is acidic; sulfonamides typically have pK_a values ranging from 10-12. The effect of pH on the emission was examined by recording fluorescence spectra of 3 (6×10^{-5} M) at pH 10.6 and 12.1. The intensity of the spectrum at pH 12.1 was one third of that at pH 10.6. The spectral shapes were identical. The diminished intensity of the spectrum acquired at higher pH is likely due to a lack of fluorescence from the sulfonamide anion. Use of this label as a fluorescent tag must therefore be limited to media of pH < 10.

Polymer Absorption and Steady-State Emission Spectra

UV Absorption Spectrum

Figure 4 shows the UV absorption spectra of pyrensulfonamide-labelled polymers 1 and 2 in DI H_2O. The absorption spectra above 220 nm are qualitatively identical to those for the model compounds 3 and 4 in Figure 1. This is evidence that the pyrenesulfonamide label has maintained its integrity during the polymerization process. However, the polymer absorption spectra in Figure 4 are red-shifted compared to those of the model compounds (Figure 1). Comparison of Figures 1 and 4 reveals that the polymer absorption extends to 400 nm; the model compounds, however, fail to absorb appreciably at wavelengths longer than 390nm. The significance of this effect will be further discussed in a later section.

Steady-State Emission

Steady-state emission spectra of surfactant-polymerized 1 and solution-polymerized 2 are shown in Figure 5. Both labelled polymers display the three peaks assigned to monomer emission, as shown for the model compounds in Figure 2. Excimer emission, centered around 519 nm, is also observed for the labelled polymers. Excimer emission is definitely a polymer-enhanced effect; since the content of the label is 7×10^{-5} M for copolymer 1 and 9×10^{-5} M for copolymer 2. No excimer intensity was observed for the model compounds in this concentration range (Figure 2).

Although 2 contains slightly more pyrenesulfonamide label (0.35 mole % for 2 and 0.25% mole % for 1), the excimer emission intensity of 1 is dramatically enhanced relative to 2. A greater *local concentration* of the label therefore exists for 1 relative

to **2**, strongly suggesting that microstructural differences exist between these polymers. We believe that copolymer **2**, prepared in homogenous solution, has a more random structure and surfactant-polymerized **1**, which possesses a blocky microstructure[35]. The microheterogeneous surfactant produces partitioning of the hydrophobic pyrenesulfonamide monomer within the micelle during copolymerization allowing some degree of blockiness even a low feed composition. Clearly the number of consecutive pyrensulfonamide label repeat units is determined to some extent by the pyrenesulfonamide monomer label-to-surfactant ratio. Effects of surfactant polymerization methods upon polymer microstructure have been noted elsewhere. In separate studies, Peer[18], and Dowling and Thomas[19], investigated copolymers synthesized from acrylamide and a hydrophobic comonomer by a surfactant copolymerization technique. The microstructures of these systems are also believed to have blocky characteristics. The copolymers demonstrated either intra- or intermolecular solution behavior[18], apparently depending upon the choice of hydrophobic comonomer, polymerization conditions and other factors.

The concentration dependence of excimer-to-monomer ratios, I_E/I_M, for the two copolymers is shown in Figure 6. The concentrations of the polymers were viewed over a range of 10^3, from 2.0×10^{-4} gm/dl to 0.2 gm/dl. The concentration dependence of I_E/I_M values are dramatically different. The I_E/I_M values for **2** , the polymer synthesized in homogeneous solution, show only a small concentration dependence, signifying little or no change in the pyrene environment and therefore in polymer conformation. However, I_E/I_M values for **1**, the polymer synthesized in the presence of surfactant, increase dramatically at concentrations above ca. 0.1 gm/dl, indicating that the pyrene groups are in an increasingly hydrophobic environment presumably caused by increasing intermolecular associations.

The increases of I_E/I_M values with polymer concentration (Figure 6) are paralleled by changes in viscosity, a bulk or macroscopic property. In Figure 7, I_E/I_M and reduced viscosity of copolymer **1** are plotted as a function of concentration. Viscosity and I_E/I_M both increase dramatically above a criticial concentration, C^* (ca. 0.1 gm/dl), providing strong evidence that intermolecular hydrophobic associations of the pyrenesulfonamide labels are responsible. As concentration increases, intermolecular hydrophobic association of the labels is facilitated. It has been proposed that hydrophobic molecules can locate each other at distances greater than 100 angstroms due to the strong influence of water-structuring[20-22]. This is reflected on a molecular level by enhancement of I_E/I_M values. On a macroscopic scale, hydrophobic associations are indicated by a sharp increase in the viscosity profile at C*. To our knowledge this represents the first associative thickener which relies on a fluorescence label as the sole hydrophobic moiety. Also, the parallel response of I_E/I_M and η_{red} vs concentration (Figure 7), along with previous literature studies allow rational suggestions to be made on the mode of the micellar or surfactant polymerization, as well as the nature of the aggregation responsible for the associative thickening phenomenon.

Concentration dependencies of η_{red} and I_E/I_M are shown in Figure 8 for copolymer **2** prepared in DMF/H_2O. The zero Huggins constant of the reduced viscosity vs concentration curve suggests a compact polymer conformation that is independent of polymer concentration. The I_E/I_M values confirm this premise. The microstructure of this polymer - random label distribution - no doubt strongly influences the polymer conformation. In water, the hydrophobic labels are compelled to aggregate by the hydrophobic effect. The random interspacing of the hydrophobe along the polymer backbone leads to compaction of the polymer coil due to intramolecular associations. Such a compact structure is reflected in the viscosity profile of **2**, as we have shown.

In order to further elucidate the nature of the hydrophobic associates, additional studies were conducted. Excitation spectra for polymers **1** and **2** are shown in Figures 9 and 10, wherein emission was monitored at both monomer (419nm) and excimer (510nm) wavelengths. In each case, the excitation spectrum of the excimer emission is red-shifted by 4 nm from the monomer excitation spectrum. This suggests that preformed, ground-state aggregates of the pyrenesulfonamide labels are the source of excimer emission. The loss of vibrational structure is consistent with ground state association.

Typically, in polymer systems, excimer emission results from chromophores which encounter one another through a diffusional process. A chromophore absorbs light, is promoted to the excited state, and, during its excited state lifetime, encounters a ground state chromophore. In this case, monomer and excimer excitation spectra are identical, since the initial absorbing species are identical. In our case, however, hydrophobic associations of the pyrenesulfonamide label appear to facilitate the formation of ground-state aggregates. Hydrophobic interactions of the pyrenesulfonamide labels provide a means for facilitating perturbation of the ground-state and yielding a species of lower energy. This results in a red-shift in both the absorption spectrum and the excitation spectrum when emission is monitored in the excimer, or perhaps more appropriately, excited aggregate region.

The phenomenon of pyrene absorption and excitation spectral shifts in the context of ground-state interactions has been previously documented. In a fundamental study, Avis and Porter[23] examined the photophysics of pyrene dissolved in a poly(methyl methacrylate) matrix as a function of pyrene concentration. At pyrene concentrations ≥ 0.01 mol dm^{-3}, excimer emission was observed and absorption and excitation spectra were red-shifted relative to the spectra of pyrene at lower concentrations. Van der Waals interactions of proximate pyrene molecules, resulting in aggregates of lower ground-state energy, were proposed to explain the observed spectral shifts.

Precedence also exists for the aggregation of pyrene-labelled, water-soluble polymers in aqueous media. Winnik and coworkers[7-10] have studied the aggregation behavior of pyrene-labelled (hydroxypropyl)celluloses in water. Excimer excitation

spectra were red-shifted relative to monomer excitation spectra indicating ground-state interactions of pyrene labels. No rise times were observed for the decay profiles, verifying the preformed nature of the aggregate. Frank and coworkers[6] have reported similar results for pyrene end-labelled poly(ethylene glycol) in H_2O. In both Winnik's and Frank's studies, comparative spectroscopic studies of pyrene-labelled polymers were performed in methanol as well as in water. No ground-state aggregation of the label moieties was observed in methanol, thus emphasizing the importance of the hydrophobic effect.

Additional evidence for aggregation in polymers **1** and **2** was obtained by excitation of aqueous solutions of **1** and **2** (Figure 11) at 395 nm. Emission in the monomer region is very low for both polymers (compare with Figure 2). The broad red-shifted emission dominates indicating that indeed the pyrene aggregate is responsible for excimer emission in solutions of **1** and **2**. The small amount of monomer emission which seems to be present could be due in part to dissociation of the excited aggregate.

Transient Emission Studies

Analysis of Transient Decay--Background.

The Birks[24,25] Scheme for excimer formation/dissociation indicates that monomer fluorescence decays as the sum of two exponential terms while the excimer decay can be described as the difference of two exponential terms. The Birks kinetic scheme adequately describes the transient decay behavior of low molar mass systems and some model polymer systems. However, many labelled polymer systems exhibit a complex decay response and this has been our experience with both **1** and **2**.

The fluorescence decay profiles of the models in water or dioxane are monomexponential (Table I). The difference in the lifetimes in water (ca.13 nsec) and dioxane (ca.30 nsec) is quite large, demonstrating the effect of microenvironmental polarity on the decay of the excited state.

The decay profiles of the two polymers **1** and **2** in aqueous solution were complex but could be approximately fit by a sum of two exponentials. In both cases, the decay curve could be fit to a longer lived component (ca.15 nsec) and a shorter lived component (ca.11 nsec). Detailed interpretation is impossible, probably because labels in many different environments are contributing to the emission decay. One point, however, is particularly informative. The decay profile of the monomer emission (400nm) of **1** is invariant, within experimental error, with change in the concentration from 2.2×10^{-3} g/dL to 2.2×10^{-1} g/dL. However, as noted previously, both reduced viscosity and the I_E/I_M ratio of **1** increase at concentrations on the order of 2.2×10^{-1} g/dL (Figure 7), It appears as though the local environment of the species responsible for emission at 400 nm in **1** is modified

little, if at all, as polymer aggregation occurs.

While it is difficult to interpret the excimer decay profile of the polymer samples, it is worth noting that the excimer decay profiles of **1** and **2** obtained at 550 nm do not exhibit a rise time (characteristic of the diffusion time for excimer formation.) The rise times at 550 nm (excimer or excited aggregate emission region) and 400 nm (monomer emission region), are essentially identical. Although specific decay times were not obtained, in general we note that the decay profile has a long lived decay component on the order of 30 nsec. The decay profiles in the excimer region suggest the presence of a ground state dimer. This idea is supported by the work of Wang *et al.*[28] who performed picosecond excimer fluorescence spectroscopy on poly(1-pyrenylmethyl-methacrylate) in chloroform. In this study an essentially instantaneous rise was observed for the excimer fluorescence profile on a picosecond time scale, signifying ground-state interactions of the pendent pyrene moieties.

For pyrene labelled hydroxypropyl cellulose, Winnik *et al.*[7] also identified ground-state pyrene aggregates via excitation spectra and the lack of a rise time for the excimer decay. Frank and coworkers[27] also attributed the emission of pyrene end-labelled PEG to excitation of preformed pyrene aggregates.

Quenching Studies.

In order to further probe the microenvironment of the pyrene fluorophore, the fluorescence of the polymers and the model compounds was quenched by nitromethane (N), iodide ion (I), methyl pyridinium chloride (MPC), and cetylpyridinium chloride (CPC). In the case of N and I, quenching data fit the Stern-Volmer equation (1),

$$I_o/I = 1 + K_{SV}[Q] \qquad (1)$$

where K_{SV} = $k_Q\tau_o$
and I_o = emission intensity in the absence of quencher, Q
I = emission intensity in the presence of Q
[Q] = quencher concentration
K_{SV} = Stern-Volmer quenching constant
k_Q = quenching rate constant
τ_o = lifetime of unquenched fluorophore

such that plots ('Stern Volmer Plots') of I_o/I vs.[Q] were linear for [Q] <ca.0.01M. The same plots for MPC and CPC quenching frequently showed upward curvature (Figures 12 to 15), even at low concentrations of Q, indicative of both static (complexation of Q to fluorophore) and dynamic quenching processes. Attempts to fit these curved plots using several currently available kinetic treatments[36,37] failed. Thus, we will discuss the results using the simplest possible kinetic model (Equation 2) for static plus dynamic quenching of a fluorophore M, by Q, in which K_G is the association constant for formation of the complex, MQ. Provided the extinction coefficients of M and MQ

at the wavelength of excitation are the same (i.e. Q does not significantly perturb the absorption spectrum of M), the excited complex MQ* is non-fluorescent, and MQ* does not revert significantly to M*, then the modified Stern-Volmer expression (2) holds.[29] This reduces to (3) for purely static quenching ($K_{SV} = 0$). This has

$$I_o/I = 1 + (K_{SV} + K_Q)[Q] + K_{SV}K_Q[Q]^2 \quad (2)$$

$$I_o/I = 1 + (K_Q[Q] \quad (3)$$

the same I_o/I vs. [Q] dependence as purely dynamic quenching but can be distinguished from the latter by measurement of the fluorophore lifetime in the absence (τ_o) and presence (τ) of Q for which equation (4) applies. Thus,

$$\tau_o/\tau = 1 + K_D[Q] \quad (4)$$

for purely dynamic quenching $K_{SV} = K_D$ whereas for purely static quenching $K_D = 0$, i.e. the fluorophore lifetime is independent of [Q], although the fluorescence intensity drops as [Q] increases. Finally, from equation (2), the slopes of upwardly curving Stern-Volmer plots should tend to a value of $(K_{SV} + K_Q)$ approaches 0.

Stern-Volmer constant (K_{SV}) for quenching of monomer emission at 400 nm by N, an amphiphilic quencher, and I, an anionic heavy atom quencher, are given in Table II. From the known lifetimes (τ_o) of the fluorophores (Table I) of the model compounds, both N and I quench fluorophore fluorescence at or near the diffusion-limited rate ($k_Q = 4 = 7 \times 10^9 M^{-1}s^{-1}$). Exact quenching constants (k_Q) were not calculated for the polymers **1** and **2** since a single fluorescence lifetime was not obtained for these materials. However, it is worth noting that K_{SV} values for models **3** and **4** are consistently greater than those for the polymer bound labels. The (approximately) two component fluorescence decay of the polymers, with $\tau \sim 15$ and 11 ns, has a similar 'average' lifetime to the single component decay ($\tau_o \sim 13$ ns) of the models (Table I), suggesting k_Q for the polymers is two to four times smaller than k_Q for the models. This is attributable to the bulk of the polymers and the enhanced viscosity of the medium. The approximate k_Q values for the polymers (ca. $1 \rightarrow 4 \times 10^9 M^{-1}s^{-1}$) are in the range of being diffusion-limited and indicate ready accessibilitly of these quenchers to the pyrene label.

In order to further probe the hydrophobicity of the labelled polymers, CPC, a hydrophobic quencher, was employed for intensity quenching. CPC is a surfactant with a critical micelle concentration (CMC) of 8×10^{-4} M[28]; its pyridinium ring is an oxidative quencher. For comparative purposes, N-methyl-pyridinium chloride (MPC), a less hydrophobic analog of CPC, was also used.

Figures 12-15 are the monomer intensity quenching curves (Stern Volmer plots) of the pyrenesulfonamide model compounds and labelled polymers for the alkyl pyridinium quenchers. Fluorescence quenching of **1** and **2** by CPC is shown for two

label concentrations (Figures 14 and 15). In no instance did we observe evidence of exciplex formation in either absorption or emission spectra. Many of the plots show upward curvature. This is probably indicative of a combined static and dynamic quenching process. In the case of MPC quenching of fluorescence of **3** and **4** (Figure 12), the curvature of the plots is less pronounced than for CPC, despite the fact that concentrations of MPC were typically over a hundred times greater than for CPC. Stern-Volmer plots for MPC quenching of fluorescence of **1** and **2** (Figure 12) are essentially linear. In all other cases we estimated initial slopes of Io/I vs. [Q] plots. Some experiments were also conducted in which fluorophore lifetimes were measured in the presence of Q in order to obtain K_D and k_Q via equation (4).

A summary of the data for fluorescence quenching of **1**, **2**, **3**, and **4** by MPC and CPC is given in Table III. In the case of fluorescence of **3** quenched by CPC (Figure 13) a very large initial slope (35000 M^{-1}) was obtained. This is attributed to complexation of the large hydrophobic carboxylate anion of **3** (a carboxylic acid, but above its pK_a) with the large hydrophobic cation, CPC. Quenching of fluorescence of **4** by MPC (Figure 12) must be almost entirely a dynamic process since $K_{SV} \sim K_D \sim 35$ M^{-1}. The quenching rate constant for this process is $2.7 \times 10^9 M^{-1}s^{-1}$ since $\tau_o = 13.1$ ns for **4** in DI H_2O (Table I). In contrast, CPC quenching of fluorescence of **4** (Figure 13) gave an initial slope of $4000 M^{-1} >> K_D = 60$ M^{-1}, indicating a large component of static quenching by CPC. Since **4** is neutral (in contrast to 3), its association with CPC is hydrophobically driven. A hydrophobic salt is formed which is non-fluorescent and leads to predominantly static quenching, in contrast to MPC, which quenches by a purely dynamic mechanism. For CPC quenching of the fluorescence of **4** a value of $k_Q = 4.6 \times 10^8$ $M^{-1}s^{-1}$ can be obtained from K_D and τ_o. Thus, dynamic quenching of fluorescence of **4** by both MPC and CPC occurs at near diffusion limited rates.

The analysis of MPC and CPC quenching data for the polymers **1** and **2** is hindered by the complex fluorescence decay behavior of the label in the polymer. This precludes our obtaining k_Q values for the polymers using equation (4). However, careful examination of the Stern Volmer plots of I_o/I vs [Q] leads to some intriguing conclusions. Thus, MPC quenching of fluorescence of **1** and **2** (Figure 12) gives essentially identical, linear Stern-Volmer plots with slopes of 18 and 20 M^{-1}, respectively. The linear plots indicate either purely dynamic (slope = K_{SV}) or purely static (slope + K_Q) quenching. Concentrations of MPC in the same range used for the I_o/I vs. [Q] experiments, markedly reduced the (non-exponential) decay of fluorescence of **1** and **2**[28]. Although it is not meaningful to obtain a k_Q value for such a non-exponential decay, this result indicates that MPC quenches the fluorescence of the polymers by a predominantly dynamic, diffusional process. In this respect MPC is analogous to both N and I in its quenching behavior. Once again, the lower values of KSV for polymers **1** and **2** relative to models **3** and **4** can be attributed to the bulk of the polymers and the enhanced viscosity of the medium.

The CPC quenching of fluorescence of low concentrations of **1** and **2** (Figure 14) give quite a different result from the MPC quenching. The Stern Volmer plot for the surfactant polymer **1** plus CPC is approximately linear with a slope of ca. 3800 M^{-1} for [CPC] < ca. 4 x 10^{-4}M whereas the plot for the solution polymer **2** plus [CPC] is distinctly curved upwards over the same range of [CPC] with a much lower initial slope of ca. 1900 M^{-1}. The near linear plot for CPC and its high slope must be a consequence of predominantly static quenching with K ~ 3800 M^{-1}. Assumption of dynamic quenching (i.e. K_{SV} ~ 3800 M^{-1}) would lead to an unreasonably high k_Q of ca. 3 x 10^{11} $M^{-1}s^{-1}$ if τ_o = 13 ns is assumed for the polymer. Indeed, the slope of 3800 M^{-1} for **1** plus CPC is very similar to the value of 4000 M^{-1} obtained for neutral model **4** plus CPC. We note that the (nonexponential) fluorescence decay is minimally affected by addition of CPC quencher relative to MPC -- thus verifying the static nature of the CPC-polymer label interaction[38]. Presumably association of both **1** and **4** with CPC is hydrophobically driven. The solution polymer **2** also gives a large but lower initial slope (1900 M^{-1}) of the Stern Volmer plot for CPC quenching. The lower initial slope indicates less complexation and the curvature of the plot suggests a larger contribution of dynamic quenching for this polymer with randomly spaced pyrene labels. Stern-Volmer plots for quenching of the fluorescence of higher concentrations of **1** and **2** by CPC are shown in Figure 15. Both plots show marked upward curvature most probably a consequence of the CPC concentrations (up to 5 x 10^{-4}M) being comparable to label concentrations. Once again the effect of CPC on the fluorescence of **1** is greater than on fluorescence of **2** at low [CPC], suggesting the surfactant quencher interacts more strongly with polymer **1** that has blocks of hydrophobic pyrene labels. Thus hydrophobically modified polymers form (static) hydrophobic aggregates with surfactants such as CPC, even below the critical micelle concentration of the surfactant. Formation of such aggregates is the dominant mechanism of fluorescence quenching by CPC, the effect being most striking for the surfactant polymer **1**. Such polymer-surfactant complexes are of interest from both fundamental[30] and pratical[31] points of view. It may also be significant that, at low polymer concentrations, K_{SV} for fluorescence of **1** quenched by CPC is about twice as large as the initial slope for **2** quenched by CPC (recall that KSV values for **1** and **2** plus MPC are essentially identical). This may indicate that the hydrophobic CPC has some preference for association with the blocky regions of **1** rather than the more randomly spaced hydrophobic labels in **2**. A number of other groups[1,10,11,32-34] have employed photophysical techniques to observe surfactant interactions with pyrene-labelled polymers. Our study differs in that we have also employed a quenching process to observe these interactions.

Conclusions

This work dealt with the photophysics of pyrenesulfonamide-labelled water-soluble polymers prepared by either a microheterogeneous surfactant copolymerization technique or by a homogeneous solution polymerization technique. The surfactant copolymerization technique yielded a pyrensesulfonamide-labelled copolymer **1**, which

proved to be a model associative thickener. Viscosity profiles of this polymer in aqueous media exhibit a low critical overlap concentration--typical associative thickener behavior. A blocky microstructural tendency was demonstrated for this polymer I_E/I_M ratios of the pyrenesulfonamide label. This microstructure is a consequence of the microheterogeneity present during the surfactant copolymerization. Hydrophobic interactions of the label, as evidenced by I_E/I_M, parallel that of the viscosity profile. The viscosity response of the polymer is therefore driven by the molecular, hydrophobic interactions of the pyrensulfonamide label. These hydrophobic interactions lead to a formation of static, ground state aggregates of the pyrene labels as denoted by excitation studies and lifetime measurements. Quenching studies of the pyrenesulfonamide label imply that it resides in an open, aqueous environment accessible to hydrophilic quenchers such as iodide ion. The hydrophobic character of the label was verified by its interactions with the hydrophobic CPC quencher - a static hydrophobic complex was formed.

The solution polymerization technique gave a pyrenesulfonamide-labelled copolymer **2**, with largely intramolecular associative behavior. Fluorescence measurements suggested this copolymer has a random microstructure, as would be expected to result from the copolymerization of two acrylamide monomers in a homogeneous medium. The random microstructure of this polymer appears to facilitate a compact conformation due to intramolecular hydrophobic interactions of the interspaced pyrenesulfonamide label. The Huggins profile of this polymer in aqueous solutions has zero slope, demonstrating a compact, non-interacting conformation. On a molecular level I_E/I_M values are independent of polymer concentration, paralleling the viscosity response of this system. Associations of the pyrene label are also static. Although the polymer conformation is compact, fluorescence quenching and lifetime measurements suggest the pyrenesulfonamide labels reside in a relatively aqueous microenvironment, and are approached and encountered by small molecules at or near the diffusional rate. Quenching of this copolymer with the hydrophobic CPC confirmed the hydrophobic character of the pyrenesulfonamide label and its tendency to form static aggregates via hydrophobic associations in H_2O.

In summary, we have employed photophysical techniques to elucidate the associative behavior of pyrenesulfonamide-labelled polyacrylamides in aqueous media. Correlations between macroscopic (visocmetric) and molecular (photophysical) characterization methods have allowed us to develop structure-property relationships for systems in which the pyrenesuflonamide moiety serves as the sole hydrophobe responsible for associative behavior.

References

1. Herkstroetrer, W. G.,; Martic, P.A.; Hartman, S. E.; Williams, J. L. R.; Faird, S. *J. Polym. Sci., Polym. Chem. Ed.*, **1983**, *21*, 2473.

2. Chu, D. Y.; Thomas, J. K. *Macromolecules*, **1984**, *17*, 2142.

3. Turro, N. J.; Arora, K. S. *Polymer*, **1986**, *27*, 783.

4. Arora, K. L.; Turro, N. J. *J. Polym. Sci., Polym. Chem. Ed.*, **1987**, *25*, 259.

5. Stramel, T. D.; Nguyen, C.; Webber, S. E.; Rodgers, M. A. J. *J. Phys. Chem.*, **1988**, *92*, 2934.

6. Char, K.; Frank, C. W.; Gast, A. P.; Tang, W. T. *Macromolecules*, **1987**, *20*, 1833.

7. Winnik, F. M.; Winnik, M. A.; Tazuke, S.; Ober, C. K. *Macromolecules*, **1987**, *20*, 38.

8. Winnik, F. M. *Macromolecules*, **1987**, *20*, 2745.

9. Winnik, F. M. *Macromolecules*, **1989**, *22*, 734.

10. Winnik, F. M. *J. Phys. Chem.*, **1989**, *93*, 7452.

11. Winnik, F. M. *Langmuir*, **1990**, *6*, 522.

12 Winnik, F. M. *Macromolecules*, **1990**, *23*, 233.

13. Oyama, H. T.; Tang, W. T.; Frank, C. W. *Macromolecules*, **1987**, *20*, 1839.

14. Hemeker, D. J.; Garza, V.; Frank, C. W. *Macromolecules*, **1990**, *23*, 4411.

15. Oyama, H. T.; Hemeker, D. J.; Frank, C. W. *Macromolecules*, **1989**, *22*, 1255.

16. Nakaro, Y.; Komiyama, J.; Iijima, *J. Coll. Polym. Sci.*, **1987**, *265*, 139.

17. Horak, V.; Crist, D. R. *J. Chem. Ed.*, **1975**, *52*, 665.

18. Peer, W. J. In *Polymers in Aqueous Media*; Glass, J. E., Ed.; Advances in Chemistry Series No. 223; American Chemical Society: Washington, D. C., 1989, p. 411.

19. Dowling, K. C.; Thomas, J. K. *Macromolecules*, **1990**, *23*, 1059.

20. Israelachvili, J.; Pashley, R. *Nature*, **1982**, *300*, 341.

21. Israelachvili, J.; *Acc. Chem. Res.*, **1987**, *20*, 415.

22. Char, K.; Frank, C. W.; Gast, A. P. *Macromolecules*, **1989**, *22*, 3177.

23. Avis, P.; Porter, G. *J. Chem. Soc.*, Faraday Trans. 11, **1974**, *70*, 1057.

24. Birks, J. B. *Photophysics of Aromatic Molecules*; Wiley-Interscience; New York, 1970, Chapter 7.

25. Winnik, M. A.; Pekcan, O.; Egan, L. *Polymer*, **1984**, *25*, 1767.

26. Wang, F. W.; Lowry, R. E.; Cavanagh, R. R. *Polymer*, **1985**, *26*, 1657.

27. Char, K.; Gast, A. P.; Frank, C. W. *Langmuir*, **1988**, *21*, 989.

28. Kalyanasundaram, K. *Photochemistry in Microheterogeneous Systems*; Academic: Orlando, **1987**, p. 126.

29. Lakowicz, J. R. *Principles of Fluorescence Spectroscopy*; Plenum: New York, **1983**, Chapter 9.

30. Goddard, E. D. *Colloids Surf.*, **1986**, *19*, 255.

31. Breuer, M.M.; Robb, I. D. *Chem. Ind.*, **1972**, 530.

32. Chankdar, P.; Somasundaran, P.; Turro, N. J. *Macromolecules*, **1988**, *21*, 950.

33. Winnik, F. M.; Ringsdorf, H.; Venzmer, J. *Langmuir*, **1991**, *7*, 905.

34. Winnik, F. M.; Ringsdorf, H.; Venzmer, J. *Langmuir*, **1991**, *7*, 912.

35. McCormick, C. L.; Ezzell, S. A.; previous paper in this series submitted to *Macromolecules*.

36. Chu, D.; Thomas, J. K. *J. Am. Chem. Soc.*, **1986**, *108*, 6270.

37. Ettink, M. R.; Ghiron, C. A. *J. Phys. Chem.*, **1976**, *80*, 486.

38. Ezzell, S. A.; Ph.D. dissertation, University of Southern Mississippi, **1990**.

Table I - Fluorescence

Lifetimes of Model Compounds in Homogeneous Solution[a]

Sample	Solvent	C, M	T, ns
3	H_2O	2.5×10^{-7}	13.3
	Dioxane	2.6×10^{-7}	30.9
4	H_2O	3.1×10^{-7}	13.1
	Dioxane	3.1×10^{-7}	30.3

[a]Excitation at 340 nm, monitoring at 400 nm

Table II. Quenching of Fluorecence[a] of Polymers 1 and 2 and Model Compounds 3 and 4 by Nitromethane (N) and Sodium Iodide (I) in Water

Compound	Q	[Polymer]g/dl	[label],M	K_{SV}, M^{-1}	k_Q, $M^{-1}s^{-1}$
3	N	-	2.5×10^{-8}	49	3.7×10^{9}
4	N	-	3.1×10^{-7}	58	4.4×10^{9}
1	N	2.18×10^{-1}	7.1×10^{-5}	11	-
1	N	2.18×10^{-3}	7.1×10^{-7}	23	-
2	N	1.93×10^{-1}	9.3×10^{-5}	12	-
2	N	1.93×10^{-3}	9.3×10^{-7}	17	-
3	I	-	1.8×10^{-7}	74	5.6×10^{9}
4	I	-	2.6×10^{-7}	85	6.5×10^{9}
1	I	2.0×10^{-3}	6.5×10^{-7}	49	-
2	I	2.2×10^{-3}	1.1×10^{-6}	43	-

[a]Excitation at 340 nm, quenching at 400 nm.

Table III. Quenching of the Fluorescence[a] of Polymers and Model Compounds by Methyl Pyridinium Chloride (MPC) and Cetyl Pyridinium Chloride (CPC) in Water

Compound	Q	[Polymer]g/dl	[label],M	Slope, M^{-1}	k_D, M^{-1}
3	MPC	-	1.8×10^{-7}	58[b]	-
3	CPC	-	1.8×10^{-7}	35,000[b]	-
4	MPC	-	2.6×10^{-7}	36[b]	35
4	CPC	-	2.6×10^{-7}	4,000[b]	60
1	MPC	2.0×10^{-3}	6.5×10^{-7}	18[c]	-
2	MPC	2.2×10^{-3}	1.1×10^{-6}	20[c]	-
1	CPC	2.0×10^{-3}	6.5×10^{-7}	3,800[c]	-
2	CPC	2.0×10^{-3}	1.0×10^{-6}	1,900[b]	-
1	CPC	2.0×10^{-1}	6.5×10^{-5}		-
2	CPC	2.0×10^{-1}	1.0×10^{-4}		-

[a]Excitation at 340 nm, monitoring at 400 nm.
[b]Non-linear Stern-Volmer plots. The slope is at the linear portion at low [Q].
[c]Slopes at linear Stern-Volmer plots.

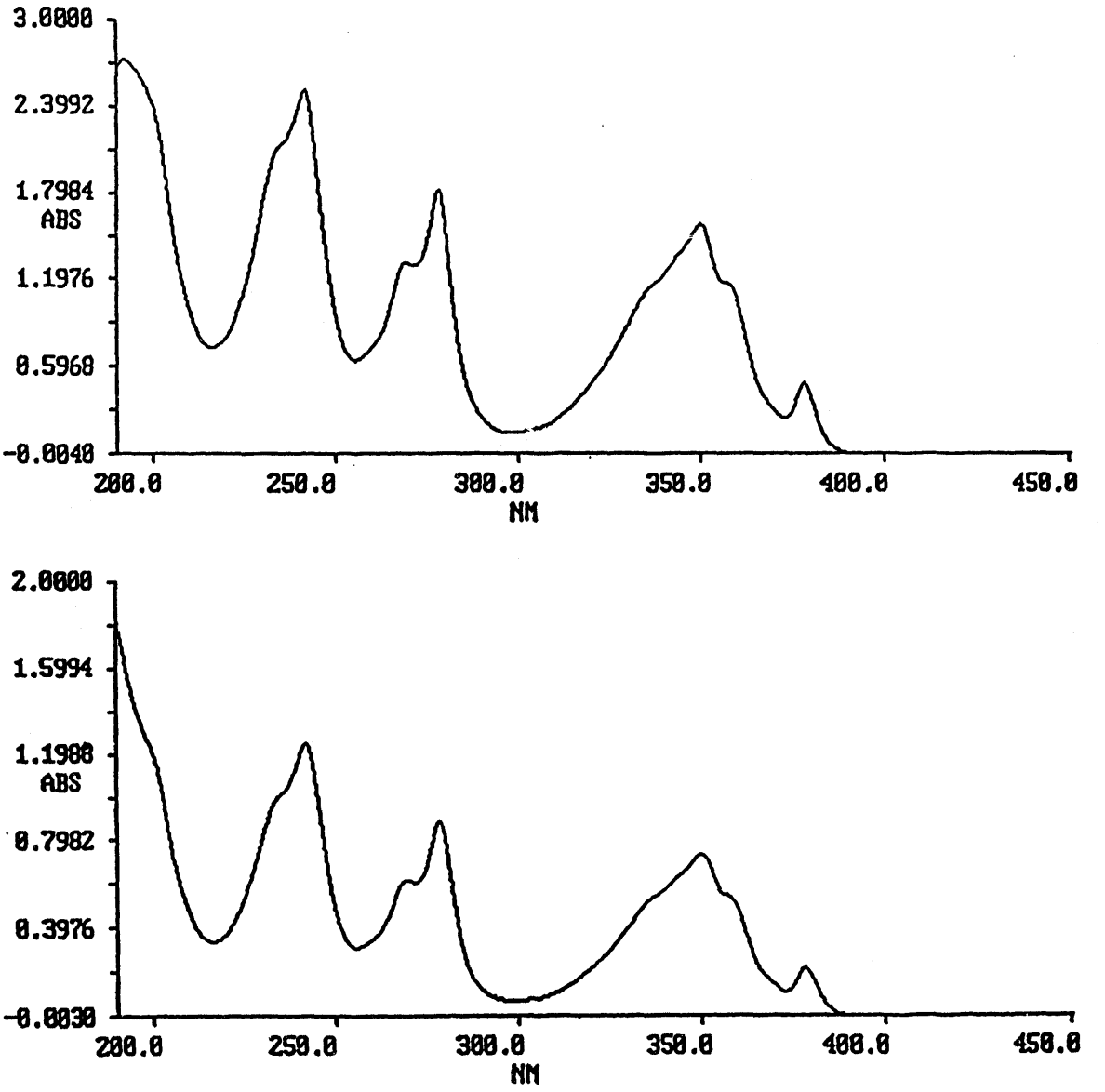

Figure 6-1. UV Absorption Spectra of **3** (Top) and **4** (Bottom) in H_2O (C = 10^{-5} M).

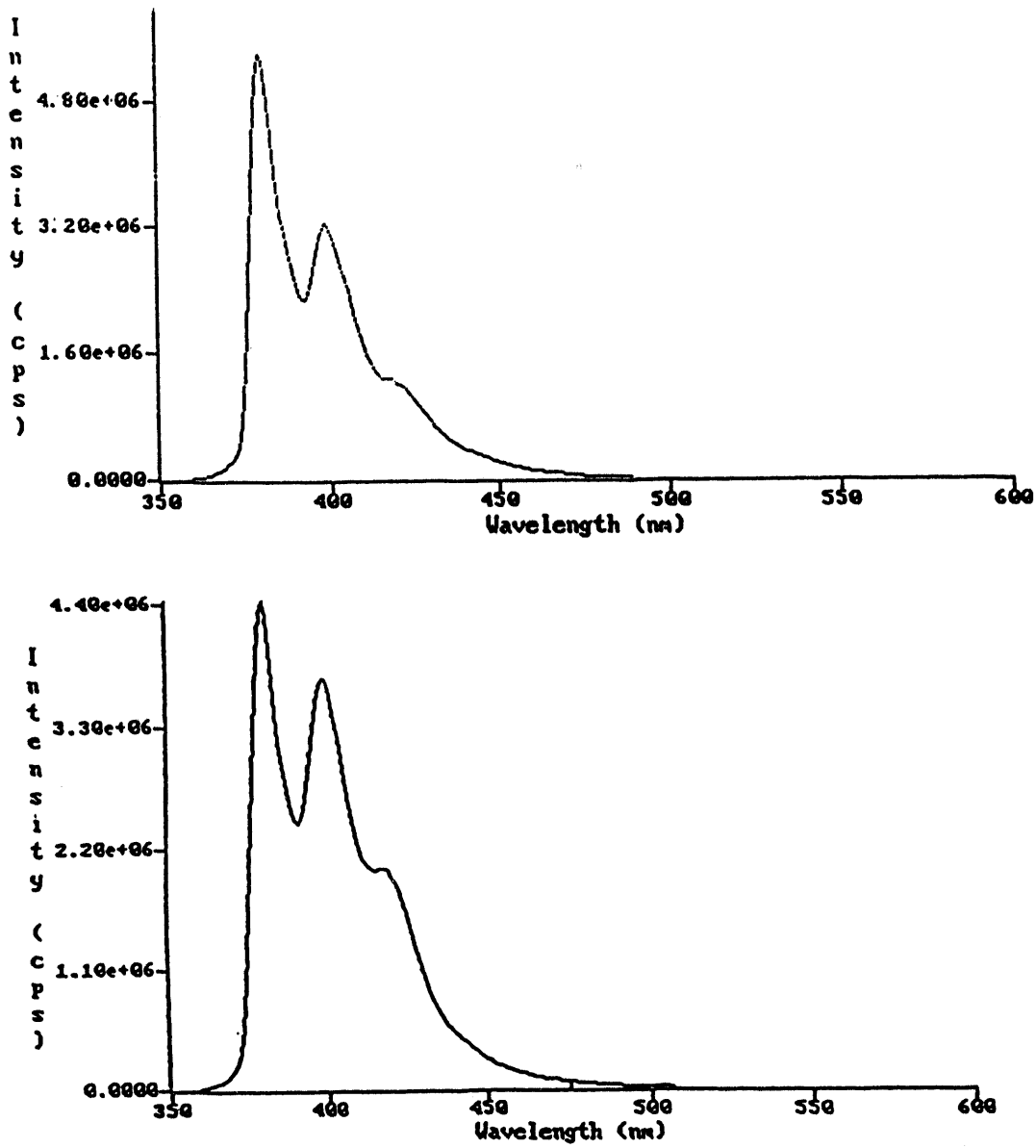

Figure 6-2. Steady-State Fluorescence Spectra of 3 (Top) and 4 (Bottom) in H_2O ($C = 10^{-5}$ M).

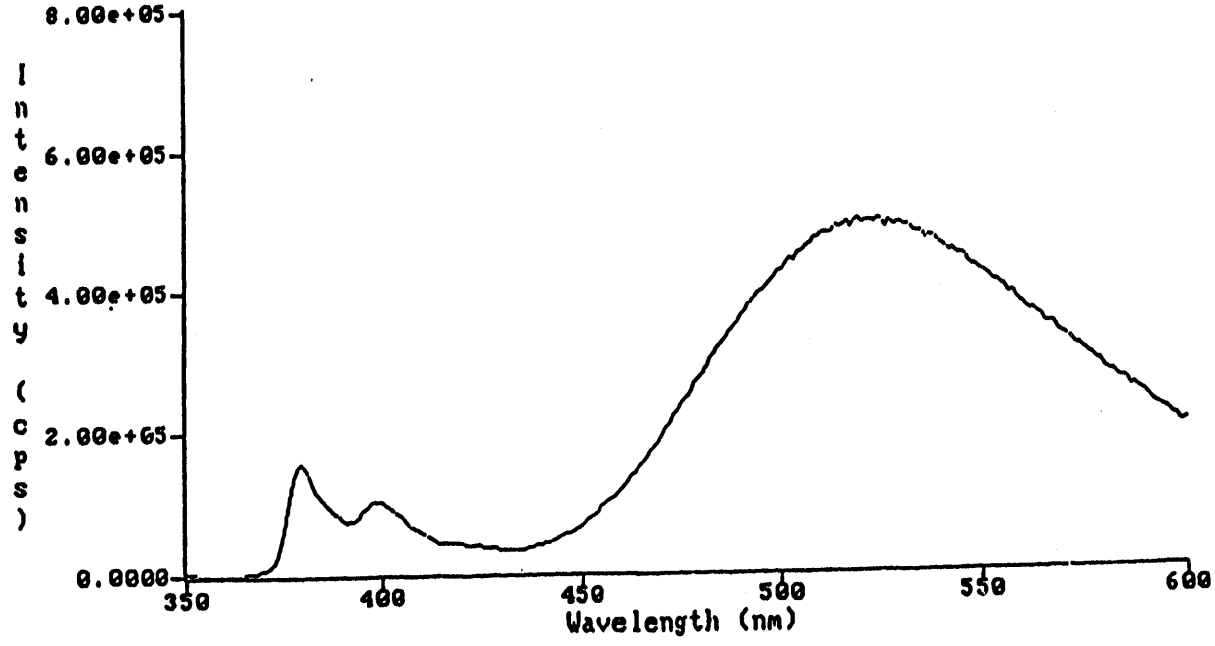

Figure 6-3. Steady-State Emission Spectrum of 3 (Sodium Salt, C ≈ 10^{-2} M) in H_2O.

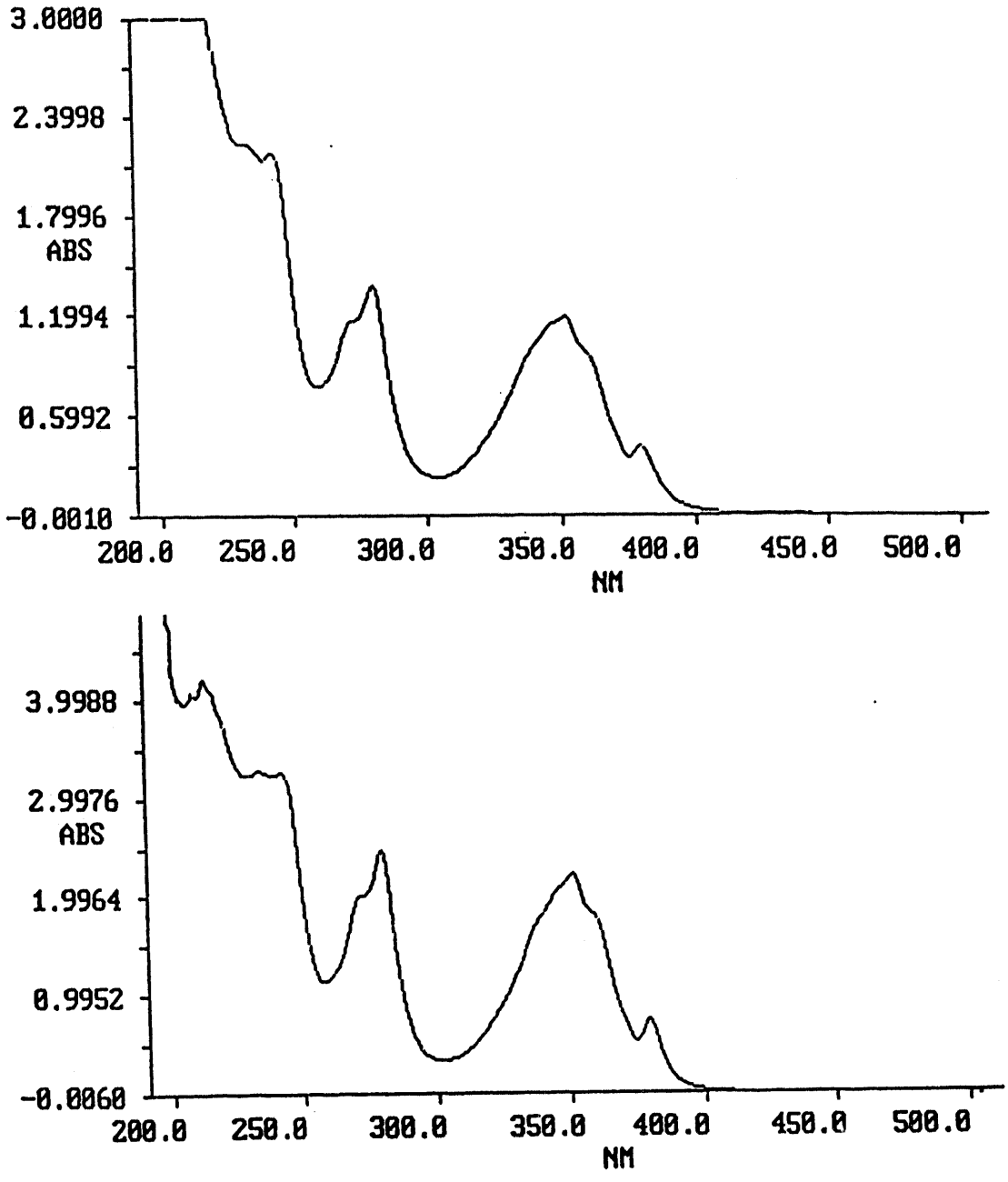

Figure 6-4. UV Absorption Spectra of 1 (Top) and 2 (Bottom) in H_2O (C = 0.15 g/dL).

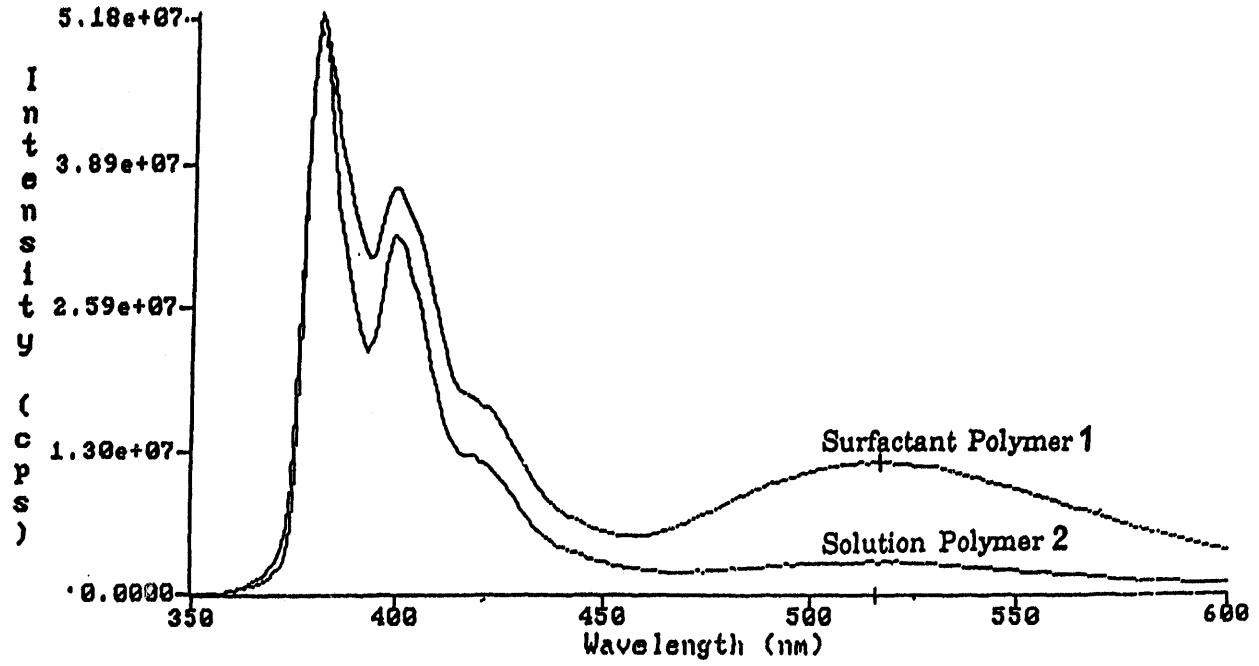

Figure 6-5. Steady-State Emission Spectra of 1 (Copolymer C = 218 mg/dL, Fluorophore C = 7.13 x 10^{-5} Mol/L) and 2 (Copolymer C = 193 mg/dL, Fluorophore C = 9.28 x 10^{-5} Mol/L) in H_2O.

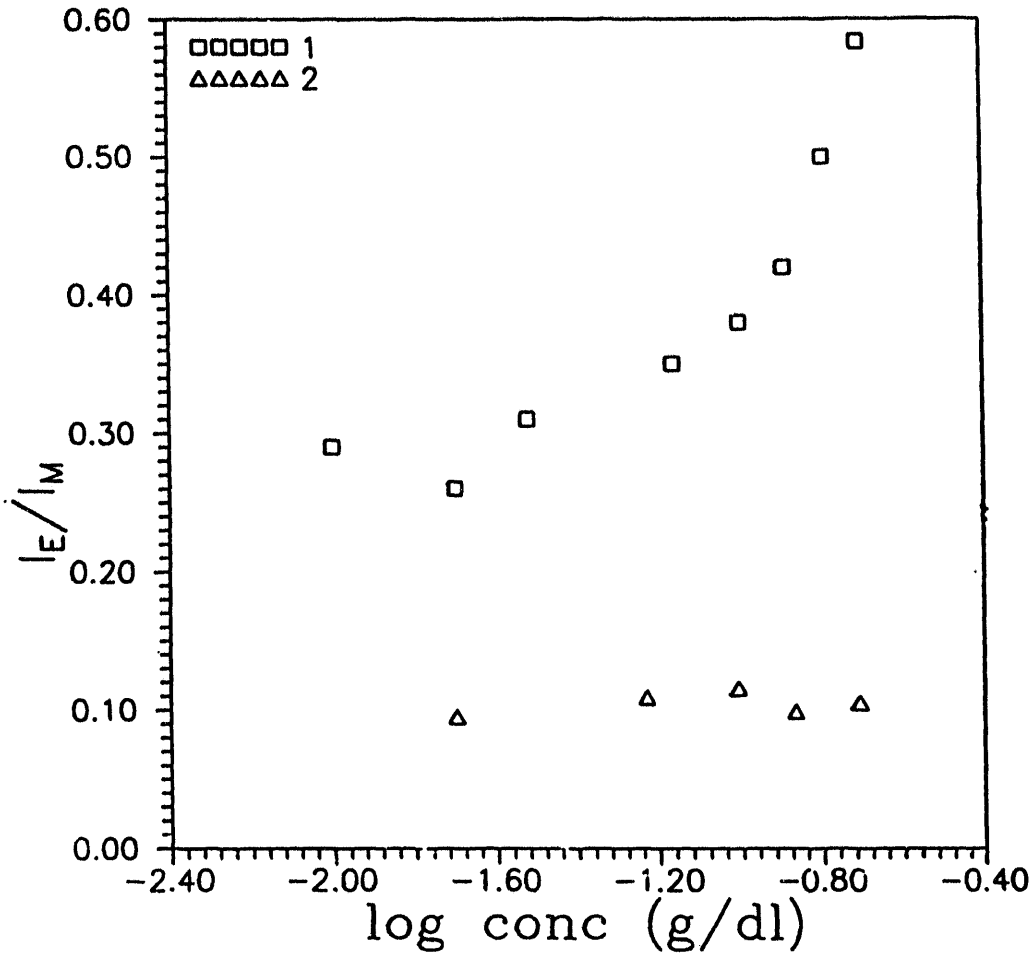

Figure 6-6. I_E/I_M as a Function of Log Polymer Concentration of 1 and 2 in H_2O.

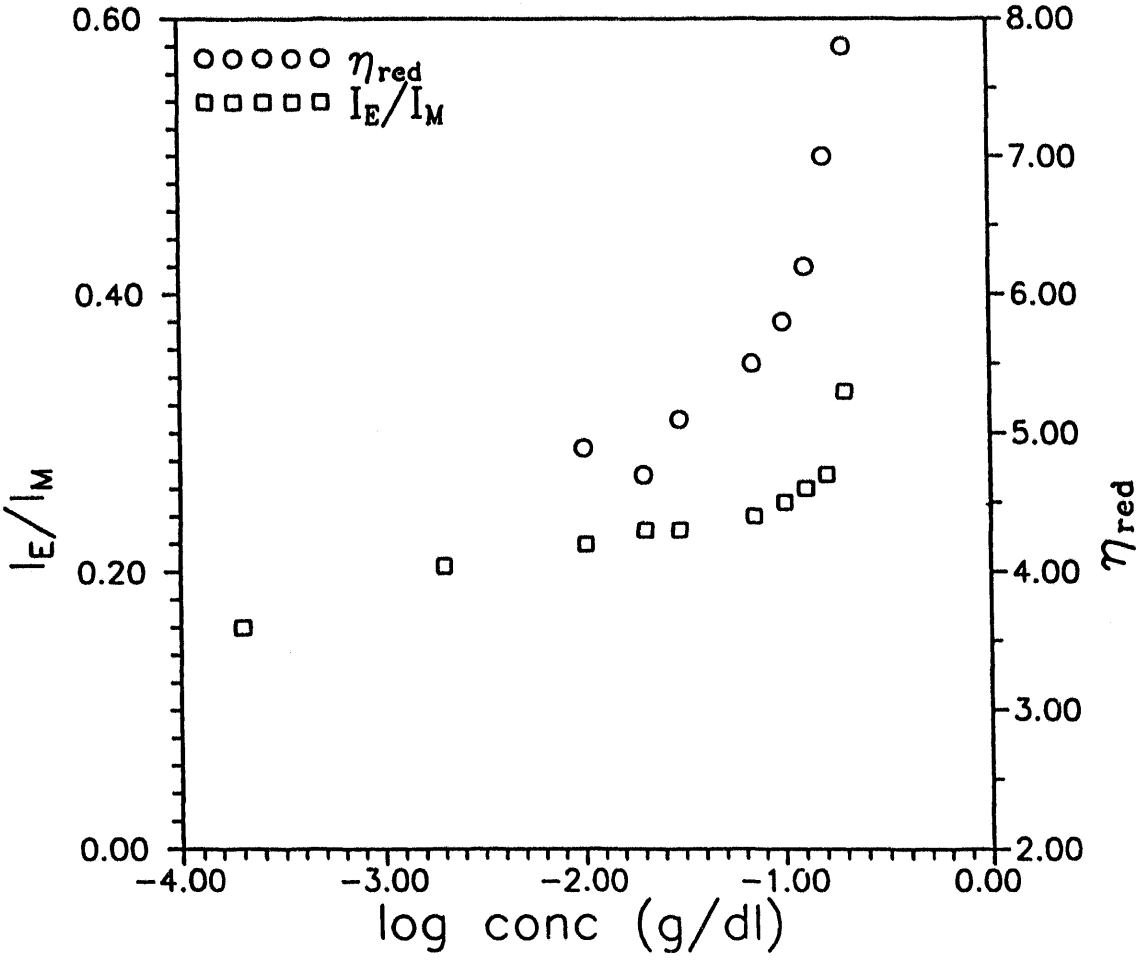

Figure 6-7. η_{red} and I_E/I_M as a Function of Log Polymer Concentration for 1 in H_2O.

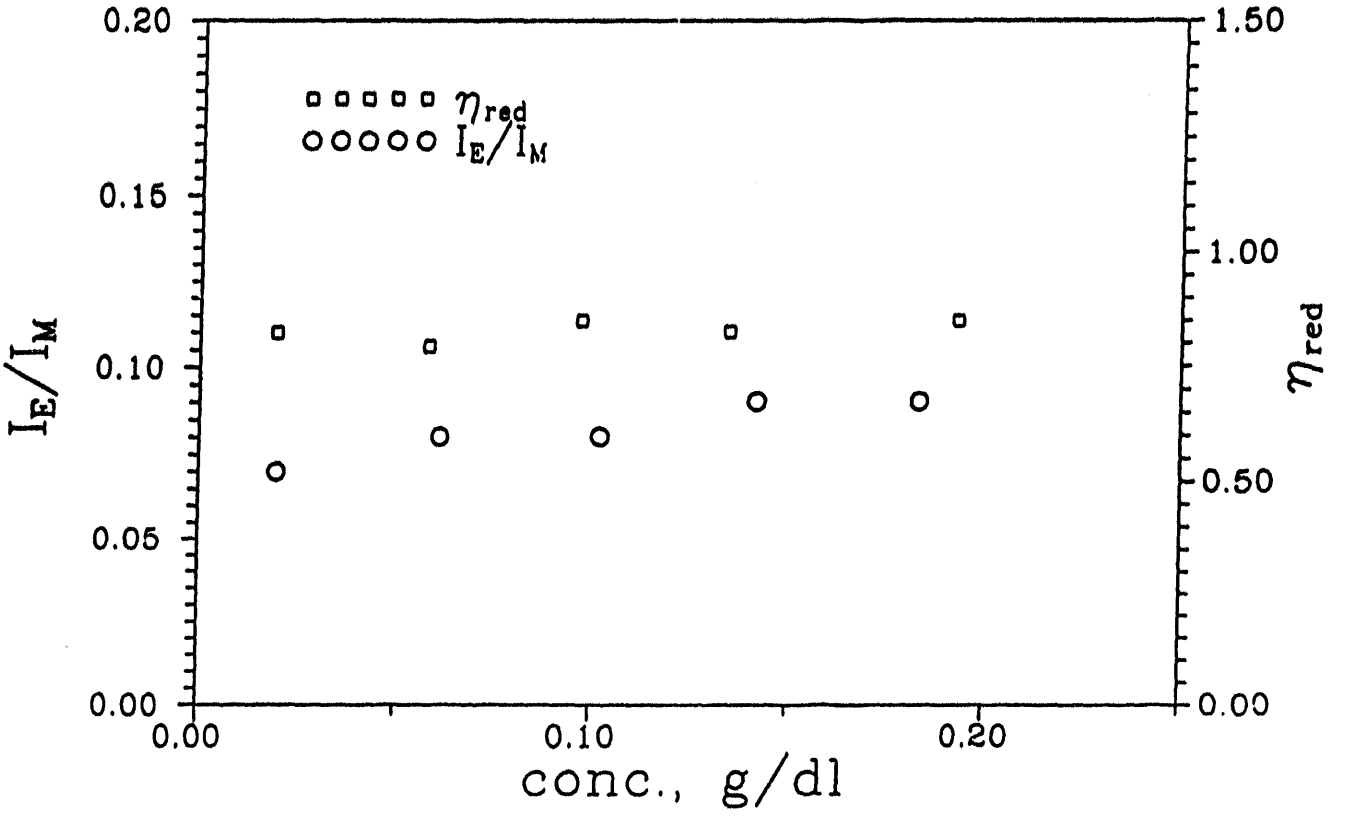

Figure 6-8. η_{red} and I_E/I_M as a Function of Polymer Concentration for **2** in H_2O.

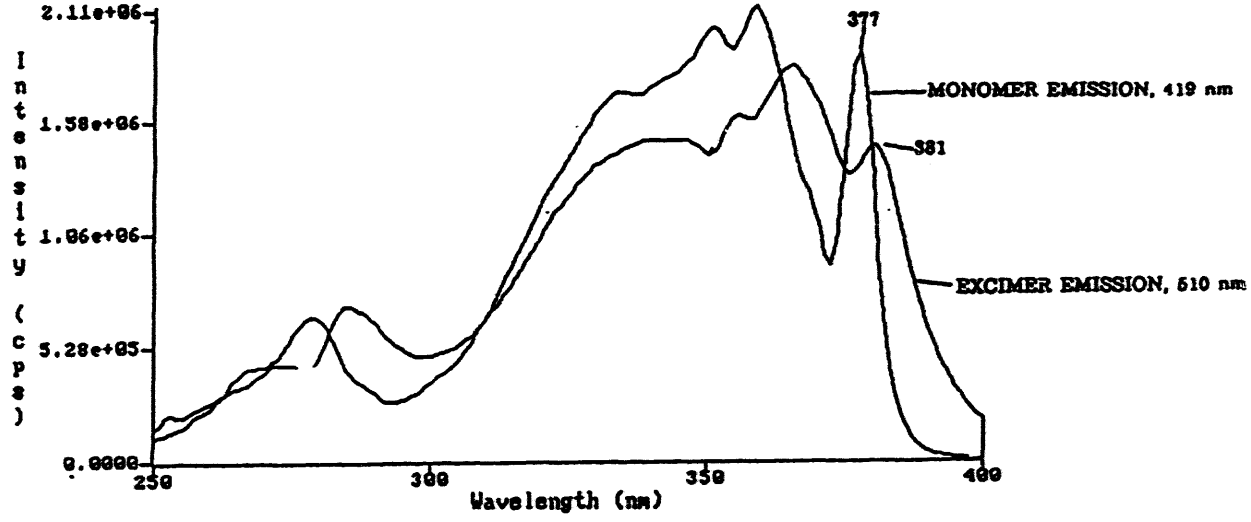

Figure 6-9. Excitation Spectra at Monomer and Excimer Emission of 1 in H_2O, C = 0.22 g/dL.

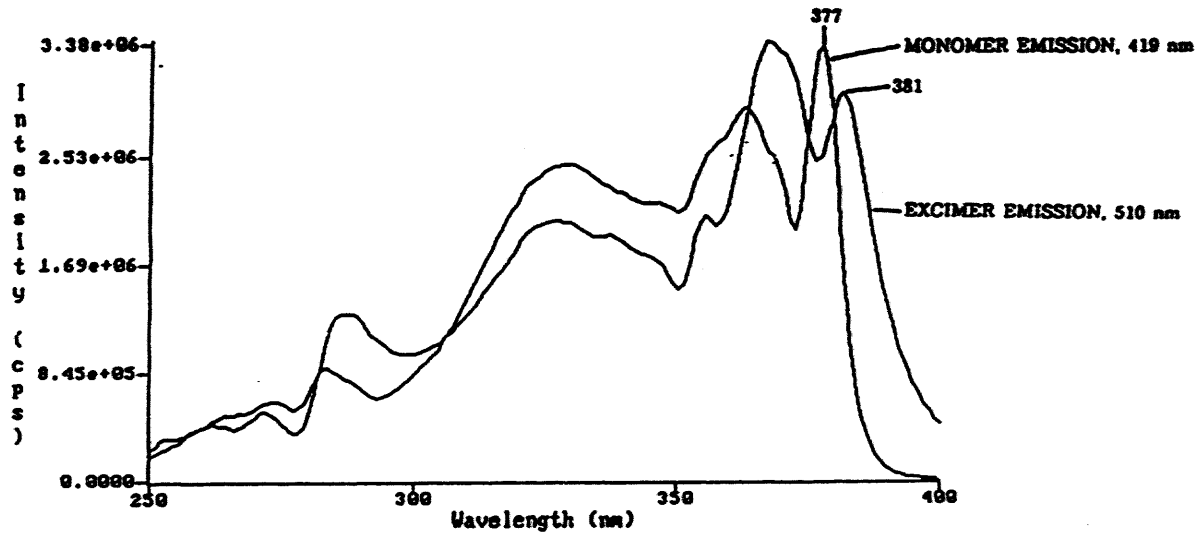

Figure 6-10. Excitation Spectra at Monomer and Excimer Emission of 2 in H_2O, C = 0.19 g/dL.

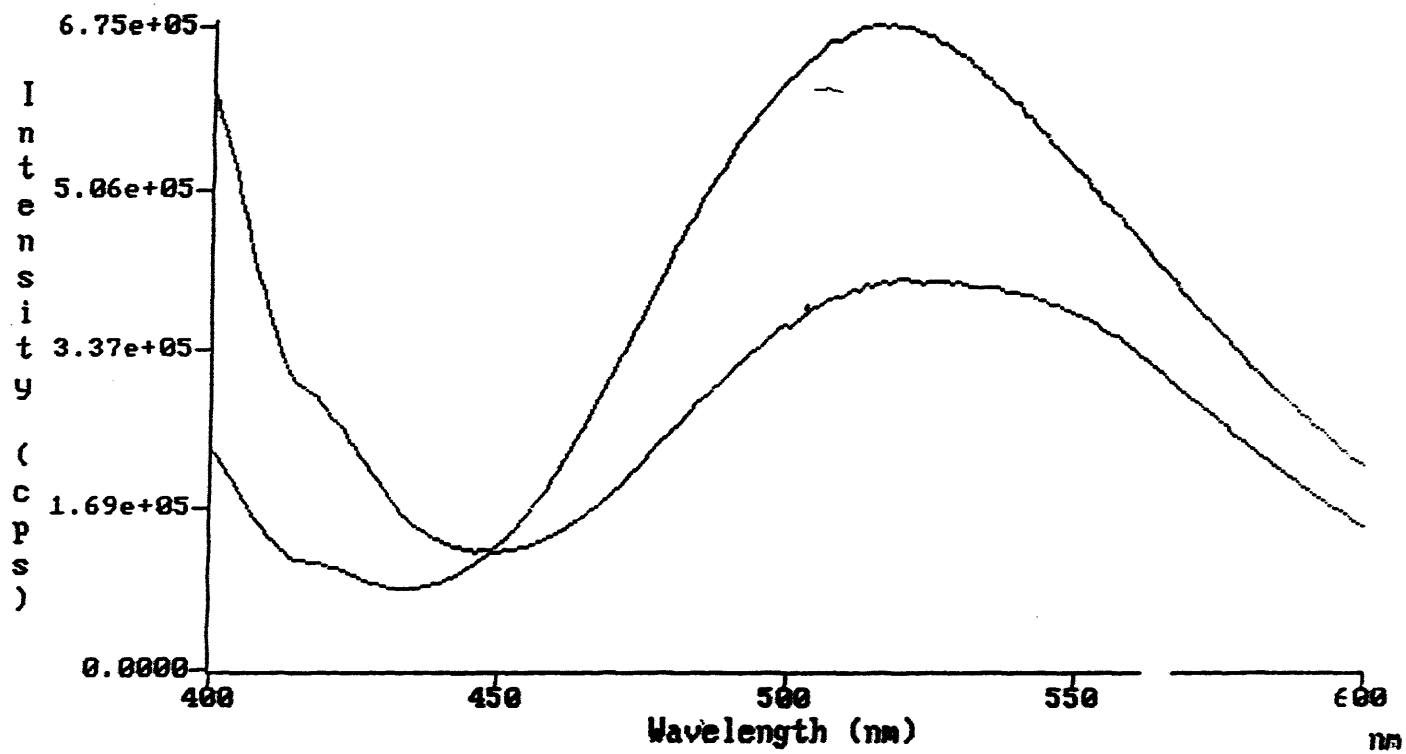

Figure 6-11. Steady-State Emission Spectra of 1 and 2 in H_2O (Excitation of Aggregates at 395 ± 1 nm).

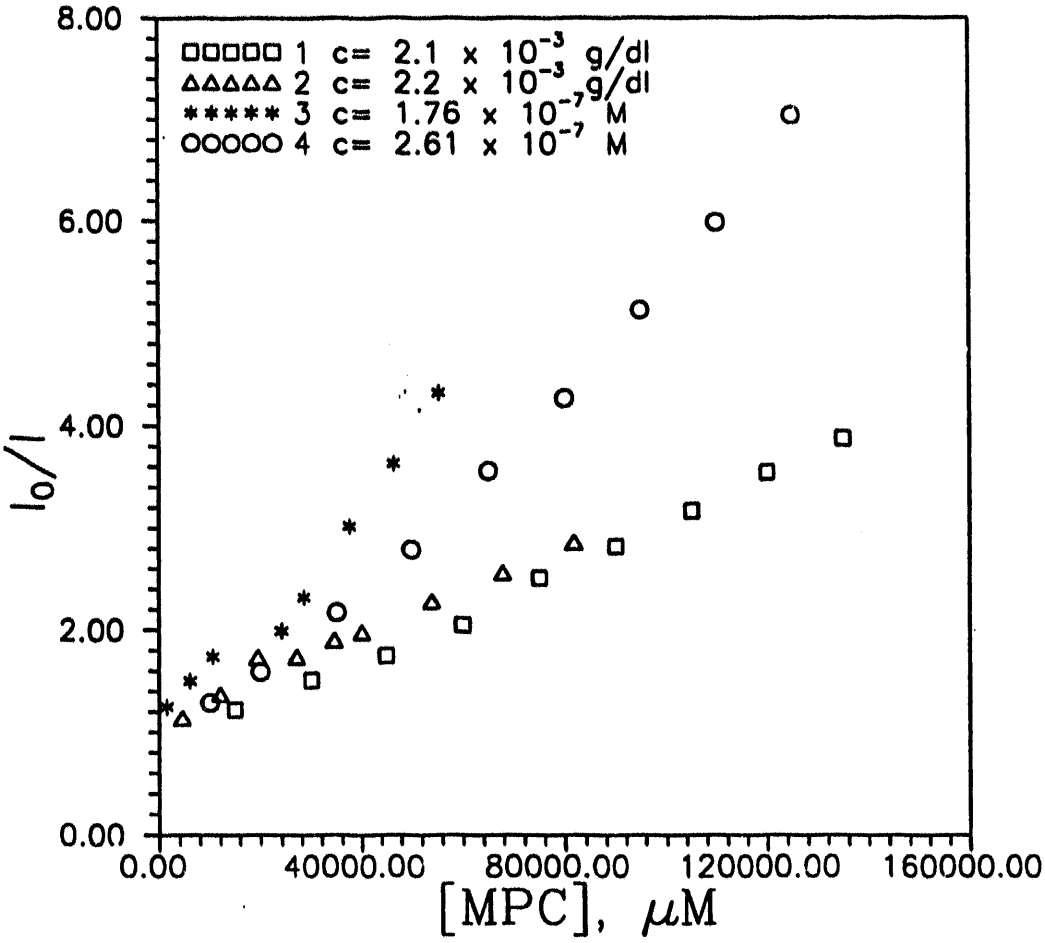

Figure 6-12. MPC quenching of pyrenesulfonamide polymers and models.

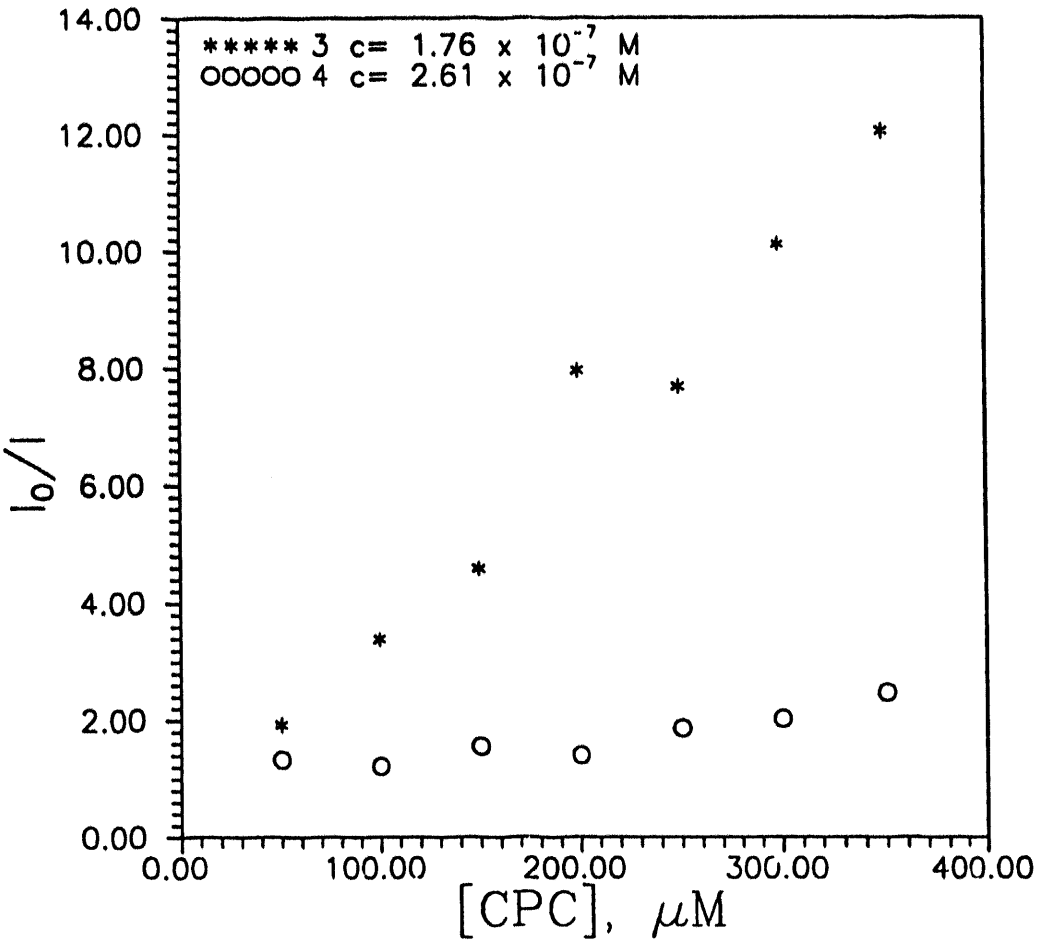

Figure 6-13. CPC quenching of pyrenesulfonamide models (label conc. ≈ 10^{-5} M).

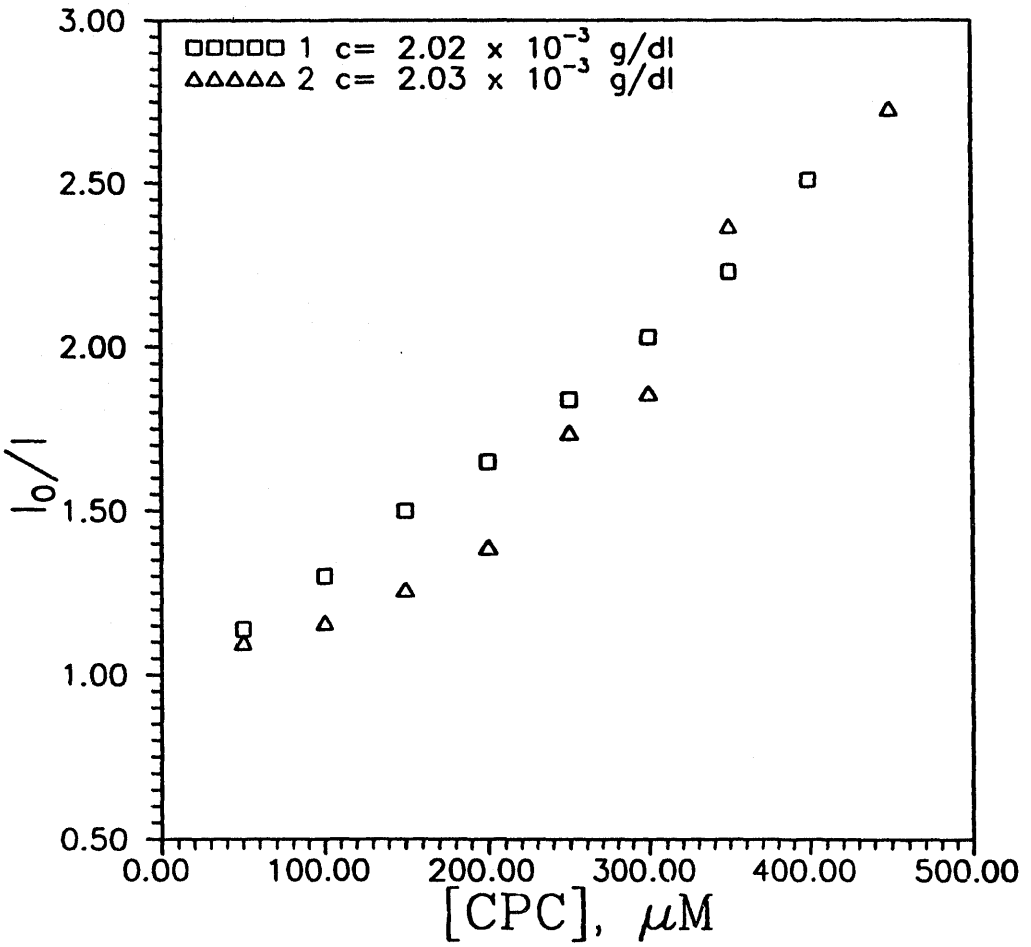

Figure 6-14. CPC quenching of pyrenesulfonamide polymers (label conc. ≈ 10^{-7} M).

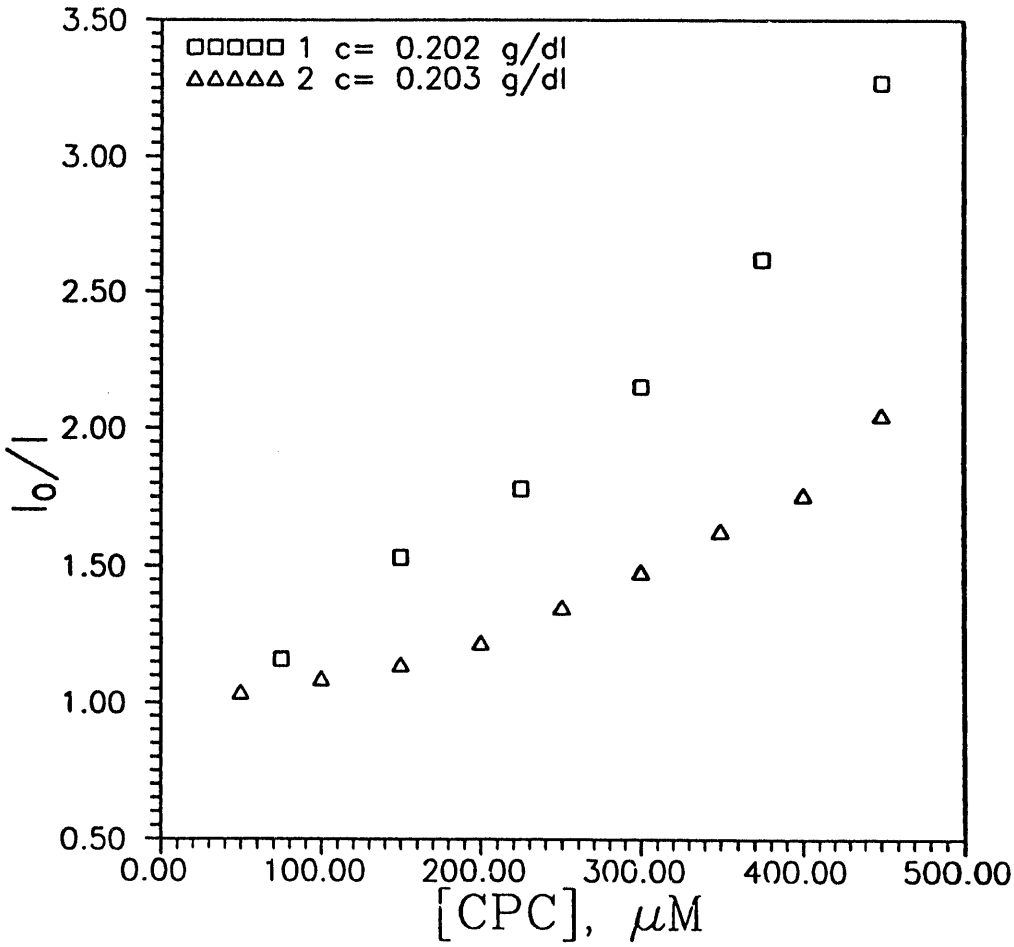

Figure 6-15. CPC quenching of pyrenesulfonamide polymers (label conc. ≈ 10^{-4} M).

CHAPTER SEVEN: AMPHOLYTIC COPOLYMERS OF SODIUM 2-ACRYLAMIDO-2-METHYLPROPANESULFONATE WITH 2-ACRYLAMIDO-2-METHYLPROPANETRIMETHYLAMMONIUM CHLORIDE

Abstract

Copolymers of sodium 2-acrylamido-2-methylpropanesulfonate (NaAMPS) with 2-acrylamido-2-methylpropanetrimethylammonium chloride (AMPTAC) have been prepared by free-radical polymerization in a 0.5M NaCl aqueous solution using potassium persulfate as the initiator. Copolymer compositions were obtained by ^{13}C NMR and elemental analysis. Reactivity ratios were calculated by the methods of Fineman-Ross ($r_1 = 0.58$; $r_2 = 0.87$) and Kelen-Tüdös ($r_1 = 0.50$; $r_2 = 0.62$). An r_1r_2 value of 0.31 indicates an alternating microstructure for NaAMPS and AMPTAC monomer units. Molecular weights, second virial coefficients, diffusion coefficients, and average diameters were found using classical and quasielastic low angle laser light scattering. As the compositions of the copolymers approach equal molar concentrations of NaAMPS and AMPTAC, polyampholyte behavior is observed. The second virial coefficients can be used to distinguish the polyelectrolyte/polyampholyte transition as a function of copolymer composition. The dilute solution properties of the copolymers, as well as those of the NaAMPS and AMPTAC homopolymers, have been studied as related to composition, pH, temperature and added electrolytes.

Introduction

Water-soluble copolymers showing tolerance to added electrolytes have been the subject of research in our laboratories in recent years. Of particular interest have been hydrophilic polyampholytes that exhibit enhanced viscosity with added salts[1-9]. Such copolymers containing acidic and basic moieties were reported as early as the 1950's. For example Alfrey and Morawetz reported the synthesis of vinyl polyampholytes from copolymerization of 2-vinylpyridine and methacrylic acid[10]. These polyampholytes behaved as polyanions in alkaline solution, and as polycations in acid solution. Ehrlich and Doty copolymerized 2-dimethylaminoethyl methacrylate with methacrylic acid, varying the composition of the latter from 23 to 57 mol %[11]. The solution and light scattering properties of the copolymer which had 53.7 mol % methacrylic acid were studied at the isoelectric point. The polymer coils possessed negative second virial coefficients A_2 indicating that the hydrodynamic volume of the coils was reduced by intramolecular attractions between the positive and negatively charged groups.

More recently Salamone et al. studied polyampholytes made by pairing anionic and cationic monomers then polymerizing them into highly alternating copolymers[12-16]. The observed solution behavior was consistent with that of high charge density polyampholytes. We reported polyampholytes containing the cationic monomer 2-acrylamido-2-methylpropanedimethylammonium hydrochloride (AMPDAC)[3-6]. The cationic copolymers

at low pH were subject to dehydrochlorination to reduce segmental repulsions making structure/behavior assessment more difficult. The quaternary cationic monomer 2-acrylamido-2-methylpropanetrimethylammonium chloride (AMPTAC) was synthesized to solve this problem [8,17]. This monomer not only features a quaternized ammonium moiety which remains charged regardless of pH but the amide group is protected from hydrolysis by geminal methyl groups. This paper reports copolymers of AMPTAC and NaAMPS, the ATAS series (Figure 1). In this ATAS series the monomers will retain their respective charges over a wide pH range; therefore the monomer ratio will dictate polymer net charge and the resulting solution properties.

Experimental

Materials and Monomer Synthesis

2-Acrylamido-2-methylpropanesulfonic acid (NaAMPS) was obtained from Fluka and purified by recrystallization from a methanol/2-propanol solvent system. Methyl iodide from Aldrich was used without further purification. Synthesis of 2-acrylamido-2-methylpropanetrimethylammonium chloride (AMPTAC) by a multistep procedure has been previously reported [17]. Briefly, 2-acrylamido-2-methylpropanedimethylamine was reacted with a ten-fold excess of methyl iodide in refluxing diethyl ether and then ion-exchanged to yield the product AMPTAC. Potassium persulfate from J.T. Baker was recrystallized twice from deionized water prior to use.

Synthesis of Copolymers of Sodium 2-Acrylamido-2-methylpropanesulfonate with 2-Acrylamido-2-methylpropanetrimethylammonium Chloride

The homopolymers of NaAMPS and AMPTAC, and the copolymers of AMPTAC with NaAMPS (the ATAS series) were synthesized by free radical polymerization in a 0.5M NaCl aqueous solution under nitrogen at 30°C using 0.1 mol % potassium persulfate as the initiator. The synthesis and purification procedures have been reported previously[17,18]. The feed ratio of NaAMPS:AMPTAC was varied from 90:10 to 30:70 mol % with the total monomer concentration held constant at 0.45M. Aqueous NaCl solutions as the reaction medium insured that the copolymers remained homogeneous during polymerization.

All copolymers were soluble in deionized water except for ATAS-50. This copolymer precipitated from solution during dialysis and remained insoluble until NaCl was added. This "hydrogel" was washed repeatedly with deionized water to remove any remaining salt or monomer and was then lyophilized. Conversions were determined gravimetrically. Table I lists reaction parameters for the copolymerization of AMPTAC with NaAMPS, and the homopolymerizations of NaAMPS and AMPTAC. FT-IR: Copolymer: ATAS-50, N-H 3440 cm^{-1} (s), 3296 cm^{-1} (s); C-H 3063-2935 cm^{-1} (m); C=O 1655 cm^{-1} (s), 1549 cm^{-1}; S-O 1208 cm^{-1} (s). ^{13}C NMR: Copolymer: ATAS-50, NaAMPS C=O 178.8 ppm; AMPTAC C=O 178.2 ppm; Quat CH_3 57.8 ppm; Chain CH_2 37.8 ppm; Chain CH 45.0 ppm; Gem Methyls CH_3 29.4 ppm

Copolymer Characterization

Elemental analyses for carbon, hydrogen, nitrogen, and sulfur were conducted by M-H-W Laboratories of Phoenix, AZ on the low conversion copolymer samples. Copolymer compositions were confirmed using ^{13}C NMR by integration of the amide carbonyl peaks[19]. ^{13}C NMR spectra were obtained using 10 wt/wt % aqueous (D_2O) polymer solutions with DSS as the reference. FT-IR spectra were obtained using a Perkin-Elmer 1600 Series FT-IR spectrophotometer. Molecular weight studies were performed on a Chromatix KMX-6 Low Angle Laser Light Scattering instrument. Refractive index increments were obtained using a Chromatix KMX-16 Laser Differential Refractometer. For quasielastic light scattering a Langley-Ford Model LF1-64 channel digital correlator was used in conjunction with the KMX-6. All measurements were conducted at 25°C in 1M NaCl.

Viscosity Measurement

Stock solutions of sodium chloride (0.10, 0.20, 0.30, 0.50 and 0.75M NaCl) were prepared by dissolving the appropriate amount of salt in deionized water. Polymer stock solutions were then made by dissolving a specified amount of polymer in solvent from these salt solutions. The solutions were then diluted to required concentrations and allowed to age for two to three weeks before being analyzed with a Contraves LS-30 rheometer. Triplicate samples were prepared of each concentration to reduce experimental error. Intrinsic viscosities were evaluated using the Huggins equation[20].

Results and discussion

The ATAS series of copolymers was synthesized by varying the ratio of NaAMPS and AMPTAC from 90:10 to 30:70 mol % in the feed. Reaction parameters and the resulting copolymer compositions determined by elemental analysis or ^{13}C NMR are given in Table I. The number appended to the acronym ATAS refers to the amount of AMPTAC in the feed. This series differs from the previously studied ADAS series[3,4] in which AMPDAC was the cationic monomer. The quaternary ammonium group of AMPTAC has been shown to be a stable cationic moiety which remains charged over a wide pH range[17]. When AMPDAC was used in the ADAS copolymers, the exact number of cations present was never precisely known due to loss of HCl from the tertiary amine hydrochloride in aqueous solution. The AMPTAC monomer and ATAS copolymers have no facile route for charge elimination other than counterion condensation, making them better suited for structure/property studies.

Compositional Studies

Elemental analysis was used to determine the copolymer compositions from nitrogen and sulfur content represented by equations (1) and (2).

$$\% N/14.01 = A + 2B \quad (1)$$

$$\% S/32.06 = A \quad (2)$$

The coefficients *A* and *B* are the number of moles of NaAMPS and AMPTAC, respectively, in a normalized amount of copolymer, e.g. one gram. The mole percent of each monomer in the copolymer may then be determined using equations (3) and (4).

$$\text{mol \% NaAMPS} = A/(A + B) \times 100\% \quad (3)$$

$$\text{mol \% AMPTAC} = B/(A + B) \times 100\% \quad (4)$$

Integration of ^{13}C NMR amide carbonyl peaks also gave the mole percent of NaAMPS and AMPTAC in the copolymers. This information agrees favorably with that derived from elemental analysis. The low and high conversion data differ significantly only for ATAS-10 in which compositional drift would be expected for an alternating copolymerization as indicated by the values of r_1 and r_2. The copolymer compositions as a function of feed composition are shown in Figure 2. A copolymerization in which an ideally random copolymer would be formed is represented by the dashed line.

Reactivity Ratio and Microstructure Studies

Reactivity ratios for the ATAS series were determined from the feed ratios of the monomers and the resultant copolymer compositions obtained by elemental analysis. The traditional methods of Fineman-Ross[21] and Kelen-Tüdös[22] were employed to determine the monomer reactivity ratios from the low conversion copolymer samples. The Fineman-Ross method gave reactivity ratios for NaAMPS (M_1) and AMPTAC (M_2) of $r_1 = 0.58$ and $r_2 = 0.87$. The Kelen-Tüdös method produced reactivity ratios of 0.50 and 0.62 for r_1 and r_2 respectively and $r_1r_2 = 0.31$, Table II. The copolymer compositions as a function of feed composition for the ATAS series are shown in Figure 2. The experimental data suggest the ATAS copolymers, like the previously reported series ADAS, are highly alternating.

Microstructural information was obtained statistically using the equations of Igarashi[23] and Pyun[24] and is presented in Table III. The Igarashi method calculates the fractions of NaAMPS-NaAMPS, AMPTAC-AMPTAC, and NaAMPS-AMPTAC units in the copolymers as a function of reactivity ratios and copolymer compositions. The Pyun method calculates the mean sequence length of the monomers in each copolymer. The data clearly indicate the alternating tendency of the monomer sequences. The ATAS copolymers, however, do not possess the degrees of alternation obtained for the ADAS copolymers. For example, ADAS-50 had a 15 mol % higher alternation value than the analogous ATAS-50. This is indicative of NaAMPS:AMPDAC having a stronger interaction than the NaAMPS:AMPTAC ion pair.

Light Scattering Studies

Classical and quasielastic light scattering data for the ATAS series are presented in Table IV. The polymers have molecular weights ranging from 1.47×10^6 g/mol for the ATAS-100 homopolymer, to 7.92×10^6 g/mol for ATAS-40-2. The second virial coefficients (A_2) were found to exhibit dependence on copolymer composition. ATAS-50-2 with a 50:50 mol % charge composition is better solvated in the presence of electrolytes than the copolymers with charge imbalances. ATAS-25-2 has a negative A_2 value while ATAS-50-2 has an A_2

value of 0.763 ml·mol/g^2. Similar results had been observed for the ADAS copolymers in which ADAS-50 had the highest A_2 value for the series. The data are consistent with the expected polyelectrolyte/polyampholyte transitions depending on the extent of AMPTAC incorporation in the copolymers. Higgs and Joanny have presented theoretical predictions which agree with our results[25].

The narrow distribution of experimental values for the diffusion coefficients (D_o) and average hydrodynamic diameters (d_o) are consistent with the viscosity behavior of the copolymers in electrolyte solutions. In 1M NaCl, the ATAS copolymers are neither chain extended nor chain constricted due to charge screening. In deionized water, large differences would be expected for polyampholytes, i.e., ATAS-50-2, and polyelectrolytes, i.e., ATAS-10-2 and ATAS-70-2 (Table IV), where strong electrostatic effects would dominate. Experimental difficulties, unfortunately, preclude meaningful light scattering studies of the high charge density polyampholytes in deionized water. Viscometric studies, however, support the above discussion.

Viscometric Studies

The dilute solution behavior of the ATAS series was studied with respect to composition, temperature, pH and added electrolytes. Apparent viscosities of the polymers were measured at polymer concentrations below C* using a Contraves LS-30 low shear rheometer. The solutions were aged two to three weeks to allow equilibration of polymer conformations in solution. Intrinsic viscosities were calculated using the Huggins relationship.

The solution behavior of the homopolymer ATAS-100 was previously examined in the pH range of 3 to 11 in 0.1M NaCl[17]. No dependence of apparent viscosity was observed. Each copolymer of AMPTAC with the sulfonate monomer NaAMPS should be non-dependent on changes in pH above 3 since the sulfonate group remains ionized.

Intrinsic viscosities for the copolymers ATAS-50 and -70 and the homopolymer ATAS-100 are relatively independent of temperature when measured in deionized water and in 0.5M NaCl in the temperature range of 25°C to 60°C. Most polyelectrolytes exhibit reductions in viscosity as a function of increasing temperature due to the elimination of rotational restrictions. Increase in conformational freedom may be offset by water restructuring around the NaAMPS and AMPTAC ions pairs.

Effects of Copolymer Composition

The apparent viscosities of the ATAS copolymers in deionized water plotted as a function of composition are shown in Figure 3. A decrease in the apparent viscosity develops as the molar ratio of NaAMPS and AMPTAC approaches unity. The curve is discontinuous due to the insolubility of ATAS-50-2 in the absence of added electrolytes. This is the result of decreasing polymer hydrodynamic volume caused by increasing intramolecular associations. The ADAS copolymers displayed a similar effect[3,4].

The effects of composition on intrinsic viscosity in NaCl solutions are displayed in Figure 4. The homopolymer ATAS-0 and the copolymers ATAS-10-2, -25-2, -40-2 and -50-2 have comparable molecular weights which lead to similar viscosities in 0.75M NaCl. In 0.1M NaCl, the polyelectrolyte effect dominates solution viscosity and significant differences due to composition can be discerned. Copolymers with more NaAMPS than AMPTAC act as polyanions. As the amount of AMPTAC in the copolymers increases to 50 mol %, the viscosity decreases as a result of increasing polyampholyte character. This behavior agrees with the second virial coefficient data. The copolymer ATAS-70-2 which has 65.7 mol % AMPTAC and the homopolymer ATAS-100 have low intrinsic viscosities due to polycationic character. The intrinsic viscosity of ATAS-50-2, which is insoluble in deionized water, increases with increasing ionic strength.

Effects of Added Electrolytes

The effects of sodium chloride on the intrinsic viscosities of the ATAS copolymers and ATAS-0 and ATAS-100 were determined at a shear rate of 5.96 sec^{-1} at 25°C (Figure 5). ATAS-0, the anionic homopolymer of NaAMPS, shows the greatest decrease in viscosity as the NaCl concentration increases. As more AMPTAC is incorporated into the copolymer this effect becomes less pronounced due to the transition from polyelectrolyte to polyampholyte character. ATAS-40-2 lies near the polyampholyte composition region but still possesses a net charge. This leads to a small change in viscosity for ATAS-40-2 with increasing ionic strength. At equal molar concentrations of each monomer, (ATAS-50-2) there is an increase in the viscosity. The copolymer ATAS-70-2 lies on the edge of the polyelectrolyte/polyampholyte transition and thus shows a small decrease in intrinsic viscosity.

The intrinsic viscosity of each sample was plotted as a function of the inverse square-root of the ionic strength (Figure 6). Polyelectrolytes show a direct linear dependence when plotted in this manner[26]. The polymers ATAS-0, -10-2, and -100 exhibit linear behavior and positive slopes. The copolymers ATAS-50-2 and -40-2 exhibit slightly negative slopes indicative of polyampholyte nature and consistent with the second virial coefficient data. Intermediate behavior is observed for ATAS-25-2 and ATAS-70-2.

Conclusions

Homopolymers of NaAMPS and AMPTAC, and the copolymers of NaAMPS with AMPTAC (the ATAS series), have been synthesized by free radical polymerization in 0.5M NaCl. The presence of NaCl allows the polymerizations to remain homogeneous yielding copolymers with microstructures less alternating than those of the previously studied ADAS series. Copolymer compositions were obtained by elemental analysis and ^{13}C NMR. Reactivity ratios determined by the methods of Fineman-Ross and Kelen-Tüdös yield $r_1r_2 = 0.31$. Molecular weights range from 1.47 to 7.92 x 10^6 g/mol for the AMPTAC homopolymer and the ATAS-40 copolymer respectively. Second virial coefficients indicate a copolymer with an equal molar concentration of each monomer to be better solvated than copolymers with charge imbalances. Second virial coefficients and ionic strength changes

may be used to detect polyampholyte/polyelectrolyte transitions with compositional changes. ATAS-0, -10, -25, -75, and -100 behave as polyelectrolytes while ATAS-40 and -50 show polyampholyte behavior.

In the absence of added electrolytes, decreasing viscosities are observed as copolymer compositions approach equal molar values. This is attributed to decreasing polymer hydrodynamic volumes caused by increasing intramolecular associations. In 1M NaCl the copolymers are neither chain extended nor chain constricted due to charge screening by the added electrolytes. The use of the quaternary ammonium monomer AMPTAC allows the synthesis of high charge density polyelectrolytes and polyampholytes with precisely known charge ratios thus allowing accurate assessment of structure/property relationships.

References

1. C. B. Johnson, Ph.D. Dissertation, University of Southern Mississippi (1988).

2. L. C. Salazar, Ph.D. Dissertation, University of Southern Mississippi (1991).

3. C. L. McCormick and C. B. Johnson, *Macromolecules, 21*, 686 (1988).

4. C. L. McCormick and C. B. Johnson, *Macromolecules, 21*, 694 (1988).

5. C. L. McCormick and C. B. Johnson, *Polymer, 31*, 1100 (1990).

6. C. L. McCormick and C. B. Johnson, *Macromol. Sci., Chem., A27(5)*, 539 (1990).

7. C. L. McCormick and L. C. Salazar, *ACS Polym. Preprints, 30(2)*, 344 (1989).

8. C. L. McCormick, L. C. Salazar, and E. E. Kathmann, *ACS Polym. Preprints, 32(1)*, 98 (1991).

9. C. L. McCormick and L. C. Salazar, *Water-Soluble Polymers: Synthesis, Solution Properties, and Applications, 467*, ACS, 1991, p. 119.

10. T. Alfrey, R. M. Fuoss, H. Morawetz and H. Pinner, *J. Am. Chem. Soc., 74*, 438 (1952).

11. G. Erlich and P. Doty, J. *Am. Chem. Soc., 76*, 3764 (1954).

12. J. C. Salamone, W. Volksen, S. C. Israel, A. P. Olson and D. C. Raia, *Polymer, 18*, 1058 (1977).

13. J. C. Salamone, C. C. Tsai and A. C. Watterson, *J. Macromol. Sci. Chem., A13(5)*, 665 (1979).

14. J. C. Salamone, C. C. Tsai, A. P. Olsen and A. C. Watterson, in *Advances in the Chemical Sciences: Ions in Polymers, 187,* ACS, 1980, p. 337.

15. J. C. Salamone, C. C. Tsai, A. C. Watterson and A. P. Olson, *Polymeric Amine and Ammonium Salts,* E. J. Goethals Ed., Pergamon Press, New York, 1980.

16. J. C. Salamone, N. A. Mahmud, M. U. Mahmud, T. Nagabhushhanam and A. C. Watterson, *Polymer, 23,* 843 (1982).

17. C. L. McCormick and L. C. Salazar, Water Soluble Co-Polymers 41. Copolymers of Acrylamide and Sodium 3-Acrylamido-3-Methylbutanoate, submitted for publication.

18. C. L. McCormick and L. C. Salazar, Water Soluble Co-Polymers 42. Cationic Polyelectrolytes of Acrylamide and 2-Acrylamido-2-Methylpropanetrimethylammonium Chloride.

19. C. L. McCormick and B. H. Hutchinson, *Polymer, 27(4),* 623 (1988).

20. M. L. Huggins, *J. Am. Chem. Soc., 64,* 2716 (1942).

21. M. Fineman and S. Ross, *J. Polym. Sci., 5(2),* 259 (1950).

22. T. Kelen and F. Tüdös, *J. Macromol. Sci. Chem., A9,* 1, (1975).

23. S. Igarashi, *J. Polym. Sci., Polym. Lett. Ed., 1,* 359 (1963).

24. C. W. Pyun, *J. Polym. Sci., A2(8),* 1111 (1970).

25. P. G. Higgs and J. F. Joanny, *J. of Chem. Phys., 94(2),* 1543 (1991).

26. C. Tanford, " Physical Chemistry of Macromolecules", Wiley, New York, 1961, p.506.

TABLE I

Reaction Parameters for the Copolymerization of Sodium 2-acrylamido-2-methylpropanesulfonate (NaAMPS) with 2-Acrylamido-2-methylpropanetrimethylammonium Chloride (AMPTAC).

Sample Number	Feed Ratio NaAMPS:AMPTAC	Reaction Time (hrs)	Conversion (%)	Weight (% C)	Weight (% N)	Weight (% S)	AMPTAC in Copolymer (mol %)[a]	AMPTAC in Copolymer (mol %)[b]
ATAS-10-1	90:10	3.3	22.3	31.26	5.79	9.86	14.7 ± 0.4	--
ATAS-10-2	90:10	3.8	38.3	--	--	--	--	21.3 ± 1.3
ATAS-25-1	75:25	1.5	16.2	42.52	7.79	8.38	36.1 ± 1.1	--
ATAS-25-2	75:25	3.3	42.0	--	--	--	--	36.1 ± 2.2
ATAS-40-1	60:40	1.4	28.9	45.55	8.80	7.58	45.4 ± 1.4	--
ATAS-40-2	60:40	3.5	34.6	--	--	--	--	40.0 ± 2.4
ATAS-50-1	50:50	3.3	15.0	46.92	9.37	6.84	51.7 ± 1.6	--
ATAS-50-2	50:50	16	61.2	--	--	--	--	51.0 ± 3.1
ATAS-70-1	30:70	1.5	14.2	47.40	9.81	4.65	65.7 ± 2.0	--
ATAS-70-2	30:70	2.5	24.7	--	--	--	--	62.0 ± 3.7
ATAS-0	100:0	5.8	58.6	--	--	--	0[c]	0[c]
ATAS-100	0:100	5.5	41.2	--	--		100[c]	100[c]

[a] Determined from Elemental Analysis
[b] Determined from ^{13}C NMR
[c] Theoretical

Table II

Reactivity Ratios for the ATAS and ADAS Copolymer Series Determined using the Methods of Kelen-Tüdös and Fineman-Ross.

	ATAS			ADAS		
Method	r_1	r_2	r_1r_2	r_1	r_2	r_1r_2
Kelen-Tüdös	0.50 ± 0.02	0.62 ± 0.02	0.31	0.22 ± 0.02	0.31 ± 0.04	0.07
Fineman-Ross	0.58 ± 0.06	0.87 ± 0.09	0.50	0.22 ± 0.03	0.33 ± 0.05	0.07

Table III

Structural Data for the Copolymers of Sodium 2-Acrylamido-2-methylpropanesulfonate (NaAMPS, M_1) with 2-Acrylamido-2-methylpropanetrimethylammonium Chloride (AMPTAC, M_2).

Sample Number	AMPTAC in Copolymer (mol %)[a]	Blockiness (mol %)		Alternation (mol %)	Mean Sequence Length	
		M_1-M_1	M_2-M_2	M_1-M_2	M_1	M_2
ATAS-10	14.7	71.4	0.8	30.5	5.5	1.1
ATAS-25	36.1	35.1	7.3	54.0	2.5	1.2
ATAS-40	45.4	22.9	13.6	63.2	1.8	1.4
ATAS-50	51.7	16.3	19.6	64.1	1.5	1.6
ATAS-70	65.7	6.4	37.8	54.5	1.2	2.5

[a] Determined from Elemental Analysis

Table IV

Classical and Quasielastic Light Scattering Data for Copolymer of Sodium 2-Acrylamido-2-methylpropanesulfonate (NaAMPS) with 2-Acrylamido-2-methylpropanetrimethylammonium Chloride (AMPTAC)

Sample Number	AMPTAC in Copolymer (mol %)[a]	dn/dc	Mw x 10^{-6} (g/mol)	A_2 x 10^4 (ml-mole/g^2)	D_o x 10^8 (cm^2/g)	d_o (Å)	DP x 10^{-4}
ATAS-0	0.0	0.1116	6.12	0.921	3.87	1265	2.23
ATAS-10-2	14.7	0.1190	8.22	0.494	4.19	1297	2.67
ATAS-25-2	36.1	0.1229	6.20	-0.023	4.73	1048	3.61
ATAS-40-2	45.4	0.1405	7.92	0.594	3.85	1285	2.75
ATAS-50-2	51.7	0.1445	7.68	0.763	4.63	1000	3.52
ATAS-70-2	65.7	0.1454	4.98	0.340	4.06	1252	3.42
ATAS-100	100.0	0.1458	1.47	2.115	6.37	916	0.67

[a] Determined from Elemental Analysis

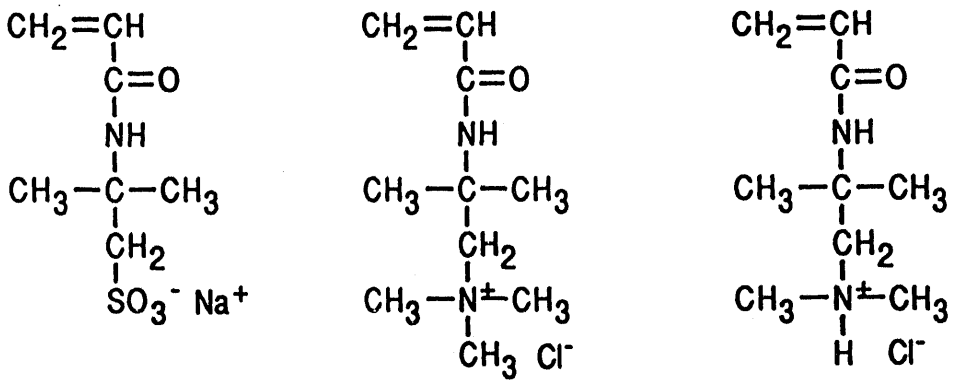

Figure 7-1. Structures for the monomers Sodium 2-Acrylamido-2-methylpropanesulfonate (NaAMPS), 2-Acrylamido-2-methylpropanetrimethylammonium Chloride (AMPTAC) and 2-Acrylamido-2-methylpropanedimethylammonium Hydrochloride (AMPDAC).

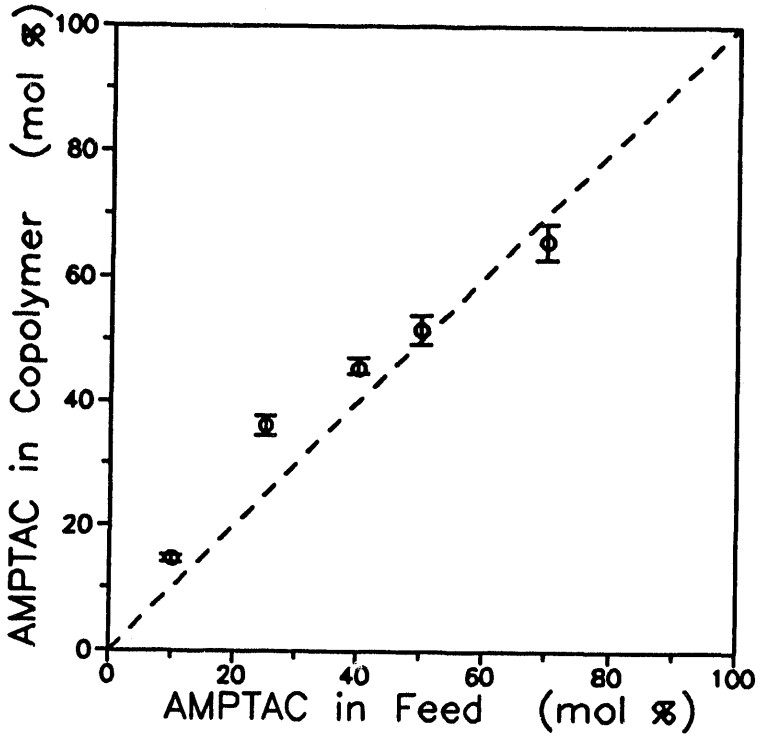

Figure 7-2. Mole percent AMPTAC incorporated into the ATAS copolymers as a function of comonomer feed ratio. The dashed line represents ideal random incorporation.

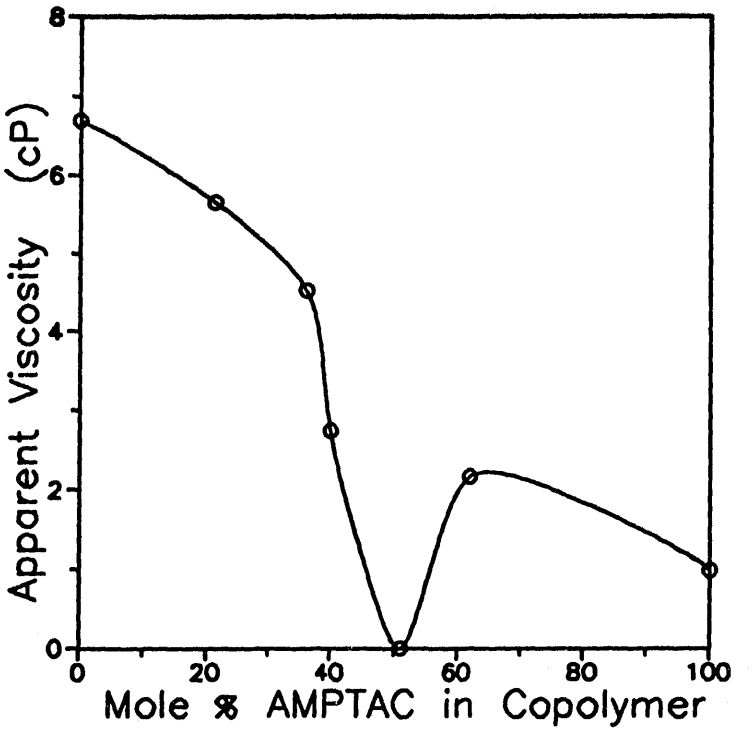

Figure 7-3. Effect of copolymer composition on the apparent viscosity of 0.025 g/dL ATAS polymer solutions in deionized water at 25°C at a shear rate of 5.96 sec^{-1}.

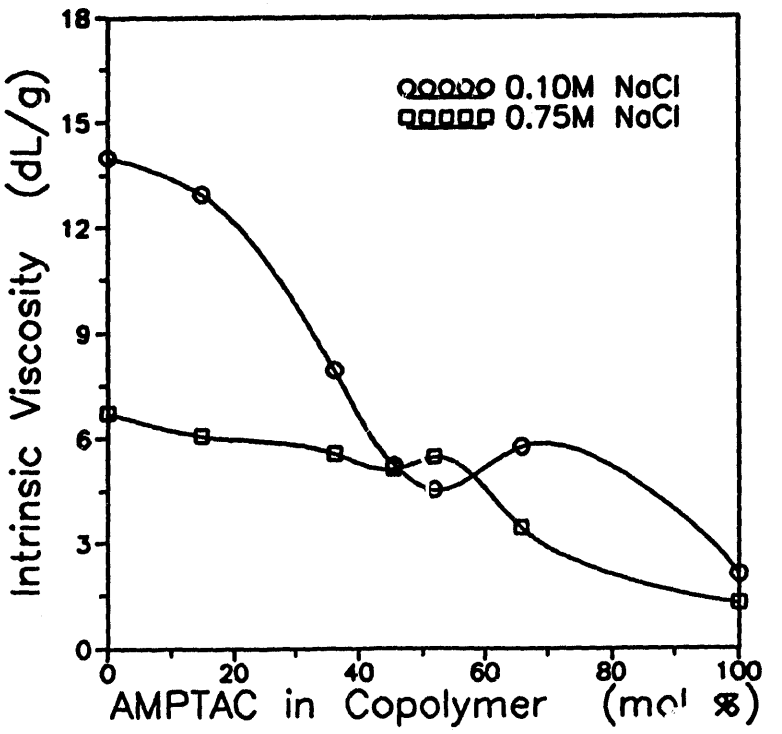

Figure 7-4. Intrinsic viscosity of the ATAS copolymer series as a function of composition in 0.10M and 0.75M NaCl determined at a shear rate of 5.96 sec^{-1} at 25°C.

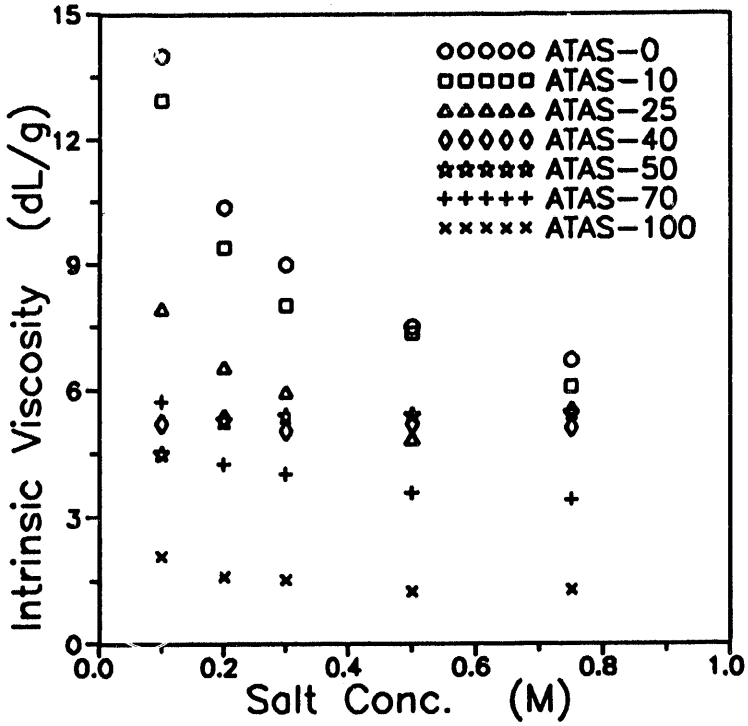

Figure 7-5. Intrinsic viscosities for the ATAS copolymers as a function of NaCl concentration determined at a shear rate of 5.96 sec^{-1}.

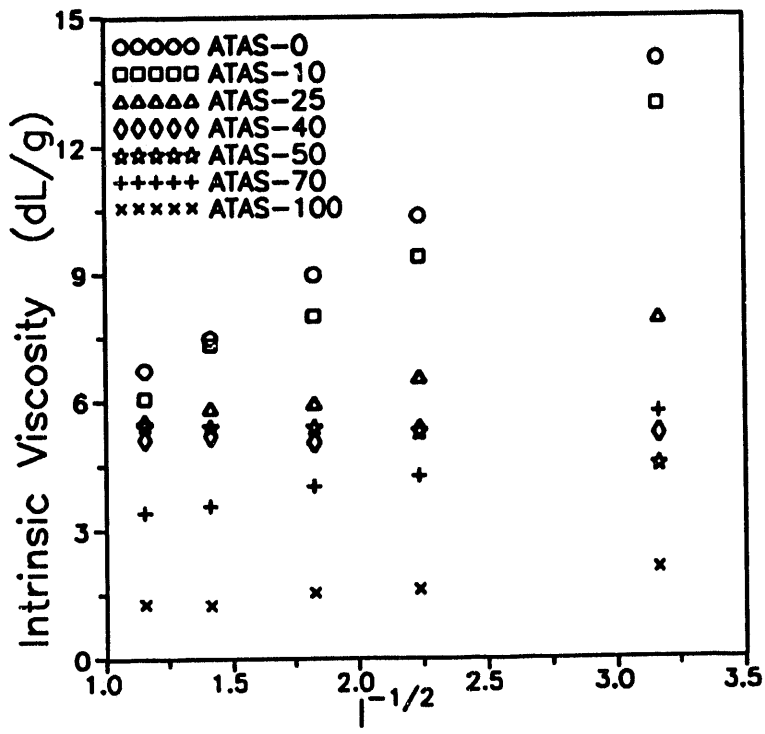

Figure 7-6. Intrinsic viscosities for the ATAS copolymers as a function of the inverse square root of ionic strength.

CHAPTER EIGHT: AMPHOLYTIC TERPOLYMERS OF ACRYLAMIDE WITH SODIUM 2-ACRYLAMIDO-2-METHYLPROPANESULFONATE AND 2-ACRYLAMIDO-2-METHYLPROPANETRIMETHYLAMMONIUM CHLORIDE

Abstract

Low charge density ampholytic terpolymers of acrylamide (AM) with random distributions of sodium 2-acrylamido-2-methylpropanesulfonate (NaAMPS) and 2-acrylamido-2-methylpropanetrimethylammonium chloride (AMPTAC) have been synthesized by free radical polymerization in 0.5M NaCl aqueous solutions. Terpolymer compositions were obtained by ^{13}C NMR. Low angle laser light scattering provided molecular weights and second virial coefficients which varied from 2.8 to 6.8 x 10^6 g/mol and 1.31 to 2.95 ml·mol/g^2 respectively. Dilute solution properties of the terpolymers were measured with respect to composition, concentration and added electrolytes. Polyampholyte behavior was observed for the polymer with as little as 0.5 mol % of each charged group and became significant when 7 mol % of each charged monomer was incorporated. At 12 and 15 mol % incorporation of each charged monomer, solution behavior becomes complex consistent with the existence of intermolecular interactions at low ionic strengths and intramolecular associations at medium salt concentrations.

Introduction

Few studies have been reported for polyampholytes with low charge densities[1-8] although copolymers and terpolymers of this type have great potential as rheology modifiers. Applications include drag reduction, enhanced oil recovery, personal care and coatings formulations. The "antipolyelectrolyte" effect or increased viscosity in salt solutions has not been commercially exploited. Microstructural charge placement, polymer concentration, and ionic strength are important in determining viscosity behavior. For polyampholytes with hydrophilic mers, the lower the charge density the greater the solubility in deionized water and the less added electrolyte necessary for dissolution[2-,4,17].

Peiffer and Lundberg[7,8] studied polyampholytes with low charge densities by incorporating the neutral monomer acrylamide (AM) along with methacrylamidopropyltrimethylammonium chloride and sodium styrene sulfonate yielding properties not readily attainable with the high charge density polyampholytes. Polymers were soluble in deionized water as well as in the presence of added electrolytes. In the absence of added electrolytes, the low

charge density polyampholytes, (< 10 mol %) showed intermolecular associations while the polymers with higher charge densities favored intramolecular ionic associations. The rheology of high ionic strength aqueous solutions could be controlled by adjusting the net charge and the anion-cation charge density of the polyampholytes.

Our laboratories have previously explored polyampholyte behavior using high charge density copolymers[9,10] and low charge density terpolymers[1,5,6]. Low charge density terpolymers (the ADASAM terpolymer series) were made using acrylamide (AM) as a neutral hydrophilic monomer along with sodium 2-acrylamido-2-methylpropanesulfonate (NaAMPS) and 2-acrylamido-2-methylpropanedimethylammonium hydrochloride (AMPDAC) as the charged monomers (Figure 1). The terpolymers were soluble in deionized water and exhibited enhanced viscosity as electrolytes were added. Both intra- and intermolecular associations could be observed in rheological studies.

This paper reports the study of a new series of terpolymers (the ATASAM series) made with 2-acrylamido-2-methylpropanetrimethylammonium chloride (AMPTAC) as the cationic monomer. This monomer features a quaternized ammonium functionality which is resistant to hydrolysis and readily copolymerizable[2,11]. The methods used to synthesize these terpolymers and their dilute solution behavior are discussed and compared to the previously studied ADASAM series.

Experimental

Monomer Synthesis

2-Acrylamido-2-methylpropanesulfonic acid (NaAMPS) obtained from Fluka was purified by recrystallization from a methanol/2-propanol solvent system followed by drying under vacuum at room temperature. Synthesis of 2-acrylamido-2-methylpropanetrimethylammonium chloride (AMPTAC) by a multistep procedure has been previously reported[11]. Briefly, 2-acrylamido-2-methylpropanedimethylamine was reacted with a ten-fold excess of methyl iodide in refluxing diethyl ether then ion-exchanged to yield the product AMPTAC.

Synthesis of Terpolymers of Acrylamide with Sodium 2-Acrylamido-2-methylpropanesulfonate with 2-Acrylamido-2-methylpropanetrimethylammonium Chloride

Terpolymers of AM with NaAMPS and AMPTAC (the ATASAM series) were synthesized by free radical polymerization in 0.5M NaCl aqueous solutions under nitrogen at 30°C using 0.1 mol % potassium persulfate as the initiator. The feed ratio of AM:NaAMPS:AMPTAC was varied from 99.0:0.5:0.5 to 70:15:15 mol % with the total monomer concentration held constant at 0.45M.

The use of 0.5M NaCl as the reaction medium insured that the terpolymers remained in solution during polymerization.

In a typical synthesis, specified quantities of each monomer were dissolved in small volumes of NaCl solution. After the pH was adjusted to 7, the separate solutions were combined and diluted to a 0.45M total monomer concentration. The reaction mixture was sparged with nitrogen for twenty minutes then initiated with 0.1 mol % potassium persulfate. The reaction was usually terminated at <30% conversion due to the high viscosity of the reaction medium and as a precaution against terpolymer compositional drift. The polymers were precipitated in acetone, redissolved in deionized water, then dialyzed using Spectra/Por 4 dialysis bags with molecular weight cutoffs of 12,000 to 14,000 g/mol. After isolation by lyophilization, the polymers were stored in desiccators with a nitrogen atmosphere.

All terpolymers were soluble in deionized water except for ATASAM 10-10 and ATASAM 15-15. These terpolymers precipitated from solution during dialysis. These hydrogel-like materials were washed repeatedly with deionized water to remove any remaining salt, or monomer, and then lyophilized. Conversions were determined gravimetrically. Table I lists reaction parameters for the terpolymerization of AM with NaAMPS and AMPTAC. FT-IR: Typical terpolymer: ATASAM 15-15, N-H 3515-3200 cm^{-1} (s); C-H 2933 cm^{-1} (m); C=O 1674-1658 cm^{-1} (s); S-O 1208 cm^{-1} (s). ^{13}C NMR: ATASAM 15-15, AM C=O 181.1 ppm; AMPTAC C=O 179.2 ppm; NaAMPS C=O 178.0 ppm; Chain CH 45.0 ppm; Chain CH_2 38.0 ppm; Quat CH_3 57.1 ppm; Gem CH_3 29.5 ppm.

Terpolymer Characterization

Terpolymer compositions were determined from ^{13}C NMR by integration of the amide carbonyl peaks[12]. ^{13}C NMR spectra were obtained using 10 wt/wt % aqueous (D_2O) polymer solutions with DSS as the reference. FT-IR spectra were acquired using a Perkin-Elmer 1600 Series FT-IR spectrophotometer. Molecular weight studies were performed on a Chromatix KMX-6 Low Angle Laser Light Scattering instrument. Refractive index increments were obtained using a Chromatix KMX-16 Laser Differential Refractometer. For quasielastic light scattering a Langley-Ford Model LF1-64 channel digital correlator was used in conjunction with the KMX-6. All measurements were conducted at 25°C in 1M NaCl.

Viscosity Measurement

Stock solutions of sodium chloride were prepared by dissolving the appropriate amount of salt in deionized water. Polymer stock solutions were made by dissolving a specified amount of polymer in solvent from these salt solutions. The solutions were then diluted to required concentrations and

allowed to age for two to three weeks before being analyzed with a Contraves LS-30 rheometer. Triplicate samples were prepared of each concentration to reduce experimental error. Intrinsic viscosities were evaluated using the Huggins equation[13].

Results and discussion

The ATASAM terpolymers were synthesized by varying the ratio of AM:NaAMPS:AMPTAC from 99:0.5:0.5 to 70:15:15 mol % in the feed. Reaction parameters and the resulting compositions for the polymers are given in Table I. The number appended to the acronym ATASAM refers to the concentration of NaAMPS and AMPTAC in the feed respectively. This series differs from the previously studied ADASAM series in that AMPTAC replaces AMPDAC as the cationic monomer. The quaternary ammonium of AMPTAC has been shown to provide a hydrolytically stable cationic moiety which remains charged regardless of solvent pH [2,11].

Compositional Studies

Terpolymer compositions were determined by the integration of acrylamido carbonyl peaks obtained from ^{13}C NMR. This method gave the mol % AM, NaAMPS and AMPTAC in the terpolymers with the exception of ATASAM 0.5-0.5 and ATASAM 2.5-2.5 which were assumed to have compositions equivalent to their feed. Previous studies of acrylamide copolymers with NaAMPS or AMPTAC showed low concentrations of charged monomers in the feed provided random incorporation regardless of the conversion[2,11,14]. The terpolymerizations were terminated at low conversion (< 30 % except for ATASAM 0.5-0.5) as an added precaution against compositional drift. Relatively good agreement between the feed compositions and the terpolymer compositions is shown in Table I.

In these terpolymerizations it is unlikely that the charged units exist in pairs along the polymer chain. Previous studies have demonstrated that addition of sodium chloride lowers monomer-monomer and monomer-polymer electrostatic interactions during polymerization[2,15,16]. A similar shielding effect would be expected to eliminate monomer pairing thus producing polyampholytes with charged monomers distributed randomly along the polymer chain. It is also interesting that attempts to synthesize these polyampholytes without added electrolytes were not successful due to phase separation of the reaction mixture.

Light Scattering Studies

Classical and quasielastic light scattering data for the ATASAM series are presented in Table II. Molecular weights range from 2.78 to 6.77 x 10^6

g/mol. Terpolymers with similar degrees of polymerization show decreasing second virial coefficient (A_2) values with increasing charge density. This trend is consistent with that of recently prepared sulfobetaine copolymers of acrylamide with the zwitterionic monomer 3-(2-acrylamido-2-methylpropane-dimethylammonio)-1-propanesulfonate[2-4].

The mean polymer diffusion coefficients (D_o) and hydrodynamic diameters (d_o) are consistent with degrees of polymerization and A_2 values. Decreasing solvation is indicated by decreasing A_2, lower d_o, and larger D_o values. The terpolymer ATASAM 5-5 has a degree of polymerization similar to ATASAM 10-10 but has greater A_2 and d_o values.

Viscometric Studies

The dilute solution behavior of the ATASAM series was studied in relationship to copolymer composition and added electrolyte concentration. Apparent viscosities of the polymers were measured at polymer concentrations below C^* using a Contraves LS-30 low shear rheometer. The solutions were aged two to three weeks to allow complete solvation. Intrinsic viscosities were calculated using the Huggins relationship.

Effects of Terpolymer Composition

The terpolymers with approximately balanced molar concentrations of NaAMPS and AMPTAC exhibit polyampholyte behavior. ATASAM 5-10 displays polyelectrolyte behavior as a direct result of the charge imbalance. For ATASAM 0.5-0.5 and ATASAM 2.5-2.5 the charge density is not sufficient to produce major changes in viscosity, however slight increases in intrinsic viscosity were observed with increasing salt concentration.

Effects of Added Electrolytes

The effects of sodium chloride on the intrinsic viscosities of the ATASAM terpolymers were measured at a shear rate of 5.96 sec^{-1} at 25°C as shown in Figure 2. ATASAM 5-5 displays a dramatic increase in viscosity with the addition of a small amount of sodium chloride. This is indicative of the elimination of intramolecular interactions and the resulting coil expansion.

The terpolymers ATASAM 10-10 and ATASAM 15-15 display complex behavior with increasing salt concentration. The presence of a small amount of electrolyte is required to solubilize both terpolymers. A slight increase in the ionic strength initially produces a decrease in intrinsic viscosity, likely due to the elimination of intermolecular molecular interactions with increasing ionic strength[2,7]. As the ionic strength increases further, the intrinsic viscosities

increase as intramolecular interactions are reduced and chain solvation is enhanced.

Figure 3 displays the reduced viscosity of ATASAM 10-10 as a function of polymer concentration at three ionic strengths. Intermolecular interactions exist in 0.05M NaCl as suggested by the large reduced viscosities above C^* (approximately 0.13 g/dL polymer concentration). Polymer aggregation is likely occurring at low salt concentration. In 0.25M NaCl the reduced viscosities above C^* decrease as intermolecular interactions are disrupted. Remaining intramolecular interactions in 0.25M NaCl are eliminated resulting in increased reduced viscosity at 1.0M NaCl.

Conclusions

Synthesis of the ampholytic ATASAM terpolymers in NaCl solutions allowed the incorporation of charged monomers in equal amounts and in random sequences. Molecular weights and second virial coefficients varied from 2.8 to 6.8 x 10^6 g/mol and 1.31 to 2.95 ml mol/g^2 respectively. Solution properties were studied as functions of terpolymer composition as determined by ^{13}C NMR and ionic strength. Polyampholyte behavior was observed for the polymer with as little as 0.5 mol % of each charged group and became significant when 7 mol % of each charged monomer was incorporated. ATASAM 5-5 displayed an 80 % increase in intrinsic viscosity in 1M NaCl compared to deionized water. At 12 and 15 mol % incorporation of each charged monomer, the solution behavior was complex with increasing ionic strength. These polymers were insoluble in deionized water but dissolved in 0.05M NaCl. Increasing the ionic strength to 0.1M NaCl led to a decrease in intrinsic viscosity, the result of elimination of intermolecular interactions, i.e., aggregates. Further increases in ionic strength led to disruption of intramolecular interactions; and an increase in intrinsic viscosity.

References

1. C. B. Johnson, Ph.D. Dissertation, University of Southern Mississippi (1988).

2. J. C. Salamone, I. Ahmed, E. L. Rodriguea, L. Quach and A. C. Watterson, *J Macromol. Sci.-Chem., A25(5-7)*, 811 (1988).

3. C. L. McCormick and L. C. Salazar, *Water-Soluble Polymers: Synthesis, Solution Properties, and Applications, 467,* ACS, 1991, p. 119.

4. C. L. McCormick and L. C. Salazar, *ACS Polym. Preprints, 30(2)*, 344 (1989).

5. C. L. McCormick and C. B. Johnson, *Macromol. Sci.-Chem. A27(5)*, 539 (1990).

6. C. L. McCormick and C. B. Johnson, *Polymer, 31*, 1100 (1990).

7. D. G. Peiffer and R. D. Lundberg, *Polymer, 26*, 1058 (1985).

8. D. G. Peiffer, R. D. Lundberg and I. Duvdevani, *Polymer, 27*, 1453 (1986).

9. C. L. McCormick and C. B. Johnson, *Macromolecules, 21*, 686 (1988).

10. C. L. McCormick and C. B. Johnson, *Macromolecules, 21*, 694 (1988).

11. C. L. McCormick and L. C. Salazar, Water Soluble Co-Polymers 42. Cationic Polyelectrolytes of Acrylamide and 2-Acrylamido-2-Methylpropanetrimethylammonium Chloride, submitted for publication.

12. C. L. McCormick and B. H. Hutchinson, *Polymer, 27(4)*, 623 (1988).

13. M. L. Huggins, *J. Am. Chem. Soc., 64*, 2716 (1942).

14. C. L. McCormick and G. S. Chen, *J. Polym. Sci., Polym. Chem. Ed., 20*, 817 (1982).

15. C. L. McCormick and L. C. Salazar, *Polym. Mat. Sci. Eng., 57*, 859 (1987).

16. C. L. McCormick and L. C. Salazar, Water Soluble Co-Polymers 41. Copolymers of Acrylamide and Sodium 3-Acrylamido-3-Methylbutanoate, submitted for publication.

17. J. C. Salamone, E. L. Rodriguez, S. C. Israel, I. Ahmed and A. C. Watterson, *Current Topics in Polymer Science, Volume I*, R. M. Ottenbrite, L. A. Utracki and S. Inoue, editors, Hanser Publishers, *292*, (1987).

TABLE I

Reaction Parameters for the Terpolymerization of Acrylamide (AM) with Sodium 2-acrylamido-2-methylpropanesulfonate (NaAMPS) and 2-Acrylamido-2-methylpropanetrimethylammonium Chloride (AMPTAC).

Sample Number	Feed Composition (mol %) AM:NaAMPS:AMPTAC	Reaction Time (hr)	Conversion (%)	Terpolymer Composition[a] (mol %) AM:NaAMPS:AMPTAC
ATASAM 0.5-0.5	99.0:0.5:0.5	2.5	51.6	99[b]:0.5[b]:0.5[b]
ATASAM 2.5-2.5	95.0:2.5:2.5	2.5	25.0	95[b]:2.5[b]:2.5[b]
ATASAM 5.0-5.0	90.0:5.0:5.0	2.5	19.5	86.0:6.9:7.0
ATASAM 10-10	80.0:10.0:10.0	2.5	26.1	76.0:11.9:12.1
ATASAM 15-15	70.0:15.0:15.0	2.5	29.0	69.5:15.8:14.7
ATASAM 5-10	85.0:5.0:10.0	3.0	13.9	82.2:6.4:11.5

[a] Determined from ^{13}C NMR
[b] Theoretical

Table II

Classical and Quasielastic Light Scattering Data for Terpolymers of Acrylamide (AM) with Sodium 2-Acrylamido-2-methylpropanesulfonate (NaAMPS) with 2-Acrylamido-2-methylpropanetrimethylammonium Chloride (AMPTAC)[a].

Sample Number	dn/dc	Mw x 10^{-6} (g/mol)	A_2 x 10^4 (ml·mole/g^2)	D_o x 10^8 (cm^2/g)	d_o (Å)	DP x 10^{-3}
ATASAM 0.5-0.5	0.1426	6.03	2.95	4.23	1037	8.48
ATASAM 2.5-2.5	0.1481	2.78	1.65	5.77	835	3.91
ATASAM 5-5	0.1510	5.07	2.00	3.81	1192	5.48
ATASAM 10-10	0.1395	5.87	1.57	4.49	1094	5.44
ATASAM 15-15	0.1344	6.77	1.31	4.33	1184	5.74
ATASAM 10-5	0.1376	3.88	1.56	4.13	1278	3.95

[a] Determined in 1.0M NaCl at 25°C.

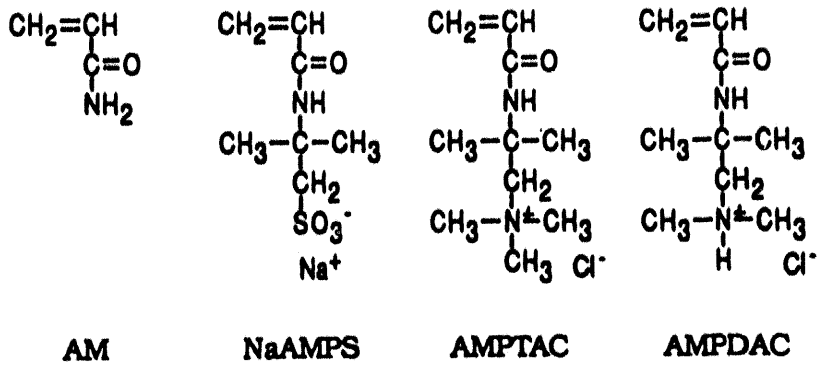

Figure 8-1. Structures for the monomers Acrylamide (AM), Sodium 2-Acrylamido-2-methylpropanesulfonate (NaAMPS), 2-Acrylamido-2-methylpropanetrimethylammonium Chloride (AMPTAC), and 2-Acrylamido-2-methylpropanedimethylammonium Hydrochloride (AMPDAC).

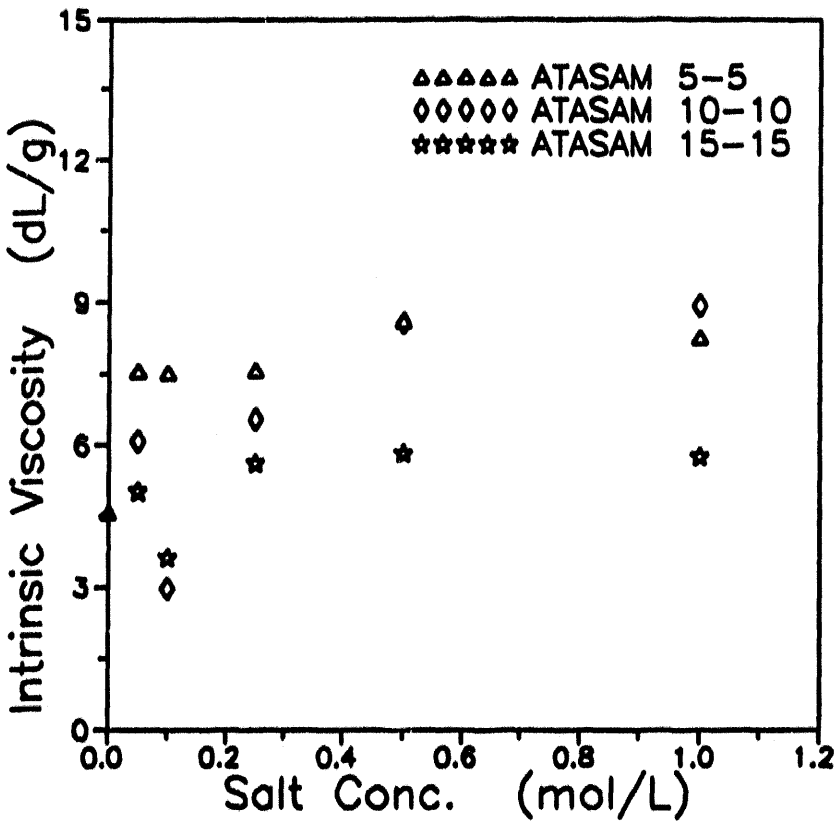

Figure 8-2. Effects of sodium chloride on the intrinsic viscosities of ATASAM terpolymers determined at 25°C at a shear rate of 5.96sec^{-1}.

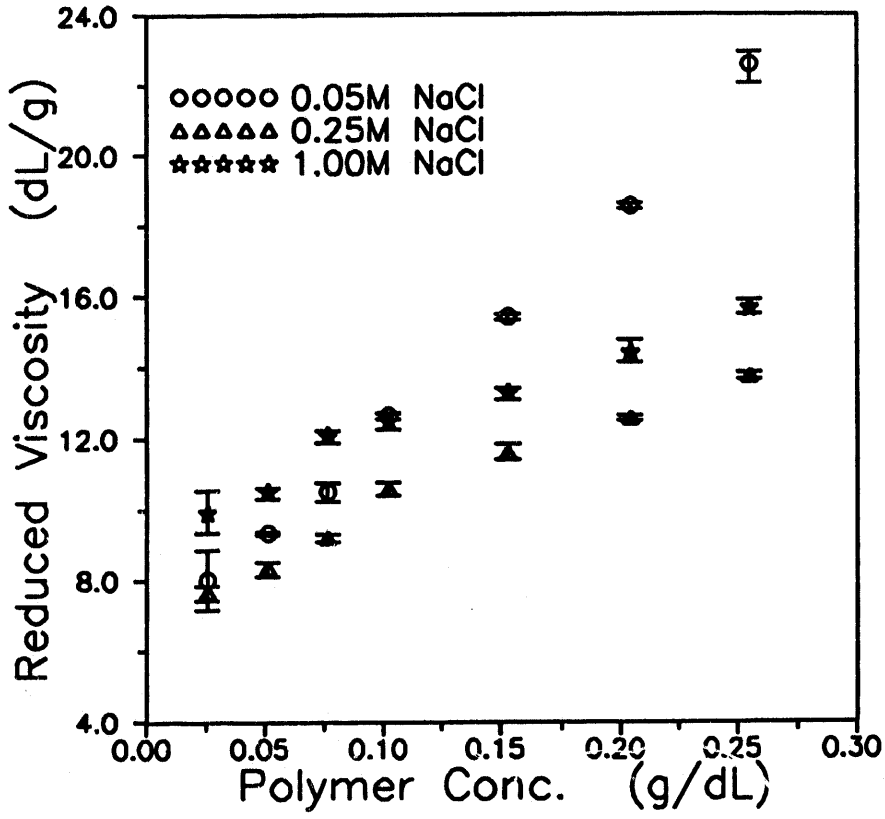

Figure 8-3. Reduced viscosities of the ATASAM 10-10 terpolymer in various ionic strengths determined at a shear rate of 5.96 sec^{-1} at 25°C. The bars represent the distribution of the data.

CHAPTER 9 : POLYMER SOLUTION EXTENSIONAL BEHAVIOR IN POROUS MEDIA

Introduction

Considerable efforts have been undertaken to define the flow properties of polymer solutions through porous media. Both the shear and elongational viscosity properties of high molecular weight polymer solutions in a porous media must be characterized as a function of macromolecular structure and solvent-polymer interactions so that mobility performance for a polymer reservoir injection can be optimized.

Flow Through Beds of Packed Spheres

Dimensional analysis has been used to define the major parameters controlling the flow resistance or mobility of a polymer solution through beds of uniform spherical particles. Dimensionless groups have been used to show correlation between parameters. The bed Reynolds number, N_{Re}, and fluid friction factor, f, are defined as

$$N_{Re} \equiv \frac{v d \rho}{\eta_s (1 - \phi)} \tag{1}$$

$$f \equiv \frac{d \phi^3}{v^2 (1 - \phi) \rho} \frac{\Delta P}{\Delta \ell} \tag{2}$$

$$\Lambda = N_{Re} f \tag{3}$$

Within these two dimensionless groups the nature of the porous media is given by the diameter of the spherical particles, d, forming a bed having porosity, ϕ. The driving force for fluid flow through the bed is given by the pressure drop per unit length of bed, $\Delta P/\Delta \ell$. Flow conditions through the bed are defined by the average fluid velocity, v. This velocity is based on the cross section area of an empty bed. The fluid velocity

within the pore channels comprising the bed would be the empty bed velocity divided by the bed porosity. Solution fluid properties of shear viscosity, η_s, and density, ρ, are also used in the dimensionless groups.

Newtonian Fluids

The N_{Re} establishes flow conditions and the friction factor is a measure of fluid resistance at the given flow conditions. For Newtonian fluids, such as water, experimentation has found that[1]

$$\Lambda = 175 + 1.75N_{Re} \tag{4}$$

Non-Newtonain Fluids

When the Newtonian fluid contains large water-soluble polymers the relationship described by equation (4) is not valid. At a critical flow condition the polymer coils within the solvent passing through the porous media begin to elongate and produce additional resistance to flow. This resistance due to polymer coil elongation is called the solution elongational viscosity, η_e. At certain flow conditions the resistance due to the solution's elongational viscosity can be two or three orders of magnitude greater than that due to the shear viscosity.

Dilute Polymer Solution Behavior in Extensional Flow

Usually a polymer coil starts to elongate when the product of its response time, τ, and the elongation rate, Γ, equal 0.1. This dimensionless product is called the Deborah Number,[2] N_{De}

$$N_{De} = \Gamma\tau \tag{5}$$

The fluid elongation rate is the change in fluid velocity with respect to direction of flow. For a porous media of spheres the elongation rate is dependent on the fluid velocity and bed porosity.

$$\Gamma = \frac{\sqrt{2}}{\phi}\,\frac{v}{d} \tag{6}$$

The coil response time, τ, can be estimated from the intrinsic viscosity of the polymer, $[\eta]$ and the polymer's molecular weight, M.

$$\tau = \frac{\eta_s [\eta] M}{RT} \tag{7}$$

In equation 7, R and T are the gas law constant and temperature, respectively.

The magnitude of the Deborah number is a measure of a polymer coil's ability to react by extension (its response time) to a given flow condition (the fluid elongation rate). The degree of coil extension depends upon the Deborah number. When the Deborah number is much less than one, minimum coil extension is experienced. However when the Deborah number is greater than one, the coil is fully extended. This extension followed by a relaxation to a random coil state converts kinetic energy to heat and thereby increases resistance to fluid flow through a porous media.

At Deborah numbers greater than one, a maximum flow resistance has been reported by Durst[3]. The maximum friction factor observed by Durst, fm, when compared to the solvent friction factor, fs, is defined by equation 8 for a solution containing polymer coils at concentration, C, which have N number of macromolecular sub-elements in the coil capable of contributing to the elongation of the coil.

$$\frac{fm - fs}{fs} = \left[\frac{N[\eta]C}{50}\right]^{2/3} \left[\frac{1}{1 + [\eta]C}\right] \tag{8}$$

The number of macromolecular sub-elements can be determined if the polymer's repeat unit (monomer) molecular weight, M_o, and the length of the repeat unit, ℓ_o, are known.

$$N = \left(\frac{\ell_o}{M_o}\right)^2 \left(\frac{\Phi}{[\eta]}\right)^{2/3} M^{4/3} \tag{9}$$

In equation 9, Φ is the Fox-Flory constant[4].

Combination of equations 8 and 9 shows how macromolecular structure (coil size, capacity to elongate, monomer influence, concentration and polymer interaction with solvent) should affect the maximum fluid flow resistance experienced when a polymer solution is forced through a porous media. Note that the maximum mobility change per volume fraction of polymer coils in solution, $(f_m - f_s)/(f_s[\eta]C) = \psi_{max}$, predicted by equation 10 is a product of a constant, $(\Phi^4/[50^6\ A^6])^{1/9}$, the contour length of the macromolecule, $(\ell_o M/M_o)^{4/3}$, the hydrodynamic size of the coil, $(M[\eta])^{2/9}$, and the

number of polymer coils per unit volume of solution $[AC/M]^{2/3}$.

$$\psi_{max} = \frac{fm - fs}{f_s[\eta]C} = \left(\frac{\Phi^4}{50^6 A^6}\right)^{1/9}\left(\frac{\ell_o M}{M_o}\right)^{4/3}\left(\frac{[M[\eta]]^{2/9}}{([\eta]C)^2 + [\eta]C}\right)\left[\frac{AC}{M}\right]^{2/3} \quad (10)$$

In equation 10, A is Avogadro's number. This equation was developed for dilute solutions of linear, non-association polymer coils which elongate as finitely extensible non-linear elastic springs[5]. A dilute solution exists when the volume fraction of polymer in solution, $[\eta]C$, is less than about 0.50.

Equation 10 gives the maximum expected normalized mobility decrease, $(f_m - f_s)/(f_s[\eta]C) = \psi_{max}$, for a polymer solution in which the macromolecular coils are fully expanded. As previously discussed, the amount of coil expansion depends upon the Deborah number developed within the porous media produced by the flow field. Data published by Durst[3] using high molecular weight polyacrylamide in aqueous solutions suggest the dependence of solution mobility on the Deborah number can be given by

$$\psi = \psi_{max}\frac{1 + erf\left(\frac{N_{De} - \mu}{\sigma}\right)}{2} \quad (11)$$

where $\psi = (f_p - f_s)/(f_s[\eta]C)$ and f_p is the friction factor of the polymer solution. When all polymer coils in the solution experience full extension ($N_{De}>1$) then $f_p = f_m$ and $\psi = \psi_{max}$.

Comparison to Porous Media Flow Data

Equation 11 contains adjustable parameters μ and σ. Values for these parameters probably depend upon the variation of the porous media structure and/or the distribution of polymer coil sizes found in the solution. Figure 9-1 shows good agreement between the Durst experimental ψ values and the ψ function given by equation 11.

Equation 11 can be simplified by expressing it as

$$\psi = \psi_{max}^{\xi} \quad (12)$$

where ψ is the normalized solution mobility, ψ_{max} is the maximum mobility change per volume fraction of polymer coils, and ξ is an exponent which controls the extent to which the maximum mobility change conditions develop. ψ_{max} is a function of polymer molecular properties and concentration. The exponent ξ is defined by equation 13.

$$\xi = \frac{1 + \text{erf}\left(\frac{N_{De} - \mu}{\sigma}\right)}{2} \tag{13}$$

Application to Sandstone Porous Media

We will now expand the above analysis to polymer flooding in sandstone reservoirs. These reservoirs have porosities, ϕ, which range from 0.1 to 0.4 and permeabilities, k, which vary from 1.0×10^{-10} to 3.0×10^{-8} cm^2 (10 to 3000 md). For many sandstone reservoirs, ϕ can be related to k in the following manner.

$$\phi = a + b \log k \tag{14}$$

The parameters a and b vary with the particular reservoir. Woodbrine sandstone values for a and b are 0.465 and 0.025, respectively, where k is expressed in cm^2 dimensions.[6]

Although a sandstone reservoir is composed of compressed or consolidated sand particles, this porous media can be roughly characterized by an average sand sphere diameter, d. This diameter can be estimated from ϕ and k values of the reservoir using the Kozeny-Carman relationship.[7]

$$d = \frac{1 - \phi}{\phi} \sqrt{\frac{180\,k}{\phi}} \tag{15}$$

The reservoir characteristic particle diameter, d, can be used to estimate the extension rate, Γ, for a fluid forced through the media at velocity, v. As previously discussed,

$$\Gamma = \frac{\sqrt{2}}{\phi} \frac{v}{d} \tag{16}$$

The fluid velocity in the porous media, v, varies with distance from the wellhead. For cylindrical wells having volumetric injection rates Q through a pay length of L, the local fluid velocity at radial distance r can be calculated.

$$v = \frac{Q}{2\pi r L} \tag{17}$$

Combination of Equations 15, 16 and 17, shows that the fluid extension rates in

sandstone near the wellhead can be determined by

$$r = \frac{Q}{\pi r L(1-\phi)} \sqrt{\frac{\phi}{360k}} \qquad (18)$$

If one uses a relationship such as Equation 14 to define porosity in terms of permeability, then the fluid extension rate is a function of only well injection rates, Q/L, reservoir permeability, k, and radial distance from the well, r.

Model Predictions

The above relationship was used with Equation 12 to model the approximate near well reservoir resistance to injection of high molecular weight polyacrylamide solutions. Using this model, Figure 9-2 was constructed to show the solution to solvent friction factor ratios, f_p/f_s, as a function of polymer molecular weight, M, solution dimensionless concentration, $[\eta]C$, reservoir permeability, k, and radial distance from the wellhead, r. A constant injection rate of 20 barrels per day per foot of pay thickness was used to construct this figure.

Examination of Figure 9-2 reveals the following:

1. Extension of polymer molecules, and thus significant increased fluid flow resistance, occurs very near the wellhead.
2. The total fluid flow resistance, which is proportional to the area under a curve increases with polymer molecular weight (compare conditions A to C and B to D), polymer concentration (compare conditions A to B and C to D) and lower reservoir permeabilities.
3. Complete polymer extension and thus, maximum fluid resistance, can easily develop near the wellhead using typical injection conditions. This is shown by the flattening of the curves to zero slope under conditions C and D.
4. Although not shown by Figure 9-2, an increase in wellhead fluid injection rates magnifies fluid flow resistance significantly.

The above analysis was done for injection of dilute polymer solutions ($[\eta]C < 0.50$). Many of the arguments used to develop this extension model are less accurate or invalid as polymer concentration increases. Usually, injected polymer flooding solutions are much more concentrated ($[\eta]C >> 0.50$). Under more concentrated conditions, fluid resistance due to polymer coil extension is expected to be much greater. In addition, injection conditions using concentrated solutions can degrade the polymer because extensional forces exceed macromolecular covalent bonding forces.[8]

Concentrated Polymer Solution Behavior in Shear

As previously noted, the polymer solutions used for enhanced oil recovery are almost always injected at high concentrations. Usually the dimensionless concentration, (the product of the polymer's intrinsic viscosity, [η], and the polymer concentration in solution, C), is greater than 0.50. Under these conditions considerable overlap exists between individual macromolecular coils and the resulting entanglement between coils greatly affects solution rheological behavior. Solutions of entangled polymer coils have greater shear viscosities and much greater elongational viscosities than dilute polymer solutions.

The shear viscosities of typical concentrated polymer solutions show pseudoplastic or shear thinning behavior where the apparent shear viscosity, η_a, decreases with shear rate, $\dot{\gamma}$. This behavior can be expressed using a power law relationship of the form

$$\eta_a = m\dot{\gamma}^{X-1} \tag{19}$$

where the solution's apparent shear viscosity, η_a, is equal to the product of the fluid shear rate, $\dot{\gamma}$, to the power X - 1 and in which m is a material constant (the consistency index). The shear rate experienced by a power law fluid flowing in a porous media having permeability, k, and porosity, ϕ, can be estimated from the following relationship:

$$\dot{\gamma} = \frac{3v(3X+1)}{(150X^2k\phi)^{1/2}} \tag{20}$$

where v is the fluid velocity through the porous media. In addition, the Reynold's number, N_{Re}, and friction factor, f, for flow of a power law fluid of density, ρ, through a porous bed made of particles having diameter, d, can be given by[9]

$$N_{Re} = \frac{12d^X v^{2-X}\rho\phi^{2X}}{150m(1-\phi)^X\left(9+\frac{3}{X}\right)^X\phi^2} \tag{21}$$

$$f = \frac{\left(9+\frac{3}{X}\right)^X d\phi^3\phi^{2-2X}\Delta P}{12v^2\rho(1-\phi)^{2-X}\Delta\ell} \tag{22}$$

In equation 22, $\Delta P/\Delta \ell$ is the fluid pressure loss per unit length of porous media. If Λ equals the product of N_{Re} and f then

$$\Lambda = \frac{\phi^3 d^{1-x} \quad \Delta P}{(1-\phi)^2 m v^2 \Delta \ell} \tag{23}$$

As previously discussed, the N_{Re} establishes flow conditions and the friction factor is a measure of fluid resistance at the flow conditions. Experimentation indicates that

$$\Lambda = 175 + 1.75 N_{Re} \tag{24}$$

is a good predictor of a power law fluid's flow behavior in a porous media provided the fluid has simple Trautonian extensional viscosity properties. A fluid is a simple Trautonian if its extensional viscosity, η_e, is always three times its shear viscosity, i.e. $\eta_e = 3\eta_s$. Polymer solutions are non-Trantonian and therefore the above relationships are not valid but must be modified.

Concentrated Polymer Solution Behavior in Extensional Flow

Polymer solutions are not simple Trautonian fluids. They can have extensional viscosities which vary with the fluid extension rate. This phenomena is magnified when the solutions are concentrated, $[\eta]C > 0.50$, and pass through a porous media where the flow field has a significant extensional strain component. The extensional flow strain, ϵ, is the product of the extension rate, Γ, and the time of extension, t.

$$\epsilon = \Gamma t \tag{25}$$

For flow through porous media composed of packed spherical particles having diameter, d, the following relationships exist:

$$\Gamma = \frac{\sqrt{2}}{\phi} \frac{v}{d} \tag{26}$$

and

$$t = \frac{d\phi}{2v} \tag{27}$$

Equations 26 and 27 are only approximate, average conditions, but if we accept these averages, the fluid traveling through the porous media has an extensional strain which is a constant, regardless of the extension rate and is probably equal to $1//\overline{2}$.

This is an important conclusion because it implies that the fluid extensional strain is independent of both porous media particle size and fluid volumetric flow rate. Note that when the extension rate is high, the time of extension is low, and vice versa. This fact imposes constant fluid extensional strain conditions for porous media composed of spheres.

When polymer coils in solution experience an extensional flow field, the degree of coil extension into a stretched state depends upon both its extension rate and time of extension. If its extension rate is below a critical value, Γ^*, little or no coil extension occurs. Γ^* is inversely proportional to the polymer coil's response time, τ, which is a function of polymer properties. As previously discussed, when the Deborah Number ($N_{De} = \Gamma \tau$) increases to unity, $\Gamma > \Gamma^*$, then full coil extension would occur provided that the time of extension is large. If the time for extension is insufficient then full polymer coil stretch will not develop regardless of the magnitude of the extension rate. When polymer stretch is absent or minimized the solution would have a much lower resistance to flow through the porous media.

Denn and Marucci Extensional Flow Model

Denn and Marucci have developed a model to estimate a polymer solution's extensional behavior.[10] This model which incorporates extension rates (Deborah Numbers) and time of coil extension can be used to develop the following relationship to find the Durst normalized solution mobility parameter, ψ.

$$\psi = A - B - C - D \tag{28}$$

where

$$A = 1/\{C\,[\eta]\,(1 - 2N_{De})\,(1 + N_{De})\}$$

$$B = 2 \exp [(2N_{De} - 1)\, t/\tau] / \{C\,[\eta]\,(1 - 2N_{De})^3\}$$

$$C = \exp [-(N_{De} + 1)\, t/\tau] / \{C\,[\eta]\,(1 + N_{De})^3\}$$

$$D = 1/\{C\,[\eta]\}$$

This model, when used with the Durst published data[3] for polyacrylamide solution flow through a bed of packed spheres, gave a rough fit of the fluid behavior observed. Figure 9-3 shows a fit of the Durst experimental data and the model. The extensional strain of the Denn and Marucci model was adjusted to give a best fit to the data. The extension strain determined by this procedure gave a value of 2.1. This value is three

times greater than the maximum expected macromolecular extensional strain of $1/\sqrt{2}$. Thus we can conclude that the Denn and Marucci model is not consistent with the expectation that polymer coil extension during flow through a porous media of spherical particles is restricted by the time of extension. This is not logical and implies that this model is insufficient in simulating polymer solution extensional fluid flow behavior in porous media.

Conclusion

Two theoretical models for explaining polymer solution extensional flow resistance in porous media have been reviewed. The Durst model was rearranged to reveal what macromolecular parameters are important in producing solution resistance in an extensional flow field. However this model predicts a maximum fluid resistance which is larger than observed. Empirical fitting parameters had to be introduced for this model to be consistent with experimental data. The model inadequacy is probably due to its failure to correctly incorporate the cyclic and limited extensional strains experienced by macromolecules when flowing through The contracting and expanding channels of typical porous media. Unfortunately when the Denn and Marucci model was analyzed using porous media extensional flow data, it predicted a macromolecular extensional strain that is excessive and is inconsistent with logical expectations. Thus although both models are based on valid theoretical assumptions and explain some aspects of fluid flow extensional resistance, they are inadequate in explaining all porous media fluid flow resistance properties under all experimental conditions.

References

1. Bird, R. B., W. E. Stewart, E. N. Lightfoot, *Transport Phenomena*, John Wiley & Sons, NY, p. 196-200 (1960).

2. Reiner, M., *Physics Today*, p. 62, January 1964.

3. Durst, F. and R. Haas, *Rheol. Acta 20*, 179-92 (1981).

4. Flory, P. J., *Principles of Polymer Chemistry*, Cornell University Press, London, p. 602-612 (1953).

5. Bird, R. B., C. F. Curtiss, R. C. Armstrong, O. Hassager, *Dynamics of Polymeric Liquids, V2 Kinetic Theory,* John Wiley & Sons, NY, p. 85-88 (1987).

6. R. E. Collins, *Flow of Fluids Through Porous Materials*, Petroleum Publishing Company: Tulsa, 1976; p. 17.

7. A. E. Scheidegger, *The Physics of Flow Through Porous Media, 3rd Ed.*, University of Toronto Press: Toronto, 1974; p. 141.

8. Odell, J. A., A. Keller *J. Poly. Sci., Part B, 24,* 1889, 1986.

9. Wang, F. H., "Influences of Polymer Solution Properties on Flow in Porous Media," Ph.D. Thesis, Penn. State University, November, 1978.

10. Denn and Marucci, *J. Applied Polymer Sci., 21,* 841, 1977.

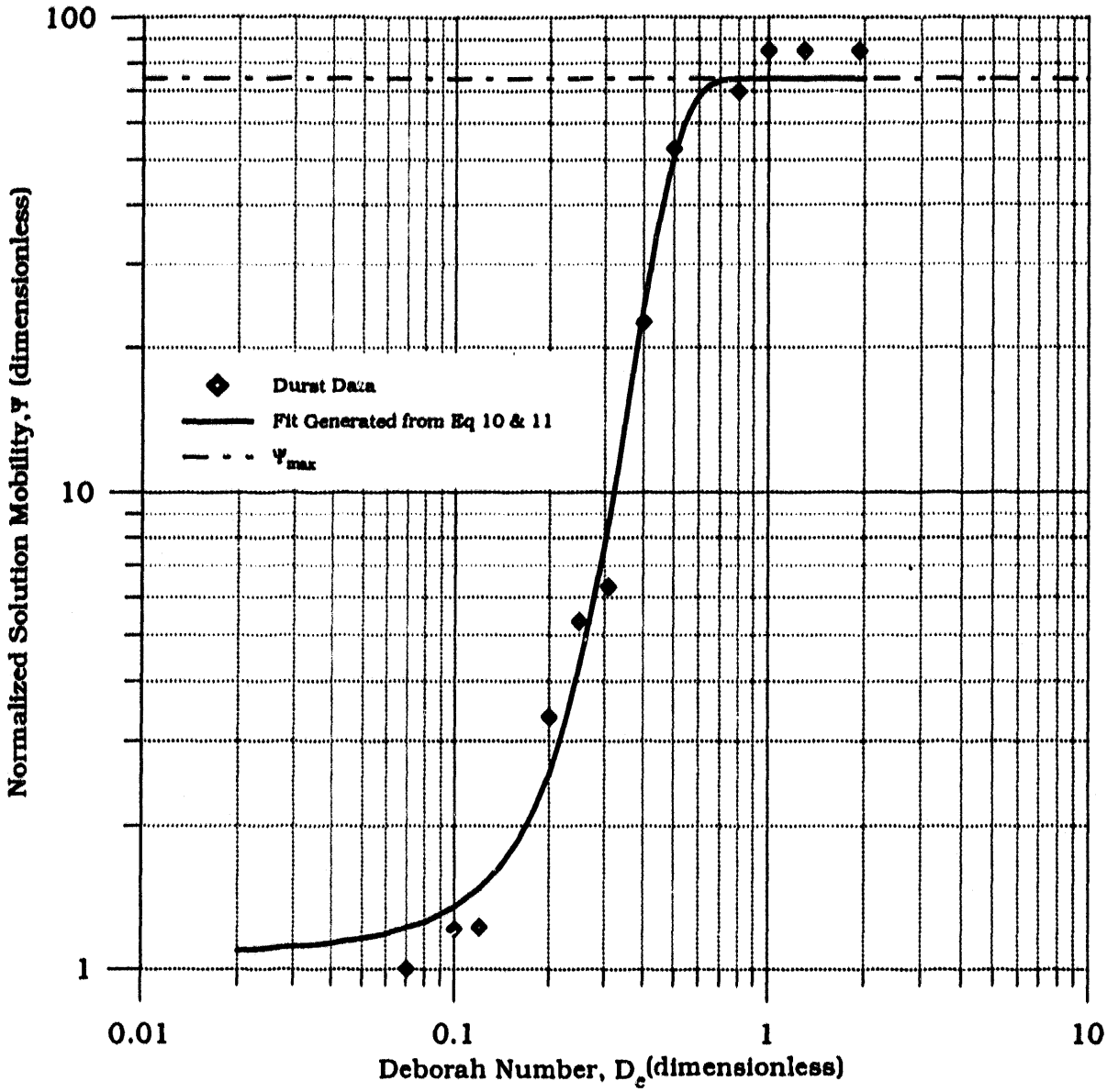

Figure 9-1, Mobility Plot for PAM in 0.5M NaCl

Parameter Values

Symbol	Description	Value	Dimensions
M-	Polymer mol. wt.	10.71×10^{6}	g/mol
l_o-	Monomer length	2.51×10^{-8}	cm
M_o-	Monomer mol. wt.	71	g/mol
Φ-	Fox-Flory constant	2.8×10^{23}	1/mole
C-	Polymer concentration	25	ppm
[η]-	Intrinsic viscosity	2200	cm^3/g
μ-	Error function fit parameter	0.31	
σ-	Error function fit parameter	0.20	

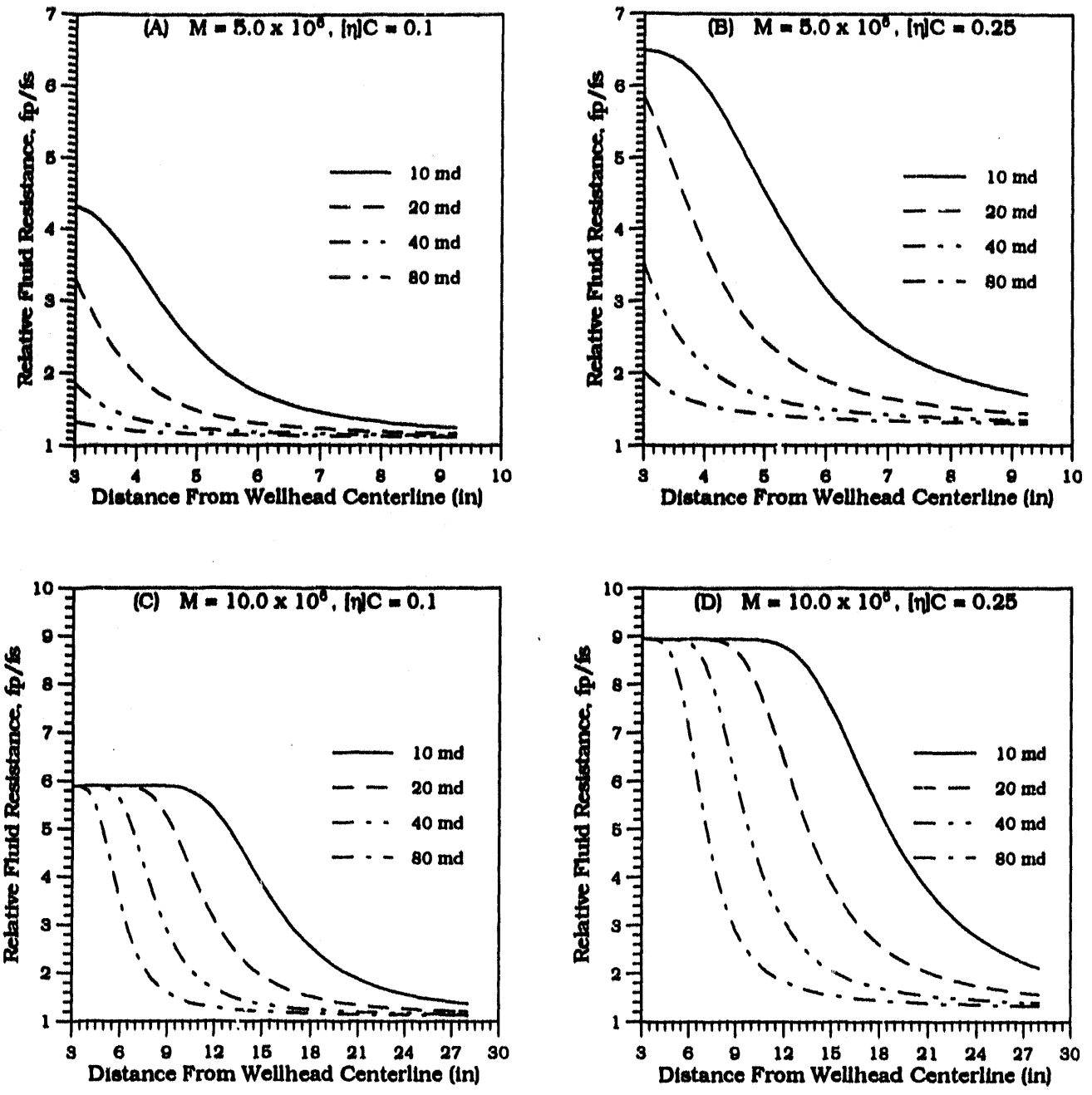

Figure 9-2

Predicted polyacrylamide dilute solution flow resistance in typical Woodbrine sandstones near a 6 inch diameter wellhead at injection rates of 20 barrels per day per foot of pay.

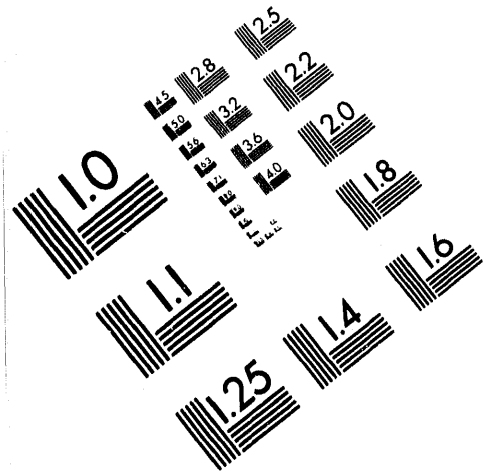

Association for Information and Image Management
1100 Wayne Avenue, Suite 1100
Silver Spring, Maryland 20910
301/587-8202

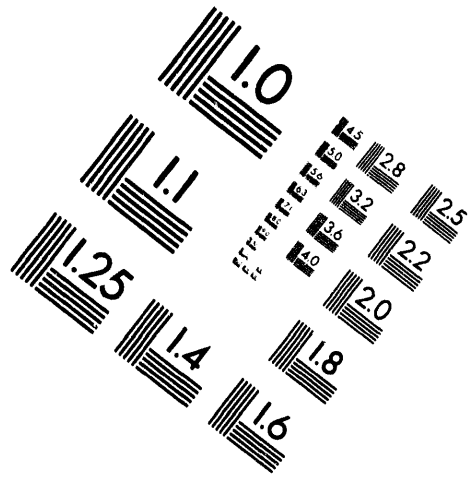

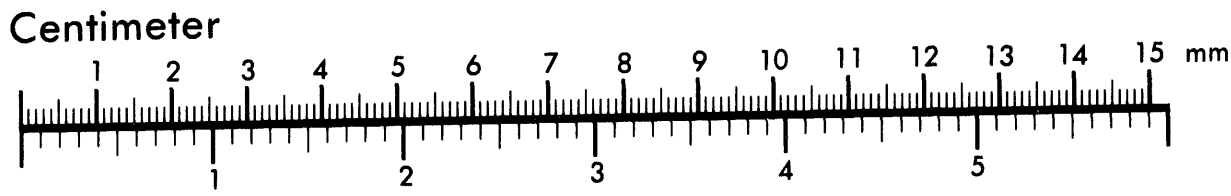

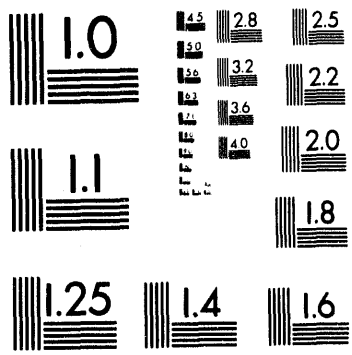

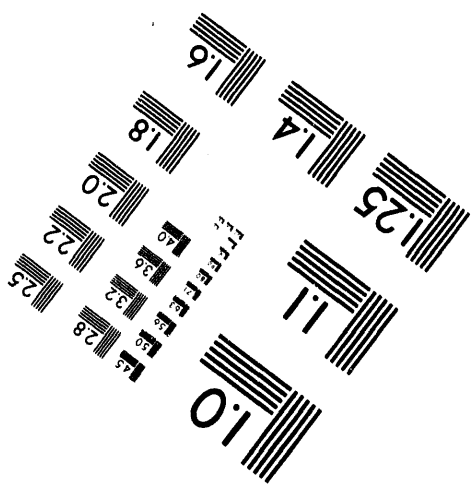

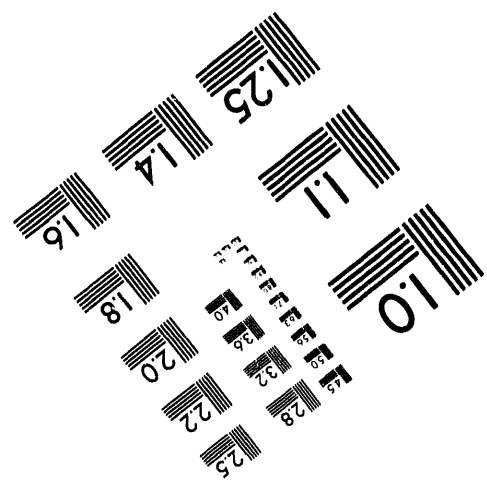

MANUFACTURED TO AIIM STANDARDS
BY APPLIED IMAGE, INC.

3 of 3

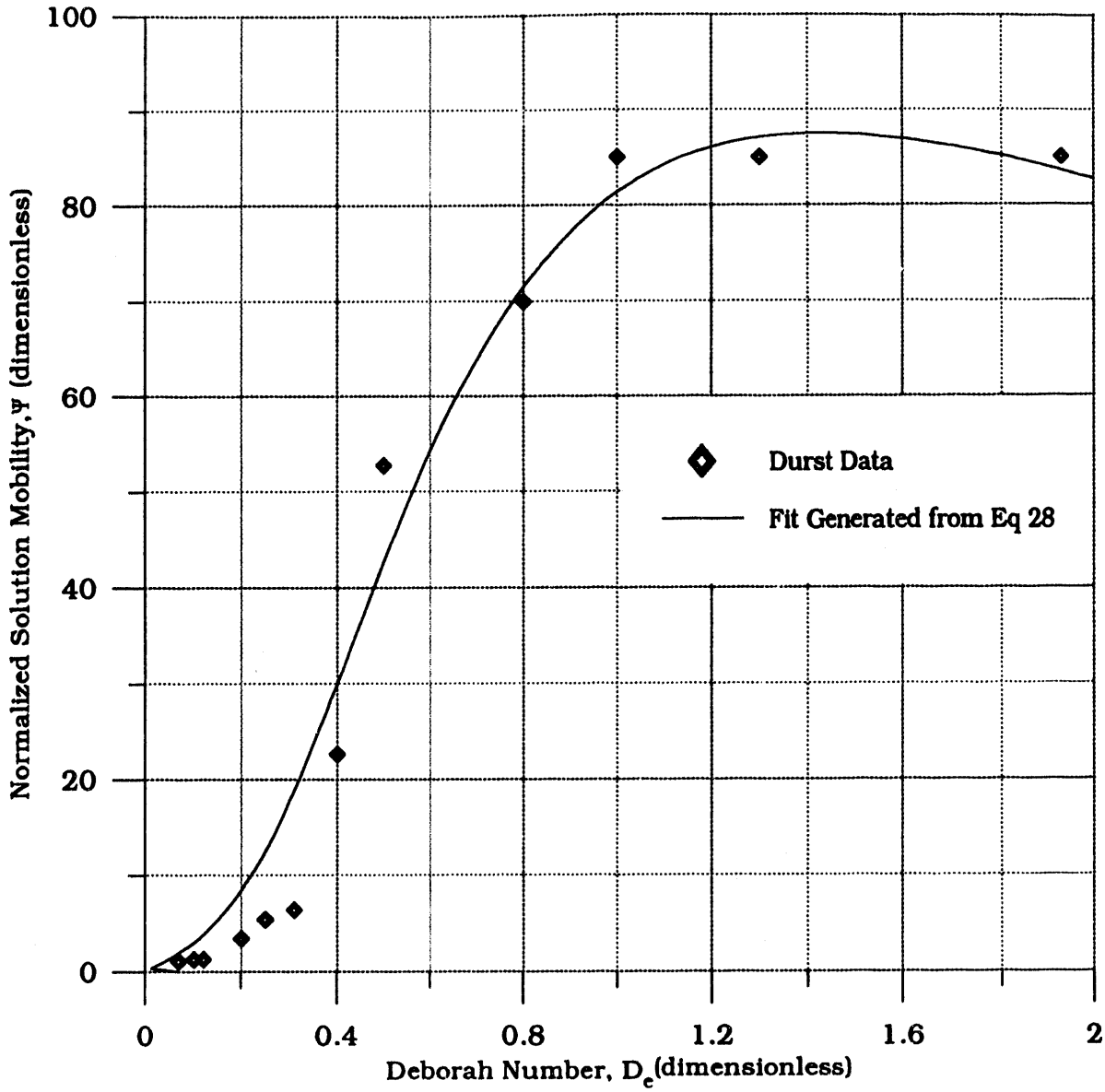

Figure 9-3, Mobility Plot for PAM in 0.5M NaCl

Parameter Values

Symbol	Description	Value	Dimensions
M-	Polymer mol. wt.	10.71×10^{6}	g/mol
l_o-	Monomer length	2.51×10^{-8}	cm
M_o-	Monomer mol. wt.	71	g/mol
Φ-	Fox-Flory constant	2.8×10^{23}	1/mole
C-	Polymer concentration	25	ppm
[η]-	Intrinsic viscosity	2200	cm^3/g
ε-	Extentional Strain	2.1	

☆U.S. GOVERNMENT PRINTING OFFICE: 1994 - 560-030/00033

DATE
FILMED
10/17/94
END